

THE AVIAN REOVIRUS TRICISTRONIC S1 mRNA: NEW INSIGHTS INTO
CONTROL OF TRANSLATION INITIATION

by

Trina Racine

Submitted in partial fulfilment of the requirements
for the degree of

Doctor of Philosophy

at

Dalhousie University
Halifax, Nova Scotia
May 2010

© Copyright by Trina Racine, 2010

DALHOUSIE UNIVERSITY

DEPARTMENT OF MICROBIOLOGY AND IMMUNOLOGY

The undersigned hereby certify that they have read and recommend to the Faculty of Graduate Studies for acceptance a thesis entitled THE AVIAN REOVIRUS TRICISTRONIC S1 mRNA: NEW INSIGHTS INTO CONTROL OF TRANSLATION INITIATION by Trina Racine in partial fulfilment of the requirements for the degree of Doctor of Philosophy.

Dated: May 17th, 2010

Supervisor: _____

Readers: _____

Departmental Representative: _____

DALHOUSIE UNIVERSITY

DATE: May 17th, 2010

AUTHOR: Trina Racine

TITLE: THE AVIAN REOVIRUS TRICISTRONIC S1 mRNA: NEW
INSIGHTS INTO CONTROL OF TRANSLATION INITIATION

DEPARTMENT OR SCHOOL: Department of Microbiology and Immunology

DEGREE: PhD CONVOCATION: October YEAR: 2010

Permission is herewith granted to Dalhousie University to circulate and to have copied for non-commercial purposes, at its discretion, the above title upon the request of individuals or institutions.

Signature of Author

The author reserves other publication rights, and neither the thesis nor extensive extracts from it may be printed or otherwise reproduced without the author's written permission.

The author attests that permission has been obtained for the use of any copyrighted material appearing in the thesis (other than the brief excerpts requiring only proper acknowledgement in scholarly writing), and that all such use is clearly acknowledged.

I would like to dedicate this thesis to the research Gods . . . I hope you like it!

TABLE OF CONTENTS

LIST OF FIGURES	ix
ABSTRACT.....	xi
LIST OF ABBREVIATIONS USED	xii
ACKNOWLEDGEMENTS.....	xiv
CHAPTER 1: Introduction	1
1.1 Overview	1
1.2 The Scanning Model Of Translation Initiation	2
1.3 Factors Affecting AUG Recognition And Ribosome Scanning	5
1.3.1 Nucleotide Context	5
1.3.2 Leader Length	6
1.3.3 Non-AUG Initiation	6
1.3.4 <i>Cis-</i> And <i>Trans-</i> Acting Factors	7
1.4 Translational Enhancement Via mRNA Circularization	7
1.4.1 Poly(A) Binding Protein	7
1.4.2 Translation Enhancer Elements Located In The 3'-UTR	8
1.5 Global And mRNA-Specific Control Of Translation Initiation	9
1.6 Translation Elongation, Termination And Ribosome Recycling	12
1.7 Alternate Mechanisms Of Translation Initiation	14
1.7.1 Leaky Scanning	14
1.7.2 Reinitiation	15
1.7.3 Ribosomal Shunting	21
1.7.4 Internal Ribosome Entry Sites	25
1.7.5 Additional Alternate Mechanisms of Initiation	30
1.8 Translational Control In Cancer Development	32
1.9 Translation Summary	33
1.10 The Family <i>Reoviridae</i>	34

1.10.1 Virion Morphology	34
1.10.2 Virus Replication	34
1.11 The Genus <i>Orthoreovirus</i>	37
1.12 Avian Reovirus	38
1.13 The S1 Genome Segment	38
1.14 Objectives	42
CHAPTER 2: Materials and Methods	43
2.1 Cells	43
2.2 Competent Cells	43
2.3 Plasmids	43
2.4 Mutagenesis	44
2.4.1 Site-Directed Mutagenesis	44
2.4.2 Deletions And Insertions	45
2.5 DNA Ligation	46
2.6 Transformation Of <i>E. coli</i>	46
2.7 Transfection	47
2.7.1 DNA Transfection	47
2.7.2 RNA Transfection	47
2.8 Immunostaining	48
2.9 Quantitative Western Blotting	48
2.10 Antibodies	49
2.11 Total RNA Extraction And RNA Purification	50
2.12 Northern Blotting	50
2.13 <i>In vitro</i> Transcription	51
2.14 <i>Renilla</i> Luciferase Assay	52
2.15 Quantitative Real-Time Polymerase Chain Reaction (qRT-PCR)	52
CHAPTER 3: Results	54
3.1 Expression From The Internal σ C Start Site Occurs Efficiently From A Full-Length Tricistronic mRNA	54

3.2 Quantitative Western Blot Analysis	56
3.3 Leaky Scanning Coordinates Expression Of The p10 And p17 ORFs, But Has Minor Effects On σ C Expression	58
3.4 Translation Of σ C Is IRES-Independent	61
3.5 Expression Of The σ C ORF Occurs In An eIF4G-Dependent Manner	64
3.6 Reinitiation Is Not Responsible For σ C Translation Initiation	67
3.7 S1 RNA Transfection Results In Inefficient Protein Expression For Detection By Western Blot	69
3.8 Development Of A Quantitative Reporter System For σ C Expression	71
3.9 Translation Of The Internal σ C Start Site Is Cap-Dependent	75
3.10 Optimization Of uAUGs In The S1 mRNA Has Differential Effects On Translation Of Downstream Open Reading Frames	78
3.11 Optimized uAUGs Exert Different Effects On Downstream Translation Depending On The Context Of The mRNA	81
3.12 Consistency Within The RL Assay System	83
3.13 Effect Of A Short 5' Leader And Stable Hairpin Structure On Downstream Initiation	83
3.14 The 3'- But Not The 5'-End Of The S1 Genome Segment Is Required For σ C Translation Initiation	88
3.15 The p17 Start Codon And The Presence Of Additional AUG Triplets Within The p17 Region Block Scanning Ribosomes	91
3.16 S1 Nucleotides 366-392 Facilitate Cap-Dependent Internal Initiation	97
3.17 An Optimized p17 Start Site Inhibits Leaky Scanning In A Heterologous mRNA	107
CHAPTER 4: Discussion	109
4.1 Overview	109
4.2 Translation Of The σ C ORF Occurs Efficiently From The Full-Length mRNA	109
4.3 Quantitative Analysis Of Western Blots, Luciferase Assays And Real-Time PCR	111

4.4 Expression Of The σ C ORF Is Not Mediated By Previously Described Alternate Translation Initiation Mechanisms	112
4.4.1 IRES-Independent	112
4.4.2 Reinitiation-Independent	113
4.4.3 Ribosome Shunting	114
4.4.4 Leaky Scanning	117
4.5 Ribosome Handoff	125
4.6 The Mechanism(s)	136
4.7 Conclusions And Perspectives	139
APPENDIX A: Letters Of Copyright Permission	141
APPENDIX B: Plasmid List	160
APPENDIX C: Primer List	163
REFERENCES	170

LIST OF FIGURES

Figure 1. Linear scanning model of translation initiation	3
Figure 2. Translation elongation and termination	13
Figure 3. Alternate mechanisms of translation initiation	16
Figure 4. Formation of a TURBS element	20
Figure 5. Avian reovirus morphology	35
Figure 6. Polycistronic ORF arrangement	39
Figure 7. Gene arrangement of the ARV S1 genome segment	41
Figure 8. Translation of the σ C ORF occurs from a full-length tricistronic mRNA with reasonable efficiency	55
Figure 9. Analysis of pixel densities obtained by quantitative Western blot analysis	57
Figure 10. Optimization of the p10 start site inhibits p17 production	59
Figure 11. Optimization of either the p10 or p17 start sites, in a plasmid based construct, exerts little effect on σ C expression	60
Figure 12. The poliovirus 2A protease is capable of enhancing IRES activity in a bicistronic construct	62
Figure 13. The ARV S1 genome segment does not display IRES activity	63
Figure 14. Expression of σ C is eIF4G-dependent	65
Figure 15. The 5'-proximal region of the S1 mRNA is required for downstream initiation when expressed from a DNA plasmid	68
Figure 16. A reinitiation-independent mechanism of translation is responsible for σ C expression	70
Figure 17. S1 RNA transfection results in inefficient protein expression for detection by western blot	72
Figure 18. Gene arrangement of the chimeric ARV σ C-RL genome segment	73
Figure 19. Translation of the plasmid-derived ARV σ C-RL chimera results in a similar σ C expression trend seen via Western blot analysis	74
Figure 20. RNA transfection of <i>in vitro</i> transcribed σ C-RL RNA is sensitive enough for quantitative analysis	76
Figure 21. Expression of the σ C-RL ORF is cap-dependent	77
Figure 22. <i>In vitro</i> transcribed ARV σ C-RL chimeric RNA results in a similar σ C expression trend seen via Western blot analysis	79

Figure 23. Addition of RNase A to RNA transfected cells is necessary for accurate qPCR determination	80
Figure 24. Optimization of a heterologous sequence results in substantial translation inhibition of the downstream ORF	82
Figure 25. Transfection of different RNA preparations on different days results in a range of RLUs but the same overall trend	84
Figure 26. Extension of the S1 5'-UTR does not promote further inhibition of σ C-RL expression	85
Figure 27. Expression of the σ C-RL ORF was not abolished by the presence of a stable hairpin structure	87
Figure 28. The 3'-terminal region of the S1 mRNA affects upstream reporter Production	89
Figure 29. Translation initiation at the σ C start codon is independent of the 5'-proximal 147 nucleotides	91
Figure 30. The p17 start site acts as an efficient barrier against scanning ribosomes	92
Figure 31. Insertion of exogenous sequence containing AUG codons impairs but does not abolish σ C-RL synthesis	94
Figure 32. Creation of additional AUG codons within the p17 reading frame significantly inhibit but do not eliminate σ C-RL production	96
Figure 33. Expression of the σ C-RL reporter ORF is independent of the translation termination location of the p17 protein	98
Figure 34. ARV S1 nucleotides 366-392 enhance downstream initiation	100
Figure 35. ARV S1 nucleotides 366-392 do not enhance leaky scanning	102
Figure 36. Expansion of Δ 366-751RL with exogenous sequence does not rescue reporter translation	104
Figure 37. Disruption of the putative 18S rRNA complementarity region inhibits reporter synthesis	105
Figure 38. Alignment of S1 cDNA sequences	106
Figure 39. The optimized p17 start site functions according to the leaky scanning model when present within a heterologous mRNA	108
Figure 40. Schematic representations of the ribosomal tethering and clustering mechanisms of translation initiation	132
Figure 41. Model of translation initiation on the tricistronic S1 mRNA	137

Abstract

The S1 genome segment of avian reovirus is functionally tricistronic, encoding three independent protein products (named p10, p17 and σ C) from three sequential, partially overlapping open reading frames (ORFs). The dogma of translation initiation, the cap-dependent scanning model, suggests that ribosomes would normally only translate the 5'-proximal ORF. Four alternate mechanisms of translation initiation could account for translation of the downstream σ C ORF; an IRES element, reinitiation, ribosome shunting, and leaky scanning. The objective of my doctoral research was to investigate the translation initiation mechanisms that are operative on the S1 mRNA.

Translation of the p10 and p17 ORFs was revealed to be coordinated via standard leaky scanning, while none of the known mechanisms of translation initiation could account for expression of the σ C ORF. Further investigation determined that two alternate cap-dependent mechanisms contribute to translation initiation at the σ C AUG codon. The first mechanism involves a modified version of enhanced leaky scanning. Although insertion of upstream elements known to impede scanning ribosomal subunits dramatically inhibited translation of the downstream ORF in the context of other mRNAs, the same elements only marginally reduced σ C translation. Specific features of the S1 mRNA therefore function to promote leaky scanning and translation of the σ C ORF. The inability to eliminate σ C expression beyond a threshold retention level of ~20-30%, despite the presence of eight upstream start codons that should eliminate leaky scanning, strongly suggests that ribosomes must also utilize a scanning-independent means to access the internal σ C start site. This mechanism for σ C translation initiation, which I termed ribosome handoff, allows ribosomes to bypass upstream elements, and requires a sequence-dependent translation enhancer element present within S1 nucleotides 366-392 that may function to mediate handoff via complementarity with 18S ribosomal RNA.

Translation initiation at the σ C start site is therefore made possible by two alternative mechanisms, enhanced leaky scanning and ribosome handoff from the 5'-cap. The novelty of these two mechanisms highlights the complexity of the translation initiation process and the potential heterogeneity of cellular ribosomes, which raises the possibility that internal initiation may be far more common than currently appreciated.

LIST OF ABBREVIATIONS USED

AFM	Atomic force microscopy
aa-tRNA	Aminoacyl-transfer RNA
ARV	Avian reovirus
ATP	Adenosine triphosphate
BiP	Immunoglobulin heavy-chain binding protein
BRV	Baboon reovirus
BTE	BYDV cap-independent translation element
BYDV	Barley yellow dwarf virus
CaMV	Cauliflower mosaic virus
CrPV	Cricket paralysis virus
dsRNA	Double stranded ribonucleic acid
<i>E. coli</i>	<i>Escherichia coli</i>
eEF	Eukaryotic elongation factor
EGFP	Enhanced green fluorescent protein
eIF	Eukaryotic initiation factor
EMCV	Encephalomyocarditis virus
FAST	Fusion associated small transmembrane
FCV	Feline calicivirus
GAP	GTPase activating protein
GCN2	General control non-derepressible 2
GEF	Guanine nucleotide exchange factor
GTP	Guanosine triphosphate
HAV	Hepatitis A virus
HCV	Hepatitis C virus
IGR	Intergenic region
IRES	Internal ribosome entry site
ITAF	IRES <i>trans</i> -acting factor
kb	Kilobase
LB	Luria-Bertani
miRNA	MicroRNA
mRNA	Messenger RNA
MRV	Mammalian reovirus
NBV	Nelson Bay reovirus
NLS	Nuclear localization signal
NSP3	Non-structural protein 3
ORF	Open reading frame
PABP	Poly(A) binding protein
PBS	Phosphate buffered saline
PCR	Polymerase chain reaction
PEI	Polyethylenimine
Pri-miRNA	Precursor microRNA
pgRNA	Pregenomic RNA

PTB	Polypyrimidine tract-binding protein
PTV-1	Porcine teschovirus-1
PVDF	Polyvinylidene difluoride
QM5	Quail fibroblast cell line
qRT-PCR	Quantitative reverse transcription polymerase chain reaction
RdRP	RNA-dependent RNA polymerase
RHDV	Rabbit hemorrhagic disease virus
RIPA	Radioimmunoprecipitation assay
RISC	RNA induced silencing complex
RISP	Re-initiation supporting protein
RLU	Relative light unit
RRM2	RNA recognition motif 2
rRNA	Ribosomal RNA
RRL	Rabbit reticulocyte lysate
RTBV	Rice tungro bacilliform virus
SD	Shine-Dalgarno
SDS-PAGE	Sodium dodecyl sulfate polyacrylamide gel electrophoresis
sORF	Short open reading frame
SSC	Sodium chloride sodium citrate
TAV	Transactivator protein
TURBS	Termination upstream ribosomal binding site
uAUG	Upstream AUG codon
Unr	Upstream of N-ras
uORF	Upstream open reading frame
UTR	Untranslated region
4E-BP	eIF4E-binding protein
4-thioU	4-thiouridine

ACKNOWLEDGEMENTS

I would like to start by thanking my supervisor, Dr Roy Duncan. Roy, I couldn't have asked for a better mentor. You provided the perfect balance of supervision and independence. Thank you for your confidence and for always going the extra mile. Only those who were fortunate enough to be in your lab know how lucky we were to have you as a supervisor. As Deniz would say, you put the "super" in supervisor!

I would also like to thank my committee members, Dr Christine Barnes, Dr. Melanie Dobson and Dr Patrick Lee. Thank you for your guidance and help over the years. You made my committee meetings something to be anticipated and always memorable. Chris, I would like to thank you personally for your technical assistance and for letting me use your lab for my radiation work. I know everyone in my lab also thanks you for that!

Roberto and Jing! What can I say but thank you! Roberto, thank you for being able to look at any old, broken, piece of equipment, and know just what to do to fix it. On more than one occasion I was able to come to you with something I had given up on and you somehow, were able to magically make it work again. Thank you for having the patience to going over math problems with me. You saved more than one of my experiments. Jing, I'm going to miss our early morning conversations. No matter what the topic, science, fashion, religion, cultural trends, I always enjoyed our talks. You are one of the most kind, generous and helpful people I have ever met. We all are immensely indebted to you.

Jayne and Deniz, I can't talk or think about one of you without thinking of the other. I still remember my first e-mail from you. We were arranging my arrival in Halifax for my interview and you guys said that one of you would be holding a sign with my name on it, while the other would be holding a sign with a different name as a negative control! I knew right then that we were going to get along. So Deniz, can you believe it? The newbie is finally finishing! I have to admit, despite what I may have said at the time, I did enjoy your teasing and my numerous nicknames.

Eileen and Chris, thank you both for always being the life of the party. Conversation was never boring when either of you were around. Chris, your commitment to science and your first love, hockey, is truly inspiring. Eileen, I will truly miss your creativity, your spirit, your ability to tell it like it is, and your Halloween costumes! Never before have I known someone who could not only come up with the best costume idea ever, but also pull it off, and with style!

Marta, to you, I pass on my title of senior grad student. Wear it, and wear it proud. Thank you for opening my eyes to the diversity in music and style that exists in the world. You are truly a unique individual, and I hope that one day you get to stop working on liposomes!

FuiBoon, it has been great getting to know you over the last couple of years. It was wonderful having company in the lab on weekends! I know that you will succeed at everything you try, but remember, don't work too hard!

Jolene and Tim, you both bring to the lab a wonderful new set of skills that will be most beneficial. I have confidence that between the two of you the Duncan lab will reach an equilibrium between organization and chaos.

Julie, it was so nice to be able to talk about Winnipeg locations and restaurants with you. Every time I go to Wasabi I'll be thinking of you. Although I know that I will never have half the talent you do, you have inspired me to take up knitting and cup-cake decorating. I will always remember your laugh.

Although we have not had much of a chance to get to know one another, Hiren, I do know that you are an excellent addition to the Duncan lab. I hope you enjoy your time as much as I have.

Laura, I don't even know where to start. I guess all I can say is thank you. Without you I never would have been able to finish this thesis, literally! Your friendship over the last couple of years has meant so much to me. Thank you for the countless rides to the airport, for picking up my mail on my extended trips out of town, for coming with me to Montreal and especially for letting me be a third wheel in your relationship. I hope that one day I can repay all the favours.

I would also like to thank my parents for their love and support. I would not be here today if it had not been for their encouragement and their confidence in my abilities.

And last, but definitely not least, I would like to thank my loving and every so supportive husband Patrick. Thank you for always being there for me, even when you lived 3500 Km away! Thank you for always understanding how much my work means to me and for always trying to make me laugh. My life would not be the same without you.
I LOVE YOU!!!

CHAPTER 1: Introduction

1.1 Overview

Translation control is an essential aspect of eukaryotic gene expression and as such, it is tightly regulated. The greatest level of regulation occurs at the initiation stage of translation. Recent developments indicate that even modest changes in the function or concentration of translation initiation factors have detrimental effects on protein expression that can ultimately lead to disease. Translation control occurs not only at the level of the factors involved in initiation, but also at the level of the messenger RNA (mRNA) itself. For instance, the presence of upstream open reading frames (ORFs) can help regulate the expression of the functional downstream ORF on the mRNA. Alternate mechanisms of translation initiation can also result in more than one polypeptide being translated from a single species of mRNA, which has major implications on understanding the complexity of cellular proteomes. Despite the wealth of knowledge on the mechanisms of translation control, we still do not have a complete picture of all the factors at play. Appreciating the complexity of the translation initiation process therefore requires continuing analysis of novel translation initiation mechanisms.

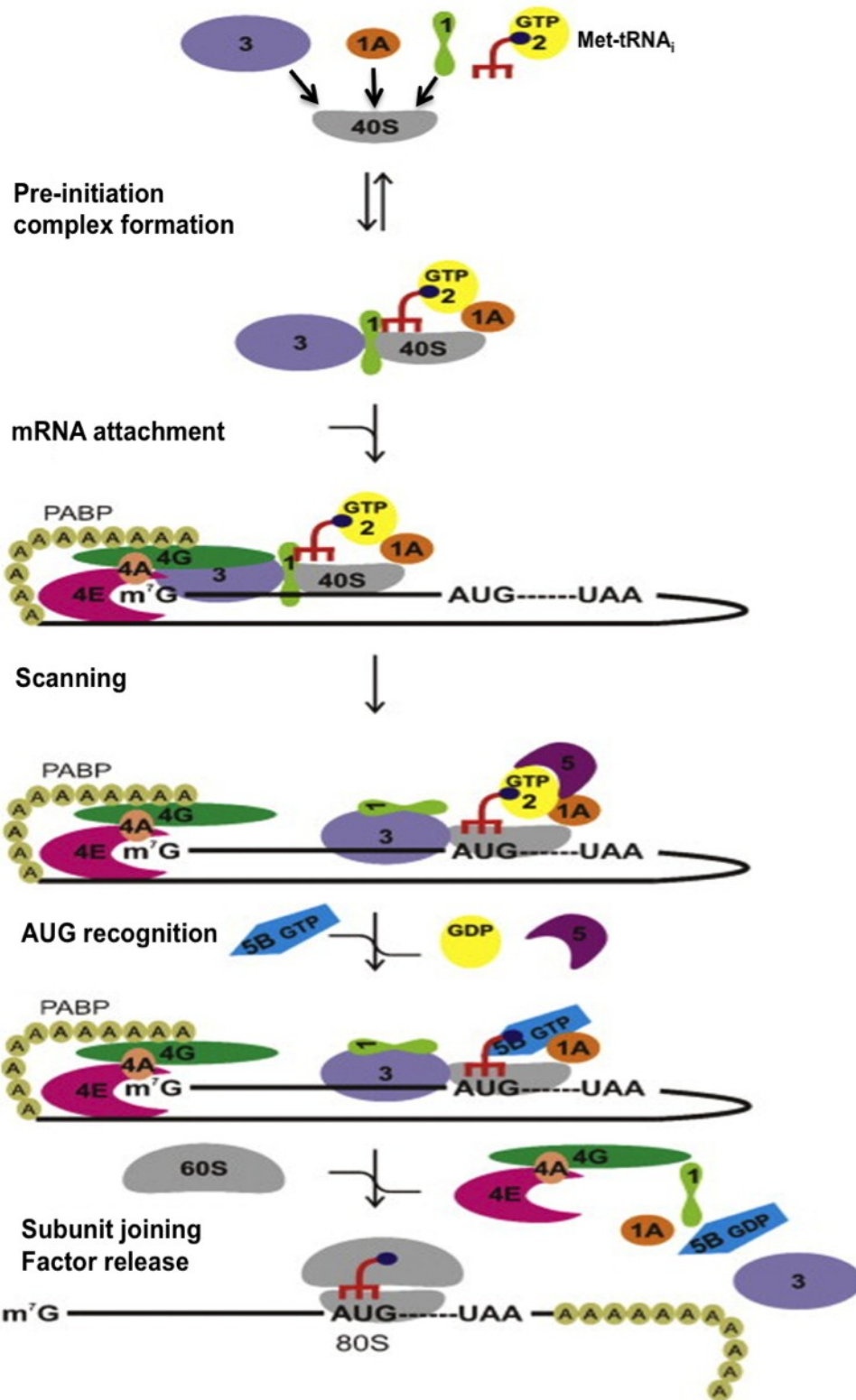
The most common method of eukaryotic mRNA translation initiation involves a cap-dependent scanning mechanism of a monocistronic strand of mRNA. Not all mRNAs adhere to the scanning-dependent, monocistronic rule however. It is through the study of such exceptions that a number of alternate translation initiation mechanisms have been discovered. My PhD research has focused on the molecular analysis of translation initiation on the tricistronic avian reovirus (ARV) S1 mRNA, an exception to the monocistronic rule. The ARV S1 mRNA is a rarity in the eukaryotic world and pushes the limit of the coding capacity of a eukaryotic mRNA, encoding three different proteins from three sequential, partially overlapping ORFs. The third ORF on the functionally tricistronic mRNA, which encodes the structural protein σ C, initiates 630 nucleotides distal from the 5'-cap and downstream of two functional ORFs encoding the p10 and p17 proteins. The main objective of my PhD research was to determine how ribosomes access the internal σ C start site. Before describing the system under investigation, I will first provide an overview of translation initiation and the features of the various mechanisms used to regulate this important process.

1.2 The Scanning Model Of Translation Initiation

Translation control is an important aspect of eukaryotic gene expression, and as such, is highly regulated. The most tightly regulated step is the initiation stage of translation. The scanning mechanism of translation accounts for most initiation events in eukaryotic cells (Kozak, 2002). The scanning model postulates that the small (40S) ribosomal subunit, equipped with eukaryotic initiation factors (eIFs) 1, 1A, 3 and 5, binds a ternary complex composed of the specific initiator tRNA, Met-tRNA_i, and eIF2 coupled to GTP, to form the 43S pre-initiation complex (Figure 1; Gebauer and Hentze, 2004). Most eukaryotic mRNAs possess a 5'-cap (m⁷GpppN, where N is any nucleotide and m is a methyl group) structure (Furuichi et al., 1975; Muthukrishnan et al., 1975), which is bound by the cap-binding complex eIF4F. The ternary eIF4F complex is composed of eIF4E, an initiation factor with specific affinity for the methylated 5'-cap, eIF4A, a DEAD family helicase thought to help unwind the mRNA in an ATP-dependent manner, and finally eIF4G, a large modular scaffolding protein that is capable of interacting directly with cap-bound eIF4E, eIF4A, and eIF3. Through the eIF3-eIF4G interaction, eIF4G is also capable of indirect interaction with the 40S ribosomal subunit. The poly(A) binding protein (PABP) is thought to stimulate translation by promoting mRNA circularization through simultaneous interactions with eIF4G and the 3' poly(A) tail (Imataka, Gradi, and Sonenberg, 1998; Tarun and Sachs, 1996). The interaction of eIF3 and eIF4E with eIF4G allows the 43S pre-initiation complex to load onto the mRNA, thus forming a 48S initiation complex that is now competent to start scanning the mRNA in a 5' to 3' direction until it encounters the first AUG start codon. The eIF3 subunit j, one of 13 subunits making up eIF3, is in part responsible for regulating 40S binding to mRNA (Fraser et al., 2007). eIF3j is located near the 40S aminoacyl site (A site) and mRNA entry channel, and interacts with eIF1A, also bound near the A-site, reducing the 40S subunit's affinity for mRNA until the ternary complex has bound the 40S subunit.

It has been reported that the 40S subunit can scan distances as great as 1700 nucleotides *in vivo* without losing significant initiation efficiency (Berthelot et al., 2004). Together, eIF1, bound to the 40S subunit near the peptidyl site (P site), and eIF1A, bound near the A-site, promote scanning by maintaining the 40S subunit in an open conformation in the mRNA binding cleft (Passmore et al., 2007). mRNA scanning is also

Figure 1. Linear scanning model of translation initiation. **1.** Initiator tRNA (Met-tRNA_i), in a ternary complex with eIF2 and GTP, is delivered to the 40S ribosomal subunit, which is already bound to eIF1, eIF1A and eIF3. **2.** The 43S pre-initiation complex binds the 5'-cap (m⁷G) structure with the aid of poly(A)-binding protein (PABP) bound to the 3' poly(A) tail and eIF4F, which consists of the cap-binding protein eIF4E, an RNA helicase, eIF4A, and a large modular scaffolding protein, eIF4G. **3.** The 48S complex is capable of scanning the mRNA. **4.** Recognition of the start codon commits the complex to initiate translation by hydrolyzing GTP and releasing inorganic phosphate from eIF2. In addition, eIF1, eIF2 and eIF5 are displaced and eIF5B-GTP binds the 40S subunit. **5.** The resulting complex binds the 60S subunit and undergoes ribosome-induced GTP hydrolysis by eIF5B, stimulating the dissociation of the remaining initiation factors and 80S ribosome formation. Figure adapted from Rodnina and Wintermeyer (2009) *Curr Opin Cell Biol.* **21**(3), 435-43.



aided by the eIF4G/eIF4A complex bound to the exit site (E site) of the 40S subunit, which implies that eIF4A “pulls” mRNA through the mRNA-binding cleft, rather than unwinding it at the leading edge of the 40S subunit, providing the 5′ to 3′ directionality observed in ribosome scanning (Siridechadilok et al., 2005). Once an AUG triplet reaches the P-site, it is recognized as the start codon by base-pairing with the CAU anticodon in Met-tRNA_i (Cigan, Feng, and Donahue, 1988). AUG recognition may result in either release or displacement of eIF1 from its original location near the P-site. At this point the 40S subunit stops scanning and eIF5, a GTPase activating protein (GAP), induces the hydrolysis of GTP bound to eIF2 and the subsequent removal of eIF2-GDP from the 48S initiation complex (Das, Ghosh, and Maitra, 2001; Das and Maitra, 2001). This hydrolysis event culminates in 60S ribosomal subunit joining and displacement of initiation factors from the 40S subunit, mediated by eIF5B, a ribosome-dependent GTPase (Pestova et al., 2000), ultimately forming the 80S ribosome.

1.3 Factors Affecting AUG Recognition And Ribosome Scanning

1.3.1 Nucleotide Context

In addition to the important roles of the eukaryotic initiation factors in start site selection, in particular eIF1 and eIF1A (Mitchell and Lorsch, 2008; Pestova and Kolupaeva, 2002), the efficiency with which ribosomes recognize the first AUG codon is influenced by the nucleotide context surrounding the start codon. The sequence cc(A/G)cc**AUGG** (where the initiating AUG is shown in bold), referred to as the Kozak consensus sequence, is considered optimal for eukaryotic (at least in metazoans) ribosome recognition (Kozak, 1986b; Kozak, 1987a; Kozak, 1987b). In plants and animals, a purine at position -3 (preferentially an A), with the adenine of the start codon considered +1, is the most highly conserved and functionally important flanking nucleotide (Kozak, 1984a; Kozak, 1987a). The G at position +4 is also important, especially when position -3 is anything but an A. The initiation efficiency of a start codon with a “poor context” can be improved through the insertion of a hairpin structure 12-15 nucleotides downstream of the start site (Kozak, 1990; Kozak, 1991b). The presence of a stable secondary structure at this position stalls the ribosomal subunit momentarily with its AUG-recognition center right over the AUG codon, thereby facilitating initiation. In

addition, the statistically significant conservation between orthologous mammalian mRNAs in the 30 nucleotides upstream of the initiation site suggests that there may be additional determinants of start site selection yet to be discovered (Shabalina et al., 2004).

1.3.2 Leader Length

The length of the 5'-untranslated region (UTR) also affects translation initiation efficiency. A 5' leader of less than 8-12 nucleotides results in leaky scanning (mentioned below), while lengthening the leader beyond this progressively increases initiation efficiency (Kozak, 1991a; Pestova and Kolupaeva, 2002). This limit on leader length likely stems from the fact that the 48S initiation complex bound to a start codon occupies approximately 12 nucleotides upstream and 15 nucleotides downstream of the AUG codon (Lazarowitz and Robertson, 1977), suggesting that an extremely short leader would lack potential stabilizing interactions between the mRNA and the initiation complex, allowing the complex to scan past the first AUG start codon.

1.3.3 Non-AUG Initiation

Initiation of translation can also occur at non-AUG codons (Kozak, 2002; Peabody, 1989). In general, non-AUG codons tend to differ from the canonical start codon by only one nucleotide and are situated in an optimal Kozak consensus sequence. Mechanistically, many of the initiation factors play a role in monitoring the codon/anti-codon interaction. For example, mutations in any of the three subunits of eIF2 or in eIF5 that increase the rate of GTP hydrolysis and subsequent eIF2-GDP dissociation from the 43S pre-initiation complex allow significant recognition of non-AUG codons (Huang et al., 1997). These results imply that GTP hydrolysis by the ternary complex is normally suppressed at non-AUG triplets during scanning. Also, omission of eIF1 from 43S complexes results in scanning-competent complexes, but these complexes are no longer able to discriminate between cognate and noncognate initiation codons, nor are they able to sense the context surrounding these codons, thus enabling initiation at non-AUG triplets (Pestova and Kolupaeva, 2002). The ability to initiate translation at these rare non-AUG codons may confer some advantages to the cell. First, the low level of initiation that occurs at these sites allows for the modulation of expression for a protein

that is normally only required/tolerated in low concentrations. Second, the presence of a non-AUG initiation codon upstream of the main start site allows for the expression of more than one protein from a single mRNA.

1.3.4 *Cis-* And *Trans-*Acting Factors

Scanning can be strongly affected by *cis-* and *trans-*acting factors that interfere with ribosomal subunit loading or block a scanning ribosome. *Cis* factors include strong secondary structures ($\Delta G \sim -60$ kcal/mol for complete inhibition) present at the extreme 5'-end or within the 5'-UTR that impede 40S subunit loading (Byrd, Zamora, and Lloyd, 2005) or block scanning subunits on the 5' side of the secondary structure (Kozak, 1986a; Kozak, 1989a; Pelletier and Sonenberg, 1985). Also, multiple upstream start codons (uAUGs) can decrease initiation efficiency at the main ORF (Kozak, 1989b; Kozak, 1992). *Trans-*acting factors tend to be mRNA specific, and as such, often result in translational regulation during particular cellular events and/or locations. *Trans* factors include RNA-binding proteins that can also block ribosome loading or scanning (Paraskeva et al., 1999; Stripecke et al., 1994), and miRNAs (discussed below).

1.4 Translational Enhancement Via mRNA Circularization

1.4.1 Poly(A) Binding Protein

The 3'-UTR and the poly(A) tail present on most eukaryotic mRNAs play important roles in translation initiation. A cellular factor, PABP, is able to interact simultaneously with the 3' poly(A) tail through its RNA recognition motif 2 (RRM2) and with eIF4G, thus bringing about the circularization of the mRNA (Imataka, Gradi, and Sonenberg, 1998; Tarun and Sachs, 1996). Interaction between the cap and poly(A) tail synergistically enhances translation, most likely resulting from increased eIF4E affinity for the 5' cap (Borman, Michel, and Kean, 2000; Gallie, 1991; von Der Haar, Ball, and McCarthy, 2000), and stimulation of 60S ribosomal subunit joining (Kahvejian et al., 2005). As mentioned above, eIF5 and eIF5B are thought to bring about 60S subunit joining. In yeast, two putative RNA helicases are thought to inhibit the function of these initiation factors, and therefore inhibit 60S subunit joining. The yeast equivalent of PABP, Pab1p, is thought to bring about 60S subunit joining by inhibiting the action of

these putative RNA helicases, thus derepressing the inhibition of eIF5B (Searfoss, Dever, and Wickner, 2001). It is still unknown whether PABP functions in a similar manner in multi-cellular eukaryotes.

In addition to its role in mRNA circularization, yeast Pab1p is capable of stimulating translation of capped, poly(A) tail-deficient mRNAs by acting in *trans* (Otero, Ashe, and Sachs, 1999). The Pab1p RRM2 is required for this *trans*-activation, although the eIF4G-Pab1p interaction induced by RRM2 is not necessary, indicating that the RRM2 domain may interact with an as yet unidentified component of the pre-initiation complex.

1.4.2 Translation Enhancer Elements Located In The 3'-UTR

Circularization of the mRNA is so important for efficient translation that viral mRNAs that lack a poly(A) tail have evolved various means to bring about this circularization. For example, the 3' UTR of the Dengue virus mRNA lacks a poly(A) tail but is highly structured, possessing a terminal stem-loop structure preceded by two dumbbell-like structures. Translation enhancement of the Dengue virus mRNA is postulated to involve PABP interaction with the A-rich sequence flanking the dumbbell structures in an eIF4G-dependent manner (Polacek, Friebe, and Harris, 2009). Similarly, rotavirus, a member of the *Reoviridae* family, has also evolved a unique mechanism to bring about the circularization of their capped but non-polyadenylated mRNAs (Piron et al., 1998; Poncet, Aponte, and Cohen, 1993). The viral non-structural protein 3 (NSP3) simultaneously binds the sequence UGACC, present at the extreme 3'-terminus of all 11 mRNA segments, and eIF4G, bringing about the circularization of the mRNA. Not only does the NSP3/eIF4G interaction cause circularization, it also evicts PABP from eIF4G, ultimately resulting in the reduction of host protein synthesis (Piron et al., 1998). However, recent evidence suggests that NSP3 binding to the 3'-terminus may not be necessary for viral translation, but may be required to prevent these transcripts from being used in viral replication (Montero, Arias, and Lopez, 2006). The latter example highlights some of the unique features associated with macromolecular synthesis mediated by RNA viruses, where plus-strand RNAs can serve as templates for either transcription or translation, both of which need to occur in the cytoplasm. Furthermore, in

plus strand RNA viruses, the same RNA serves as the genome and must be packaged inside progeny virions.

An interesting mechanism of 3'-end induced translational enhancement is seen in many plant viruses that encode uncapped, non-polyadenylated mRNAs. The best-studied example of this cap-independent 3'-end mediated mechanism of translation initiation occurs in the Barley yellow dwarf virus (BYDV; Guo, Allen, and Miller, 2001; Rakotondrafara et al., 2006; Wang, Browning, and Miller, 1997). The BYDV genome is composed of a single strand of positive sense RNA that is approximately 5.7-kb in length and contains a complex 3'-UTR of 869 nucleotides (Miller, Waterhouse, and Gerlach, 1988). Within this extensive 3'-UTR lies a translational enhancer region, a stem-loop called the BYDV cap-independent translation element (BTE), which is responsible for mediating cap-independent translation initiation at the 5'-proximal AUG through its interaction with a complementary stem-loop present within the 5'-UTR (Rakotondrafara et al., 2006). It was recently demonstrated that the 3' BTE is capable of binding eIF4F, more specifically, eIF4G, with high affinity (Treder et al., 2008). The current model of translation initiation on the BYDV mRNA posits that the 3' BTE recruits eIF4F, and possibly other proteins, and delivers them to the 5'-UTR through long-distance base-pairing of the 5' and 3' "kissing loops". Once the eIF4F complex is near the 5'-end, the 40S subunit is recruited and competent to scan the mRNA in the traditional fashion until it encounters the first AUG codon (Guo, Allen, and Miller, 2001; Rakotondrafara et al., 2006; Treder et al., 2008).

The fact that so many viral mRNAs have evolved to be able to form a closed loop, regardless of their terminal structures, highlights the importance of the 3'-termini and mRNA circularization in translation initiation. Continued examination of mRNAs lacking a poly(A) tail may result in the discovery of additional mechanisms that promote mRNA circularization.

1.5 Global And mRNA-Specific Control Of Translation Initiation

Control of translation initiation can occur on a global or mRNA-specific level, with mRNA-specific control usually exerted through regulatory elements in either the 5'- or 3'-UTR, while global control results from changes in the state of phosphorylation of the

translation initiation factors or their regulators. An example of global control occurs with eIF2. Heterotrimeric eIF2 is covalently modified by phosphorylation in a reversible manner on Ser-51 of its α subunit in response to environmental and pathological stresses (Gebauer and Hentze, 2004). Four different eIF2 α kinases are found in mammalian cells: PKR (protein kinase R), induced by double-stranded RNA in virus infection; PERK (protein kinase R-like endoplasmic reticulum kinase), induced by unfolded proteins in the ER; HRI (heme-regulated inhibitor), induced by heme deprivation; GCN2 (general control non-derepressible 2), induced by amino acid starvation (reviewed in, Ron and Harding, 2007). Phosphorylation of eIF2 α makes it a competitive inhibitor of eIF2B, a guanine nucleotide exchange factor (GEF), ultimately blocking the exchange of GDP for GTP during the recycling of the eIF2 complex. This leads to inhibition of functional ternary complex formation and a global shut down of translation. Paradoxically, eIF2 α phosphorylation induces expression of a gene, *GCN4*, encoding a transcription factor by overcoming the inhibitory effects of four upstream ORFs (uORFs) on reinitiation at the *GCN4* ORF (see section on Reinitiation). A similar up-regulation in translation of the mammalian transcription factor ATF4 is seen upon eIF2 α phosphorylation (Vattem and Wek, 2004).

eIF4F complex formation and activity is also important in global translation control. A family of translation repressor proteins, eIF4E-binding proteins (4E-BPs), are key modulators of eIF4F formation. The cap-binding factor eIF4E, normally present in limited concentrations (Duncan, Milburn, and Hershey, 1987), is bound by the repressor protein 4E-BP in a phosphorylation-dependent manner, inhibiting the ability of eIF4E to interact with eIF4G (Haghighat et al., 1995; Pause et al., 1994). Phosphorylation of 4E-BP on specific serine and threonine residues by the downstream effectors of the phosphoinositide 3-kinase pathway in response to mitogens, hormones, and growth factors, reduces the affinity of 4E-BP for eIF4E, ultimately restoring cap-dependent translation (Gingras et al., 1998; Lin et al., 1994; Mendez et al., 1996). However, there is some evidence that additional *trans*-acting factors may be required to promote eIF4F complex assembly in growth-arrested cells other than the simple release of eIF4E from 4E-BP (Walsh and Mohr, 2006). The level of eIF4E phosphorylation may also mediate translation regulation. Depending on the virus, eIF4E phosphorylation can either be

beneficial (HSV-1; Walsh and Mohr, 2004) or inhibitory (adenovirus; Cuesta, Xi, and Schneider, 2000), to productive viral infection. eIF4E is partially phosphorylated in exponentially growing cells and the extent of phosphorylation is reduced in response to heat shock (Duncan, Milburn, and Hershey, 1987), although the exact role of eIF4E phosphorylation in protein synthesis, if any, has not been fully resolved.

Translation of specific endogenous mRNAs can also be controlled through small noncoding RNA molecules, approximately 20 nucleotides in length, called microRNAs (miRNAs; for review, see Wehner and Sarnow, 2007). Transcription of miRNA genes by RNA polymerase II results in the production of a precursor miRNA (pri-miRNA) characterized by a large hairpin structure that contains the mature miRNA (Cai, Hagedorn, and Cullen, 2004). The pri-miRNA is processed in the nucleus by the ribonuclease III endonuclease Drosha into an imperfect hairpin called pre-miRNA that is approximately 60-80 nucleotides in length. The pre-miRNA is then transported out of the nucleus by an exportin 5/RanGTP complex (Bohnsack, Czaplinski, and Gorlich, 2004; Lund et al., 2004) into the cytoplasm where it again undergoes cleavage, this time by the enzyme Dicer, into an ~20 nucleotide RNA duplex with a 3' two-nucleotide overhang. The duplex is incorporated into a multi-protein complex termed RISC (RNA-induced silencing complex), and is unwound starting at its most thermodynamically unstable end. The strand that has its 5' end at the less stable end of the duplex (the guide strand) remains associated with the protein complex and guides it to a target mRNA with miRNA complementarity (Sullivan and Ganem, 2005; Wehner and Sarnow, 2007). The first miRNA discovered, *lin-4* found in *Caenorhabditis elegans* (*C. elegans*), acts on its target, *lin-14*, by binding the 3'-UTR of *lin-14* and blocking *lin-14* protein synthesis after the initiation of translation (Ambros, 1989; Olsen and Ambros, 1999; Wightman et al., 1991; Wightman, Ha, and Ruvkun, 1993). Most miRNAs function by down-regulating the expression of their target mRNA either by promoting degradation of the mRNA (Wu, Fan, and Belasco, 2006) or translation inhibition (Humphreys et al., 2005; Pillai et al., 2005). More recently, exceptions to this rule have been discovered. For example, the liver-specific *miR-122* mediates an up-regulation in hepatitis C virus (HCV) RNA abundance (Jopling et al., 2005) and translation rate (Henke et al., 2008). There is a functional basis for targeting miRNAs to the non-coding regions of an mRNA, usually

the 3'-UTR, as indicated by the modification of a target gene so that the ORF extends into the miRNA target sequence (Gu et al., 2009). Such a modification impedes miRNA-programmed RISC association with the target gene and ultimately results in a loss of translation inhibition.

In summary, global control of translation occurs in response to cell stress or growth stimuli and is affected by the availability of initiation factors, whereas mRNA-specific translation regulation occurs in response to *cis*-acting sequences (uORFs, secondary structure, miRNA targeting elements) normally found within their non-coding regions.

1.6 Translation Elongation, Termination And Ribosome Recycling

Following the initiation stage of translation, which is the rate-limiting event in protein translation, protein synthesis continues with translation elongation, termination and ribosome recycling. Elongation involves the stepwise attachment of amino acids to the growing peptide chain (Figure 2A). During elongation, a ternary complex composed of aminoacyl-tRNA (aa-tRNA), GTP and the elongation factor eEF1, composed of two subunits, eEF1A, a GTPase, and eEF1B, a GEF, is delivered to the A-site of the 80S ribosome. Once bound to the A-site, the ternary complex can interact with the peptidyl-tRNA, triggering the elongation of the nascent peptide chain by one amino acid. Following the peptidyl-transfer reaction, the ribosomal subunits undergo a spontaneous and reversible ratchet-like relative rotation that places the 3' ends of the P- and A-site tRNAs in the E- and P-sites, respectively. This "hybrid state" is stabilized by elongation factor eEF2, which utilizes the energy of GTP hydrolysis to finalize the translocation of peptidyl-tRNA and deacylated tRNA into the P and E sites, respectively. eEF2 is thought to provide the directionality of tRNA and mRNA movement through the ribosome (Rodnina and Wintermeyer, 2009; Zaher and Green, 2009). When a termination codon is present in the decoding center, a high affinity eRF1/eRF3 complex (release factors) binds to the A-site through the ability of eRF1 to recognize all three termination codons (Figure 2B). GTP hydrolysis by eRF3 facilitates a large conformation change that may place eRF1 in the peptidyl transferase center, thus stimulating peptide hydrolysis and release (Rodnina and Wintermeyer, 2009).

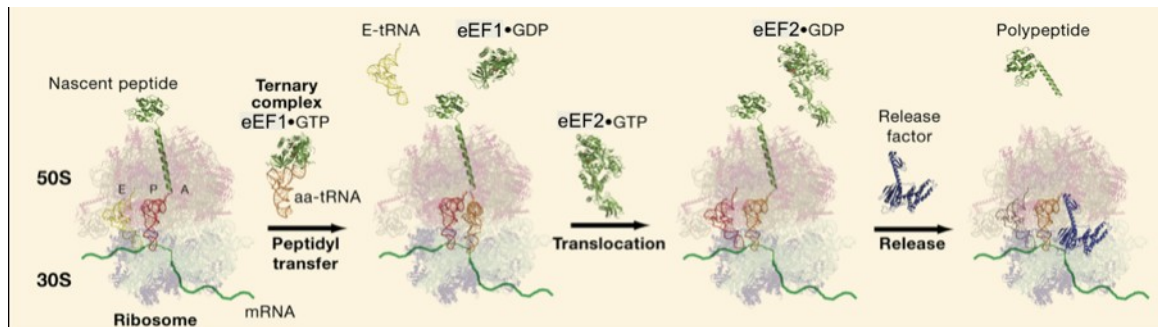


Figure 2. Translation elongation and termination. During the elongation cycle, peptidyl transfer takes place in which a ternary complex composed of the elongation factor eEF1, aminoacyl-tRNA (aa-tRNA), and GTP is deposited into the aminoacyl (A) site and reacts with the peptidyl-tRNA, elongating the nascent peptide by one amino acid. Subsequent translocation of the mRNA in the ribosome is mediated by elongation factor eEF2, which couples the energy of GTP hydrolysis to directional movement of the mRNA-tRNA complex. As a result, the peptidyl-tRNA and the deacylated tRNA move from the A and peptidyl (P) sites into the P and exit (E) sites, respectively. Termination of protein synthesis occurs when a stop codon enters the A-site. Stop codons are recognized by release factors, which trigger a hydrolytic reaction that results in the release of the growing polypeptide chain from the tRNA. Figure adapted from Zaher and Green *Cell* (2009).

The factors involved in eukaryotic ribosome recycling have only recently been discovered (Pisarev, Hellen, and Pestova, 2007). Post-termination complexes consist of deacylated tRNA present in the P-site of the 80S ribosome, still bound to mRNA. The initiation factor eIF3 catalyzes the dissociation of the 60S subunit from the 40S-tRNA-mRNA complex. This action is enhanced by additional initiation factors, namely eIF1, eIF1A and the loosely associated eIF3j subunit. Release of tRNA is mediated by eIF1, while eIF3j ensures subsequent mRNA dissociation. Pisarev and co-workers (2007) hypothesize that the translational enhancement stimulated by PABP through mRNA circularization most likely results from the interaction of eIF3 on post-termination 40S subunits with eIF4G bound to the 5' end.

1.7 Alternate Mechanisms Of Translation Initiation

Although the scanning model of translation initiation accounts for the majority of protein expression, a significant portion of eukaryotic mRNAs (approximately 10%) may not utilize 5' cap-dependent linear scanning to initiate translation (Futterer, Kiss-Laszlo, and Hohn, 1993; Hinnebusch, 1997; Morris and Geballe, 2000; Pelletier and Sonenberg, 1988; Yueh and Schneider, 1996). These mRNAs tend to contain long, structured, 5'-UTRs that may also include one or more uAUGs, and include mRNAs that encode growth-related factors, tumor suppressors, transcription factors, and proto-oncogenes (Ryabova, Pooggin, and Hohn, 2002). Viral 5'-UTRs are also often highly structured and complex. Moreover, up to 40% of eukaryotic mRNAs may contain uAUGs in their 5'-leaders, and the number of uAUGs correlates with the relative length of the leader suggesting there is no negative selection against the presence of these AUGs (Chappell et al., 2006, and references therein). Such UTRs pose a challenge but alternative mechanisms have evolved. It has been through the study of viral mRNAs that many of the alternative mechanisms of translation initiation were discovered.

1.7.1 Leaky Scanning

Leaky scanning is a modified form of the scanning model of translation initiation and can occur when an mRNA includes one or more uAUGs (Figure 3A). Leaky scanning occurs in a cap-dependent manner when the 40S ribosomal subunit “leaks” or

scans past the 5'-proximal start codon due to its close proximity (8-12 nucleotides) to the 5'-cap (Kozak, 1991a; Sedman, Gelembiuk, and Mertz, 1990), when the start codon is a non-AUG codon in an optimal context (with ccA/GccAUGG being optimal) or an AUG codon in a suboptimal context (Kozak, 1989b). The presence of a stable hairpin structure 12-15 nucleotides downstream of the potential start site can cause the 40S subunit to pause scanning, allowing the subunit sufficient time to recognize a suboptimal start codon (Kozak, 1990; Kozak, 1991b). A modified version of leaky scanning can also occur when two AUG codons are positioned very close together (Matsuda and Dreher, 2006; Williams and Lamb, 1989). Leaky scanning can result in the production of two or more proteins with a common C-terminus when the start sites are in the same reading frame, or two totally different proteins when they are in different reading frames.

As mentioned previously, the proper functioning of the initiation factor eIF1 plays a major role in start site selection (Pestova and Kolupaeva, 2002). In addition to its role in scanning processivity by maintaining the 40S subunit in an open conformation, eIF1 also plays a role in leaky scanning by rejecting codon-anticodon mismatches in the P-site, and by eliminating 48S assembly at AUG triplets in a suboptimal sequence context and at AUGs located within 8-12 nucleotides from the 5'-cap structure.

1.7.2 Reinitiation

Another means by which a ribosome is capable of initiating translation at an internal start site is through the cap-dependent mechanism of translation reinitiation (Figure 3B). Upon translation termination of an uORF, the 40S ribosomal subunit is able to remain associated with the mRNA and resume scanning. The efficiency with which the 40S subunit can reinitiate translation at a downstream start codon depends on *cis*-elements and *trans*-acting factors (reviewed in, Morris and Geballe, 2000). The fundamental requirement for reinitiation to occur is the ability of the post-termination 40S subunit to acquire *de novo* the ternary complex needed to recognize the next AUG start site. For this to happen two main rules must be followed. First, the uORF being translated must be short, usually no greater than 30 codons, and second, the intergenic region between ORFs must be a minimum distance of approximately 80 nucleotides (Futterer and Hohn, 1992; Kozak, 1987c; Luukkonen, Tan, and Schwartz, 1995).

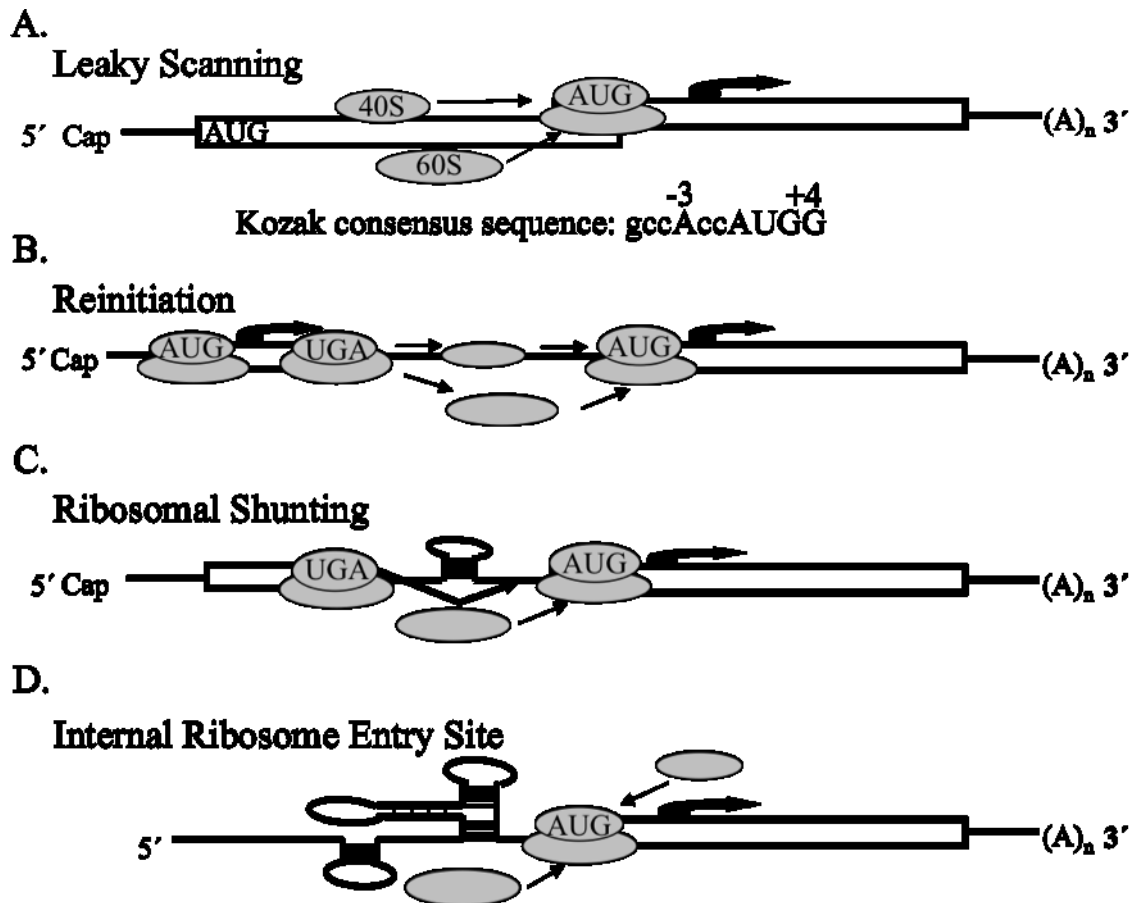


Figure 3. Alternate mechanisms of translation initiation. Diagrams of the structural features of mRNA, represented by the black line, with or without the m⁷G cap (Cap), along with ORFs denoted by the open rectangles and the two ribosomal subunits, 40S and 60S. Most eukaryotic mRNAs also possess a poly(A) tail at their 3'-end (A)_n. **A. Leaky Scanning** – The 40S ribosomal subunit binds the 5'-cap and leaks past the 5'-proximal AUG and initiates at the next proximal start site in a favourable context. **B. Reinitiation** – Upon termination of a short uORF initiated in the normal cap-dependent fashion, the 40S subunit remains bound to the mRNA and proceeds to scan the mRNA until it encounters the next proximal AUG codon where it then reacquires the 60S subunit and initiates another round of translation. **C. Ribosomal shunting** – As in reinitiation, a short uORF is translated in a cap-dependent manner. Upon termination the 40S subunit encounters mRNA secondary structure at the base of which is a shunt donor and acceptor site. The 40S subunit is translocated from the shunt donor to the shunt acceptor site where it then scans the mRNA and initiates translation at the next proximal start site. **D. Internal Ribosome Entry Site** – The presence of extensive secondary structure, normally within the 5'-UTR, enables the 40S subunit to bind the mRNA at an internal position without the need for the 5'-cap structure. The 40S subunit is then capable of scanning the mRNA in search of an AUG codon or it is placed directly at the start site where it initiates translation.

Translating ribosomes appear to lose initiation factors as they synthesize the polypeptide, and as such, need to reacquire said factors before another round of initiation can commence. As the length of the uORF increases, the frequency of reinitiation decreases suggesting that translation of a short ORF does not result in complete initiation factor disassociation from the 40S subunit and thus can be used in a subsequent round of initiation (Kozak, 1987c). It was recently demonstrated that eIF3h is responsible for maintaining reinitiation competency, possibly by facilitating post-initiation retention of eIF3 on the ribosome (Roy et al., 2010). The requirement for a minimum intercistronic length most likely represents the minimum time necessary for the scanning subunit to reacquire the ternary complex and other required initiation factors. Other factors can also influence the scanning of a post-termination 40S subunit, for example, the sequence surrounding the uORF stop codon (Miller and Hinnebusch, 1989), and the structure of the uORF peptide (Hill and Morris, 1993; Lovett and Rogers, 1996). The last codon plus ten base-pairs immediately adjacent to the termination codon of uORF4 on the *GCN4* mRNA are sufficient to convert a normally weak barrier to scanning ribosomes (uORF1) into an efficient translation barrier. This result suggests that the characteristics of uORF4 translation termination are largely responsible for uORF4 preventing translation initiation at the *GCN4* AUG codon (Miller and Hinnebusch, 1989). The peptide encoded by certain uORFs can interfere with the function(s) of the translating ribosome and are thus considered *cis*-acting negative regulators of translation. These peptides tend to exert their function, for example attenuating translation or preventing ribosome release from the mRNA at the uORF stop codon, before fully emerging from the ribosome (Lovett and Rogers, 1996).

The best documented case, and initial observation, of reinitiation occurs in the yeast *GCN4* mRNA (reviewed in, Hinnebusch, 2005). Although translation of the *GCN4* mRNA occurs constitutively, it is inhibited under nutrient-rich conditions by a process that is dependent on the presence of four short (two or three codons) uORFs (uORF1-4). In nutrient-rich cells, the ribosome encounters and translates uORF1 according to the scanning model of initiation. Upon termination of uORF1 translation, the 40S subunit remains bound to the mRNA and is capable of recruiting a ternary complex *de novo* and reinitiating at uORFs2-4. In nutrient-deprived cells however, the kinase Gcn2p

phosphorylates eIF2 α (Dever et al., 1992) resulting in a failure to produce ternary complex. The depletion in ternary complex concentration slows the rate of 40S subunit and ternary complex interaction, allowing approximately 50% of rescanning ribosomes to bypass uORF4 before acquiring the ternary complex and thus reinitiating at the main *GCN4* ORF.

An interesting, but poorly understood aspect of *GCN4* translation is the disparate roles uORF1 and uORF4 play in reinitiation. Mutational analysis has revealed that AU-rich sequences in the triplet preceding the termination codon and in sequences flanking the uORF1 stop codon are beneficial for reinitiation, while GC-rich sequences surrounding the uORF4 termination codon actually inhibit reinitiation (Grant and Hinnebusch, 1994). Additionally, sequences 5' to uORF1 are also required for reinitiation (Grant, Miller, and Hinnebusch, 1995). Interestingly, it was recently demonstrated that eIF3 remains associated with the 40S subunit throughout uORF1 translation, and upon termination, the N-terminal domain of eIF3a interacts with sequences 5' of uORF1 to promote resumption of scanning for reinitiation (Szamecz et al., 2008).

Ribosomes may also reinitiate translation upon termination of a long ORF, and the details of this unique reinitiation mechanism are starting to come to light (Luttermann and Meyers, 2009; Meyers, 2003; Poyry et al., 2007). Rabbit hemorrhagic disease virus (RHDV) and feline calicivirus (FCV) are both non-enveloped, positive strand RNA viruses that belong to the family *Caliciviridae*. Both viruses produce a bicistronic subgenomic mRNA, with the two structural protein cistrons overlapping by four nucleotides (AUGA). Termination-dependent reinitiation allows translation of the second cistron. Reinitiation at the 3'-proximal ORF (ORF2) requires translation and termination of the uORF (ORF1) and the presence of an RNA element, termed "termination upstream ribosomal binding site" (TURBS), present within the 3'-terminal ~80 nucleotides of ORF1 (Meyers, 2003). Reinitiation at ORF2 can occur upstream of the ORF1 termination codon, as in RHDV, or four nucleotides downstream of the ORF1 termination codon, as in FCV, and at non-AUG start codons. Shifting the ORF1 termination codon or the ORF2 start site away from the RNA element abrogates reinitiation. Impressive cross-linking studies performed by Poyry and colleagues (2007) demonstrated that the RNA element has the potential to bind both the 40S ribosomal subunit and eIF3. These results agree

nicely with the recent insights into the mechanism of post-termination ribosome disassembly established by Pisarev and co-workers (2007). The TURBS element possesses three important motifs (Figure 4A). Motif 1 is conserved throughout the caliciviruses, and is responsible for base pairing between mRNA and 18S ribosomal RNA (rRNA). Motif 2, located proximal to the stop/start site, forms intramolecular base pairs with motif 2*, located upstream of motif 1 (Figure 4B). This interaction induces the formation of a stem-loop structure and positions motif 1 in the unpaired bulge where it can form intermolecular interactions with 18S rRNA (Luttermann and Meyers, 2009). The postulated mechanism of reinitiation after a long ORF suggests that upon translation termination of the uORF, eIF3 stimulates the release of the 60S subunit from the ribosome, while the TURBS element is capable of tethering and stabilizing the eIF3/40S complex such that the 40S subunit is positioned with the restart codon in the ribosomal P-site (Luttermann and Meyers, 2009; Poyry et al., 2007). Tethering the 40S subunit to the TURBS element would allow the ribosome time to bind the initiation factors necessary for another round of translation. Similar translation termination-reinitiation strategies are employed by the calicivirus murine norovirus (Naphthine et al., 2009) and by influenza B virus (Powell et al., 2008).

This mechanism of reinitiation after a long ORF is quite similar to the method of translational coupling and termination-reinitiation used to express prokaryotic bicistronic (and polycistronic) mRNAs. In prokaryotes, translation initiation generally utilizes the Shine-Dalgarno (SD) sequence present just upstream of the AUG codon to help recruit the small (30S) ribosomal subunit to the mRNA through the complementary sequence motif present at the 3'-terminal end of the 16S rRNA. Although each cistron on a eubacterial polycistronic mRNA usually has its own SD motif, not every motif is capable of recruiting the initiation machinery *de novo*. One of the mechanisms used by prokaryotes to overcome these “weaker” SD motifs is to couple translation termination and reinitiation (for review, see Jackson, Kaminski, and Poyry, 2007). Upon termination of an upstream cistron, the small subunit may undergo bidirectional diffusion for a very short period of time before dissociating from the mRNA. If a stabilizing element is present, such as a weak SD sequence, that element may be able pause the diffusing 30S subunit long enough for it to reacquire the initiation factors necessary for it to initiate

another round of translation. Therefore, the ability of a weak SD sequence in stabilizing a post-termination 30S subunit on an mRNA through its interaction with the 16S rRNA, thus making it competent for reinitiation, is reminiscent of the interaction between the TURBS element and the 18S rRNA present within 40S subunits.

1.7.3 Ribosomal Shunting

Ribosomal shunting, or discontinuous scanning, is yet another means by which ribosomes are capable of initiating translation at an internal start codon, downstream of multiple short ORFs and stable secondary structure (Figure 3C). Shunting was first described in Cauliflower mosaic virus (CaMV) (Futterer et al., 1990; Futterer, Kiss-Laszlo, and Hohn, 1993), and then in Rice tungro bacilliform virus (RTBV) (Futterer et al., 1996; Pooggin et al., 2006), two plant pararetroviruses. Ribosomal shunting relies upon the presence of two essential elements; the presence of a 5'-proximal short ORF (sORF; sORF A in CaMV), which terminates in front of a stable hairpin structure, and the secondary structure of the mRNA itself, which brings the main ORF into close proximity with sORF A. The shunt model postulates that the 43S ternary complex enters the mRNA in a cap-dependent manner and scans until it reaches the 5'-proximal sORF A. The ribosome translates and terminates sORF A at the stop codon, the shunt donor site, and disassociates, providing a fraction of 40S subunits competent to be translocated downstream to the shunt acceptor site, at which point the 40S subunit resumes scanning and is capable of initiating another round of translation. The actual initiation factors involved in the resumption of scanning are still unknown, although recent work demonstrated that for efficient reinitiation to occur, the central one-third fragment of eIF4G must have participated in translation of the upstream sORF (Poyry, Kaminski, and Jackson, 2004).

As in reinitiation, several parameters must be upheld in order for shunting to be successful. First, the sORF length is limited to 2 to 15 codons; a stop codon immediately after the start codon (start-stop ORF) inhibits shunting (Hemmings-Mieszczak, Hohn, and Preiss, 2000; Pooggin, Hohn, and Futterer, 2000). Second, the optimal spacing between the sORF termination codon and the base of the stem structure is five to ten nucleotides (Dominguez et al., 1998; Pooggin, Hohn, and Futterer, 2000). Shifting the termination

codon of the sORF A closer to the stem structure would allow the translating ribosome to unwind more of the stem causing the shunt acceptor site to shift to a position further upstream. Moving sORF A further from the stem base would prevent unwinding of the stem by the translating ribosome and, as a consequence, it would shift the shunt landing site further downstream. Therefore, the position of the shunt acceptor site depends on the shunt donor site, which in itself is dependent on the position of the sORF termination codon.

Another interesting feature of shunting ribosomes is their ability to shunt and reinitiate relatively efficiently and precisely at non-AUG codons at the base of the shunt acceptor site, as seen in RTBV (Futterer et al., 1996). The RTBV pregenomic RNA (pgRNA) serves as mRNA for the virus and is functionally tricistronic with ORF I preceded by a leader sequence more than 600 nucleotides long that forms a stable secondary structure and includes 12 sORFs. As in CaMV ribosome shunting, ribosomes translate RTBV mRNA sORF 1 (Pooggin et al., 2006) and are then translocated to the ATT start codon of ORF I (Futterer et al., 1996). The shunt mechanism is precise in that a non-AUG codon 12 nucleotides upstream of the ORF I start site is not used to initiate translation (Futterer et al., 1996).

Reinitiation on the yeast *GCN4* mRNA is reliant upon the cellular concentration of ternary complex, while a virally-encoded translational transactivator protein, TAV, enhances reinitiation efficiency on the CaMV 35S mRNA (Bonneville et al., 1989; Futterer and Hohn, 1991; Pooggin, Hohn, and Futterer, 2000). The translational transactivator protein TAV is capable of many protein-protein interactions, including interaction with the eIF3g subunit (Park et al., 2001) and the recently identified plant protein called reinitiation supporting protein (RISP; Thiebauld et al., 2009). The model of TAV action in reinitiation postulates that TAV recruits RISP to reinforce TAV interaction with eIF3 and the 60S ribosomal subunit. The TAV-eIF3 interaction either stabilizes eIF3 upon eIF4B release allowing eIF3 to remain bound to the 40S subunit during elongation, or the eIF3/TAV complex gets shifted to the 60S subunit during elongation due to the ability of TAV to bind 60S ribosomal proteins, and then shifted back to the 40S subunit during termination (Ryabova, Pooggin, and Hohn, 2006). Either way, the TAV protein appears to aid in maintaining 40S – initiation factor interaction.

In addition to advantageously avoiding the extensive secondary structure and multiple sORFs present in the CaMV leader, ribosomal shunting prevents unwinding of the secondary structure that would occur by scanning ribosomes. This is beneficial for CaMVs in that these viruses house their packaging signal at the apical portion of the hairpin (Guerra-Peraza et al., 2000). This phenomenon would reduce the requirement for host helicase activity, normally found in the limiting eIF4F complex, and thus reduce the need for the virus to compete with the host cell for its translation machinery.

The sORF-stem-mediated mechanism of ribosomal shunting that occurs in pararetroviruses may be well characterized, but it is not the only mechanism of ribosomal shunting present in the literature. Animal viruses, such as adenovirus (Yueh and Schneider, 1996), Sendai virus (Curran and Kolakofsky, 1989; Latorre, Kolakofsky, and Curran, 1998) and human papillomavirus (Remm, Remm, and Ustav, 1999), have all been reported to utilize some form of shunt-mediated mode of translation initiation.

Human adenovirus late mRNAs are capped at their 5'-ends and all possess a common 5'-UTR called the tripartite leader sequence. This leader sequence is relatively unstructured for the first 80 nucleotides and then contains a series of stable hairpin structures (Zhang, Dolph, and Schneider, 1989). The tripartite leader sequence utilizes three conserved regions, which have a striking complementarity to 18S rRNA, to facilitate ribosomal shunting (Yueh and Schneider, 2000). The first is located in the unstructured region of the leader while the other two are located within the hairpin series. In uninfected cells, translation initiation of host mRNAs or adenovirus late mRNAs occurs by both scanning and shunting mechanisms with approximately similar efficiencies (Yueh and Schneider, 1996). During late-stage viral infection, initiation due to scanning is completely abrogated and shunting is solely used. During shunting the 43S pre-initiation complex binds the 5'-cap and scans the cap-proximal end of the tripartite sequence until it encounters the first of the stable stem structures. Through the interaction of the virally-encoded L4-100K protein with the 40S subunit, the subunit is translocated downstream, past the series of stable stem structures (Xi, Cuesta, and Schneider, 2004). The L4-100K protein is thought to enhance ribosomal shunting by binding the tripartite leader sequence in a phosphotyrosine-dependent manner (Xi, Cuesta, and Schneider, 2005), and through the ability of L4-100K to bind not only the 40S subunit, but also the

eukaryotic initiation factors eIF4G and PABP (Xi, Cuesta, and Schneider, 2004).

L4-100K is capable of interacting with eIF4G at its C-terminus, the region normally occupied by the kinase Mnk1 (Cuesta, Xi, and Schneider, 2000). This displaces Mnk1 from eIF4G and prevents phosphorylation of eIF4E. Dephosphorylated eIF4E is sequestered by 4E-BP, inhibiting the formation of the eIF4F complex. This results in a decrease in active eIF4F and ultimately a decrease in cap-dependent translation initiation. Late adenovirus expression is not inhibited by this decrease because the structured region of the tripartite sequence does not need to be unwound as it can be bypassed with the shunt mechanism. It has been postulated that the enhanced binding of eIF4G and PABP to L4-100K drives 40S subunit recruitment and utilization on the tripartite leader sequence (Xi, Cuesta, and Schneider, 2004).

The Sendai virus, a paramyxovirus, produces a polycistronic P/C mRNA that contains two overlapping ORFs. From these two ORFs, multiple proteins are synthesized in a cap-dependent manner. The second ORF expresses a subunit of the polymerase protein termed P. The first ORF encodes an N-terminally nested set of proteins designated C', C, Y1 and Y2, respectively, that derive from alternate translation start sites in the same reading frame. Initial work on the P/C mRNA suggested that expression from the C', C and P start sites occurred via leaky scanning, while Y1 and Y2 expression was due to ribosomal shunting (de Breyne, Monney, and Curran, 2004; de Breyne et al., 2003; Latorre, Kolakofsky, and Curran, 1998). It has since been discovered that the majority of Y1 and Y2 expression *in vivo* is due to proteolytic processing of the C' polypeptide, while *in vitro*, synthesis of Y1 and Y2 occurs *de novo* (de Breyne, Monney, and Curran, 2004). Y protein processing can be recapitulated *in vitro* with the addition of endopeptidases (de Breyne, Stalder, and Curran, 2005). The Curran group was able to show however, that a minimal level of Y1 and Y2 production resulted from *de novo* synthesis that they speculate must arise from ribosomal shunting. Although no extensive examination of this shunting process was undertaken, it was speculated that the Sendai virus shunt does not require any specific *cis*-acting donor site, nor does it require any additional factors. The shunt mechanism does require an acceptor site that was tentatively mapped to a region just downstream of the Y2 start site (de Breyne et al., 2003).

The P/C mRNA also encodes a protein designated X that represents approximately

the C-terminal 95 amino acids of the P protein. The X protein is expressed in a cap-dependent manner at an initiation site more than 1500 nucleotides downstream of the 5'-cap (Curran and Kolakofsky, 1988). The mechanism of X protein synthesis has been postulated to occur in a scanning-independent manner, perhaps utilizing ribosomal shunting, although no work on the subject has occurred since the initial observation.

A final example of discontinuous scanning occurs on the human papillomavirus type 18 E1 protein (Remm, Remm, and Ustav, 1999). Expression of E1 occurs in a cap-dependent manner more than 700 nucleotides downstream from the 5' end, and independent of the expression of either E6 or E7. Inactivation of upstream minicistrons and insertion of stable hairpins in various locations had little to no effect on E1 production leading the authors to speculate that E1 synthesis occurs via discontinuous scanning. However, there is little direct evidence to support this prediction and there has been no characterization of the mechanism by which shunting may occur.

1.7.4 Internal Ribosome Entry Sites

Although the majority of cellular and viral mRNAs utilize a cap-dependent mechanism of translation initiation, some mRNAs possess an internal ribosome entry site (IRES) element, usually in their 5'-UTR, to direct initiation from an internal position along the mRNA in a cap-independent manner (Figure 3D). Initially discovered over 20 years ago in the 5'-UTR of the poliovirus mRNA (Pelletier and Sonenberg, 1988), IRES elements are now known to be present in many different forms in various viral and cellular mRNAs. While the number of IRES elements discovered continues to increase every year, this section will focus mainly on those elements belonging to picornavirus, HCV, and Cricket paralysis virus (CrPV), as they have been well studied and are quite divergent from one another.

Picornavirus genomes consist of a single strand of positive sense RNA with a covalently linked, virally encoded, peptide at the 5'-end followed by an unusually long 5'-UTR (~750 nucleotides) with many non-initiating AUG triplets. Clearly, the scanning model of translation initiation is inadequate to explain the mechanism of picornavirus translation, as it must proceed in a cap-independent manner. Two independent groups were able to demonstrate that insertion of the 5'-UTRs of poliovirus (Pelletier and

Sonenberg, 1988) or encephalomyocarditis virus (EMCV) (Jang et al., 1988) between adjacent cistrons in a bicistronic construct results in expression of the downstream ORF independent of the expression of the upstream cistron. Construction of such bicistronic constructs, with a sequence of interest as the intergenic region, has become the “gold standard” in deciphering whether the sequence of interest can act as an IRES element.

Subsequent studies identified four major types of IRES elements based on their sequence and secondary structure; type 1 (I) (e.g. poliovirus), type 2 (II) (e.g. EMCV), type 3 (e.g. HCV), and type 4 (CrPV). In addition to IRES types I and II, members of the picornaviridae family also possess two different minor types of IRES element, type III (e.g. hepatitis A virus [HAV]) and type IV (e.g. porcine teschovirus-1 [PTV-1]) (reviewed in, Belsham, 2009). A common feature among picornavirus IRES elements is their reliance on extensive secondary structure for activity. Even minimal changes in structure through point mutation or deletion can result in loss of function. Types I – III also share the feature of an essential polypyrimidine tract near the 3′-end of the IRES that is closely associated with an AUG codon.

The specific initiation factor requirements for each IRES type also differ. EMCV requires initiator tRNA, factors eIF2, eIF3, eIF4A, and the central portion of eIF4G, to form the 48S initiation complex (Pestova, Hellen, and Shatsky, 1996). Recent evidence revealed that the central region of eIF4G is capable of directly binding domain V of type I IRES elements in a manner analogous to type II IRESs. Once bound, eIF4G is able to recruit eIF4A to type I IRESs, thus causing a conformational change in the IRES element enabling 43S recruitment (de Breyne et al., 2009). Hepatitis A virus on the other hand requires intact eIF4F for its function (Ali et al., 2001; Borman and Kean, 1997), in addition to the factors outlined for type II IRESs. Unlike types I – III, IRESs belonging to type IV do not require any of the eIF4 factors or eIF3, however, 48S preinitiation complex formation is enhanced in the presence of eIF3, similar to their HCV cousins (Pestova et al., 1998; Pisarev et al., 2004). Additionally, CrPV, a type 4 dicistrovirus, possesses two IRES elements, one in the 5′-UTR and another within the mRNA intergenic region (Wilson et al., 2000b). Fascinatingly, the intergenic region IRES does not require any canonical initiation factors, not even initiator tRNA, as it is capable of initiating translation from a GCU triplet located in the ribosomal A-site (Wilson et al.,

2000a).

In line with the canonical initiation factor requirements just discussed, although not essential, viral proteins can also have an affect on IRES function. For example, during poliovirus infection, a virally encoded protease, 2A, is thought to participate in host cell translation inhibition by cleaving eIF4G at its N-terminal end, ultimately separating the regions that bind eIF4E and eIF3, thus preventing 40S ribosomal subunit recruitment to the 5'-cap (Etchison et al., 1982; Krausslich et al., 1987). The stimulation in poliovirus translation observed in the presence of the 2A protease may result from increased availability of initiation factors and the ability of the virus to utilize the cleaved form of eIF4G for 40S recruitment. However, subsequent research has shown that the translational enhancement of poliovirus mRNA in the presence of 2A initially occurs at a time when host cell protein synthesis has yet to be inhibited (Hambidge and Sarnow, 1992). Additionally, an alternative method of inhibiting cap-dependent translation, expression of 4E-BP2, does not stimulate IRES function (Roberts, Seamons, and Belsham, 1998), suggesting that 2A protease may be modifying another protein responsible for the change in IRES performance.

Non-canonical translation factors, also referred to as IRES *trans*-acting factors (ITAFs), are also required for efficient translation, although the exact requirement for said factors depends on the type of IRES (Belsham, 2009). As alluded to earlier, there is very little sequence or structural similarity between picornavirus type I and II IRES elements, and as such, they differ in their requirement for ITAFs. *In vitro* translation of poliovirus mRNA in rabbit reticulocyte lysate (RRL) results in inefficient and aberrant initiation unless the cell-free RRL is supplemented with the cellular factors PTB (polypyrimidine tract-binding protein) and Unr (upstream of N-ras) (Dorner et al., 1984; Hunt et al., 1999; Hunt and Jackson, 1999), while EMCV functions normally in cell-free extracts. In addition to their role as positive regulators of IRES function, the ITAF double-stranded RNA-binding protein 76, was recently found to inhibit the activity of human rhinovirus-2 in neuronal but not glioma cells, implicating ITAFs as modulators of virus tropism (Merrill, Dobrikova, and Gromeier, 2006).

Although studies of picornavirus IRES elements resulted in a better understanding of IRES structure and the factors required to recruit the ribosome to the mRNA, they did

little to help the understanding of ribosome-IRES interaction. Examination of IRES types 3 and 4 has provided initial insights into these interactions. In addition to the sequence and structural differences between IRES types 1 – 4, HCV and CrPV both utilize distinct mechanisms of IRES-mediated initiation that involve precise, factor-independent binding of ribosomes (Pisarev, Shirokikh, and Hellen, 2005). The HCV 5'-UTR can be subdivided into four different stem-loop structures, also known as domains I – IV. Domain III is the most important and complex and is further divided into six subdomains. The position of the HCV initiation codon and a short region of coding sequence downstream are also important for IRES function. Through toeprinting analysis, it was determined that the solvent side of the 40S subunit is capable of interacting directly with the HCV IRES through multiple non-contiguous contacts such that the initiation codon is placed in the ribosomal P-site, and that 48S pre-initiation complexes can be formed through the addition of the eIF2-ternary complex (Pestova et al., 1998). Although not required for 48S formation, eIF3 also directly binds the HCV IRES and enables accurate IRES function. Interestingly, the regions of high-affinity binding between HCV IRES and 40S do not necessarily match the regions on the IRES element required for function (Pisarev, Shirokikh, and Hellen, 2005). This suggests that the IRES element plays additional, as yet undiscovered, roles in initiation.

Type 4 IRES elements, such as those found within the intergenic region of the positive-strand RNA of CrPV, employ a third and final mechanism for recruiting ribosomes. Like HCV, the CrPV intergenic region (IGR) IRES is capable of recruiting 40S without the aid of any canonical initiation factors. Unlike HCV however, CrPV does not require initiator tRNA or the ternary complex to form 80S ribosomes competent to undergo elongation (Wilson et al., 2000a). Interestingly, the IGR IRES is capable of interacting with the intersubunit side of both 40S and 60S subunits, in the region normally occupied by tRNAs (Schuler et al., 2006; Spahn et al., 2004). The interaction between CrPV IRES and 40S induces a conformation change in the 40S subunit near the mRNA entry channel. Upon 60S joining, the IRES undergoes a conformational change where it retracts itself from the A-site and shifts closer to the E-site region, and the rotational movement of the 40S subunit reverses to its original, unbound, conformation (Spahn et al., 2004). Taken together, the CrPV IRES can be viewed as an RNA-based

translation factor that is capable of inducing ribosomal conformations necessary for translation initiation.

It has been known for some time that the expression of a number of cellular proteins continues under conditions where normal cap-dependent translation is inhibited, for example during viral infection, stress and mitosis. Researchers set out to determine whether these proteins were expressed via cellular IRES elements, and were quick to discover the first cellular counterpart in the 5'-UTR of the immunoglobulin heavy-chain binding protein (BiP) (Macejak and Sarnow, 1991). Despite the rapid detection of IRES elements within cellular mRNAs, very little is known regarding their mechanism of ribosome recruitment or their secondary structure (reviewed in, Elroy-Stein and Merrick, 2007). What is known is that many function in a modular fashion and possess a polypyrimidine tract that binds and utilizes PTB as an ITAF. Also, the ability of a cellular ITAF to modulate function could be related to its intracellular concentration, post-translational modification, due to some external signal, or to its subcellular localization (Lewis and Holcik, 2008). The advantage for a virus possessing an IRES element within its mRNA is three-fold. First, the existence of an IRES element capable of directing internal translation initiation in a cap-independent manner implies that these mRNAs do not require the traditional cap structure present at their 5'-ends. For example, the picornavirus mRNAs possess a virally-encoded protein linked to their 5'-ends. Second, viruses with an IRES element could inhibit host cell cap-dependent protein synthesis without interfering with their own protein expression. Third, the ability to initiate translation despite the presence of extensive secondary structure near the 5'-cap implies that the mRNA can contain additional secondary structure in this region that can be used for other things, for example RNA replication or packaging (Mason, Bezborodova, and Henry, 2002). The secondary structure bypassed in ribosome shunting also possesses signals for viral replication and RNA packaging (Guerra-Peraza et al., 2000). The advantage for cellular mRNAs in possessing an IRES element lies in their ability to maintain or induce efficient levels of protein expression during periods of cellular stress or times of global protein inhibition.

Although the list of mRNAs possessing a putative IRES element continues to grow, caution should be taken when examining the data as deficiencies may be present. Some

valid concerns regarding the method(s) used to “detect” an IRES element have recently been presented (Kozak, 2001b; Kozak, 2007). The construction of a “bicistronic” construct, the “gold standard” test for an IRES element, should only be trusted if the appropriate controls are also performed. Frequently, an mRNA believed to carry an IRES element in fact possesses a cryptic promoter or splice site, thus producing a monocistronic mRNA which undergoes traditional cap-dependent translation initiation. RNA analysis, in the form of Northern blot and quantitative polymerase chain reaction (PCR) are also required, and often forgotten, to determine whether the primary effect of a change in the putative IRES was on translation or on mRNA accumulation.

1.7.5 Additional Alternate Mechanisms of Initiation

Another form of cap-independent translation initiation, involving the direct recruitment of the 40S ribosomal subunit to a 5′-proximal poly(A) sequence in the absence of some canonical initiation factors, has recently been reported (Shirokikh and Spirin, 2008). In this study, the authors were able to demonstrate, through the use of toeprinting assays, that mRNAs with poly(A) leaders, similar to those found in the 5′-UTRs of poxviruses, do not require the canonical initiation factors eIF3, eIF4F, or PABP and thus act in an “IRES-like” manner. The poly(A) leaders do not recruit 40S subunits to a specific region within the leader, nor do they possess extensive tertiary structure. This is an interesting finding in that IRES elements may not require all the canonical initiation factors, but they do recruit 40S subunits in a modular fashion to specific locations within the IRES. The authors believe that once a 40S subunit is recruited to the mRNA, it is capable of undergoing ATP-independent “phaseless wandering” until it encounters the start codon (Shirokikh and Spirin, 2008).

Ribosome tethering and clustering have also been proposed to act as mechanisms for translation initiation (Chappell, Edelman, and Mauro, 2006). The tethering model predicts that the 40S ribosomal subunit binds a fixed point on the mRNA, the 5′-cap structure for example, and reaches the initiation codon by bypassing the intervening sequence, potentially due to the intervening sequence being folded and out of the way. The clustering model on the other hand, is a dynamic process where-by the 40S subunit reaches the initiation codon through reversible binding to and detachment from various

sites on the mRNA. These models are supported by analysis of a nine-nucleotide sequence present in the 5' leader of the mRNA encoding the homeodomain protein Gtx that is capable of acting as a ribosome recruitment site by base-pairing with 18S rRNA (Chappell et al., 2006; Chappell, Edelman, and Mauro, 2000; Chappell, Edelman, and Mauro, 2004). Mauro and colleagues demonstrated that extending the region of complementarity beyond nine nucleotides increases its binding affinity for 18S rRNA, which is inversely proportional to its ability to direct translation, with a seven nucleotide sequence being optimal for translational enhancement (Chappell, Edelman, and Mauro, 2004). In subsequent studies, the nine-nucleotide sequence was shown to be able to direct ribosomes across upstream AUGs and stable hairpin structures when the element was used in tandem as the “shunt donor and acceptor” site (Chappell et al., 2006). The Gtx element does have some restrictions on its function, in that it works best when spaced ~50 nucleotides from the 5'-cap and its ability to direct translation decreases when the initiation codon is present at increasing distances from the element (Chappell, Edelman, and Mauro, 2000; Chappell, Edelman, and Mauro, 2006). Relevant to the clustering model, the Gtx element is capable of mediating initiation at AUG codons upstream and downstream of the recruitment site (Chappell, Edelman, and Mauro, 2006).

Ultimately the authors present ribosomal tethering and clustering as alternatives to the traditional mechanism of ribosome scanning, and these alternative mechanisms invoked a ribosome filter hypothesis (Mauro and Edelman, 2002; Mauro and Edelman, 2007). The ribosome filter hypothesis proposes that specific mRNA-rRNA and mRNA-ribosomal protein interactions at sites on the ribosomal subunits are important in controlling the rate of polypeptide chain production. Therefore, the ribosomal subunits themselves are considered regulatory elements or filters that mediate interactions between particular mRNAs and components of the translation machinery. The hypothesis also suggests that the rRNA and proteins that make up the ribosome vary depending on the cell type, stage of cell differentiation or subcellular location of the ribosome. This ribosomal heterogeneity led the authors to propose four hypothetical tenets for the ribosome filter hypothesis. First, the ribosome is a regulatory structure that embodies mechanisms for preferentially translating different subsets of the message population. The ability of ribosomes to filter translation depends on their ability to specifically

interact with segments of the mRNA that bind to ribosomal proteins or rRNA. Second, ribosomes may display a continuum of regulatory effects. The influence the ribosome-mRNA interaction has on translation ranges from being beneficial to inhibitory. Third, competition for binding sites in ribosomal subunits may affect the rate of translation of different mRNAs. Interaction between one population of mRNA with ribosomes may out-compete a different set of mRNAs for the same population of ribosomes. Fourth, the filter may also be modulated as a result of altering or masking particular binding sites on ribosomes. The efficiency with which a particular mRNA is translated will differ depending on the accessibility of ribosomal binding sites. Evidence is slowly starting to emerge that suggests that ribosome biogenesis does in fact produce a heterogeneous population of ribosomes, and this heterogeneity can be cell-type-specific (Rodriguez-Mateos et al., 2009; Tseng et al., 2008).

The ribosome filter hypothesis, along with the additional alternate mechanisms of translation initiation, are consistent with the idea that translation can be controlled and facilitated by multiple mechanisms (Chappell, Edelman, and Mauro, 2006), and may help explain observations made by other researchers (Herbreteau et al., 2005; Xi, Cuesta, and Schneider, 2004). The HIV-2 gRNA, for example, carries an IRES module 50 nucleotides downstream of the AUG codon that is capable of attracting the 48S complex to this region, without the involvement of the 5'-UTR (Herbreteau et al., 2005), as the ribosomal clustering model would predict.

1.8 Translational Control In Cancer Development

Translation control occurs at the level of the global proteome and at the level of selective translation of specific mRNAs and classes of mRNAs, and as such, is a key regulator of cancer development and progression. Changes in translation result from altered activity of signal transduction pathways that control protein synthesis, and in changes in the concentration of key translation components, such as translation factors, ribosomes and tRNAs (reviewed in, Schneider and Sonenberg, 2007).

As mentioned previously, the presence of uORFs or extensively structured 5'-UTRs can regulate translation. It is interesting to note that particular groups of mRNAs harbouring such 5'-UTRs encode proto-oncogenes, anti-apoptotic proteins and growth

factors. Normally these mRNAs would be poorly translated, however, under certain conditions, such as an increase in the rate-limiting concentration of eIF4E (Duncan, Milburn, and Hershey, 1987), they benefit disproportionately compared to mRNAs bearing “normal” 5'-UTRs (Koromilas, Lazaris-Karatzas, and Sonenberg, 1992). To this end, eIF4E is considered to be a proto-oncogene in that over-expression of eIF4E results in the transformation of various cell types (Lazaris-Karatzas, Montine, and Sonenberg, 1990; Lazaris-Karatzas et al., 1992; Lazaris-Karatzas and Sonenberg, 1992; Miyagi et al., 1995), most likely due to its ability to enhance the expression of mRNAs with extensive secondary structure within their 5'-UTRs. The expression level and phosphorylation state of eIF2 α is also important in that a mutant eIF2 α that cannot be phosphorylated is transforming and promotes tumorigenesis in NIH 3T3 cells (Donze et al., 1995), while the eIF2 α subunit is over-expressed in various cancers (Rosenwald et al., 2001; Tejada et al., 2009).

Viruses, particularly DNA viruses, are also capable of inducing cancer development. One of the many ways in which this is achieved is through the promotion of core eIF4F components and eIF4F complex assembly (Arias et al., 2009; Walsh and Mohr, 2006; Walsh et al., 2005). For example, herpes simplex virus-1 encodes an eIF4F-assembly chaperone, ICP6, which is capable of interacting with the N-terminus of eIF4G to promote eIF4F assembly in growth-arrested cells (Walsh and Mohr, 2006). Another way in which viruses induce cancer development is through the generation of host-specific miRNAs (Samols et al., 2007; Swaminathan, 2008). For example, multiple miRNAs encoded by Kaposi sarcoma-associated herpesvirus are known to down-regulate thrombospondin 1 (Samols et al., 2007), a potent inhibitor of blood vessel growth, most likely aiding in tumor development.

1.9 Translation Summary

When translation control, particularly at the initiation stage is altered, various disease states can develop. Although most eukaryotic mRNAs follow the monocistronic, cap- and scanning-dependent mechanism of translation initiation, numerous exceptions have been discovered. Most of these exceptions were first ascertained through the examination of viral mRNAs, but have also been observed in rare cases of cellular gene

expression. It therefore seems prudent to continue the examination of viral mRNAs that do not follow the monocistronic rule of translation initiation as they may lead to the discovery of novel translation mechanisms.

1.10 The Family *Reoviridae*

1.10.1 Virion Morphology

Reoviridae is a large and diverse family of nonenveloped, icosahedral viruses whose protein capsid is arranged in one, two or three concentric capsid layers, with an overall diameter of 60-90 nm (Figure 5). The name “Reoviridae” is derived from respiratory enteric orphan virus since initial isolates were known to infect the respiratory and gastrointestinal tract without causing disease. The family *Reoviridae* contains 15 genera divided into two groups, turreted or nonturreted, based on the presence of a “turret” protein situated at the 12 icosahedral vertices of either the virus or core particle (Attoui et al., 2006). The outermost protein layer can be removed intracellularly within endocytic vesicles, or *in vitro* by proteases such as trypsin and chymotrypsin, ultimately forming “infectious” or “intermediate” subviral particles (ISVPs, term used to describe reovirus particles). The innermost protein layer, the core, surrounds the viral genome comprised of 9 – 12 linear segments of double stranded ribonucleic acid (dsRNA). Within the “turreted” genera, some of the enzymatically active minor proteins of the virion either form the turrets on the surface of the core or are situated near the turrets (Joklik, 1985; Zhang et al., 2005).

1.10.2 Virus Replication

While the host range and type of disease caused by various members of the *Reoviridae* family differ markedly, several features of the replication pathway are common to all viruses of this family. While the mode of entry into cells varies depending on the genera, it usually results in the loss of the outer capsid layer(s) and the release of the transcriptionally active core particle. Not only does the core particle contain one copy of each genome segment, but it also contains multiple copies of the RNA-dependent RNA polymerase (RdRp) and the mRNA-capping enzyme. The RdRp uses the negative strand of the viral genome as a template for viral transcription in a conservative manner

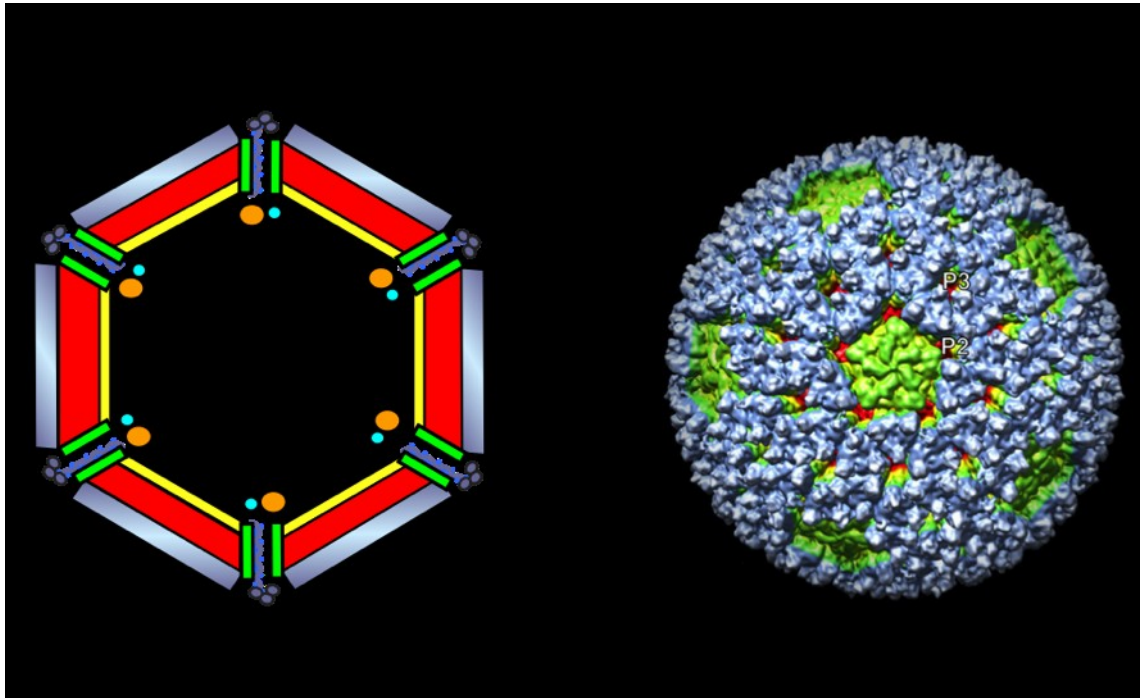


Figure 5. Avian reovirus morphology. **A.** Diagram of a *Reoviridae* family member, ARV, in cross-section demonstrating the arrangement of the structural proteins and indicating the location of the ten linear segments (L: large, M: medium, S: small) of dsRNA within the inner core. **B.** Electron cryomicroscopy image of the surface of ARV. Part B copied, with permission, from Zhang et al. (2005) *Virology* 343:25-35.

(i.e. the mRNA is identical to the positive-sense genome strand and does not displace the positive strand from the double-strand genome segment), producing an unspliced mRNA containing a 5'-methylated cap structure but lacking a poly(A) tail (Joklik, 1985; Martinez-Costas, Varela, and Benavente, 1995). The mRNA is extruded from the core through the icosahedral apices of the virus particle into the cytoplasm where they are able to interact with the host cell translation machinery. The viral mRNAs direct the synthesis of viral proteins and serve as templates for the synthesis of minus-sense RNA to form the dsRNA genome segments.

Although the exact mechanism of particle assembly and genome replication remains unknown, it does appear to take place in a concurrent manner within “viral factories” found within the cytoplasm. Studies performed on rotavirus, a member of the *Reoviridae* family, demonstrate that mRNA templates move into cores as they are replicated by the viral replicase, and once inside the core, the dsRNA is no longer susceptible to nuclease treatment (Patton and Gallegos, 1988; Patton and Gallegos, 1990). Additional research indicates that sequences found within the 5'- and 3'-ends of the mRNA can interact in *cis* forming an imperfect panhandle with a non-base-paired 3'-termini that is required to interact with the RdRp and initiate minus-strand synthesis (Chen and Patton, 1998). Since packaging of the mRNA precedes dsRNA synthesis, the mRNA must also contain *cis*-acting signals necessary for the selective packaging of equimolar concentrations of the genome segments into each virion. An interesting feature of the imperfect panhandle structure is the presence of a stable stem-loop structure that varies in its make-up depending on which genome segment is responsible for panhandle formation (Chen and Patton, 1998), suggesting that the stem-loop structures are responsible for the specific packaging and assortment of viral mRNAs within the *Reoviridae* (Patton and Spencer, 2000). The presence and strict requirement for 5'- and 3'-terminal consensus sequences adds an additional level of complexity to these viral mRNAs not found within cellular mRNAs. Cellular mRNAs are solely responsible for protein synthesis, while the dsRNA viruses of the *Reoviridae* also use their mRNA for packaging and replication.

In addition to the parental core particle, progeny cores are also involved in mRNA synthesis, providing an amplification step to virus replication. Although most genera exit

the cell through cell lysis, the syncytia forming members of the *Orthoreovirus* genus propagate the viral infection by inducing infected to uninfected cell-to-cell fusion (Salsman et al., 2005).

1.11 The Genus *Orthoreovirus*

The genus *Orthoreovirus* belongs to the turreted group of *Reoviridae* family members. Viruses belonging to this genus are isolated from a broad range of mammalian, avian, and reptilian hosts. The orthoreoviruses are best characterized by a genome comprised of ten dsRNA genome segments of three different lengths, large (L), medium (M) and small (S) based on their mobility when analyzed by standard sodium dodecyl sulfate polyacrylamide gel electrophoresis (SDS-PAGE), found within the core (Spandidos and Graham, 1976). Other features include a polycistronic S-class genome segment encoding two or three distinct proteins, a capsid approximately 80 nm in diameter, and isolation from a vertebrate host. The genus can be further subdivided into fusogenic and non-fusogenic subgroups based on the ability of the virus to induce cell-to-cell fusion and syncytium formation (Duncan, 1999; Duncan et al., 2004). Mammalian reovirus (MRV) belongs to the non-fusogenic subgroup and is the prototype member of the genus *Orthoreovirus*. There are however, two atypical mammalian reovirus isolates, Nelson Bay reovirus (NBV) and baboon reovirus (BRV), which are capable of inducing multinucleated cell formation (Duncan, Murphy, and Mirkovic, 1995; Gard and Compans, 1970). Two additional species of fusogenic orthoreoviruses have been identified; reptilian reovirus (Duncan et al., 2004), and the prototype of the fusogenic orthoreoviruses, avian reovirus (Duncan et al., 1996).

Orthoreovirus members possess a genome that is composed of ten dsRNA segments found within the inner protein layer, the core, of the capsid, most likely organized in partially ordered concentric layers and associated with an RdRp (Benavente and Martinez-Costas, 2007; Nibert and Schiff, 2001). Along with the RdRp, the core also contains a viral capping enzyme, that together produce capped, non-polyadenylated transcripts that are extruded out of channels that extend through the capsid into the cytoplasm where they are translated by the cellular machinery (Martinez-Costas, Varela, and Benavente, 1995).

Examination of various genome segment sequences revealed variation in the length of the 5'- and 3'-UTRs, but conservation in the nucleotide sequence at the extreme 5'- and 3'-terminal ends (Duncan, 1999). These conserved sequences, particularly the 3'-consensus sequence, appear to play a role in RNA replication and packaging as deletion or mutagenesis of the sequence in the rotaviruses impairs these abilities (Patton and Spencer, 2000). Most mRNAs are monocistronic, encoding only one protein, while a few mRNAs are polycistronic, encoding multiple proteins from the same messenger RNA (Figure 6). Interestingly, the S1 genome segment of all members of the *Orthoreovirus* genus encodes a polycistronic mRNA except for Baboon reovirus (BRV) where it is the S4 genome segment that is bicistronic (Dawe and Duncan, 2002). The S7 genome segment found within the Atlantic salmon reovirus (AtSRV), a member of the *Aquareovirus* genus, is equivalent to the S1 segment found within the orthoreoviruses and is also polycistronic (Racine et al., 2009).

1.12 Avian Reovirus

Avian reovirus can be isolated from domestic and wild birds and causes a variety of diseases, such as, arthritis and a gastrointestinal malabsorption syndrome (Benavente and Martinez-Costas, 2007). The pathogenicity of ARV is linked to its ability to induce syncytium formation in infected tissues and cell culture (Duncan and Sullivan, 1998). Although syncytium formation is not essential for viral replication, it is believed to aid in disseminating the virus throughout the host and consequently, augmenting the level of pathogenicity (Brown et al., 2009; Duncan et al., 1996; Salsman et al., 2005). Through the use of two monoreassortant viruses that differ in their ability to induce syncytium formation, it was discovered that the protein responsible for cell-to-cell fusion resides on the S1 genome segment (Duncan and Sullivan, 1998), which was subsequently confirmed by cloning and sequencing analysis of the S1 genome segment (Shmulevitz and Duncan, 2000).

1.13 The S1 Genome Segment

Of the ten dsRNA segments that make up the ARV genome, all are functionally monocistronic except the largest of the S class segments, S1. The S1 genome segment in

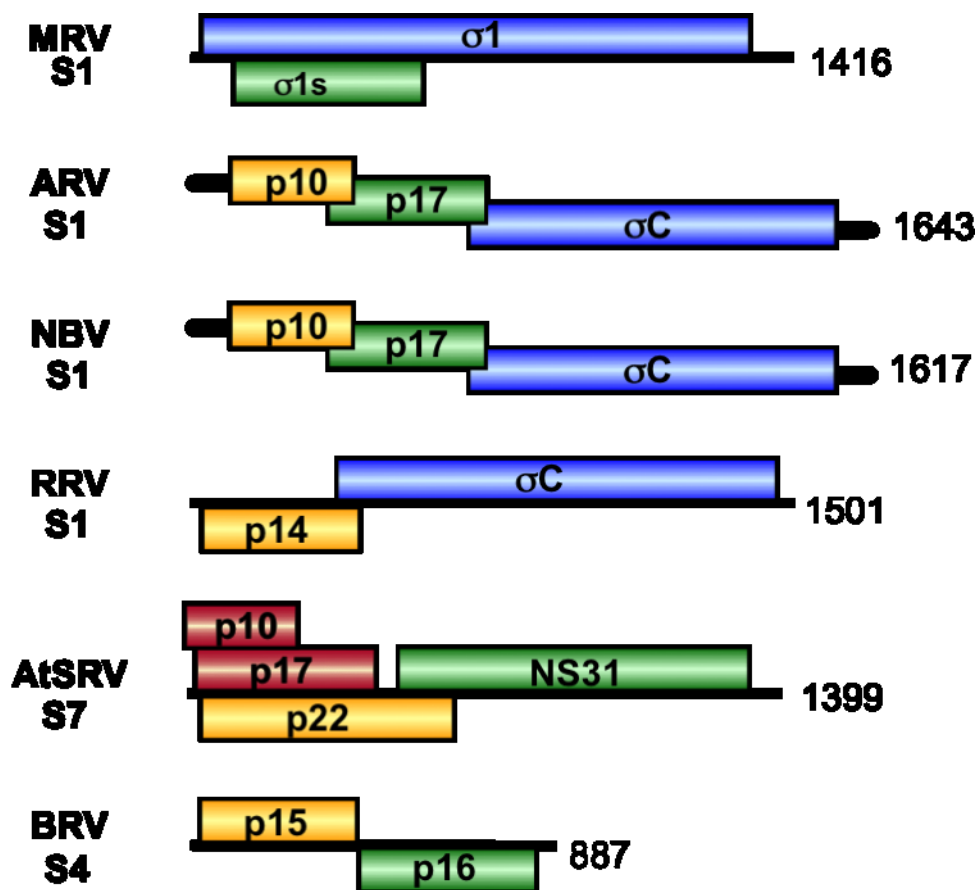


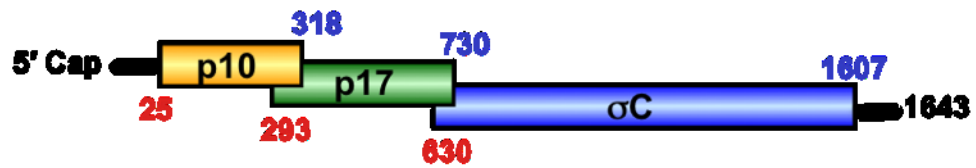
Figure 6. Polycistronic ORF arrangement. Schematic arrangement of the polycistronic genome segments found within the genera *orthoreovirus* (MRV, ARV, NBV, RRV and BRV) and *aquareovirus* (AtSRV). The ORFs are shown as coloured rectangles above and below a line representing the S1 and S4 mRNA (S7 is equivalent to S1) and are identified by the name or approximate molecular mass (in kDa) of the predicted gene product. The numbers at the end of the segment refers to the length, in nucleotides, of the segment. The virus species and the genome segment are indicated on the left. The blue boxes represent the cell attachment protein and the yellow boxes represent the FAST proteins. The function of the proteins encoded by the red and green boxes remains uncertain.

ARV is functionally tricistronic and possesses three, partially overlapping ORFs that encode three distinct proteins (Figure 7A). The 5'-proximal ORF encodes the fusion associated small transmembrane (FAST) protein, p10, that is solely responsible for cell-cell fusion and syncytium formation (Shmulevitz and Duncan, 2000). The next 5'-proximal ORF encodes p17, a nonstructural nucleocytoplasmic shuttling protein (Costas et al., 2005) that may retard cell growth through the activation of the p53 pathway (Liu et al., 2005), while the 3'-proximal ORF encodes a soluble cytoplasmic cell attachment protein, σ C, which is structurally and functionally similar to the MRV σ 1 protein (Grande et al., 2000; Guardado Calvo et al., 2005).

The distribution and function of all three proteins expressed from the S1 mRNA varies widely. Briefly, p10 is a nonstructural, integral membrane protein inserted in the plasma membrane of infected or p10-transfected cells in an $N_{\text{exo}}/C_{\text{cyt}}$ topology (Shmulevitz and Duncan, 2000). This topological arrangement results in a relatively small ectodomain incapable of forming the intricate structures necessary for enveloped virus fusion. Nonetheless, the p10 proteins function as fusion machines, and are thus the simplest representative of this class of proteins (Shmulevitz et al., 2002). The p17 protein is also a nonstructural protein, however, it lacks a transmembrane domain and as such is soluble within the cell. Costas *et al.* (2005) demonstrated that p17 contains a nuclear localization signal (NLS) in its C-terminus that is required to actively shuttle p17 into the nucleus of actively transcribing cells. Although the exact function of p17 has yet to be determined, it has been postulated that nuclear p17 may block nuclear signaling pathways, thus evading the triggering of the host immune response. Alternatively, nuclear p17 may play a role in cellular transcription inhibition or diverting biosynthetic resources from the nucleus to the cytoplasm, the site of ARV replication (Costas et al., 2005). A separate study has suggested that ectopic expression of p17 retards cell growth through the activation of p53 (Liu et al., 2005). Finally, σ C is a minor outer capsid protein located at the vertices of the icosahedral capsid, and forms an elongated trimer that functions as the viral cell attachment protein (Grande et al., 2000).

Another interesting feature of the ARV S1 mRNA is the presence of only four AUG triplets (methionine codons Met1 – Met4) upstream of the σ C start site, all of which reside within the first 300 nucleotides of the mRNA (Figure 7B). Also, the sequence

A.



B.

ARV

		25
Met 1	(p10)	CG<u>U</u>CGA<u>U</u>GC
		34
Met 2	(p10)	UG<u>C</u>GUA<u>U</u>GC
		293
Met 3	(p17)	GCACAA<u>U</u>GC
		298
Met 4	(p10)	AUGCAA<u>U</u>GG
		630

Figure 7. Gene arrangement of the ARV S1 genome segment. A. The organization and arrangement of the p10, p17 and σ C ORFs (coloured boxes) within the ARV S1 genome segment. Numbers refer to nucleotide position within the mRNA, with numbers in red representing the first nucleotide of the ORF and numbers in blue representing the last nucleotide of the ORF (excluding the termination codon). **B.** The locations and flanking sequences of all potential initiator methionine codons (bold) in the ARV S1 genome segment upstream of the σ C start site are listed. The codons are identified by the first nucleotide position of the methionine codon (bold) and the nucleotides in the -3 and +4 positions are underlined. The reading frame of each methionine codon is indicated (parentheses).

context surrounding these methionine codons goes from a very poor context surrounding the p10 AUG, to a strong context surrounding the p17 start site, to a preferred context surrounding Met 4 (Figure 7B). Due to these two remarkable features of the 5' region of the S1 mRNA and the fact that the p10 ORF terminates downstream of the p17 initiation site, it was postulated previously that expression of the p10 ORF serves a dual role; first to express the p10 polypeptide, and second, to shunt ribosomes past the relatively good p17 start codon so they can reinitiate translation at the σ C start site (reviewed in, Kozak, 2002). The absence of AUG triplets between the p10 termination codon and the σ C start codon support this theory. The remarkable tricistronic arrangement of the S1 genome segment is a rarity in the eukaryotic world and the mechanism(s) that regulates its expression has only recently begun to be explored (Racine et al., 2007; Shmulevitz et al., 2002).

1.14 Objectives

The arrangement of three partially overlapping ORFs in the S1 genome segment of avian reovirus challenges the dogma of translation initiation, since the cap-dependent scanning model cannot be the sole method of start site selection. Early work on the S1 segment of ARV revealed that optimization of the relatively weak 5'-proximal p10 start site increased p10 expression approximately 15-fold with little to no effect on expression of σ C (Shmulevitz et al., 2002). This data indicated that leaky scanning, the most likely explanation for σ C expression, cannot be the mechanism responsible for initiation. Therefore, the goal of the present work was to identify the mechanism(s) of translation initiation on the tricistronic S1 mRNA of avian reovirus, particularly at the 3'-proximal ORF, σ C.

CHAPTER 2: Materials & Methods

2.1 Cells

Quail fibroblast (QM5) cells, a clonal derivative of QT6 cells that exhibit a very low spontaneous fusion index (Antin and Ordahl, 1991), were used for all transfection studies. Cells were maintained in Medium 199 with Earl's salts, supplemented with 10% fetal bovine serum (Sigma). Cells were grown in 175 cm² flasks at 37°C with 5% CO₂, and sub-cultured with trypsin digestion every two days.

2.2 Competent Cells

A starter culture, consisting of four ml of sterile Luria-Bertani (LB) medium and 100 µl DH5α *Escherichia coli* (*E. coli*), was incubated overnight at 37°C, shaking at 200 rotations per minute. The starter culture was then added to 900 ml of sterile LB medium and incubated at 37°C for approximately 2 hours or until the culture reached an OD₆₀₀ of 0.5 - 1.0. The *E. coli* cells were transferred to centrifugation bottles and pelleted by centrifugation at 5000 rpm for 15 minutes. The supernatant was decanted and the pellet was resuspended in 60 ml cold 0.1M CaCl₂ and left on ice overnight at 4°C. The following morning the cells were pelleted once more by centrifugation at 5000 rpm for 15 minutes. The cells were resuspended in 60 ml cold 0.1M CaCl₂ with 10% glycerol. The cells were pelleted with a final spin at 5000 rpm for 15 minutes. The supernatant was decanted, the pellet was resuspended in 20 ml cold 0.1M CaCl₂ with 10% glycerol. The cells were transferred to sterile eppendorf tubes in 100 µl aliquots and stored at -70°C.

2.3 Plasmids

The full-length cDNA of the ARV S1 genome segment was amplified by PCR with flanking HindIII and NotI restriction endonuclease recognition sites inserted into plasmid pcDNA3 (Invitrogen) that had been digested with HindIII and NotI to create plasmid pARV-S1. A modified *Renilla* luciferase (RL) ORF (RL AUG mutated to AGG) amplified from plasmid phpRLFL (kindly provided by Dr. Graham Belsham, Technical University of Denmark) was inserted into pARV-S1 in-frame with the σC ORF between S1 nucleotides 751 and 752 using the XbaI restriction site present within the S1 sequence at this location, resulting in the production of the plasmid pσC-RL. The RL ORF, with its

authentic AUG start site, and the S1 sequence 3' of the RL ORF were amplified by PCR from p σ C-RL using primers that created BamHI and XbaI restriction sites at the 5'- and 3'-ends, respectively. The PCR product was digested with BamHI and XbaI and cloned into a pcDNA3 BamHI/XbaI digested plasmid, creating plasmid pRL. These plasmids were the backbone for all subsequent point substitutions and PCR reactions. The region of interest, in all plasmid manipulations, was sequenced at either the Robarts (London, Ontario) or MCLab (San Francisco, California) automated sequencing facilities. All plasmids were used as templates for PCR reactions utilizing a forward primer containing the T7 polymerase promoter and an S1-specific reverse primer. These amplicons were used as templates for *in vitro* transcription. The term construct refers to either the plasmid that was manipulated (e.g. pS1-RL) or the mRNA derived from this plasmid (e.g. S1-RL). A list of all plasmids created can be found in Appendix B, while a list of primers used can be found in Appendix C.

2.4 Mutagenesis

2.4.1 Site-Directed Mutagenesis

All point substitutions were created using the PfuTurbo DNA polymerase kit (Stratagene) according to the manufacturer's instructions. Briefly, primers were designed that possessed the mutation in question, flanked on either side by more than 15 nucleotides of authentic sequence. Primers, at a concentration of 100 ng/ μ l, were mixed with 100 ng of plasmid DNA, 1 μ l of 10 mM dNTPs, 5 μ l 10X PfuTurbo reaction buffer and 1 μ l polymerase enzyme to a final volume of 50 μ l. The PCR program utilized 26 cycles of a denaturation step of 95°C for 30 seconds, a one minute annealing step where the temperature was 5°C lower than the melting temperature of the primers being used, and an elongation step at 72°C for 12.5 minutes. The reaction was then cooled to 4°C. The restriction enzyme DpnI (Stratagene) was used to digest the template DNA. One μ l of DpnI was added to the PCR reactions and incubated at 37°C overnight. Site-directed mutagenesis used to optimize the context (ccAccAUGgG) of the p10 or p17 start codons (p10opt and p17opt), to convert the four AUG codons that occur upstream of the σ C start site to AUC codons (M1-M4), to convert the two AUG codons present within the insert of miniORF1 to AUC codons, to create additional AUG start sites in a strong context

within the p17 region (M5, gcAaaAtGg; M6, ttaacatGg; M7, caacaAtgG; capitalized letters indicate the position of nucleotide point substitutions and the created AUG start codon is underlined), and to remove the three σ C AUG codons upstream of the RL ORF in p σ C-RL and to introduce a stop codon in the p17 ORF (stp 517) to create plasmid pS1-RL. Point substitutions were also created in plasmids p Δ 366-751RL and p Δ 423-751RL within regions RBS1 and RBS2 to disrupt 18S complementarity.

2.4.2 Deletions And Insertions

The p17 ORF was N-terminally FLAG-tagged through the insertion of a triple FLAG sequence using an ApaI restriction site created through site-directed mutagenesis seven nucleotides downstream of the A of the p17 ATG start codon.

Plasmid pEGFP-S1 was created through the insertion of the ARV S1 sequence using the NotI restriction site into parental plasmid pEGFP-N1 (Clontech Laboratories, Inc), which is located downstream of the GFP ORF. Plasmid pS1-IRES-GFP was created by inserting the ARV S1 sequence into plasmid pEGFP-N1 using restriction sites HindIII and KpnI. The poliovirus IRES element was subsequently inserted using restriction sites KpnI and AgeI. The GFP ORF is located downstream of both the S1 and IRES sequences.

A stable ($\Delta G = -60$ kcal/mol) hairpin structure (hp7; Kozak, 1989a) was amplified from plasmid phpRLFL and was inserted into the 5'-end of p σ C-RL either between S1 nucleotides 1 and 2 using BamHI and NheI restriction sites (php σ C-RL), between S1 nucleotides 222 and 223 (p σ CRL-hp223) or between S1 nucleotides 579 and 580 (p σ CRL-hp579) using an NheI restriction site within p σ C-RL. The BamHI and NheI restriction sites within p σ C-RL were created by nucleotides point substitution (see Primer List, Appendix C) and the endonuclease sites were added to the 5' and 3' ends of the hairpin sequence through PCR.

Plasmid p β -RL was created by subcloning into plasmid pRL the β -globin 5'-UTR using restriction sites HindIII and BamHI. Plasmids with internal deletions in the S1 sequence were created by PCR amplification of the S1 5'-terminal region of interest from pARV-S1 using a forward primer with a HindIII restriction site and a reverse primer with a BamHI restriction site. These PCR amplicons and plasmid pRL were digested and

ligated together producing plasmids p Δ 628-751RL, p Δ 593-751RL, p Δ 483-751RL, p Δ 423-751RL, p Δ 393-751RL, p Δ 366-751RL, and p Δ 312-751RL. Plasmid p σ C-RL was also modified through the insertion of either 24 (mini-ORF1) or 78 (mini-ORF2) nucleotides between S1 nucleotides 304 and 305 using an ApaI restriction site on both termini of the insert. Plasmid p Δ 366-751intRL was created through the insertion of 114 nucleotides of heterologous sequence between S1 nucleotide 365 and the A of the RL start codon. Inserts in all plasmid constructs were confirmed by sequencing.

Primers used for PCR amplification that possessed restriction endonuclease sites at their 5'- and 3'-termini were created with six exogenous nucleotides followed by a restriction site of interest at the termini. The exogenous nucleotides were present to help recognition of the restriction site by the endonuclease. PCR products were resolved in 1% Tris acetate-EDTA agarose gels to visualize the PCR product and to determine whether the product was of the appropriate size. PCR products were extracted from gel slices using the QIAquick Gel Extraction kit (Qiagen) according to the manufacturer's instructions and digested with appropriate restriction endonucleases. Products of restriction digestions were purified using the QIAquick PCR purification kit (Qiagen), which removes the restriction enzymes and other impurities.

2.5 DNA Ligation

After vectors and inserts were digested with restriction enzymes, they were ligated together with T4 DNA ligase (Invitrogen). Either 3 μ l of insert and 3 μ l dH₂O or 10 μ l of insert was combined with 2 μ l vector, 2 μ l ligase buffer, 1 μ l of ligase enzyme and incubated at room temperature for 2 to 18 h.

2.6 Transformation Of *E. coli*

Competent DH5 α cells (100 μ l) were transformed with 5 μ l of either the DNA ligation reactions or DpnI-digested PCR products. Transformation reactions were kept on ice for 30 minutes and then transferred to a water bath set at 42°C for 90 seconds. The reactions were then transferred back to ice for a minimum of two minutes. The cells were then transferred to 900 μ l of LB medium and placed at 37°C for 45 minutes with vigorous shaking. Subsequently, the 1 ml cell suspension was pelleted and the excess medium

decanted. The transformed cells were resuspended and plated onto an LB-agar plate containing 1X ampicillin (1000X stock = 100 mg / ml). The plate was incubated overnight at 37°C.

A colony was selected and incubated in four ml LB medium with 1X ampicillin at 37°C with shaking for approximately 18 hours. The plasmid DNA was isolated using the QIAprep Spin Miniprep kit (Qiagen) according to the manufacturer's instructions. The DNA concentration was measured with a UV spectrophotometer (Eppendorf Biophotometer) at 260 nm.

2.7 Transfection

2.7.1 DNA Transfection

QM5 cells in 6-well cluster plates were transfected utilizing 6 µl Lipofectamine (Invitrogen) and 2 µg cDNA per well. The 2 µg of cDNA was supplemented with serum-free Medium 199 to a final volume of 200 µl. An additional 194 µl of serum-free Medium 199 was added to the 6 µl Lipofectamine. The two solutions were mixed together and left undisturbed at room temperature for 45 minutes. Following the incubation, the serum-containing medium was aspirated from the cells and the cells were washed twice with phosphate-buffered saline (PBS). Eight hundred microliters serum-free Medium was added to each well followed by drop-wise addition of the transfection mix. The cells were incubated for four hours at 37°C at which point the transfection mix was removed and replaced with 2 ml normal maintenance medium. The length of the incubation period varied depending on the experiment.

2.7.2 RNA Transfection

QM5 cells in a 48-well cluster plate were transfected with 1 µg of *in vitro* transcribed RNA and 1.5 µg polyethylenimine (PEI; Polysciences Inc.). The appropriate volume of RNA was first transferred to 25 µl RNase-free, serum-free Medium 199 in an RNase-free tube. The 1.5 µg PEI was added to 25 µl serum-free Medium 199, and the two solutions were then combined and allowed to sit at room temperature for 15 minutes. Following the incubation, the serum-containing Medium was aspirated off the cells, the cells were washed twice with RNase-free PBS and 200 µl RNase-free, serum-free

Medium 199 was added. The 50 μ l solution was then added drop-wise to the cells. The cluster plates were incubated at 37°C for four hours at which point they were harvested for the appropriate experiment.

To accurately perform qRT-PCR experiments (see section 2.15) on QM5 cells transfected with *in vitro* transcribed RNA, the RNA remaining on the outside of the cells at the time of harvesting had to be degraded. To this end, the minimum RNase A concentration necessary to degrade all input RNA, with either no incubation period or a four hour incubation period, was determined. RNase A-PBS solution, ranging in final concentration from 500 – 1000 μ g, was added to the cells and incubated at room temperature with intermittent rocking for four minutes. The cells were washed 4X with RNase-free PBS and the cells were harvested and subjected to qRT-PCR (described below).

2.8 Immunostaining

DNA-transfected QM5 cells were first washed with PBS and then fixed by the addition of ~1 ml of 100% methanol 24 hours post-transfection. Transfected foci were detected using the polyclonal anti- σ C antiserum, diluted 1:200 – 1:1000. Foci were visualized using a goat anti-rabbit secondary antibody conjugated to alkaline phosphatase (Jackson ImmunoResearch, diluted 1:800) and the Alkaline Phosphatase Substrate kit (Vector Laboratories Inc). Images were captured using a Zeiss Axiovert microscope (200X magnification) and Axiovision software.

2.9 Quantitative Western Blotting

QM5 cells in 6-well cluster plates were either singly or doubly transfected with the appropriate plasmid. Cells were lysed in radioimmunoprecipitation assay buffer (RIPA; 50 mM Tris pH 8.0, 150 mM NaCl, 1 mM EDTA, 1% NP₄₀, 0.5% NaDOC) 24 hours post-transfection. Lysate concentrations were determined according to the Lowry method (Lowry et al., 1951). Lysates were loaded onto the gel in either 2-fold serial dilutions or in 1 μ g decreasing increments. The final volume loaded was normalized between samples through the addition of 1X protein sample buffer. Proteins were separated in 15% SDS-PAGE gels and transferred to polyvinylidene difluoride (PVDF)

membranes utilizing the Bio-Rad Trans-Blot Cell (90 min, 100 volts). The membranes were then blocked in TBST (100mM Tris-HCl pH 8.0, 500mM NaCl, 0.1% Tween-20) containing 5% skim milk for one hour at room temperature. The membranes were incubated for an additional hour in fresh blocking solution containing the appropriate dilution of primary antibody. After the hour incubation with primary antibody, the membrane was washed three times with TBST for 5, 10 and 15 minutes. Fresh blocking buffer containing a 1:10,000 dilution of either goat anti-rabbit or goat anti-mouse horseradish peroxidase-conjugated secondary antibody was added and incubated with the membranes for one hour. The secondary antibody was then removed and blots were washed extensively with TBST as above. After the final wash, blots were exposed to ECL+ (Amersham Bioscience) for five minutes. The protein bands were visualized using the Typhoon 9410 Variable Mode Imager. The ImageQuant TL software (v.2003.02, Amersham Bioscience) was used to quantitate the bands. Regression analysis of pixel densities versus concentration was used to obtain the linear exposure range. Exposures were normalized to the actin control and σ C and p10 expression levels from the various mutant constructs were compared to the expression levels obtained from the parental S1 mRNA. The mean \pm standard error, from a minimum of three independent experiments, was used to calculate the percent change in expression levels and assessed for statistical significance using a two-tailed unpaired Student *t* test.

2.10 Antibodies

Polyclonal rabbit antisera raised against purified virus particles that contained σ C but not the nonstructural proteins, p10 and p17, was generated previously (Duncan, 1996). Polyclonal monospecific antiserum was raised in rabbits against the C-terminal domain of p10 using a purified maltose-binding protein-p10 chimeric protein expressed in *E. coli*. Christopher Barry provided the p10 antiserum. Additional rabbit antisera included sera specific for actin (Sigma) and human eIF4G (a gift from N. Sonenberg, McGill University). Mouse antiserum that recognizes enhanced green fluorescent protein (EGFP) (Clontech) or the FLAG epitope tag (Sigma) were also used. Horseradish peroxidase-conjugated goat anti-rabbit (KPL, Gaithersburg, MD) or anti-mouse (Jackson ImmunoResearch) immunoglobulin was used as a secondary for Western blot analysis.

2.11 Total RNA Extraction And RNA Purification

Total RNA was extracted from QM5 cells transfected with either DNA or RNA and used for Northern blot and quantitative PCR (qPCR) analysis. Twenty-four hours post-DNA transfection the serum-containing medium was aspirated off the cells and the cells were washed 3X with PBS. The cells were re-suspended with PBS-EDTA for five minutes and collected using a sterile rubber cell scraper and transferred to an RNase-free 1.5 ml tube. The cells were pelleted and the supernatant was removed. The pellet was re-suspended in 1 ml Trizol (Invitrogen) and homogenized by passage through a 29 gauge needle. The various phases were separated through the addition of 200 μ l chloroform. After chloroform addition, the tubes were vigorously shaken, incubated at room temperature for three minutes and then centrifuged at 12 000 rpm for ten minutes at 4°C. The upper aqueous phase was then transferred to a new RNase-free 1.5 ml tube. The RNA was precipitated and purified using the RNeasy Mini Kit (Qiagen). To ensure complete removal of any contaminating DNA, the samples were subjected to on-column DNase treatment utilizing the RNase-free DNase kit (Qiagen). The RNA concentration was measured with a UV spectrophotometer (Eppendorf Biophotometer) at 260 nm. Cells transfected with RNA were harvested four hours post-transfection. The serum-free medium was removed from the cells and replaced with 1X PBS. RNase A was added to the cells to a final concentration of 1 μ g/ μ l and cells were incubated for four minutes at room temperature with intermittent rocking. The cells were then washed four times with 1X PBS. All subsequent steps were performed as outlined for total RNA isolation from DNA transfected cells.

2.12 Northern Blotting

I would like to thank Kenneth Roy for performing the Northern blot presented in the thesis and I would like to thank Dr. Christine Barnes and Yahua Song for their technical assistance.

Total RNA (5 – 10 μ g) extracted from DNA-transfected QM5 cells was fractionated in formaldehyde gels for approximately four hours at 150 volts, and stained with ethidium bromide to reveal the 28S and 18S ribosomal RNA bands. The negatively charged RNA was transferred to Hybond membranes (Amersham Biosciences) through

upward capillary blotting using 20X sodium chloride sodium citrate (SSC) transfer solution. After overnight transfer, the membranes were removed from the transfer stacks and allowed to air dry for 20 minutes. The RNA present on the membrane was immobilized through UV cross-linking utilizing the auto cross-link setting (1200 μ joules) on the UV Stratalinker 1800 (Stratagene). The membrane was blocked in pre-hybridization buffer (1M sodium phosphate pH 6.5, 20X SSC, 50X Denhardt's, formamide, 10% SDS and salmon sperm DNA) at 42°C for approximately four hours. During the pre-hybridization incubation period an isotopically-labeled DNA probe was generated using a random primer probe generation kit (Invitrogen). Probe generation required the combination of 5 μ l gel-purified cDNA specific for the full-length S1 genome segment with dNTPs (lacking dGTP), random hexamers, α -³²P-dGTP, and the large Klenow fragment of DNA polymerase I. The probe was generated over a two-hour period at room temperature. Prior to addition to the pre-hybridization mix, the probe was incubated for ten minutes at 100°C and then on ice for five minutes and cleaned to remove any unincorporated radioisotope using a NICK column (Amersham). The membranes were hybridized at 42°C overnight. Post-hybridization the membranes were washed twice, 15 minutes each, in 2X SSC, 0.1% SDS at room temperature with shaking. The blots were then washed three times with 0.2X SSC, 0.1% SDS, heated to 65°C with shaking. Bound probe was detected by autoradiography with intensifying screens.

2.13 *In vitro* Transcription

Primers were designed to flank the region of interest, with the forward primer containing the T7 polymerase binding site. These primers, along with Vent polymerase (Invitrogen) were used to amplify the sequence of interest. The PCR amplicon was resolved in a 1% Tris acetate-EDTA agarose gels and 1 μ g of cDNA extracted from gel slices was used in the MEGAscript T7 *in vitro* transcription kit (Applied Biosystems) as per the manufacturer's instructions, or 0.25 μ g of the extracted cDNA was used in the mMessage mMachine T7 kit (Applied Biosystems), as per the manufacturer's instructions. A functional (3'-0-Me-7mG(ppp)G, New England Biolabs) or non-functional (ApppA, Sigma) cap analog was added to a final concentration of 6 mM to the MEGAscript reactions. After a 2-4 hour incubation at 37°C, 1 μ l of DNase Turbo was

added to the reactions to digest the template cDNA. The digestions were incubated for an additional 15 minutes at 37°C. At this point the RNA was purified using the RNeasy mini kit (Qiagen) according to the manufacturer's instructions. The RNA concentration was measured with a UV spectrophotometer (Eppendorf Biophotometer) at 260 nm.

2.14 *Renilla* Luciferase Assay

Four hours post-transfection of QM5 cells in 48-well culture dishes, the cells were harvested according to the *Renilla* luciferase assay system (Promega). Briefly, the medium was aspirated off the cells and then washed twice with 1X PBS. The cells were lysed in 50 µl of 1X *Renilla* Luciferase Assay Lysis Buffer for 15 minutes at room temperature with rocking. The lysate was transferred to a sterile microfuge tube and centrifuged at maximum speed for 20 seconds to pellet the cell debris. A 20 µl aliquot of the supernatant was transferred to a 1.5 ml microfuge tube. The *Renilla* Luciferase Assay Reagent was prepared immediately before use by combining 10 µl of 100X *Renilla* Luciferase Substrate per ml of *Renilla* Luciferase Buffer. Samples were read in a GloMax 20/20 luminometer (Promega) after the addition of 50 µl of assay reagent to the tube containing the lysate over a period of 10 seconds and a delay of 2 seconds. Sample results were recorded as relative light units (RLUs).

All constructs tested were *in vitro* transcribed a minimum of three separate times and were only compared to their respective parental clone *in vitro* transcribed on the same day. This minimized the effect of variable capping efficiencies on the different RNA preparations. Depending on the construct tested, the RLUs ranged from an average of four million RLUs for β-RL to 300,000 RLUs for σC-RL. The S1-RL WT averaged approximately 900,000 RLUs. The variability in RLUs observed depended on the quality of the RNA preparation and on the number of QM5 cells transfected.

2.15 Quantitative Reverse Transcription Polymerase Chain Reaction (qRT-PCR)

The Moloney murine leukemia virus reverse transcriptase was used to produce cDNA through reverse transcription of 0.25 or 0.5 µg of purified total RNA. The cDNA was subjected to real time PCR utilizing either the SuperScript III Platinum Two-Step qRT-PCR Kit with SYBR Green (Invitrogen) or the QuantiFast SYBR Green PCR kit

(Qiagen). The former kit employed the MX3000p thermocycler (Stratagene) with an amplification protocol that consisted of a 10 minute hot start at 95°C, followed by 40 cycles of denaturation at 95°C for 30 seconds, annealing at 65°C for 1 minute, and elongation at 72°C for 30 seconds. The latter kit utilized the MX3000p thermocycler with an amplification protocol of a 5 minute hot start at 95°C, followed by 40 cycles of denaturation at 95°C for 10 seconds and annealing at 60°C for 30 seconds. Melting curves, as well as separation of PCR products on a 1% Tris acetate-EDTA agarose gel, were used to ensure the formation of a single product of the appropriate size. Relative gene expression normalized to β -actin expression was calculated using the $\Delta\Delta C_T$ method (Livak and Schmittgen, 2001). Briefly, a standard curve was created for the parental and endogenous control (actin) samples by performing 4-fold serial dilutions. The C_T values of duplicate ARV samples, parental or mutant, were averaged and then normalized to the average C_T value for the endogenous control obtained at the same dilution (ΔC_T). The ΔC_T value obtained for the mutant sample is subtracted from the ΔC_T value obtained from the parental sample, giving $\Delta\Delta C_T$. The relative change in transcript expression is then determined by calculating $2^{-\Delta\Delta C_T}$. The concentration of parental and mutant RNA within the cell is believed to equal if the relative change in expression ranged between 0.5 – 1.5-fold.

CHAPTER 3: Results

3.1 Expression From The Internal σ C Start Site Occurs Efficiently From A Full-Length Tricistronic mRNA

The unusual tricistronic arrangement of ORFs on the ARV S1 genome segment and the lack of correlation between expression of the 5'-proximal p10 ORF and the 3'-proximal σ C ORF (Shmulevitz et al., 2002) suggests expression of σ C is dependent on some atypical mechanism of translation initiation. Alternative explanations would be the presence of cryptic splice sites or promoters, or the ability of mRNA to be degraded upstream of an internal start site could potentially lead to the production of monocistronic mRNA from what was thought to be polycistronic mRNA (Hellen and Sarnow, 2001; Kozak, 1999). To ensure that such a trivial explanation is not responsible for expression of the σ C ORF, plasmid pARV-S1 was transfected into QM5 cells and S1-specific transcripts were detected by Northern blotting (Figure 8A). As expected, a single species of S1-specific mRNA was observed migrating slightly ahead of the ~1850 nucleotide 18S rRNA. This indicates that the primary S1 transcript in plasmid-transfected cells is the full-length mRNA, and as such, translation initiation at the σ C start site must occur downstream of two functional ORFs.

It is well documented that the presence of uORFs can have a regulatory effect on downstream cistron expression (Kozak, 2002; Meijer and Thomas, 2002; Morris and Geballe, 2000; Mueller and Hinnebusch, 1986). To examine the influence the four AUGs upstream of the σ C start site have on σ C translation initiation efficiency, all methionine codons upstream of σ C were point substituted to AUC to generate a plasmid carrying a monocistronic version of the S1 mRNA (pS1-Mono), where the σ C start codon is the most 5'-proximal AUG. Transfection of pS1-Mono followed by quantitative Western blot analysis (Figure 8B; discussed below) revealed an average 2.3-fold increase in σ C expression compared to the wild-type polycistronic transcript (Figure 8C). The uAUGs in the S1 mRNA therefore do exert some inhibitory effect on σ C translation, but it is relatively minor. By comparison, removal of the uORFs in the yeast *GCN4* or mouse ATF4 mRNAs stimulates translation of the major downstream ORF by 74-500-fold (Harding et al., 2000; Mueller and Hinnebusch, 1986). The 2.3-fold increase in σ C

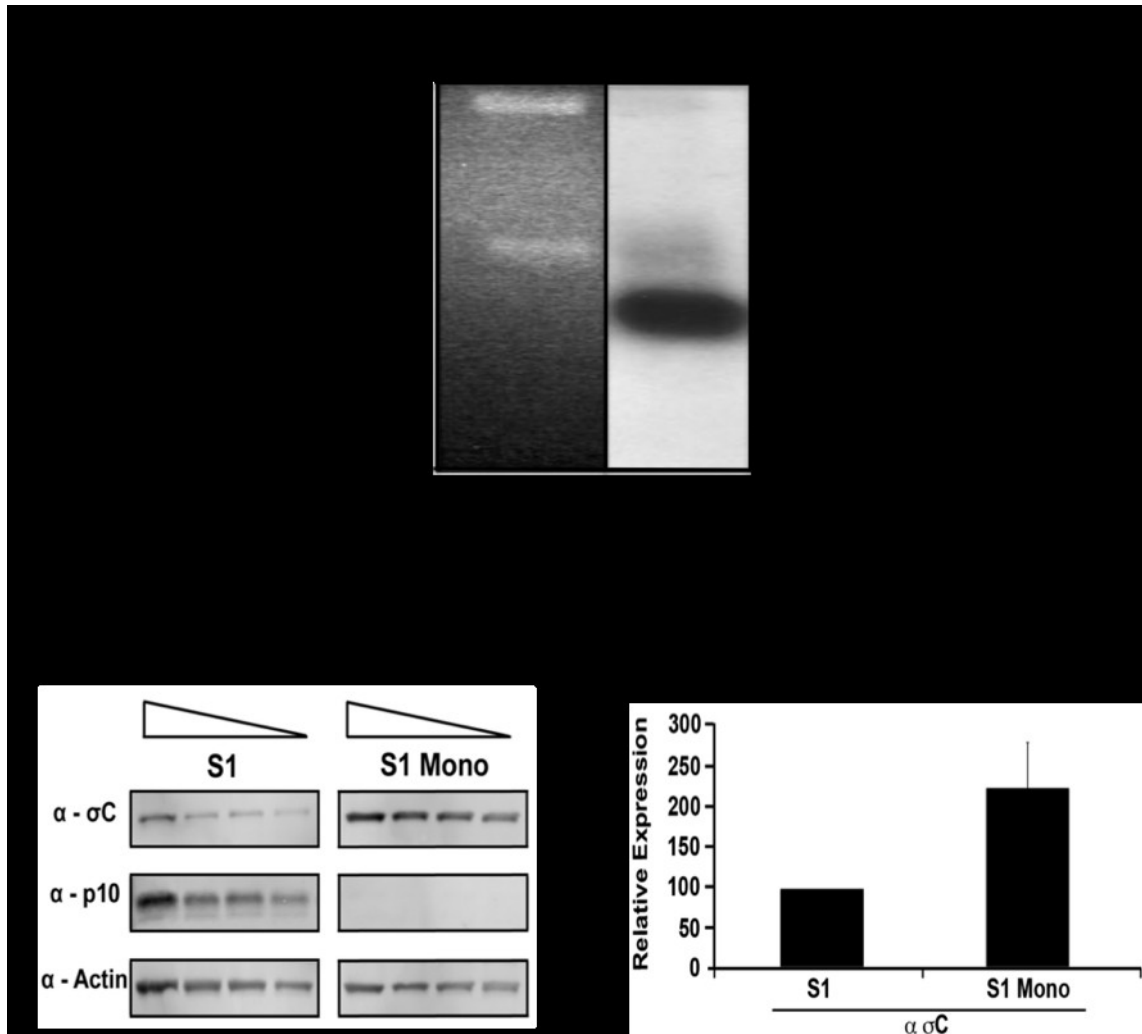


Figure 8. Translation of the σC ORF occurs from a full-length tricistronic mRNA with reasonable efficiency. **A.** S1-specific mRNA present within QM5 cells transfected with plasmid pARV-S1 as detected by Northern blotting. The left lane represents the ethidium bromide stained agarose gel loaded with 8 μ g total RNA extracted from QM5 cells, indicating the location of the 28S and 18S ribosomal RNA bands. The right lane represents the autoradiogram of the same gel indicating the location of the full-length S1 mRNA. **B.** Plasmids pARV-S1 and pS1-Mono were transfected into QM5 cells, cell lysates were harvested 24 hr post-transfection and run on a 15% SDS-PAGE gel in 1 μ g decreasing amounts to obtain a linear detection range. Expression of p10 and σC was detected with anti-sera specific for these polypeptides. The same blot was probed with an anti-actin antibody as a protein loading control. **C.** Quantitative analysis of two experiments indicating the mean \pm S.E. of the relative expression levels of σC in cells transfected with pARV-S1 (S1) and pARVS1-Mono (S1 Mono), normalized to the actin control and to expression in pARV-S1 transfected cells. Panel A provided by Kenneth Roy.

expression therefore suggests that ribosomes are normally capable of accessing the 3'-proximal cistron in a relatively efficient manner.

3.2 Quantitative Western blot analysis

The ability to detect subtle changes in protein concentration via Western blot analysis requires precise measurement of the intensity of density of protein bands that must be within the linear range of detection. To establish whether the cell lysates loaded onto the 15% SDS-PAGE gel, as in Figure 8B and all subsequent Western blots, were within the linear range, the lysates were loaded in amounts that successively decreased by 1 μg (i.e. 6, 5, 4, or 3 μg of cell lysate) and were exposed to saturating concentrations of primary antibody (i.e. 1/2500 dilution of p10, σC or actin antisera). The pixel densities obtained from the quantified protein bands were plotted versus protein concentration (Figure 9). Regression analysis provided an equation for the line in the form $y = mx + b$. By using the pixel densities obtained for each concentration, for each band detected, as the x value, the equation was solved for y. The results from each regression analysis were assigned variables; for example, the pixels obtained from the actin bands detected from the p10opt construct were designated Y1, the actin bands from the parental construct were designated Y2, the p10 bands detected from the parental sample were designated Y3, and the p10 bands detected from the p10opt construct were designated Y4. The first step in determining fold-change in protein concentration required the examination of actin band densities. Theoretically, the actin band densities should be equal because actin is stably expressed and thus should be present at comparable levels within different cell lysates of similar concentration. To compare actin band intensities, Y1 was divided by Y2. The normalized actin levels were then applied to the p10 band densities obtained from the parent S1 sample, $(Y1/Y2)Y3$. This corrects the p10 band density from the S1 sample for differences observed between the loading controls. The p10 pixel densities obtained from the p10opt construct were then divided by the actin normalized p10 band densities from the S1 construct, giving a final overall equation of $Y4/((Y1/Y2)Y3)$. This equation was applied to each concentration loaded and the average value obtained represents the percent change in protein concentration from the altered S1 mRNAs (in this example p10opt) relative to the expression from the authentic S1 mRNA. This

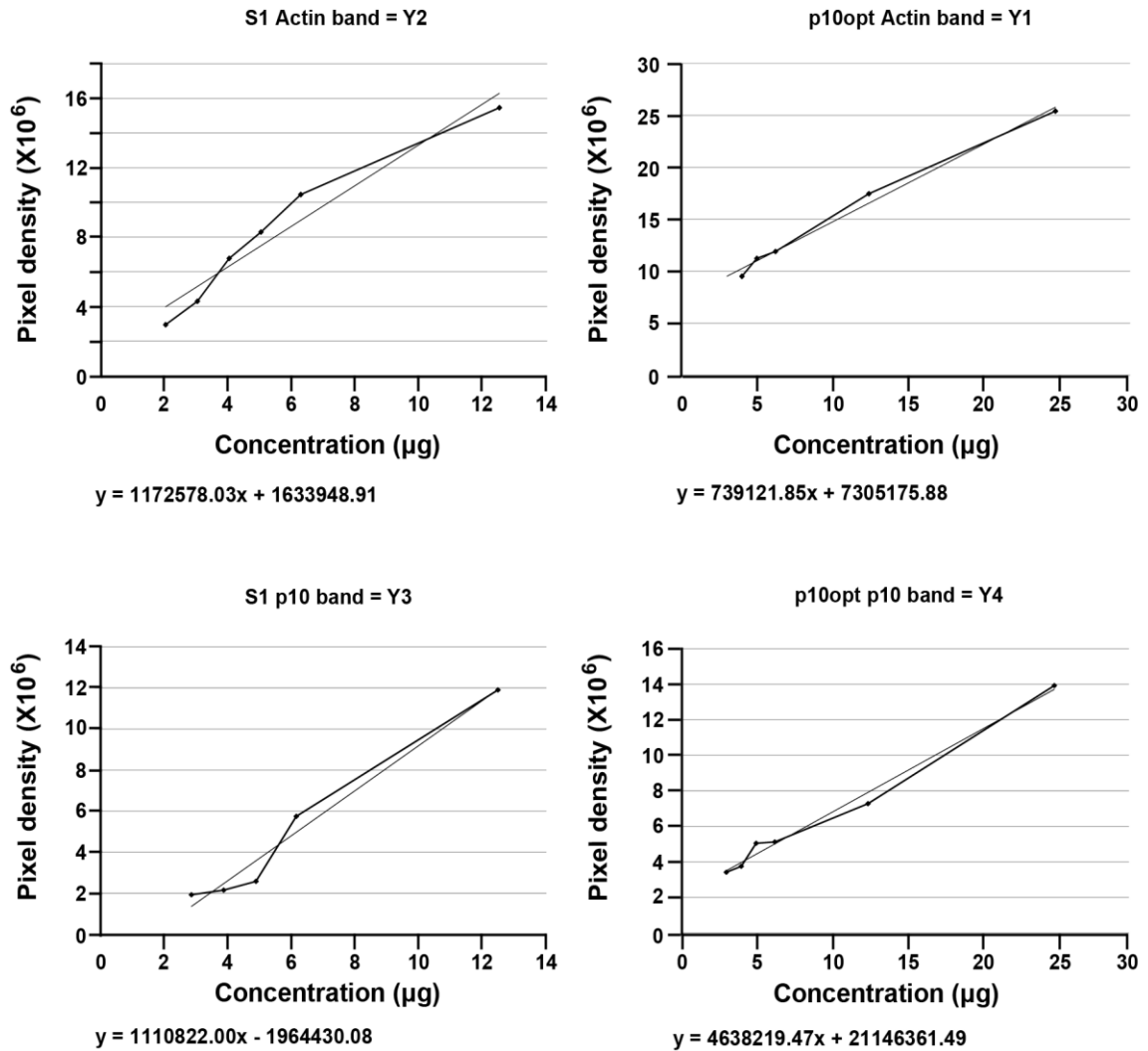


Figure 9. Analysis of pixel densities obtained by quantitative Western blot analysis. Graphical representation of the pixel densities obtained for the actin and p10 protein bands from pARV-S1 (S1) and p10opt constructs. The pixel densities were plotted against sample concentration loaded on the 15% SDS-PAGE gel. A trendline was created to obtain an equation for the line ($y = mx + b$). The equation was solved by inserting the pixel density obtained for each concentration for value x. The value obtained for y was used to normalize the pixel densities for actin concentration, which was then used to determine the fold-change in p10 band intensity obtained from p10opt compared to the parental S1 mRNA.

mathematical method of comparing pixel densities between samples was used to compare p10 and σ C concentrations from all plasmid-transfected mutant constructs to the protein concentrations obtained from pARV-S1.

3.3 Leaky Scanning Coordinates Expression Of The p10 And p17 ORFs, But Has Minor Effects On σ C Expression

Both the p10 and p17 start codons reside in a sub-optimal context, as defined by the kozak consensus sequence (p10, cgUcgAUGC; p17, gcAcaAUGC), which may explain their inability to exert any substantial effect on translation of the σ C ORF (Kozak, 2002). To explore this possibility further, the p10 and p17 start codons were individually point mutated to create the optimal Kozak consensus sequence (ccAccAUGG), generating two different expression plasmids p10opt and p17opt (Figure 10A). Due to the low specificity of the p17 antiserum (Shmulevitz et al., 2002), I N-terminally tagged the p17 ORF with the FLAG epitope in the S1, p10opt and p17opt constructs (FLAGp17, p10optFLAGp17 and p17optFLAGp17, respectively). Western blot analysis of QM5 cells transfected with the FLAG-tagged constructs revealed an approximate eight-fold decrease in p17 protein levels upon p10 start codon optimization (Figure 10B). These results are consistent with previous studies indicating that optimization of a start site in a sub-optimal context prevents the majority of downstream initiation by inhibiting leaky scanning (Kozak, 1984a; Kozak, 1986b). Optimization of the p17 start codon context had only a slight enhancing effect on p17 protein levels (~2-fold), most likely because the p17 AUG codon naturally resides in a good context with an A in the -3 position. Together, these results demonstrate that leaky scanning coordinates p10 and p17 expression.

To examine the effect optimized p10 and p17 start codons have on σ C expression, plasmids pARV-S1, p10opt and p17opt, all lacking the p17 N-terminal FLAG tag, were transfected into QM5 cells and the cell lysates were fractionated by SDS-PAGE using 1 μ g decreasing amounts to obtain the linear range of detection (Figure 11A). The relative mRNA levels were also quantified using qRT-PCR and the $\Delta\Delta C_T$ method (Livak and Schmittgen, 2001). In no instance did the change in protein levels correlate with a variation in mRNA levels, indicating that the change in p10 and σ C production is a consequence of differences in translation initiation. Quantitative analysis of multiple

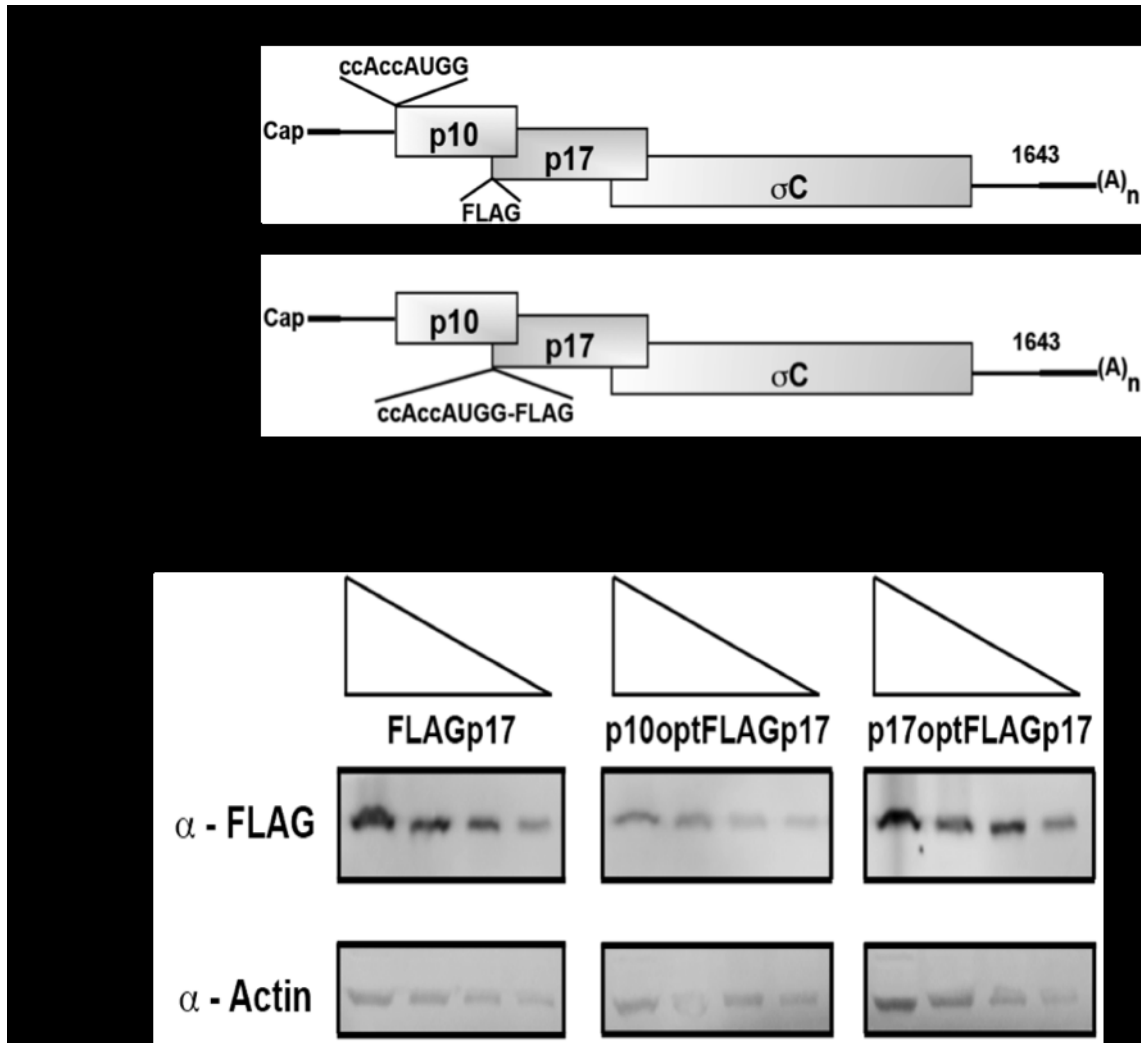


Figure 10. Optimization of the p10 start site inhibits p17 production. A. Plasmid pARV-S1 was modified by optimizing the context of either the p10 or p17 start codons (p10opt and p17opt) to conform to the optimal start sequence depicted (ccAccAUGG) and through the insertion of a FLAG-tag in-frame with the p17 start codon (p10optFLAGp17 and p17optFLAGp17). B. Western blot detection of the p17 polypeptide N-terminally tagged with the FLAG epitope from the parental plasmid (FLAGp17) and its modified versions after transfection into QM5 cells and loading of cell lysates in 2-fold serial dilutions. The same membrane was probed with an anti-actin antibody as a protein loading control.

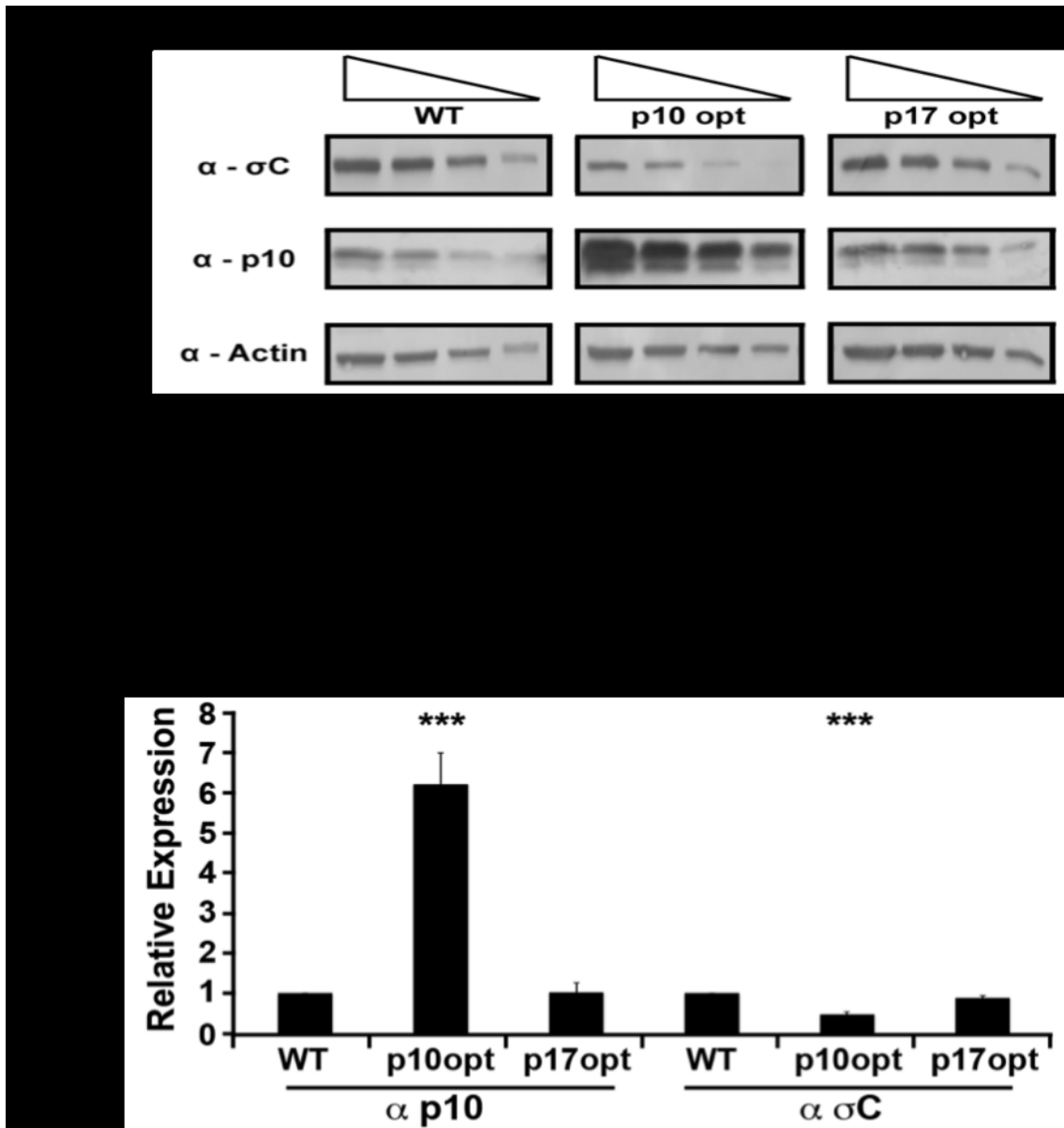


Figure 11. Optimization of either the p10 or p17 start sites, in a plasmid-based construct, exerts little effect on σ C expression. Western blot detection of polypeptides p10 and σ C from the parental plasmid (WT) and its modified versions (p10opt and p17opt) after transfection into QM5 cells and loading of cell lysates in 1 μ g decreasing increments to obtain the linear range of detection. The same blot was probed with an anti-actin antibody as a protein loading control. **B.** Quantitative analysis of several experiments (n = 7) indicating the mean \pm S.E. of the relative levels of p10 and σ C in cells transfected with pARV-S1 (WT), p10opt, or p17opt plasmids, normalized to the actin control and to expression in pARV-S1 transfected cells.

Western blots (n=7), utilizing antisera against polypeptides p10 and σ C, revealed a significant 6.1 ± 0.8 -fold increase in p10 expression in cells transfected with the p10opt construct relative to cells transfected with either pARV-S1 or p17opt (Figure 11B). However, this substantial increase in uORF expression did not inhibit σ C protein production to the extent expected from the literature (Futterer et al., 1997; Sedman and Mertz, 1988). Optimization of the p10 start site reduced expression of the σ C ORF to $52 \pm 6\%$ of the levels obtained from pARV-S1. Optimization of the p17 start codon, on the other hand, had no significant effect on σ C production, with σ C expression inhibited by only $19 \pm 9\%$ compared to expression from pARV-S1 (Figure 11B).

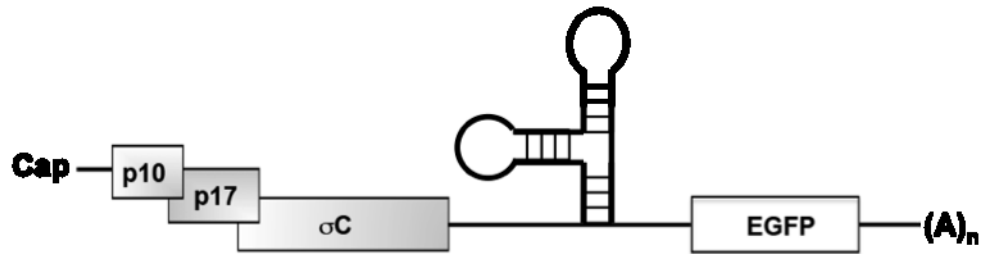
Results obtained by removal of the sub-optimal upstream start sites (Figure 8C) and optimization of the p10 and p17 start codons (Figure 11) indicate that the uORFs play only a minor role in ribosome access to the internal σ C start site. They also indicate that leaky scanning is most likely not the main mechanism by which ribosomes initiate translation at the σ C AUG on the full-length S1 mRNA, and that however ribosomes are accessing the internal start site, they are doing so in a reasonably efficient manner.

3.4 Translation Of σ C Is IRES-Independent

The S1 mRNA was next examined for the presence of an IRES element through the use of the “bicistronic” assay (Pelletier and Sonenberg, 1988). As a positive control for IRES activity, a bicistronic construct was created where the EGFP ORF, preceded by the poliovirus IRES, was cloned downstream of the ARV S1 mRNA (Figure 12A). Expression of EGFP in QM5 cells, detected by Western blotting, indicated the IRES element is capable of recruiting ribosomes to the EGFP start codon (Figure 12B). Co-transfection of this bicistronic vector along with plasmid pPV2A, which expresses the poliovirus 2A protease, resulted in a 4-fold increase in EGFP expression and a marked decrease in cap-dependent p10 expression (Figure 12B, +2A). This result was consistent with previous studies showing that the 2A protease is capable of inhibiting cap-dependent translation initiation and consequently increasing cap-independent IRES-mediated expression (Barco, Feduchi, and Carrasco, 2000; Lloyd, 2006).

To directly test whether the S1 mRNA possesses an IRES element capable of aiding in σ C expression, a bicistronic construct was created where the S1 sequence was

A.



B.

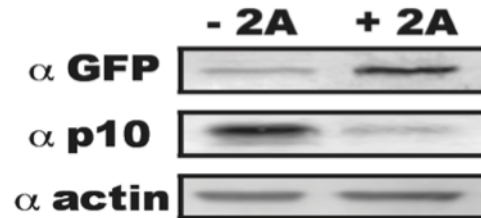
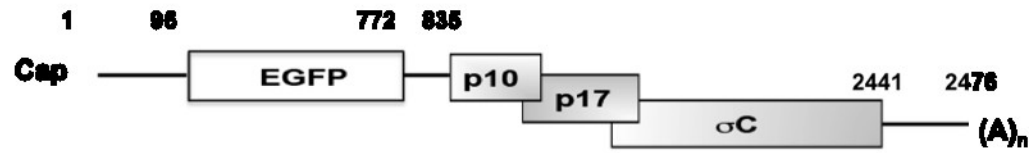


Figure 12. The poliovirus 2A protease is capable of enhancing IRES activity in a bicistronic construct. **A.** Diagram of a “bicistronic” construct designed where the entire ARV S1 sequence was cloned upstream of the poliovirus IRES element (structured element) and the green fluorescent protein (EGFP) ORF. **B.** QM5 cells were co-transfected with the bicistronic construct and either empty pcDNA3 vector (-2A) or pPV2A (+2A) and the expression of GFP and p10 were observed via Western blotting using antibodies specific for these proteins. The same membrane was probed with an actin-specific antibody as a protein loading control.

A.



B.

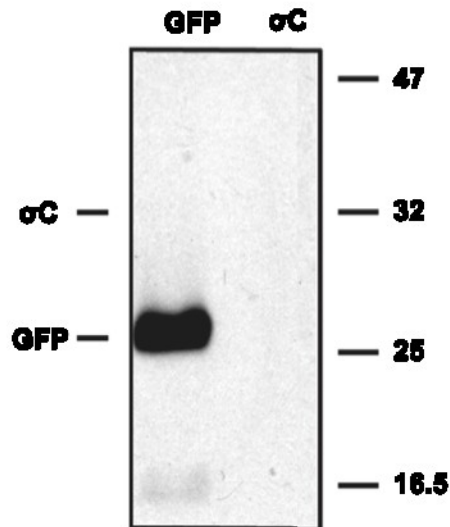


Figure 13. The ARV S1 genome segment does not display IRES activity. **A.** Diagram of a “bicistronic” construct where the authentic ARV S1 mRNA sequence was cloned downstream of the EGFP ORF. **B.** The bicistronic construct was transfected into QM5 cells and the expression of EGFP and σ C was detected by immunoprecipitation, SDS-PAGE, and autoradiography. The location of the expressed GFP protein and predicted location of the σ C protein are indicated on the left, while the molecular weight standards (kDa) are indicated on the right. Immunoprecipitation provided by Kenneth Roy.

cloned downstream of the EGFP ORF (Figure 13A). Radioimmunoprecipitation revealed high levels of the 5'-proximal EGFP protein, whereas no σ C protein was detected, even upon extended exposure of the fluorograms (Figure 13B and data not shown). If an IRES element is present within the S1 mRNA, expression of the 2A protease might be expected to show increased levels of either p10, p17 or σ C protein levels. Therefore, the S1 mRNA was co-expressed with the 2A protease in QM5 cells (see Figure 14B). Expression of the σ C ORF was actually inhibited instead of enhanced, as assessed by immunoprecipitation, indicating that the S1 mRNA does not possess an IRES element capable of allowing ribosomes access to the internal σ C start site.

3.5 Expression Of The σ C ORF Occurs In An eIF4G-Dependent Manner

Since IRES-mediated initiation is the only known alternate translation mechanism that functions in a cap-independent manner, it seemed prudent to determine whether expression of the σ C cistron was cap-dependent. The plasmid transfection procedure prevents direct comparison of σ C expression from capped and uncapped mRNAs as all mRNAs transcribed in the nucleus become capped at their 5'-ends (Perry and Kelley, 1976; Rasmussen and Lis, 1993). As an indirect test for cap-dependency, the role of eIF4F, the cap-binding complex, on the mechanism of translation initiation at the σ C start site was explored through the use of the poliovirus 2A protease. The poliovirus 2A protease cleaves eIF4G, a component of eIF4F, thus inhibiting eIF4G binding to eIF4E and subsequent 40S ribosomal recruitment to the 5'-end of the mRNA (Etchison et al., 1982). In cells co-transfected with 2A protease and GFP (plasmids pPV2A and pEGFP-N1), a dose-dependent reduction in EGFP expression was observed both by fluorescence microscopy (Figure 14A, *panels a and b*) and immunoprecipitation (Figure 14B). A similar dose-dependent reduction in σ C expression was also obtained when the pPV2A plasmid was co-transfected with the pARV-S1 expression plasmid indicating that translation initiation of the S1 ORFs requires intact eIF4G. Immunostaining cells co-transfected with full-length plasmid borne S1 (pARV-S1) and empty vector, with a polyclonal antiserum that recognizes σ C indicated antigen-positive multinucleated syncytial foci (Figure 14A, *panel c*). Co-transfection of QM5 cells with a plasmid carrying 2A protease (pPV2A) (Figure 14A, *panel d*) not only reduced the number of

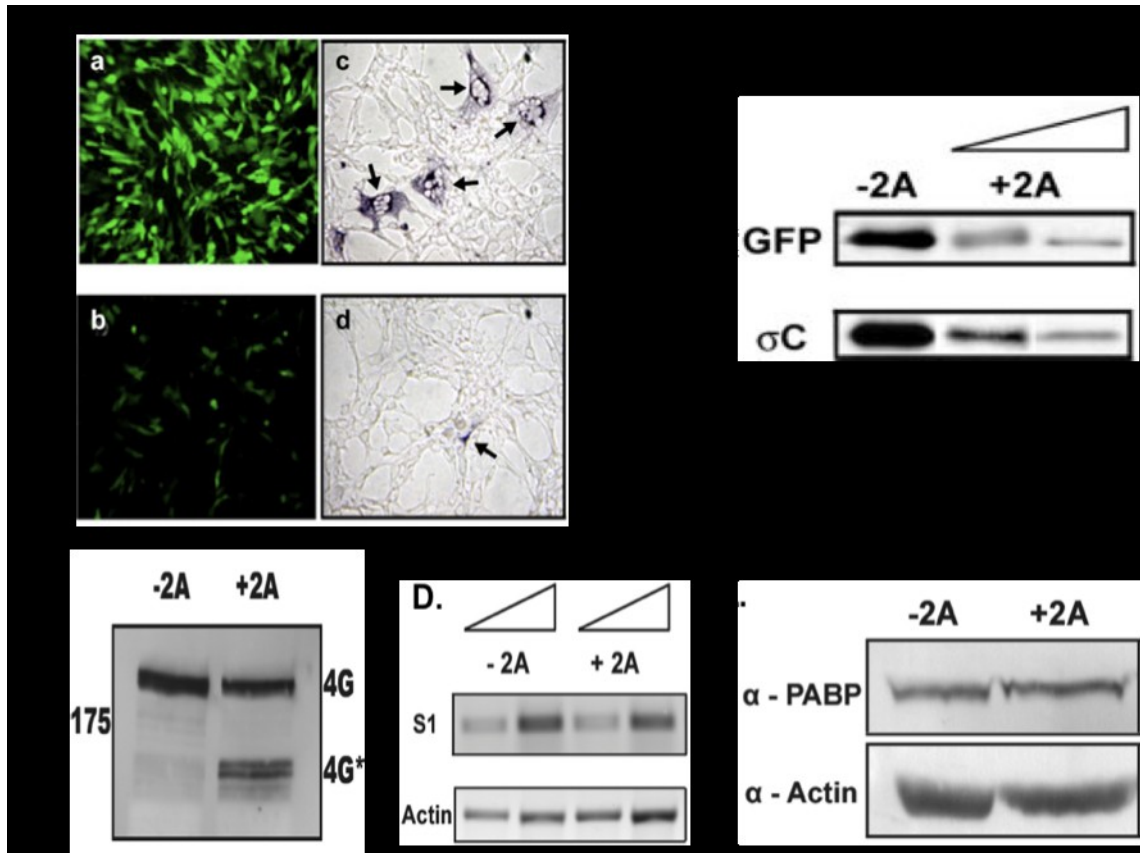


Figure 14. Expression of σC is eIF4G-dependent. **A.** Cells were co-transfected with pEGFP (Panels A and B) or pARV-S1 (Panels C and D) along with either empty vector (Panels A and C) or pPV2A (Panels B and D). Expression of EGFP was assessed by fluorescent microscopy (Panels A and B), while expression of σC was assessed by immunostaining using a polyclonal antibody that recognizes σC (Panels C and D). The presence of antigen positive (Panels C and D) and multinucleated cells (Panel C) is due to the expression of the σC and p10 proteins, respectively (arrows). **B.** Cells were co-transfected with pEGFP (GFP lanes) or pARV-S1 and either empty vector (-2A) or pPV2A in a 1:1 or 1:2 DNA ratio (+2A). Radiolabeled EGFP or σC expression was assessed by immunoprecipitation. **C.** Lysates from QM5 cells transfected with either empty vector (-2A) or pPV2A (+2A) were examined for eIF4G integrity by Western blot analysis with an antibody that recognizes eIF4G and its cleavage products. The gel mobility of molecular weight standards (kDa) are indicated on the left, while the location of the intact (4G) and the protease cleaved (4G*) products are indicated on the right. **D.** RNA was extracted from QM5 cells co-transfected with pARV-S1 and either empty vector (-2A) or pPV2A (+2A) and subjected to RT-PCR. Two-fold serial dilutions of the amplicons were visualized on an agarose gel stained with ethidium bromide. **E.** Lysates from cells transfected with either empty vector (-2A) or pPV2A (+2A) were analyzed by SDS-PAGE and Western blotting using a polyclonal antibody that recognizes the poly(A) binding protein (PABP). The membrane was also probed with an anti-actin antibody as a loading control. Panels A and B provided by Kenneth Roy.

antigen-positive cells, but also markedly decreased the number of syncytia. These results indicate that σ C expression is eIF4G-dependent, and so is expression of the p10 ORF, the protein solely responsible for syncytium formation (Shmulevitz and Duncan, 2000).

To confirm that transfection with the plasmid expressing the 2A protease resulted in cleavage of eIF4G, lysates of QM5 cells transfected with either empty vector (-2A) or pPV2A (+2A) were subjected to Western blot analysis using a polyclonal anti-eIF4G antibody (Figure 14C). The approximate 50% cleavage efficiency of eIF4G into its predicted products (Etchison et al., 1982; Ventoso et al., 1998) in the presence of 2A protease agrees with the transient transfection efficiency of QM5 cells, suggesting that 2A cleaves eIF4G efficiently.

The presence of 2A protease in cells results not only in cleavage of eIF4G and subsequent translation inhibition, but can also result in a decrease in DNA replication and inhibition of transcription (Davies et al., 1991). To ensure that the inhibition of σ C translation observed in the presence of 2A protease was directly related to eIF4G cleavage and not a reduction in transcript levels, semi-quantitative RT-PCR was performed on cells co-transfected with pARV-S1 and either empty vector (-2A) or pPV2A (+2A; Figure 14D) to measure transcript levels. Under co-transfection conditions, which result in a >90% reduction in σ C expression, S1 transcript levels are unaffected (Figure 14D, compare +2A and -2A). These results were further confirmed using qRT-PCR experiments (n=3) that indicated no significant change in S1 transcript levels in the presence of 2A protease (data not shown). The other 5' canonical translation initiation factors (eIF4E, eIF4A, eIF4B and eIF3) are not altered by the 2A protease (Duncan, Etchison, and Hershey, 1983; Etchison et al., 1984; Lee, Edery, and Sonenberg, 1985). Two independent groups have reported however, that the enterovirus and coxsackievirus 2A proteases are capable of cleaving PABP (Joachims, Van Breugel, and Lloyd, 1999; Kerekatte et al., 1999). The presence of PABP on the poly(A) tract of mRNAs is known to enhance translation of those mRNAs (Gallie, 1991; Jackson and Standart, 1990). It was therefore possible that cleavage of PABP might contribute, at least in part, to the inhibition of σ C translation observed in the presence of the poliovirus 2A protease. However, Western blot analysis of protein lysates of cells transfected with 2A protease (pPV2A) showed no cleavage of endogenous PABP (Figure 14E). These results suggest

that the 2A protease is capable of cleaving eIF4G and that the mechanism responsible for σ C expression is reliant upon an intact eIF4G, and by inference, an intact eIF4F complex.

3.6 Reinitiation Is Not Responsible For σ C Translation Initiation

It was previously postulated that ribosomes access the σ C start site through cap-dependent translation of the 5'-proximal p10 ORF, followed by translation termination and reinitiation at the σ C start codon (Kozak, 2002). Such a mechanism is thought to aid the 40S ribosomal subunit in bypassing the relatively strong context that surrounds the p17 start site, as the p10 ORF terminates downstream of the p17 start codon. This is a plausible mechanism in that the length of the intercistronic region between the end of the p10 ORF and the σ C start site is of an adequate distance (308 nucleotides) to allow the 40S ribosomal subunit to reacquire the initiation factors needed to commence another round of translation (Abastado et al., 1991; Kozak, 1987c; Luukkonen, Tan, and Schwartz, 1995; Pelletier and Sonenberg, 1988). Also, there are no AUG triplets present in any of the three reading frames in this downstream region that would cause a scanning 40S subunit to reinitiate before reaching the σ C start codon. However, reinitiation does not normally occur after translation of an ORF greater than \sim 30 codons (Hwang and Su, 1998; Kozak, 2001a; Luukkonen, Tan, and Schwartz, 1995; Ryabova, Pooggin, and Hohn, 2006). Since the p10 ORF encodes a functional polypeptide 98 amino acids long, it is unlikely that σ C expression is due to reinitiation upon termination of the p10 ORF. To test this hypothesis, the p10 ORF was shortened by progressively truncating nucleotides from the 5'-end (Figure 15A), and the effects of these truncations on p10 and σ C expression were measured via quantitative Western blot analysis (Figure 15B). Deletion of the 5'-proximal 79 (pARV- Δ 79) or 147 (pARV- Δ 147) nucleotides, which removed the 5'-UTR and either 55 or 123 nucleotides of the p10 ORF, eliminated both p10 and σ C expression. Further deletion of the S1 mRNA to nucleotide 303, which removes not only the p17 start site found at nucleotide 293 but also the final methionine codon upstream of the σ C ORF at nucleotide 298, restored σ C production. The 1.7 ± 0.4 -fold increase in σ C expression (n=3) obtained from pARV- Δ 303, a plasmid that would produce a monocistronic S1 mRNA, closely paralleled the 2.3-fold increase in σ C expression seen from pARVS1-Mono (Figure 8C), although neither of these increases

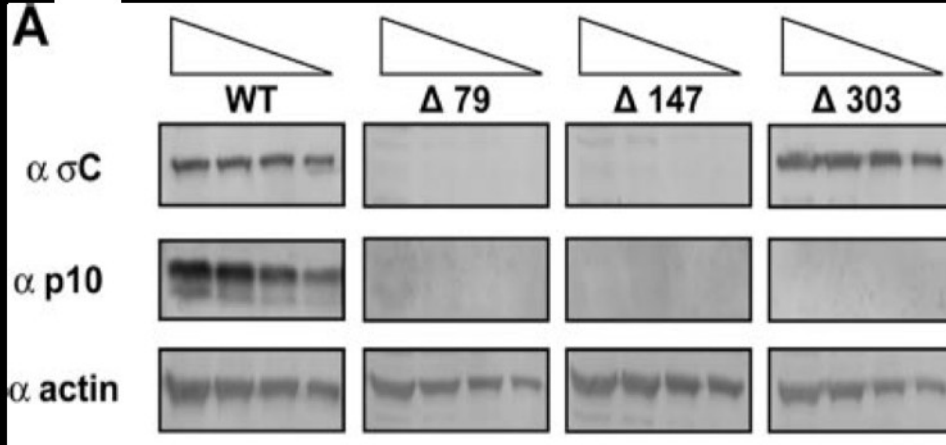
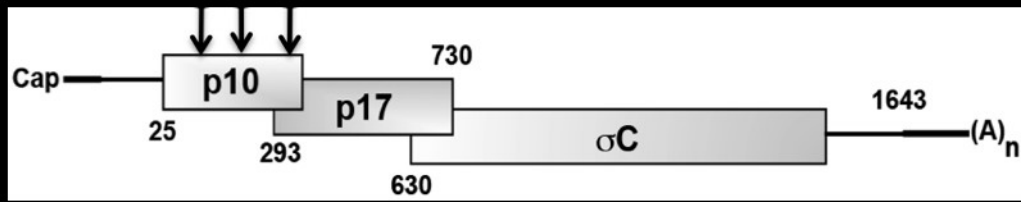


Figure 15. The 5'-proximal region of the S1 mRNA is required for downstream initiation when expressed from a DNA plasmid. **A.** Diagram of the ARV S1 mRNA transcribed from a plasmid, indicating the location of the progressive 5'-truncations ($\Delta 79$, $\Delta 147$, and $\Delta 303$; numbers refer to the number of 5'-terminal nucleotides deleted from S1). **B.** Expression of the p10 and σC polypeptides as detected via Western blot analysis from QM5 cell lysates transfected with pARV-S1 (WT) or the 5' truncations. Lysates were loaded in 1 μ g decreasing amounts in order to obtain the linear range of exposure. The membrane was also probed with an anti-actin antibody as a loading control.

was significant.

The truncation results were consistent with the idea that the p17 AUG triplet is a strong barrier to scanning ribosomes and that σ C expression may rely on the reinitiation of ribosomes terminating p10 ORF translation for expression. To directly test this hypothesis, a stop codon (CGT to TGA) was created in the plasmid pARV-S1 at nucleotide 243 (p10 stp243) through site-directed mutagenesis (Figure 16A). Ribosomes could now terminate p10 translation 50 nucleotides upstream of the p17 start site and thus could reinitiate at the p17 start codon. Quantitative Western blot analysis of cell lysates revealed expression of a truncated form of the p10 protein (Figure 16B). Contrary to the reinitiation hypothesis however, premature termination of the p10 ORF did not have a deleterious effect on σ C expression, which actually displayed a slight 1.6 ± 0.06 -fold increase in expression (n=3). To ensure that the distance between p10 termination and putative reinitiation at p17 was not an issue, another plasmid was created where a stop codon (TGT to TGA) was introduced within the p10 reading frame at nucleotide 84 (p10stp84). The RNA expressed by this plasmid should be ideal for reinitiation at p17 in that it creates a p10 “minicistron” that is only 28 codons long and increases the intercistronic distance between p10 and p17 to 209 nucleotides. Again, quantitative Western blot analysis demonstrated no inhibition in σ C expression indicating that reinitiation is most likely not responsible for translation initiation at the σ C start site.

3.7 S1 RNA Transfection Results In Inefficient Protein Expression For Detection By Western Blot

As mentioned in the introduction (section 1.11), the RdRp present within the ARV core particle produces an unspliced, capped, non-polyadenylated S1 mRNA in the cytoplasm. In contrast, nuclear transcription of pARV-S1 results in a capped S1 mRNA that is spliced and polyadenylated. In addition to the poly(A) tail, the plasmid expression vector also creates heterologous sequence at the 5'- and 3'-ends of the S1 mRNA derived from plasmid pcDNA3 due to the location of the CMV promoter transcription start site and stop sites. The differences in virus-driven cytoplasmic transcription and plasmid-derived nuclear transcription could potentially affect translation initiation on the tricistronic S1 mRNA. Before further analysis of the *cis* factors that influence ribosome

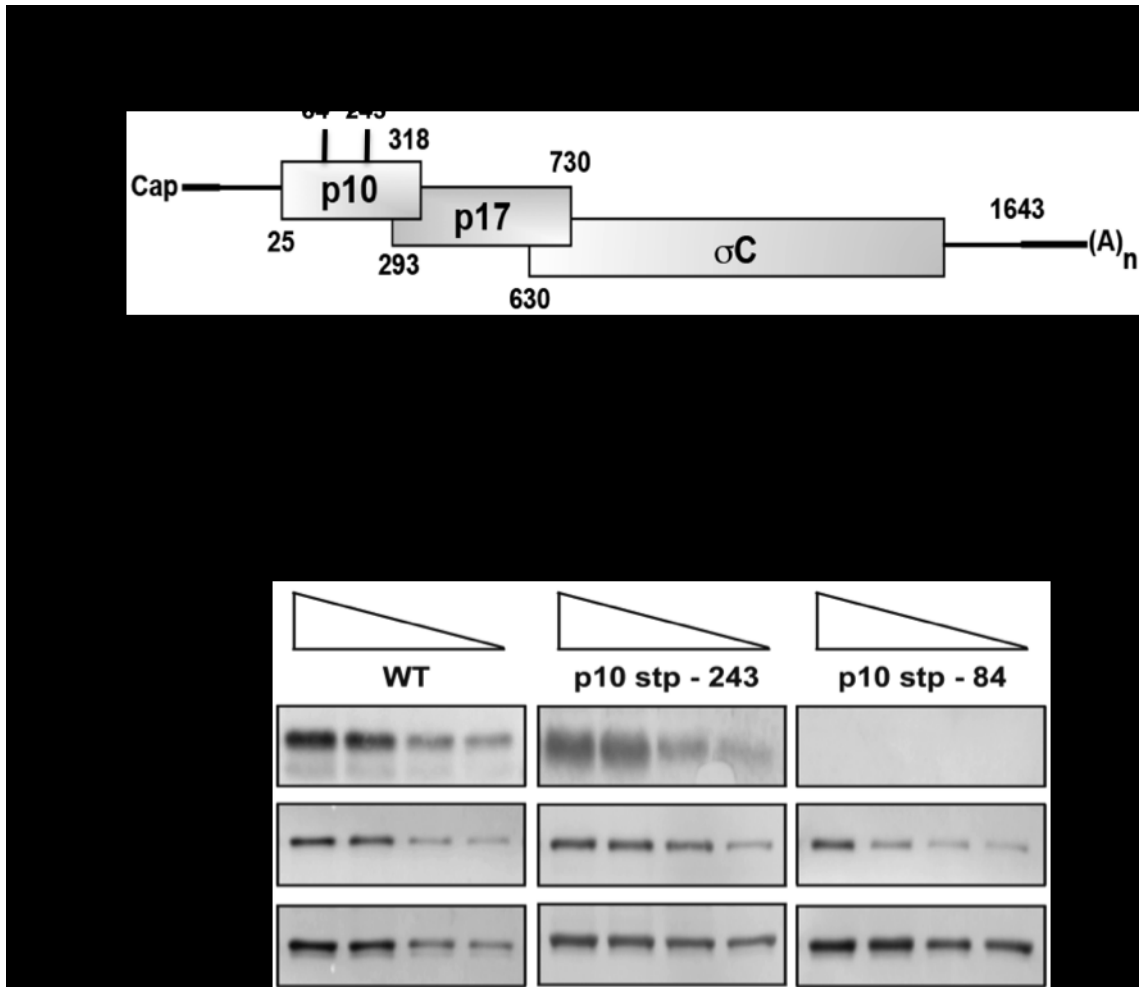


Figure 16. A reinitiation-independent mechanism of translation is responsible for σ C expression. **A.** Diagram of the ARV S1 mRNA sequence indicating the location of single nucleotide point substitutions created in the p10 reading frame through site-directed mutagenesis to introduce stop codons (stp 84 and stp 243). **B.** Expression of the p10 and σ C polypeptides as detected by Western blot analysis of QM5 cell lysates transfected with pARV-S1 (WT) or a similar plasmid carrying a stop site mutation in the p10 ORF at nucleotide 243 (p10stp243) or 84 (p10stp84). Lysates were loaded in 1 μ g decreasing amounts in order to obtain the linear range of exposure. The membrane was also probed with an anti-actin antibody as a loading control.

access to the σ C translation start site could proceed, I developed an *in vitro* transcription and RNA transfection method to examine translation of the S1 mRNA. Transcription of the S1 cDNA *in vitro* using T7 polymerase generated an unspliced, capped, non-polyadenylated S1 mRNA with authentic 5'- and 3'-termini. As demonstrated above, DNA transfection of plasmid borne S1 construct produced sufficient p10 and σ C protein for detection by Western blotting. This was not the case for lysates obtained from cells transfected with the *in vitro* transcribed S1 mRNA, although the presence of a p10 optimized start site did produce enough protein to be barely detected by Western blotting (Figure 17). The RNA transfection approach was therefore not sensitive enough to quantitatively analyze translation of the S1 mRNA via Western blotting.

3.8 Development Of A Quantitative Reporter System For σ C Expression

Due to the limited amount of ARV-specific protein detected by Western blot analysis of RNA transfected QM5 cell lysates, the quantitative *Renilla* luciferase (RL) assay system was used as a reporter for σ C expression. The RL ORF is commonly used in reporter systems as it is designed to yield reliable, linear results over a concentration range of seven orders of magnitude (Alam and Cook, 1990; Zhuang et al., 2001). Therefore, a modified RL ORF, lacking its own translation start site but the authentic stop codon, was inserted in-frame with the σ C start codon using the Xba I restriction site present in the S1 cDNA (nucleotides 746-751), ultimately producing a chimeric RL protein with 41 residues of σ C fused to the RL N-terminus (Figure 18). This construct contains the entire S1 nucleotide sequence, including the 3'-UTR and nucleotides 752 – 1607 of the σ C ORF, although this sequence was no longer translated due to the stop codon at the end of the RL ORF. To determine whether insertion of the RL ORF altered translation from the σ C start codon, expression of the chimeric construct was first tested by assaying luciferase expression in lysates from cells transfected with plasmid DNA encoding the parental p σ C-RL construct or with p σ C-RL constructs that had either the p10 or p17 start sites optimized (Figure 19A). As with the Western blot analyses presented above, optimization of either uORF decreased, but did not eliminate, translation initiation at the σ C start site (Figure 19B). Although the RL assay

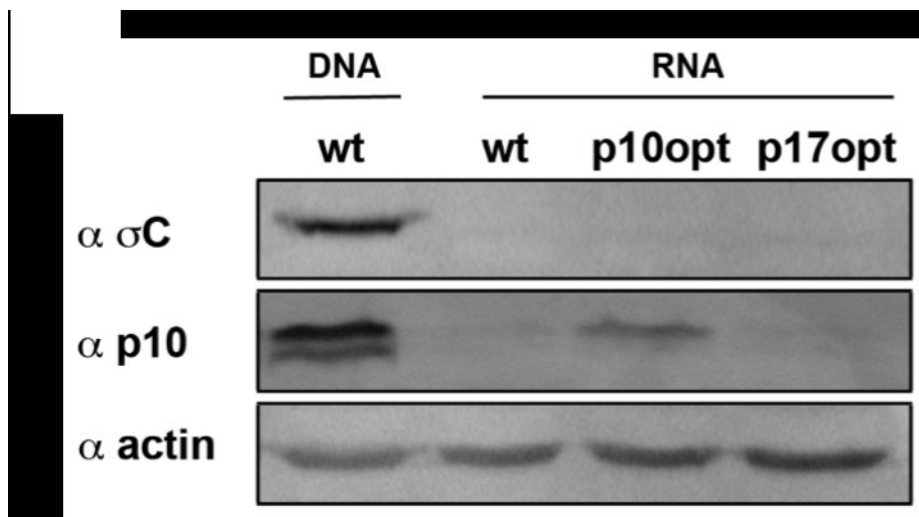


Figure 17. S1 RNA transfection results in inefficient protein expression for detection by Western blot analysis. QM5 cells were transfected with either plasmid pARV-S1 (wt DNA) or *in vitro* transcribed RNA (wt, p10opt and p17opt). Expression of the σ C and p10 proteins was analyzed by Western blotting with anti-sera specific for these proteins. The same blot was probed with an anti-actin antibody as a protein loading control.

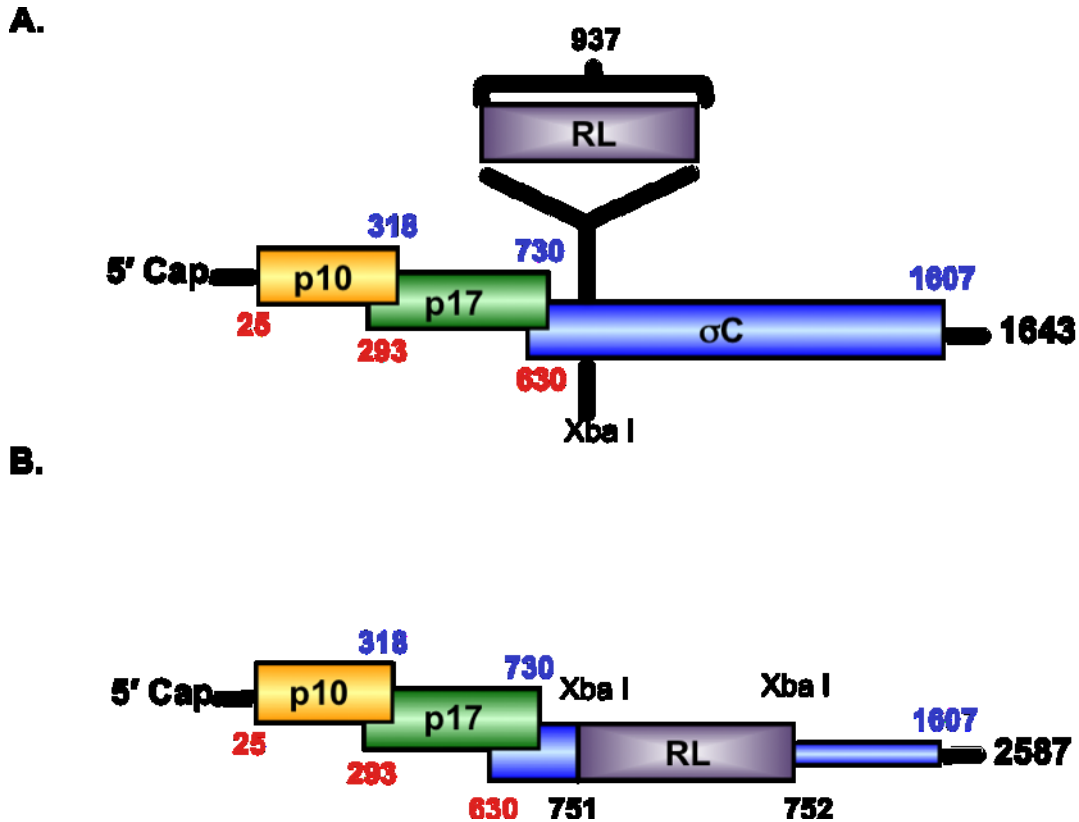


Figure 18. Gene arrangement of the chimeric ARV σ C-RL genome segment. A. Diagram of the organization of the p10, p17 and σ C cistrons (coloured rectangles) contained within the ARV S1 genome segment. Numbers in red represent the first nucleotide of the ORF and numbers in blue represent the last nucleotide of the ORF (excluding the termination codon). The RL ORF (937 nucleotides long) was inserted in-frame with the σ C start codon between S1 nucleotides 751 and 752 using the Xba I restriction site. Translation of the σ C-RL chimeric ORF produces an N-terminally extended RL protein with 41 amino acids of σ C, and terminates at the end of the RL ORF. S1 nucleotides 752 to 1643 are present downstream of the σ C-RL ORF but are not translated (thin rectangle). **B.** An alternate diagrammatic depiction of the chimeric ARV σ C-RL genome segment indicating the new length of the mRNA (2587 nucleotides). A similar version will be used in all subsequent figures.

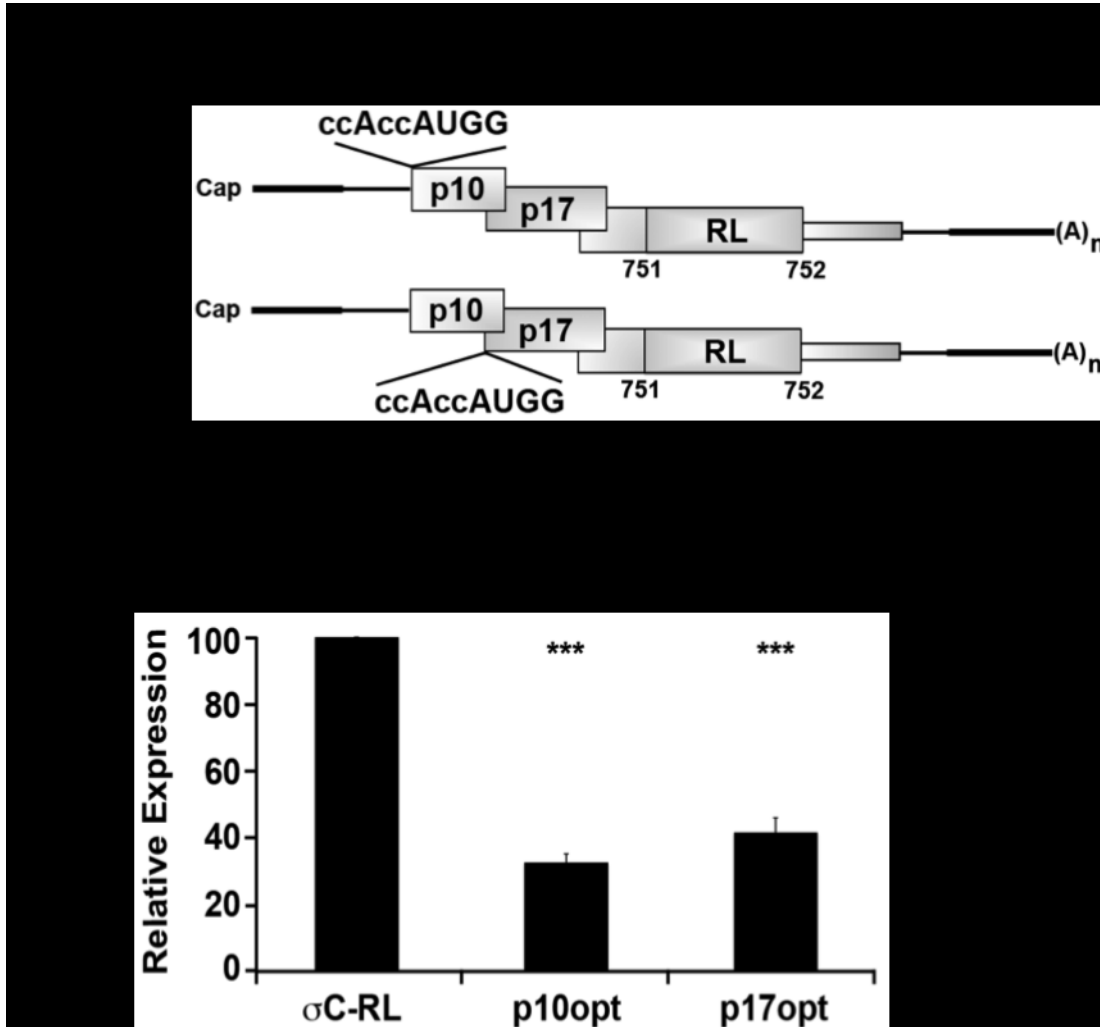


Figure 19. Translation of the plasmid-derived ARV σ C-RL chimera results in a similar σ C expression trend seen by Western blot analysis. A. Nuclear transcription of plasmid p σ C-RL results in the production of an mRNA with exogenous sequence at both the 5'- and 3'-termini (thick black lines), a poly(A) tail (A_n), and a chimeric 3'-proximal ORF where the RL ORF was inserted in-frame with the σ C start site between S1 nucleotides 751 and 752. The p σ C-RL plasmid was also modified to optimize the context of the p10 or p17 start codons (p10opt or p17opt) to conform to the optimal Kozak consensus start sequence (ccAccAUGG). **B.** The parental plasmid (σ C-RL) and the modified constructs (p10opt and p17opt) were transfected into QM5 cells using Lipofectamine. Cell lysates were harvested 24 h post-transfection and quantified for luciferase activity. Results are reported as mean \pm SE (n=4) of the relative level of σ C-RL translation, normalized to the σ C-RL construct. Expression levels significantly different from the parental construct (p<0.001) are indicated (***).

demonstrated a slightly higher level of downstream inhibition upon p10 or p17 start site optimization (~60-70%) than determined by Western blotting, the same trend was observed, with retention of significant levels of σ C expression and optimization of the p10 start site exerting a slightly more inhibitory effect on σ C translation than optimization of the p17 start site.

To determine whether RNA transfection of *in vitro* transcribed, capped σ C-RL mRNA was sensitive enough for quantitative detection, a time-course analysis was performed (Figure 20). Levels of luciferase activity peaked 4-8 h post-transfection. RNA transfection and translation of the σ C-RL mRNA, therefore, results in the production of a chimeric σ C-RL protein that can be used as a quantitative reporter for σ C expression. All subsequent studies using RNA transfection were performed at 4 h post-transfection.

3.9 Translation Of The Internal σ C Start Site Is Cap-Dependent

The ability to *in vitro* transcribe S1 mRNA enabled the direct examination of the dependency of translation initiation at the σ C start site on the 5'-cap. S1 mRNA was *in vitro* transcribed either with a functional (m7GpppG) or non-functional (ApppA) cap analog, transfected into cells and the cell lysates were analyzed using the luciferase assay (Figure 21). Expression levels were normalized to those of the non-functional cap analog. The presence of a functional cap analog at the 5'-terminus of the σ C-RL mRNA increased downstream expression >140-fold compared to the mRNA with the non-functional cap analog, indicating that initiation of σ C translation is cap-dependent. These results were further confirmed through the insertion of a stable hairpin structure ($\Delta G = -60$ kcal/mol) between S1 nucleotides one and two within the σ C-RL mRNA (Figure 21). The presence of a stable hairpin near the 5'-cap inhibits pre-initiation complex binding and thus prevents cap-dependent translation (Kumimoto, Yamane, and Ishizaki, 2005; Latorre, Kolakofsky, and Curran, 1998; Sherrill and Lloyd, 2008; Van Eden et al., 2004; Wang and Rothnagel, 2004). As indicated, insertion of the hairpin structure eliminated reporter expression, confirming that synthesis of the σ C ORF occurs in a cap-dependent manner. This result also reinforces the above results demonstrating that translation initiation at the σ C start codon occurs in an IRES-independent manner (Figure 13) and is not due to cleavage of the mRNA (Figure 8A), either one of which would have resulted

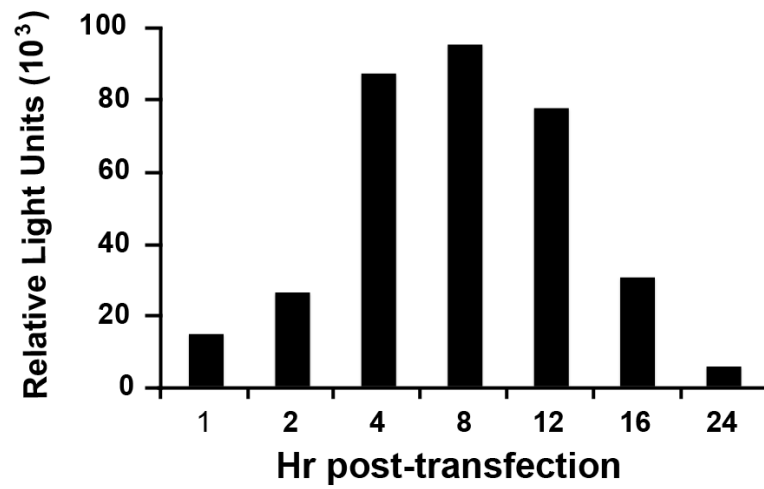


Figure 20. RNA transfection of *in vitro* transcribed σ C-RL RNA is sensitive enough for quantitative analysis. QM5 cells were transfected with 1 μ g of *in vitro* transcribed capped σ C-RL RNA and harvested for analysis of luciferase activity at the times indicated.

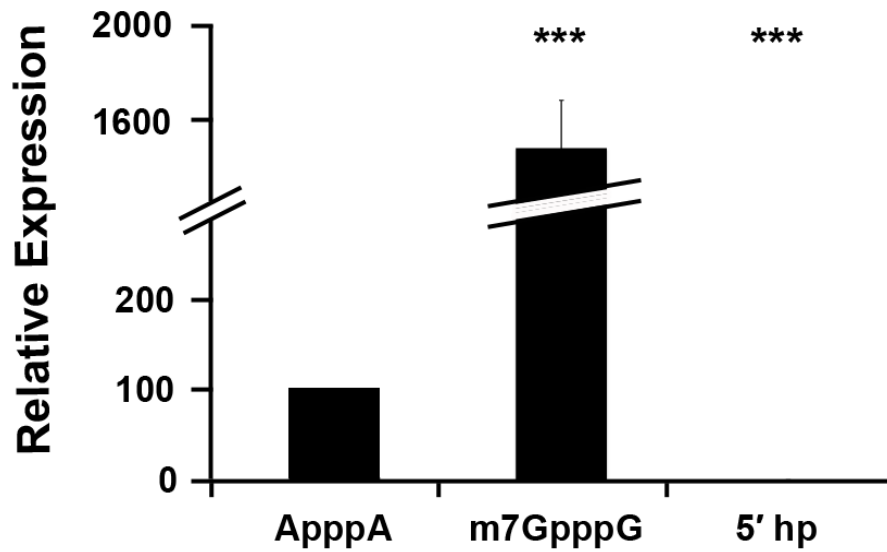


Figure 21. Expression of the σ C-RL ORF is cap-dependent. QM5 cells were transfected with σ C-RL RNA *in vitro* transcribed either with a functional cap analog (m7GpppG), a non-functional cap analog (ApppA), or with a stable hairpin structure inserted three nucleotides downstream of a functional cap analog (5' hp). Cells were harvested 4 h post-transfection for luciferase activity. Results are reported as mean \pm SE (n=4) of the relative level of σ C-RL translation, normalized to the σ C-RL construct with the non-functional cap analog. Expression levels significantly different from the parental construct ($p < 0.001$) are indicated (***).

in σ C translation in the presence of a hairpin structure or the absence of a cap at the 5'-end of the S1 mRNA.

3.10 Optimization Of uAUGs In The S1 mRNA Has Differential Effects On Translation Of Downstream Open Reading Frames

The literature indicates that optimization of some uORFs can preclude expression of downstream ORFs if the downstream ORFs are initiated by leaky scanning (Cao and Geballe, 1995; Futterer et al., 1997). To confirm results from the plasmid DNA transfections, which indicated that optimization of either the p10 or p17 start codons do not prevent expression of significant levels of residual σ C protein, the parental, p10optRL and p17optRL σ C-RL mRNAs were *in vitro* transcribed (Figure 22A), RNA transfected into QM5 cells, and the cell lysates were subjected to luciferase assays. As described above (Figure 11 and Figure 19), optimization of either uORF did result in a significant reduction in translation from the σ C start site (Figure 22B). However, also consistent with the previous experiments was the significant retention of downstream initiation at the σ C AUG codon, with translation of the p10optRL and p17optRL mRNAs producing $55 \pm 5\%$ and $70 \pm 4\%$, respectively, of the levels of σ C-RL compared to the parental mRNA. This level of inhibition was not as significant as would be expected if ribosomes were reaching the internal start site via leaky scanning (Futterer et al., 1997; Herzog, Guilley, and Fritsch, 1995). These results therefore suggested that leaky scanning does play some role in initiation at the σ C start site.

To ensure that the variation in reporter expression observed was not due to differences in mRNA levels, quantitative reverse transcription PCR (qRT-PCR) was performed on the RNA transfected QM5 cells. Prior to Trizol extraction of total cellular RNA, the RNA-transfected QM5 cells had to be treated with RNase A to degrade any RNA remaining on the outside of the cells. The presence of even minor amounts of residual RNA would interfere with accurate determination of intracellular RNA levels. To determine the minimum RNase A concentration necessary to degrade all input RNA, QM5 cells transfected with *in vitro* transcribed σ C-RL reporter RNA, with either no incubation period or a four hour incubation period, were subjected to degradation with varying concentrations of RNase A (Figure 23). Quantitative RT-PCR analysis of mock-transfected cells demonstrated the background signal, detected with primers specific for

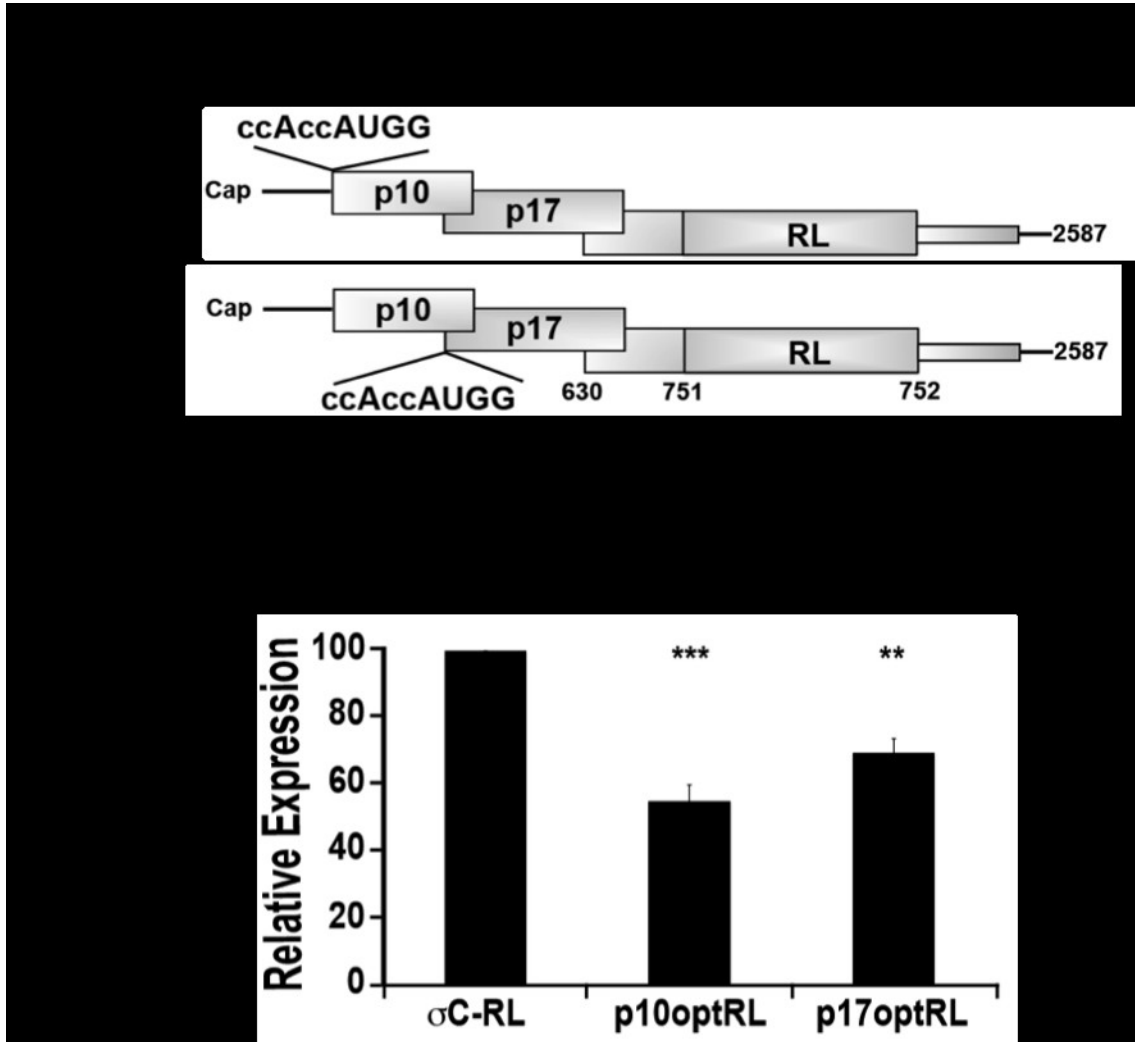


Figure 22. *In vitro* transcribed ARV σ C-RL chimeric RNA results in a similar σ C expression trend seen via Western blot analysis. A. *In vitro* transcription of σ C-RL cDNA from a T7 polymerase promoter results in the production of an authentic S1 mRNA with the addition of a chimeric 3'-proximal ORF where the RL gene has been inserted in-frame with the σ C start site between S1 nucleotides 751 and 752. The p10opt and p17opt plasmids described previously were also used to *in vitro* transcribe σ C-RL mRNA with optimized uORFs (p10optRL and p17optRL) **B.** The parental mRNA (σ C-RL) and the modified constructs were RNA transfected into QM5 cells using polyethylenimine transfection reagent. Cell lysates were harvested 4 h post-transfection and luciferase activity was quantified. Results are reported as mean \pm SE (n=4) of the relative level of σ C-RL translation, normalized to the σ C-RL construct. Expression levels significantly different from the parental construct (p<0.01 and p<0.001) are indicated (** and ***).

Treatment prior to qRT-PCR	Average C _T	
	RL primer	Actin primer
σC-RL 4hr Incubation no RNase A	20.61	21.725
σC-RL no incubation no RNase A	26.17	21.375
σC-RL no Incubation 10000ug RNase A	31.36	21.09
σC-RL no Incubation 1000ug RNase A	31.835	21.96
σC-RL no Incubation 500ug RNase A	28.42	21.875
Mock Transfected	30.975	19.825

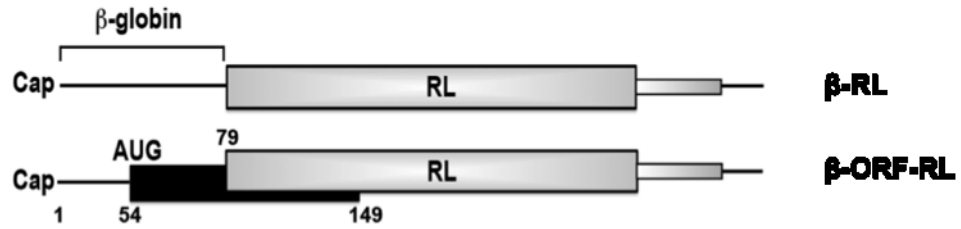
Figure 23. Addition of RNase A to RNA transfected cells is necessary for accurate qRT-PCR determination. The first column indicates the treatment conditions; RNA transfected, length of incubation, and concentration of RNase A added to the cells before harvesting. The second and third columns represent the average C_T values obtained by qRT-PCR for each treatment using primers directed against the RL or actin ORFs, respectively.

σ C-RL and actin mRNAs. An average C_T value at or near 30 is considered background (Karlen et al., 2007). Incubation of the RNA-transfected QM5 cells for four hours with no RNase A treatment revealed a 64-fold increase in σ C-RL RNA levels compared to cells exposed to the transfection mix with no incubation period (C_T 20.61 vs C_T 26.17). This indicates that a significant amount of RNA was transfected into the cells but that a significant amount still remained on the outside of the cells since the background C_T value was 30.97. Addition of 500 μ g of RNase A to cells exposed to the transfection mix degraded the vast majority of the input RNA (C_T 28.42), but it did not eliminate all input RNA. Addition of 10 000 μ g or 1 000 μ g of RNase A did, on the other hand, eliminate all RNA present within the transfection, as evidenced by C_T values at background (C_T 31.36 and C_T 31.84, respectively). Neither concentration of RNase A affected intracellular RNA, as demonstrated by the C_T values for the actin internal control. Therefore, for all further qRT-PCR experiments, 1 000 μ g RNase A was used to degrade all remaining RNA present on the outside of the cells. This method of qRT-PCR was utilized for all subsequent clones that demonstrated a significant change in initiation efficiency at the σ C start site. None of the clones demonstrated a significant difference in transcript levels indicating that all variations in protein production are due to differences in translation efficiency.

3.11 Optimized uAUGs Exert Different Effects On Downstream Translation Depending On The Context Of The mRNA

Although optimized uAUGs are expected to eliminate or dramatically reduce downstream translation initiation (Bergenheim et al., 1992; Futterer et al., 1997; Kaufman, Murtha, and Davies, 1987; Kozak, 1984a; Mueller and Hinnebusch, 1986; Sedman and Mertz, 1988), I wanted to confirm this prediction using the RL assay system. The ability of an optimized uAUG triplet to inhibit scanning ribosomes from initiating translation at a downstream ORF was therefore examined in an mRNA other than the S1 mRNA. A monocistronic mRNA containing the RL ORF preceded by the 77-nucleotide rabbit β -globin 5'-UTR was constructed (β -RL; Figure 24A). The rabbit β -globin 5'-UTR was chosen because it efficiently mediates cap-dependent translation and lacks any sequence elements or secondary structure that may significantly affect translation initiation (Kozak, 1994; Krowczynska and Brawerman, 1986). To create an uORF in this chimeric sequence

A.



B.

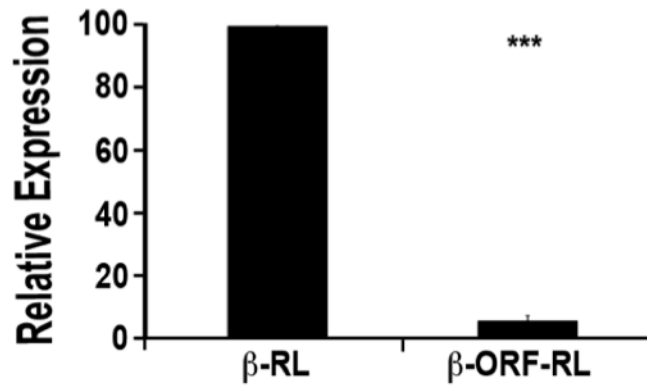


Figure 24. Optimization of a heterologous sequence results in substantial translation inhibition of the downstream ORF. **A.** Diagram depicting a capped mRNA with a β -globin 5'-UTR present upstream of the RL ORF, either with (β -ORF-RL) or without (β -RL) a single nucleotide point substitution within the β -globin UTR that creates an out-of-frame optimized ORF. The out of frame ORF commences at nucleotides 54 and terminates at nucleotides 149. The RL ORF commences at nucleotide 79. **B.** Both β -RL and β -ORF-RL were *in vitro* transcribed and transfected into QM5 cells. Harvested cell lysates were subjected to luciferase assay. Results are reported as the mean \pm S.E. (n=5) of the relative level of RL translation, normalized to the parental β -RL construct. Expression levels significantly different from the parental construct (p<0.001) are indicated (***)

the parental β -RL construct was modified by site-directed mutagenesis to create an AUG codon with the same DNA sequence surrounding the start codon as p10optRL and p17optRL (ccAccAUGG), 25 nucleotides upstream of the RL ORF (β -ORF-RL). This β -ORF-RL construct has a 48-codon ORF that overlaps, but is out-of-frame with, the RL ORF. The presence of the uORF with an optimal context for ribosome recognition reduced RL expression by $95 \pm 2\%$, indicating that optimized start sites can effectively block scanning ribosomes, but not in the context of the ARV S1 mRNA.

3.12 Consistency Within The RL Assay System

As a means of ensuring that the results reported were representative of the actual variations in translation efficiency of the σ C ORF and not a byproduct of the *in vitro* transcription/RNA transfection system, every replicate experiment performed utilized a separate batch of *in vitro*-transcribed RNA, transfected on separate days. While performing these experiments I noticed slight variations ($\sim 10\%$) in translation efficiency, expressed as differences in relative light units (RLUs), of the same clone *in vitro* transcribed on different days. This disparity is most likely the result of differences in quality of the *in vitro* transcription kits, more specifically, the ability to effectively cap the mRNA. The RLUs recorded for any particular clone also depended on the cell density of the cells being transfected. The greater the number of cells present, the higher the RLUs observed. Thus, the modified reporter constructs were only compared to their parental clone *in vitro* transcribed from the same master mix and transfected on the same day (Figure 25). Minimally, each mutant RNA was *in vitro*-transcribed and transfected on three separate occasions.

3.13 Effect Of A Short 5' Leader And Stable Hairpin Structure On Downstream Initiation

One possible explanation for the differential effects of uORF optimization in the S1 and β -globin mRNAs is the length of the 5'-UTRs. The 40S ribosomal subunit occupies approximately the first 30-40 nucleotides upon cap binding (Kozak, 1977; Lazarowitz and Robertson, 1977). The relatively short, 24-nucleotide, S1 5'-UTR might therefore facilitate leaky scanning past the optimized p10 AUG triplet (Kozak, 1988; Kozak, 1991a; Pestova and Kolupaeva, 2002; Sedman, Gelembiuk, and Mertz, 1990). To

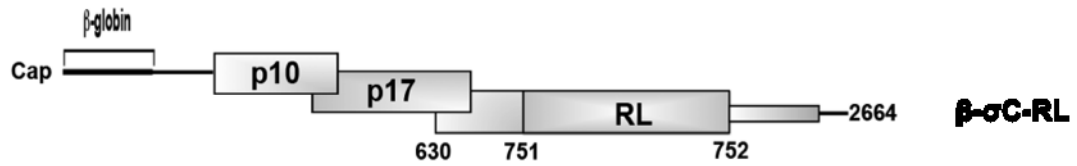
Replicate	Blank	β -RL	β -ORF-RL	β -ORF-RL
				β -RL
RNA #1 RLU	88	4,887,882	467,923	0.079217
	96	6,880,792	464,531	
RNA #2 RLU	103	4,525,243	61,260	0.012401
	147	5,111,929	58,248	
RNA #3 RLU	78	5,298,301	464,105	0.078718
	70	5,117,705	355,962	
RNA #4 RLU	81	6,762,232	269,100	0.042270
	100	6,144,979	276,670	

B.

Replicate	Blank	β - σ CRL	β -p10opt	β -p17opt	β -p10opt	β -p17opt
					β - σ CRL	β - σ CRL
RNA #1 RLU	208	210,590	172,548	169,378	0.720228	0.787070
	265	210,605	130,941	162,233		
RNA #2 RLU	185	216,365	128,739	152,665	0.657313	0.825329
	252	172,048	126,720	167,980		
RNA #3 RLU	88	321,488	211,153	186,496	0.717365	0.757655
	96	223,651	179,963	226,576		
RNA #4 RLU	103	258,774		176,910	0.706208	
	147	212,609		156,058		
RNA #5 RLU	78	217,570	106,344	127,902	0.584889	0.580749
	70	250,196	167,309	143,815		

Figure 25. Transfection of different RNA preparations on different days results in a range of RLUs but the same overall trend. **A.** β -RL and β -ORF-RL RNA were prepared on four separate occasions, transfected into QM5 cells and the cell lysates were analyzed for RL activity. Each sample was transfected in duplicate and the RLUs obtained were averaged. The average RLU obtained from the mock-transfected cells (Blank) was subtracted from the average RLU of each sample. The fold-change in expression level was obtained by dividing the RLUs from the mutant construct by the RLUs obtained from the parental construct. **B.** β - σ CRL, β -p10opt and β -p17opt RNA were prepared on four or five separate occasions, transfected into QM5 cells and the cell lysates were analyzed for RL activity. The fold-change in expression levels was determined as outline in part A.

A.



B.

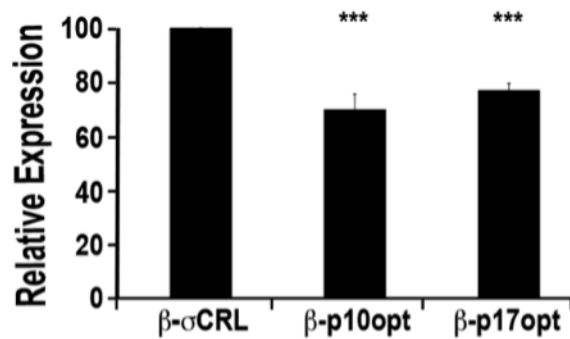


Figure 26. Extension of the S1 5'-UTR does not promote further inhibition of σ C-RL expression. **A.** Diagram depicting a capped σ C-RL mRNA 5'-terminally extended with the β -globin 5'-UTR. The 5' leader of p10opt and p17opt were also extended by the addition of the β -globin 5'-UTR. **B.** The β σ C-RL constructs were *in vitro* transcribed and transfected into QM5 cells. Cell lysates were harvested and subjected to luciferase assay. Results are reported as the mean \pm S.E. (n=4) of the relative level of σ C-RL translation, normalized to the parental β σ C-RL construct. Expression levels significantly different from the parental construct ($p < 0.001$) are indicated (***)

test this possibility, the rabbit β -globin 5'-UTR was inserted upstream of the full-length σ C-RL, p10optRL and p17optRL mRNAs (Figure 26A). Extension of the S1 5'-UTR did not alter σ C-RL expression levels when the p17 start site was optimized ($73 \pm 4\%$, compare with Figure 22), however, the extended 5'-UTR slightly increased, rather than decreased, σ C-RL synthesis from the β -p10opt construct ($67 \pm 9\%$, compare with Figure 22; Figure 26B). These results clearly demonstrate that the length of the S1 5'-UTR is not responsible for the remarkable retention in downstream initiation upon optimization of either the p10 or p17 start sites.

To further examine the role leaky scanning plays in translation initiation at the σ C AUG triplet, a stable hairpin structure capable of blocking scanning ribosomes on the 5' side of the hairpin (Kozak, 1986a; Kozak, 1989a; Pelletier and Sonenberg, 1985) was introduced into the S1 mRNA. The same hairpin structure that had previously been shown to abolish expression when inserted at the extreme 5'-end of the S1 mRNA (Figure 21) was inserted between S1 nucleotides 222 and 223 (Figure 27A, *top panel*), generating the construct σ C-RL hp 223. Luciferase assay of cells RNA-transfected with clone σ C-RL hp 223 revealed a significant reduction in downstream expression (Figure 27B; $61 \pm 4\%$) compared to the parental construct, suggesting that at least some of the ribosomes that access the σ C start site may do so by scanning through this region of the S1 mRNA, and thus can be blocked by a stable hairpin. As with the uORF optimization experiments performed above (Figure 19 and Figure 22) however, the level of inhibition observed was not as substantial as that reported in the literature (Kozak, 1986a). Most remarkably, ribosomes were still able to initiate translation at the σ C start site, although to a lesser extent ($19 \pm 1\%$), when faced with two significant barriers to scanning ribosomes in construct p10opt hp 223 that contained both the hairpin and an optimized p10 start site. If translation initiation at the σ C AUG triplet is due to ribosome scanning, ribosomes must be undergoing some form of enhanced leaky scanning in order to bypass two significant barriers.

To examine the effect the stable hairpin structure has on downstream initiation even further, the same hairpin was inserted between S1 nucleotides 579 and 580 (σ C-RL hp 579; Figure 27A, *bottom panel*). The hairpin structure was once again able to significantly inhibit σ C-RL reporter expression (Figure 27B), but unlike when present

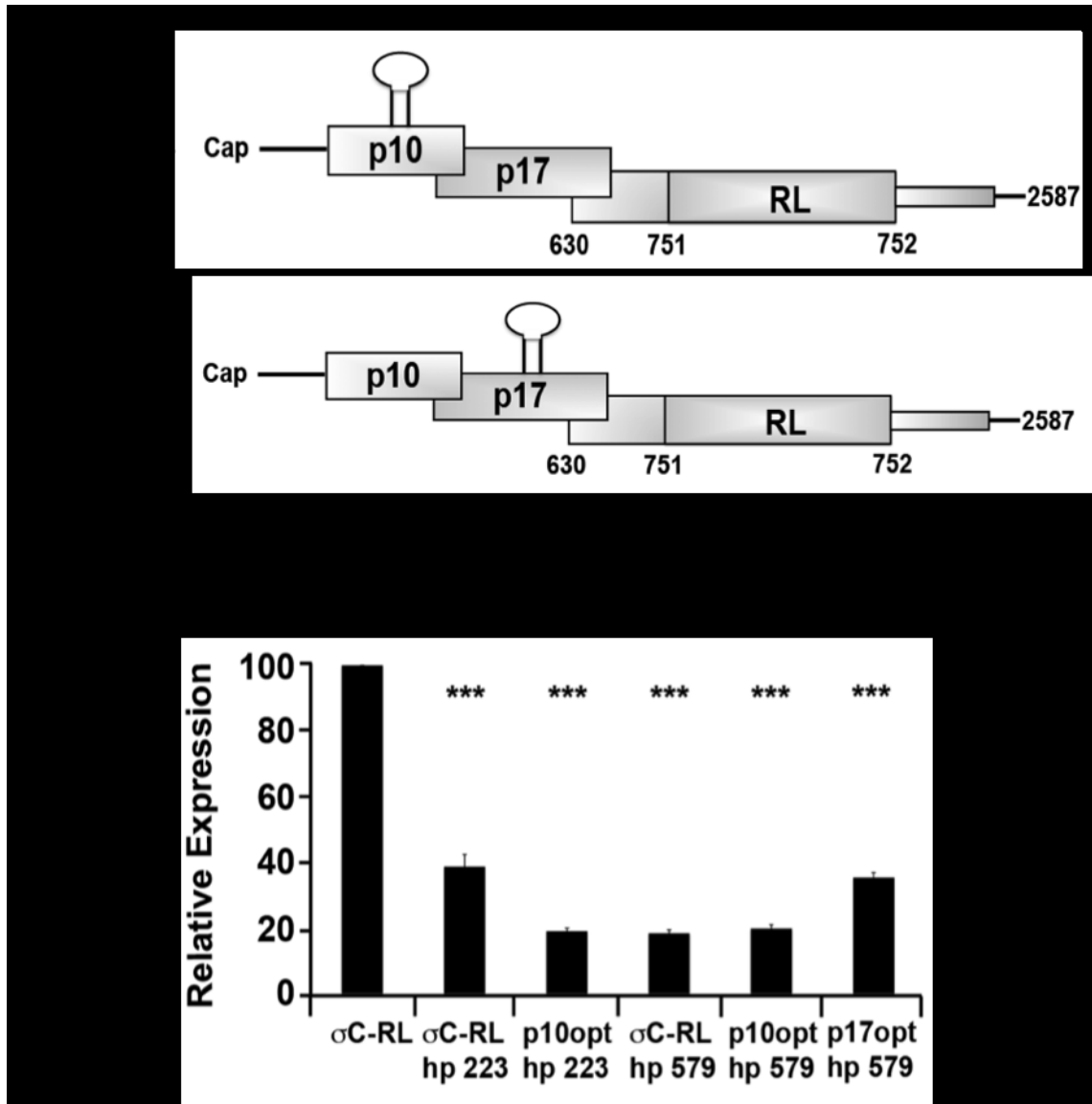


Figure 27. Expression of the σ C-RL ORF was not abolished by the presence of a stable hairpin structure. **A.** Diagram depicting a capped σ C-RL mRNA with a stable hairpin structure ($\Delta G = -60$ kcal/mol) inserted either between S1 nucleotides 222 and 223 or 579 and 580. The stable hairpin was also inserted with the p10optRL and p17optRL constructs. **B.** The parental and mutant constructs were *in vitro*-transcribed and transfected into QM5 cells. Cell lysates were subjected to luciferase assay. Results are reported as the mean \pm S.E. (n=4-5) of the relative level of σ C-RL translation, normalized to the parental σ C-RL construct. Expression levels significantly different from the parental construct ($p < 0.001$) are indicated (***)

between nucleotides 223 and 224, the presence of an optimized p10 start site did not inhibit expression any further. Surprisingly, the presence of an optimized p17 AUG codon actually relieved some of the inhibition imposed by the inserted secondary structure. Together, these results suggest that some ribosomes do scan the S1 mRNA upstream of the σ C start site, while others may access the downstream AUG triplet by some other means that may require precise folding of the S1 mRNA, since the presence of the hairpin structure appears to have differential effects depending on its location within the RNA.

3.14 The 3'- But Not The 5'-End Of The S1 Genome Segment Is Required For σ C Translation Initiation

Although most eukaryotic mRNAs possess a poly(A) tail at their 3'-terminus that synergistically enhances translation initiation through the ability of PABP to interact with the poly(A) tail and eIF4G, the ARV S1 genome segment is not polyadenylated. There are, however, many examples of viral mRNAs that lack a poly(A) tail but whose 3'-ends are still capable of enhancing translation (Guo, Allen, and Miller, 2001; Polacek, Friebe, and Harris, 2009). To examine whether the 3'-terminus of the S1 genome segment participates in translation initiation at the σ C start site, the 3'-end of the σ C-RL mRNA was progressively truncated (Figure 28A) and the resulting mRNA tested for luciferase activity. Truncation of the 3'-terminal 25 nucleotides, which removes a significant portion of the 33-nucleotide S1 3'-UTR, decreased translation from the σ C start site by ~30% (Figure 28B). Further truncations of 50, 300 or 500 nucleotides had little, if any, additional effects on σ C-RL translation. The 3'-terminus of the σ C-RL construct therefore does exert some influence on translation initiation at the σ C start site. It is unclear whether this region specifically affects ribosome access to the σ C start site or generally affects translation of the σ C-RL mRNA since the translation levels of the p10 or p17 ORFs were not examined. The exact role the 3'-terminus plays in translation is unknown, however the results suggest that this region may influence folding of the mRNA since a larger deletion of 800 nucleotides relieved the inhibition imposed by the smaller truncations (Figure 28B).

Having examined the influence of the 3'-region on translation initiation, similar experiments were conducted on the 5'-region. The σ C-RL mRNA was progressively

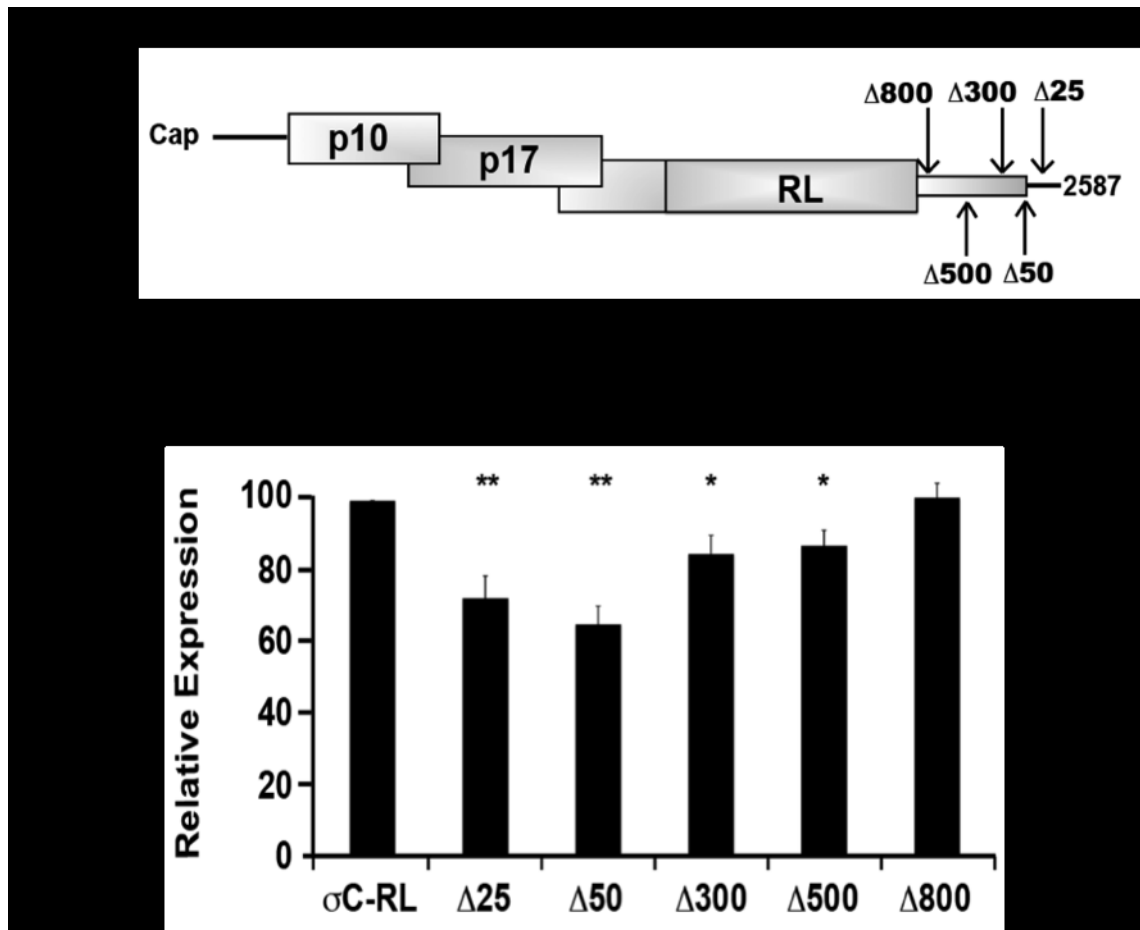


Figure 28. The 3'-terminal region of the S1 mRNA affects upstream reporter production. **A.** Diagram depicting a capped σ C-RL mRNA and indicating the location of the progressive 3'-truncations ($\Delta 25$, $\Delta 50$, $\Delta 300$, $\Delta 500$ and $\Delta 800$; numbers refer to the number of 3'-terminal nucleotides deleted from σ C-RL). **B.** The 3'-truncation transcripts were transfected into QM5 cells and the cell lysates were subjected to luciferase assay. Results are reported as the mean \pm S.E. (n=5) of the relative level of σ C-RL translation, normalized to the parental σ C-RL construct. Expression levels significantly different from the parental construct ($p < 0.05$ and $p < 0.01$) are indicated (* and **).

truncated from the 5'-terminus and tested for luciferase activity (Figure 29A). Deletion of the 5'-terminal 147 nucleotides of the σ C-RL mRNA, which removed the 5'-UTR and half of the p10 ORF including the two in-phase p10 start codons at nucleotides 25 and 34, had no significant effect on σ C translation (Figure 29B). This suggests that the two suboptimal p10 AUGs are not recognized efficiently as initiation codons and have little effect on ribosome access to the σ C start site. Deletion of the 5'-proximal 303 nucleotides, which placed the σ C start codon in the 5'-proximal position, did however cause an approximate 3.5-fold increase in σ C expression. This latter result suggests that an important negative regulatory element resides between S1 nucleotides 148-303. As mentioned above, the p17 start codon has an A residue in the -3 position, placing it in a good context for translation initiation, suggesting that it might present as a barrier to scanning ribosomes.

Interestingly, translation of the mRNAs transcribed from plasmids pARV- Δ 79 and pARV- Δ 147 resulted in no σ C expression (Figure 15). As with the RNA transfections, further truncation to Δ 303 restored σ C translation in plasmid DNA transfections to levels slightly higher than those obtained from full-length S1 mRNA. The Δ 79 and Δ 147 truncations were the only significant discrepancies observed between results obtained using the two different transfection protocols. The basis for this discrepancy is unclear, but highlighted the rationale for development of the RNA transfection approach. As previously stated, I favour the results obtained from the RNA transfections due to the presence of authentic 5'- and 3'-termini and the absence of the poly(A) tail, but recognize that insertion of the RL ORF could result in global changes in mRNA folding that affect the mechanism of ribosome access to the σ C start site.

3.15 The p17 Start Codon And The Presence Of Additional AUG Triplets Within The p17 Region Block Scanning Ribosomes

The 5'-truncation results suggested that the strong context of the p17 start codon might serve as a barrier to ribosome access to the σ C start site. To ensure that the 5'-truncations did not affect downstream translation initiation due to the altered length of the 5'-end or by affecting secondary structure, the extent of inhibition, if any, the four AUG codons (numbered sequentially, 5' to 3' and given the designation M1-M4 in Figure 30A)

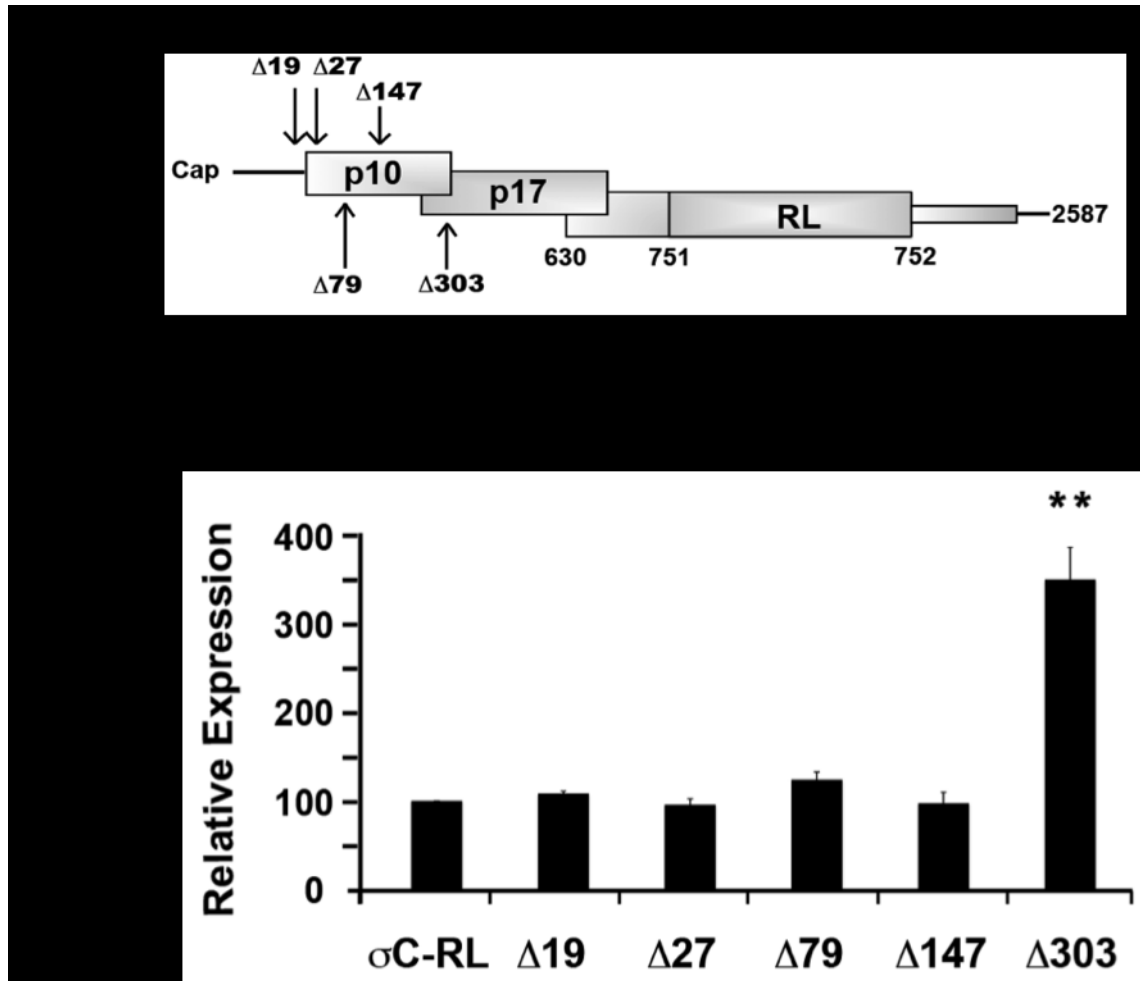


Figure 29. Translation initiation at the σ C start codon is independent of the 5'-proximal 147 nucleotides. **A.** Diagram depicting a capped σ C-RL mRNA indicating the location of the progressive 5'-truncations ($\Delta 19$, $\Delta 27$, $\Delta 79$, $\Delta 147$, and $\Delta 303$; numbers refer to the number of 5'-terminal nucleotides deleted from σ C-RL). **B.** The *in vitro* transcribed 5' truncations were transfected into QM5 cells and the cell lysates were subjected to luciferase assay. Results are reported as the mean \pm S.E. (n=3) of the relative level of σ C-RL translation, normalized to the parental σ C-RL construct. Expression levels significantly different from the parental construct ($p < 0.01$) are indicated (**).

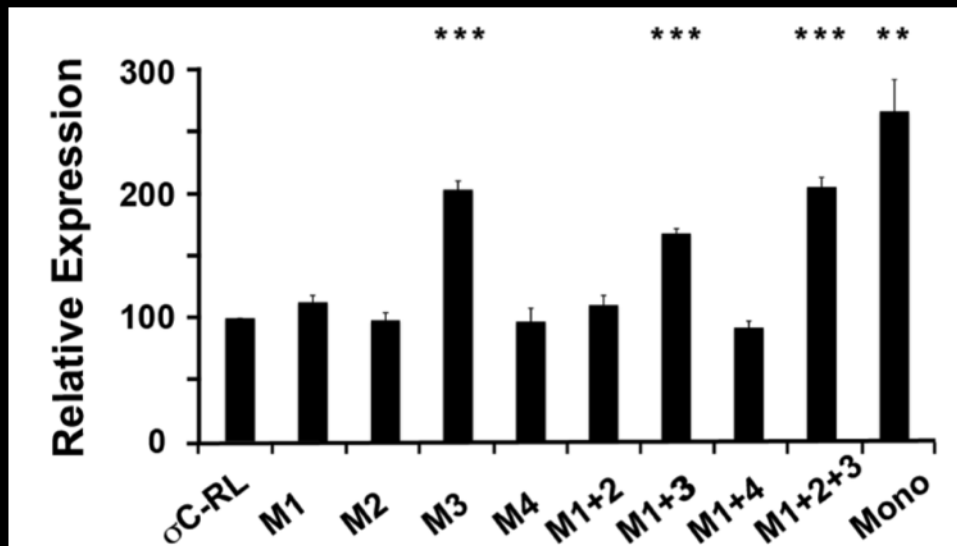
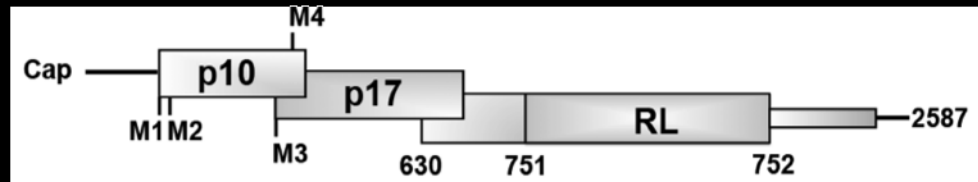


Figure 30. The p17 start site acts as an efficient barrier against scanning ribosomes.

A. Diagram depicting a capped σ C-RL mRNA indicating the location of the methionine codons located upstream of the σ C AUG codon that were subjected to site-directed mutagenesis (M1-M4), either individually or in combination. **B.** The parental (σ C-RL) and methionine point substitution transcripts were *in vitro* transcribed and subsequently transfected into QM5 cells. The cell lysates were subjected to luciferase assay. Results are reported as the mean \pm S.E. (n=3) of the relative level of σ C-RL translation, normalized to the parental σ C-RL construct. Expression levels significantly different from the parental construct (p<0.01 and p<0.001) are indicated (** and ***).

have on σ C start codon selection was examined by single nucleotide point substitution (AUG to AUC) of these codons, either individually or in various combinations. Individual or combined substitution of the two p10 start codons (M1 and M2) had no significant effect on σ C expression (Figure 30B). This result was in agreement with the 5'-truncation results suggesting these start codons do not serve as a barrier to ribosome access to the σ C start site, and coincides with the reinitiation-independent model of σ C translation initiation (Figure 16). The same situation applied to M4, the AUG codon near the end of the p10 ORF, when substituted either individually or in combination with M1 and/or M2. Despite the good context of the M4 AUG, with a purine in the -3 position and the G residue in the +4 position, the M4 AUG codon does not impede translation from the σ C AUG triplet. In contrast, rendering the M3 p17 start site non-functional had a significant stimulatory effect on σ C production (~2-fold). Mutation of the p17 start site in combination with any of the AUG codons within the p10 ORF did not result in any further increase in σ C expression. Simultaneous substitution of all four uAUGs, creating a monocistronic mRNA, resulted in ~2.7-fold increase in luciferase activity, which is higher than that observed when only the p17 start codon was removed (Figure 30) and in agreement with the level of initiation observed via Western blotting from the monocistronic S1 mRNA derived from the plasmid pS1-Mono (Figure 8C). Translation of the p17 ORF therefore does inhibit σ C expression, if only modestly, while the other uAUGs have minimal, if any, effect on translation from the σ C start site.

The scanning model predicts that insertion of an AUG codon in an optimal context upstream of a main ORF should supplant downstream translation initiation (Kozak, 1984b). This prediction, along with the observation that the p17 start site plays an inhibitory role in downstream expression, led me to examine whether the insertion of additional AUG codons, in a strong context, within the p17 region could eradicate σ C expression. Insertion of 24 heterologous nucleotides between S1 nucleotides 298 and 299 containing two additional AUG codons out of frame with the p17 ORF and in a strong context with A in the -3 and +4 positions, resulted in the creation of a mini-ORF 31 codons long that terminated 240 nucleotides upstream of the σ C start site (mini-ORF1; Figure 31A). The creation of this mini-ORF with two strong start sites reduced the expression of the chimeric σ C-RL ORF by $45 \pm 3\%$ (Figure 31B). To determine whether

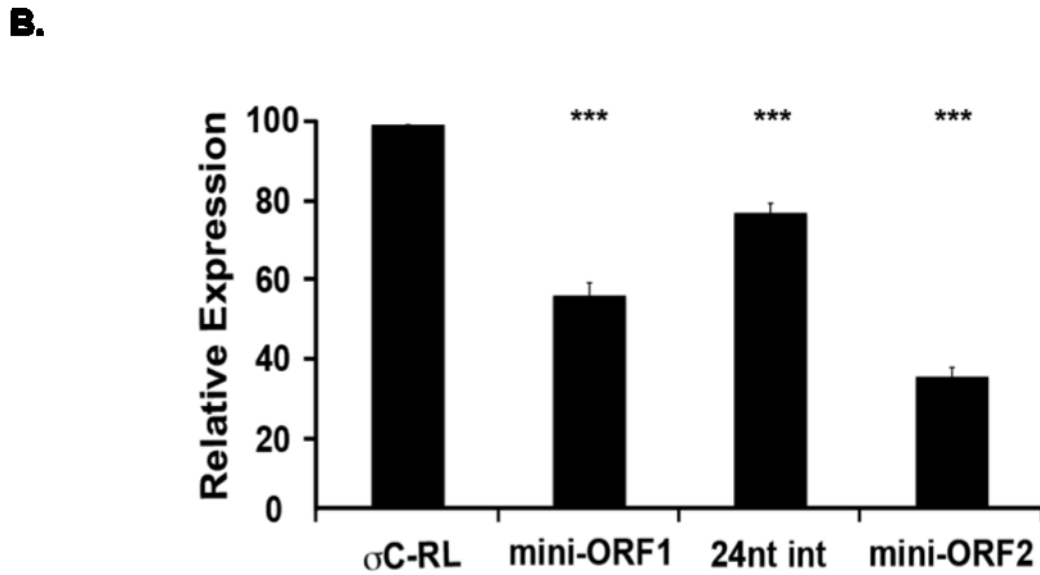
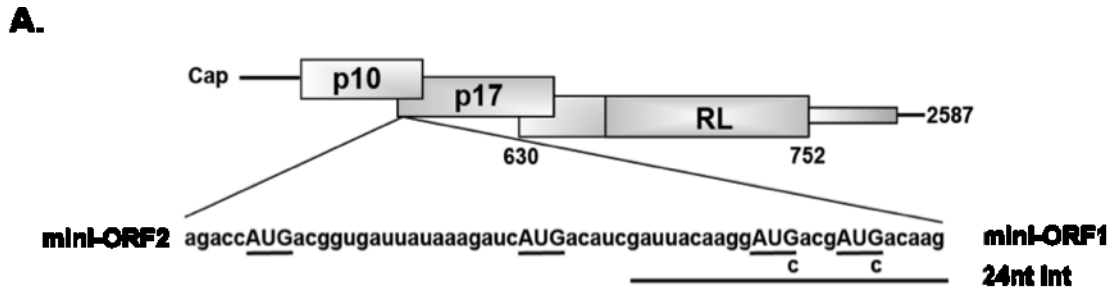


Figure 31. Insertion of exogenous sequence containing AUG codons impairs but does not abolish σ C-RL synthesis. **A.** Diagram depicting the insertion of 24 (underlined) or 78 exogenous nucleotides between S1 nucleotides 298 and 299 containing zero (24nt int), two (mini-ORF1) or four (mini-ORF2) additional AUG triplets. **B.** The parental (σ C-RL) and modified constructs were *in vitro* transcribed and transfected into QM5 cells. Cell lysates were harvested and subjected to luciferase assay. Results are reported as the mean \pm S.E. (n=3) of the relative level of σ C-RL translation, normalized to the parental σ C-RL construct. Expression levels significantly different from the parental construct ($p < 0.001$) are indicated (***).

the inserted sequence alone affected downstream translation initiation, two separate point substitutions within the 24-nucleotide insert (AUG to AUC) were created to eliminate the potential start sites (24nt int). Analysis of the 24nt int clone for luciferase activity demonstrated a slight decrease in σ C production ($23 \pm 3\%$; Figure 31B). If the level of luciferase activity obtained from clone 24nt int is considered as the parental level of σ C-RL translation (100%), the inhibitory effect of the two additional AUG start codons was relatively minor, reducing σ C production by only $28 \pm 2\%$. The inability of the inserted start sites to eliminate downstream translation initiation prompted the insertion of an additional 34 nucleotides containing two additional AUG codons in a strong context (mini-ORF2). The presence of four additional AUG codons in a strong context still did not abolish σ C expression (Figure 31B), despite the fact that the σ C start site now occurred downstream of eight uAUGs, six of which were in a good or strong context to serve as translation initiation codons.

It was possible that the residual luciferase activity observed from the constructs containing the inserted mini-ORFs was due to reinitiation at the σ C start site upon termination of the mini-ORF (Kozak, 1984b). For this reason, as well as the observation that insertion of 24 nucleotides of heterologous sequence alone affected σ C synthesis, additional uAUG codons were created without insertion of exogenous sequence and in-frame with the p17 ORF. Ribosomes initiating translation at these start sites should terminate at the p17 termination codon, downstream of the σ C AUG start codon, thus preventing the possibility of reinitiation. Site-directed mutagenesis within the region of S1 nucleotides 359-530 enabled the creation of AUG codons in a strong context (A -3, G +4), either singly or in combination (referred to as M5-M7; Figure 32A). The presence of all the uAUGs in a strong context, either singly or in combination, did significantly decrease downstream initiation, as shown by a decrease in luciferase activity (Figure 32B). However, the presence of three additional AUG codons in a strong context still resulted in a significant level of luciferase activity ($30.8 \pm 5\%$; Figure 32B). These results suggest the S1 sequence is capable of enhancing the ability of the ribosome to bypass normally inhibitory upstream elements. Interestingly, the level of translation inhibition imparted by the insertion of all three additional start codons was no more severe than the insertion of two uAUGs, suggesting that ribosome migration through the p17 region can

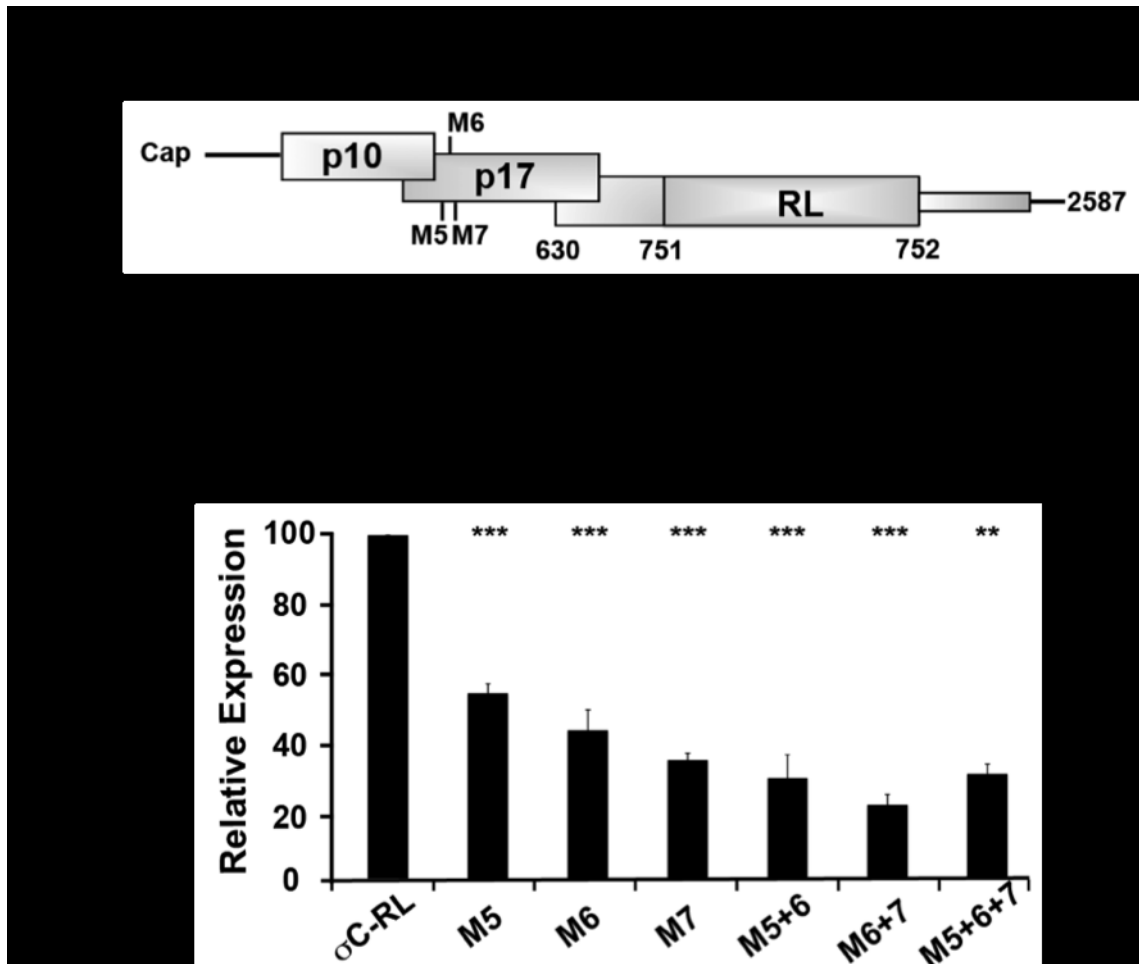


Figure 32. The presence of additional AUG codons within the p17 reading frame significantly inhibits but does not eliminate σ C-RL production. **A.** Diagram depicting the location of the AUG codons (M5-M7) created by site-directed mutagenesis within the p17 ORF. **B.** The parental (σ C-RL) and modified constructs were *in vitro* transcribed and transfected into QM5 cells. Cell lysates were harvested and subjected to luciferase assay. Results are reported as the mean \pm S.E. (n=3) of the relative level of σ C-RL translation, normalized to the parental σ C-RL construct. Expression levels significantly different from the parental construct (p<0.01 and p<0.001) are indicated (** and ***).

be completely blocked. If ribosomes were only able to reach the σ C AUG codon by scanning the S1 mRNA in a linear fashion, at some point insertion of additional start sites should completely eliminate downstream expression. Since this was not the case, the residual translation occurring at the 3'-proximal ORF may be occurring by a scanning-independent mechanism.

3.16 S1 Nucleotides 366-392 Facilitate Cap-Dependent Internal Initiation

In search of an element capable of enhancing the ability of the ribosome to bypass upstream inhibitory elements and facilitate downstream initiation, and having already examined both the 5'- and 3'-ends of the S1 mRNA, I wanted to make progressively larger internal deletions downstream of the p17 start site. The design of various IRES elements enables them to position the 40S ribosomal subunit directly on top of or just upstream of the main AUG codon (Pestova et al., 1998; Pisarev, Shirokikh, and Hellen, 2005; Reynolds et al., 1995). With this in mind, I was also interested in examining the role of the sequence surrounding the σ C start site using these internal deletions. Before this could be accomplished, however, a new parental construct had to be created (Figure 33A). The plasmid used up to this point initiated expression of σ C-RL at the σ C start codon, producing a chimeric RL protein with 41 additional amino acids at its N-terminus from the σ C ORF. Any internal deletions that eliminated the σ C start codon would therefore result in expression of authentic, non-chimeric RL with different enzymatic activity than that of the chimeric σ C-RL form of the protein. Relative luciferase activity of the internal deletions could therefore not be compared to the σ C-RL fusion protein. Thus, a new S1 expression plasmid had to be created that included the σ C sequence present upstream of the RL ORF but in a context that would prevent initiation at the σ C start site. To this end, the three AUG codons within the 121 nucleotides of the σ C ORF present upstream of the RL ORF were point substituted to AUC. Point substitution of the third σ C AUG codon in this region unfortunately also eliminated the p17 stop codon, ultimately creating a p17-RL chimera. To prevent the formation of this new chimeric protein, a stop codon was created within the p17 reading frame at nucleotide 517, upstream of the RL ORF, creating the S1-RL parental construct (Figure 33A).

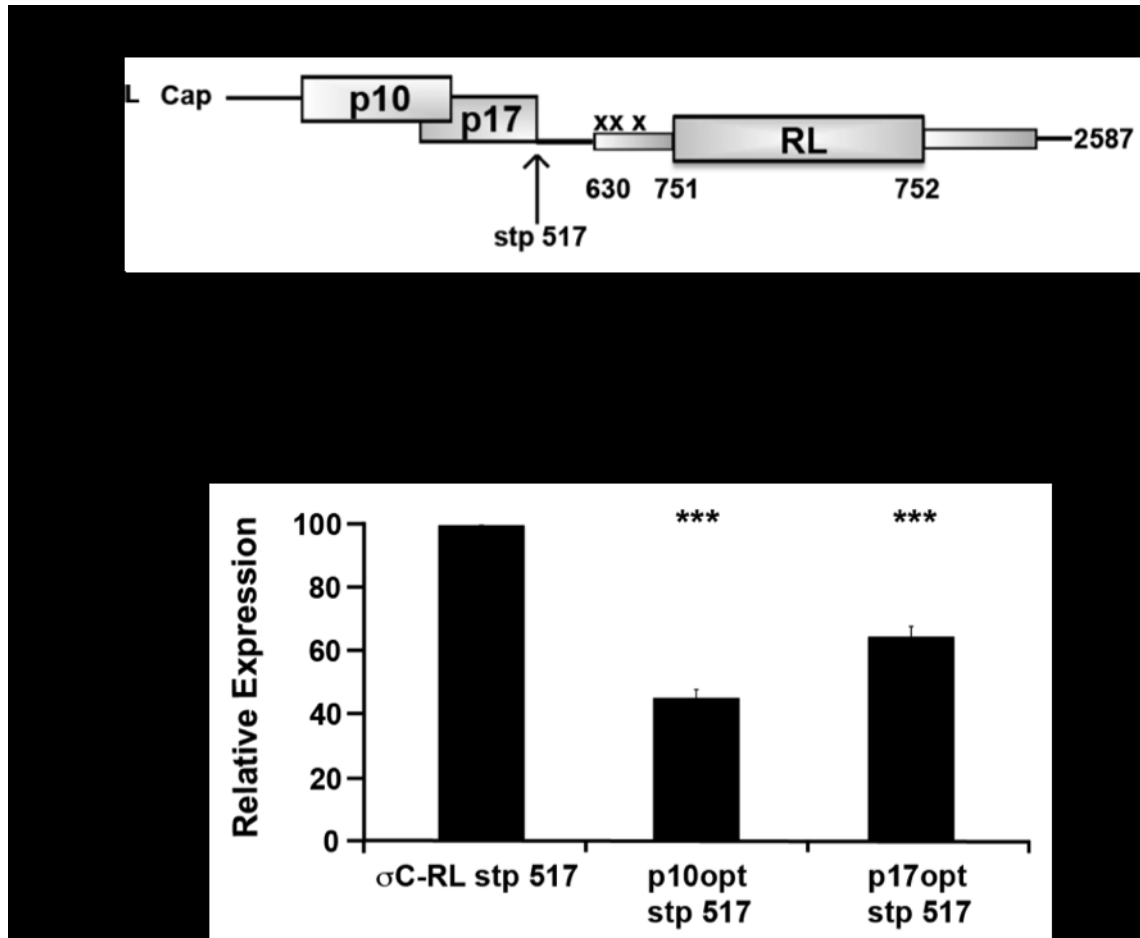


Figure 33. Expression of the σ C-RL reporter ORF is independent of the translation termination location of the p17 protein. **A.** Diagram representation of a new parental mRNA, S1-RL, where the three AUG codons present between S1 nucleotides 632 and 732 (represented by x) were point mutated to AUC. An additional point mutation was made at S1 nucleotide 517, creating a stop codon in the p17 reading frame. **B.** A stop codon was created at nucleotide 517 within the p17 reading frame through point substitution in constructs σ C-RL, p10optRL and p17optRL, thus creating σ C-RL stp 517, p10opt stp 517 and p17opt stp 517, respectively. The modified plasmids were *in vitro* transcribed and RNA transfected into QM5 cells. Cell lysates were harvested and subjected to luciferase assay. Results are reported as the mean \pm S.E. (n=3) of the relative level of σ C-RL translation, normalized to the parental σ C-RL construct. Expression levels significantly different from the parental construct (p<0.001) are indicated (***).

To ensure that creation of the stop codon at nucleotide 517 did not adversely affect the method in which ribosomes access the internal σ C start site, the same stop codon was created in the parental σ C-RL construct, and in constructs p10optRL and p17optRL (σ C-RL stp 517, p10opt stp 517 and p17opt stp 517, respectively).

Transfection of the *in vitro* transcribed RNA and subsequent luciferase assays demonstrated a similar trend in σ C expression in the presence of the stop codon at nucleotide 517, with an optimized p10 start site exerting a more pronounced inhibitory effect on σ C-RL expression than an optimized p17 start codon, but with both constructs retaining significant levels of σ C-RL expression (Figure 33B). This result validated the use of the new parental S1-RL construct, and also added to the literature on the p17 protein. Currently, all that is known about p17 is that it acts as a nucleocytoplasmic shuttling protein (Costas et al., 2005) that may retard cell proliferation (Liu et al., 2005). We can now state that the product of the p17 ORF is not required for translation initiation at the σ C start codon.

The parental S1-RL construct was then used as a template to create progressively larger internal deletions that removed regions from the p17 ORF, extending to the σ C start site (Figure 34A). These deletions included nucleotides 628-751 (Δ 628-751RL), 593-751 (Δ 593-751RL), 483-751 (Δ 483-751RL), 422-751 (Δ 422-751RL), 393-751 (Δ 393-751RL), 366-751 (Δ 366-751RL), and 312-751 (Δ 312-751RL). In all internal deletion constructs tested, except Δ 628-751RL and Δ 593-745RL, translation of the p17 ORF would terminate 71 nucleotides (not including the stop codon) downstream of the RL AUG codon, a sufficient distance downstream so as to prevent the terminating ribosomes from interfering with initiation at the RL start codon (Sachs et al., 2002). A stop codon was created at nucleotide 517 of Δ 628-751RL and Δ 593-745RL to maintain consistency with the S1-RL parental construct. Following RNA transfection of these constructs and luciferase assays, results indicated that deletion of 124 nucleotides (Δ 628-751RL), 159 nucleotides (Δ 593-751RL), 269 nucleotides (Δ 483-751RL), 330 nucleotides (Δ 422-751RL) or 359 nucleotides (Δ 393-751RL) had no effect on translation of the RL ORF (Figure 34B). However, removal of an additional 27 nucleotides (Δ 366-751RL) resulted in a substantial decrease in σ C production ($45 \pm 6\%$). Removal of an additional 54 nucleotides had no further substantial effect on translation of the RL ORF; RL

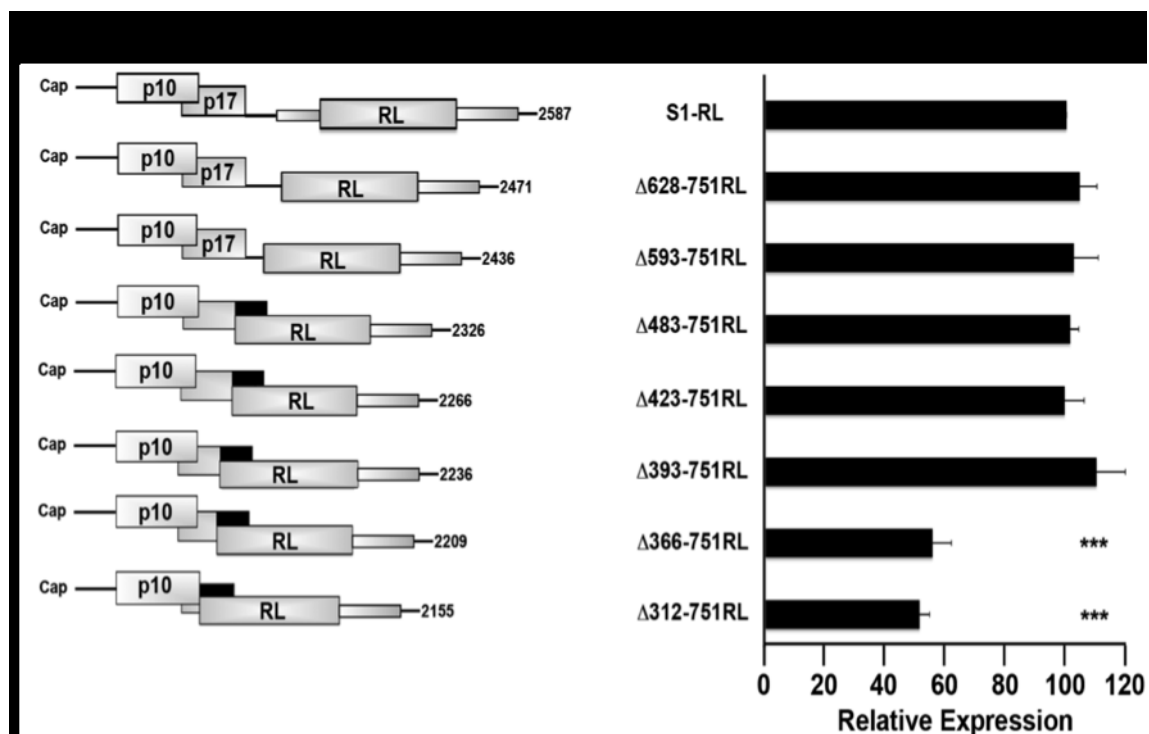


Figure 34. ARV S1 nucleotides 366-392 enhance downstream initiation. A. Diagrammatic depiction of the S1-RL cDNA modified by internal deletion (deletion of nucleotides 312 – 751, 366 – 751, 393-751, 423-751, 483-751, 593-751 and 628-751) through restriction digestion and ligation. The p17 ORF, in clones Δ312-751RL, Δ366-751RL, Δ393-751RL, Δ423-751RL and Δ483-751RL, terminates 71 nucleotides downstream of the RL AUG codon (not including the stop codon). The black portion of the p17 ORF represents translation out of frame with RL. Constructs Δ628-751RL and Δ593-751RL were point mutated at nucleotide 517 to create a stop codon within the p17 reading frame. The p17 ORF now terminates translation 84 nucleotides upstream of the RL AUG start site (not including the termination codon and including the restriction site sequence). **B.** The S1-RL parental and modified constructs were *in vitro* transcribed and transfected into QM5 cells. Cell lysates were harvested and subjected to luciferase assay. Results are reported as the mean ± S.E. (n=3-5) of the relative level of RL translation, normalized to the parental S1-RL construct. Expression levels significantly different from the parental construct ($p < 0.001$) are indicated (***)

expression was decreased by $50 \pm 3\%$ in the ($\Delta 312$ -751RL) construct. These results suggested that S1 nucleotides 366 to 392 are necessary for optimal expression of a downstream ORF in the S1 mRNA. The internal deletion constructs also indicated that the sequence immediately surrounding the σ C AUG codon is not necessary for translation from the internal start codon on the S1 mRNA, and that once the ribosome is positioned internally it is capable of initiating translation at the next proximal AUG start site.

The ability of S1 nucleotides 366-392 to promote optimal σ C production suggests that this region either enhances ribosome scanning past the strong p17 start site, or that nucleotides 366-392 contain an element involved in internal translation initiation. In attempt to distinguish between these two possibilities, the p17 AUG start codon was point substituted to AUC in the S1-RL parental background and in the $\Delta 366$ -751RL internal deletion construct (S1-RL M3 and $\Delta 366$ -751RL M3; Figure 35A). Since removal of the p17 start codon promotes translation of the downstream ORF by ~ 2 -3-fold (Figure 30), presumably by removing a barrier to scanning ribosomes, and if S1 nucleotides 366-392 are required only to promote scanning past the p17 start site, then the $\Delta 366$ -751RL construct lacking the p17 start codon should also generate levels of luciferase activity ~ 2 -3-fold higher than those observed in the parental S1-RL construct. Such was not the case; removal of the p17 start codon from the $\Delta 366$ -751RL construct did not increase levels of luciferase activity, which were in fact decreased by $\sim 30\%$ relative to the parental S1-RL construct (Figure 35B). Viewed another way, the levels of luciferase activity from the $\Delta 366$ -751RL construct (Figure 34B) and the $\Delta 366$ -751RL construct lacking the p17 start codon (Figure 35B) were similar. These results suggested that S1 nucleotides 366-392 are necessary for more than enabling enhanced scanning past the p17 start codon.

Perhaps S1 nucleotides 366-392 facilitate internal translation initiation by providing the mRNA with a suitable length in which to fold into the appropriate secondary structure. Mauro and colleagues (2006) have suggested a ribosomal tethering and clustering hypothesis to explain the ability of ribosomes to bypass uAUGs and stable hairpin structures. The tethering hypothesis posits that translation efficiency is determined in part by the accessibility of the internal initiation codon (Chappell, Edelman, and Mauro, 2006). Deletion of S1 nucleotides 366-392 could alter the natural folding of the mRNA, thus making the σ C start site inaccessible to ribosomes bound to

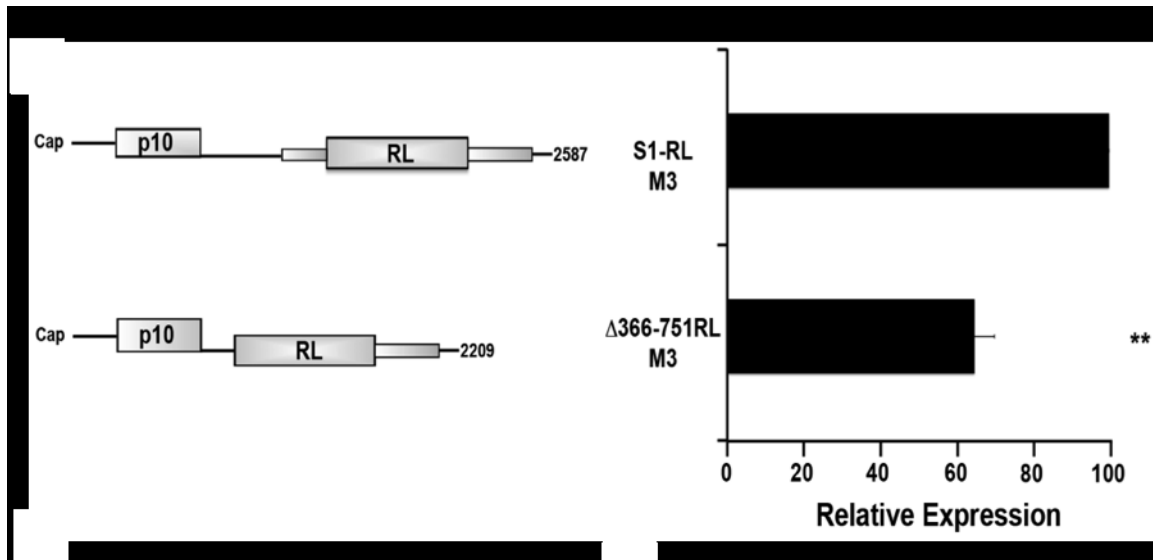


Figure 35. ARV S1 nucleotides 366-392 do not enhance leaky scanning. **A.** Diagram depicting the S1-RL and Δ 366-751 cDNAs modified by site-directed mutagenesis of the p17 start site (AUG to AUC). **B.** The parental S1-RL M3 and modified construct were *in vitro* transcribed and transfected into QM5 cells. Cell lysates were harvested and subjected to luciferase assay. Results are reported as the mean \pm S.E. (n=3) of the relative level of RL translation, normalized to the parental S1-RL M3 construct. Expression levels significantly different from the parental construct ($p < 0.01$) are indicated (**).

the 5'-cap structure. To test this hypothesis, the $\Delta 366-751\text{RL}$ construct was extended by the insertion of 114 heterologous nucleotides between the S1 sequence and the RL AUG codon ($\Delta 366-751\text{intRL}$ construct; Figure 36A). The $\Delta 366-751\text{intRL}$ mRNA is similar in length to $\Delta 483-751\text{RL}$, a construct that produced levels of luciferase activity similar to the parental S1-RL construct. Insertion of the 114 heterologous nucleotides did not rescue the ability of ribosomes to reach the RL AUG codon, as indicated by the reduced luciferase activity from $\Delta 366-751\text{intRL}$ compared to S1-RL (Figure 36B). The inhibition in downstream initiation observed from $\Delta 366-751\text{RL}$ is therefore not simply due to the length of the mRNA, suggesting that S1 nucleotides 366-392 harbour an element that is necessary for optimal leaky scanning-independent access to the 3'-proximal ORF.

The results described above indicated that the S1 mRNA sequence enhances translation of a downstream initiation codon. Closer examination of the 27-nucleotide translation enhancer region (S1 nucleotides 366-392) revealed the presence of two six-nucleotide sequences (cccauc and auaacu) that are complementary to chicken (*Gallus gallus*) 18S rRNA nucleotides 1549-1544 and 101-96 (ggguag and uauuga, respectively; Figure 37B). Alignment of the S1 cDNA sequences of 27 ARV isolates from chickens and ducks indicated complete conservation of rRNA binding site 1 (RBS1) but not rRNA binding site 2 (RBS2; Figure 38). Various reports demonstrate that 40S ribosomal subunits can be recruited to internal mRNA positions by base-pairing between the mRNA and 18S rRNA, and that this intermolecular interaction is important for translation efficiency (Chappell et al., 2006; Panopoulos and Mauro, 2008; Yueh and Schneider, 2000). To investigate the possibility that the S1 translation enhancer region base-pairs with 18S rRNA, RBS1 and RBS2 were point mutated to disrupt potential base-pairing between S1 mRNA and 18S rRNA (Figure 37C). RBS1 encompasses S1 nucleotides 370-375, while RBS2 includes nucleotides 386-391. Point mutation of S1 nucleotides 370, 371 and 375 within the $\Delta 393-751\text{RL}$ backbone (RBS1.1) inhibited RL activity by $45 \pm 7\%$, as did replacement of S1 nucleotides 372 and 373 (RBS1.2; a $47 \pm 4\%$ decrease in luciferase activity). Point mutation of nucleotides 370, 371 and 375 in the $\Delta 423-745\text{RL}$ backbone also significantly inhibited RL activity ($36 \pm 2\%$). Conversely, point substitution of S1 nucleotides 388 and 389 in RBS2 had no significant effect on

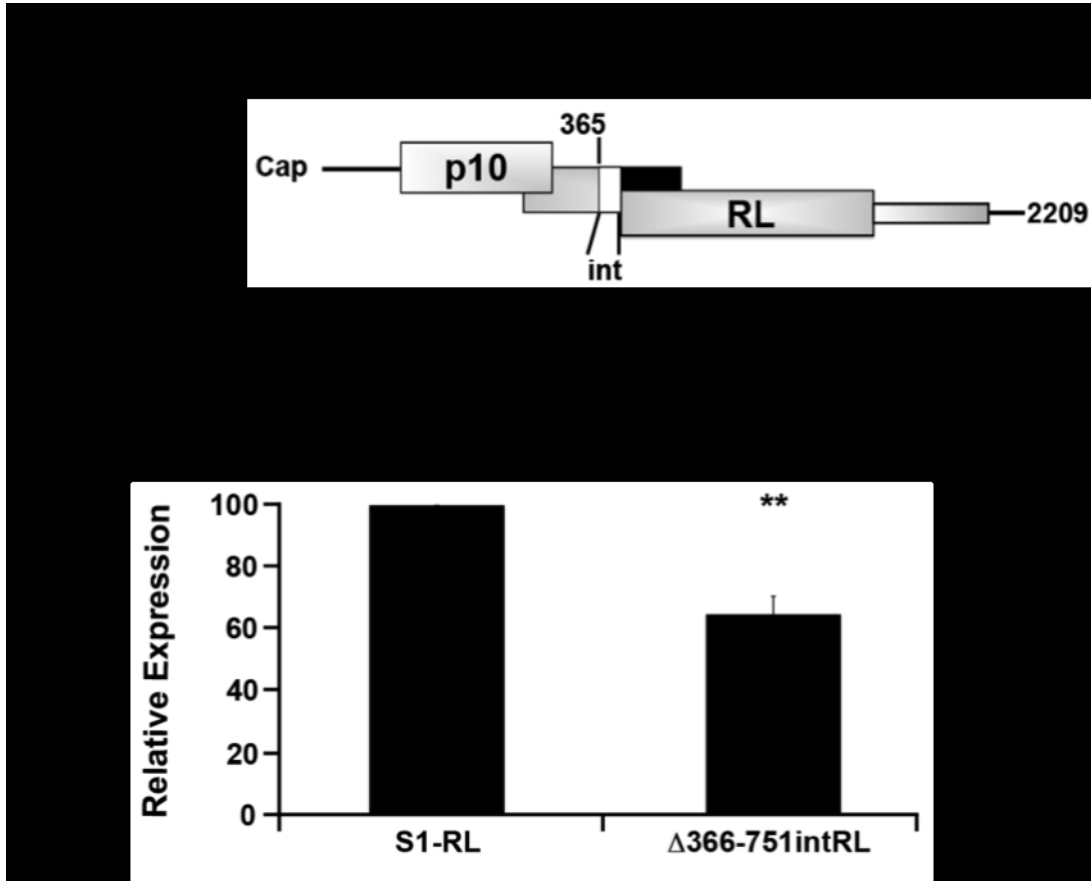


Figure 36. Expansion of $\Delta 366-751RL$ with exogenous sequence does not rescue reporter translation. **A.** Diagram indicating the location of the 114 nucleotide insert (int) into the $\Delta 366-751RL$ clone. The exogenous nucleotides were inserted between S1 nucleotide 365 and the first nucleotide of the RL ORF (denoted by white box). **B.** The S1-RL and $\Delta 366-751intRL$ clones were *in vitro* transcribed and transfected into QM5 cells. Cell lysates were harvested and subjected to luciferase assay. Results are reported as the mean \pm S.E. (n=4) of the relative level of RL translation, normalized to the parental S1-RL construct. Expression levels significantly different from the parental construct ($p < 0.01$) are indicated (**).

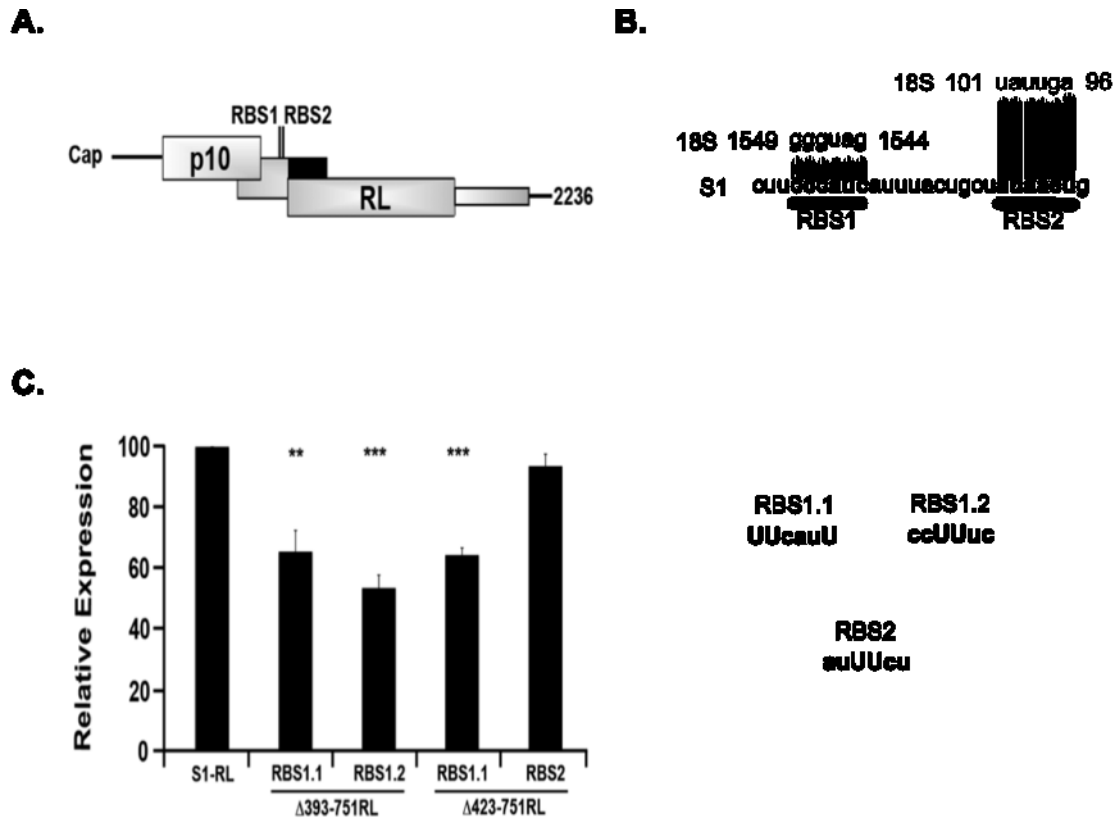


Figure 37. Disruption of the putative 18S rRNA complementarity region inhibits reporter synthesis. **A.** Diagram of the $\Delta 393-751RL$ mRNA indicating the location of the two putative ribosome binding sites (RBS1 and RBS2). **B.** S1 sequence of the 27-nucleotide translation enhancer region (S1 nucleotides 366-392), indicating the location of RBS1 and RBS2 (bold and underlined), aligned with the complementary region within 18S rRNA (numbers flanking complementary region indicate location within 18S rRNA sequence). **C.** The parental S1-RL and modified constructs were *in vitro* transcribed and RNA transfected into QM5 cells (left side). Construct $\Delta 393-751RL$ was modified by point substitution of nucleotides 370, 371 and 375 (RBS1.1) or nucleotides 372 and 372 (RBS1.2). Construct $\Delta 422-751RL$ was also modified by point substitution at S1 nucleotides 370, 371 and 375 (RBS1.1) and 388 and 389 (RBS2) (right side). Cell lysates were harvested and subjected to luciferase assay. Results are reported as the mean \pm S.E. (n=3-4) of the relative level of RL translation, normalized to the parental S1-RL construct. Expression levels significantly different from the parental construct ($p < 0.01$ and $p < 0.001$) are indicated (** and ***).

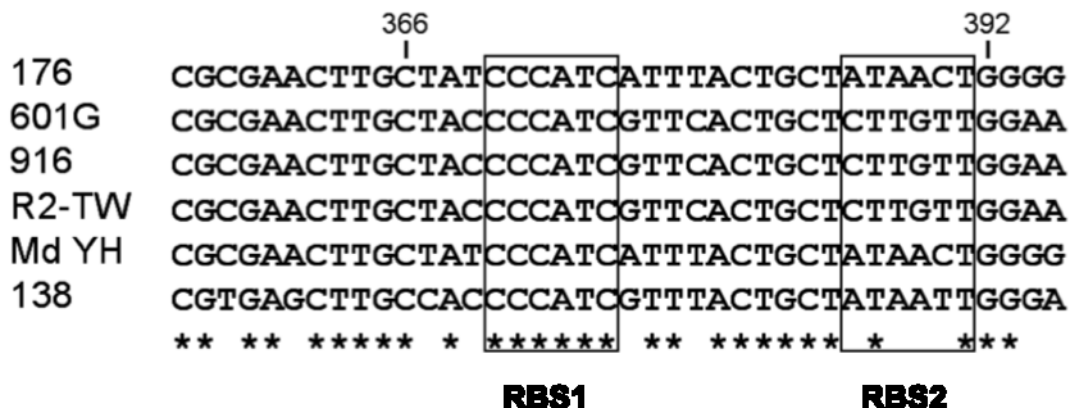


Figure 38. Alignment of S1 cDNA sequences. Alignment of S1 nucleotides 356-395 from six ARV isolates. Consensus nucleotides are indicated (*) and RBS1 and RBS2 regions are boxed.

translation of the RL ORF. These results suggest that RBS1, not RBS2, may be responsible for downstream translation initiation.

3.17 An Optimized p17 Start Site Inhibits Downstream Expression In A Heterologous mRNA

To determine whether an optimized p17 start site functions in a manner similar to that seen in the full-length S1 mRNA, S1 nucleotides 267 to 320, with an optimized p17 start codon, were inserted into the 5'-UTR of construct β -RL (Figure 39A; β -p17opt#1-RL). A larger S1 insert, S1 nucleotides 260-393 (β -p17opt#2-RL), was also created because the former insert did not include the putative translation enhancer element RBS1 identified in Figure 37. Luciferase assays of lysates harvested from QM5 cells RNA-transfected with RNA derived from β -p17opt#1-RL unexpectedly revealed a level of inhibition in RL activity ($82 \pm 4\%$; Figure 39B) more similar to the positive control β -ORF-RL (Figure 24) than the ARV p17opt mRNA (Figure 22). Surprisingly RL activity was similarly inhibited in clone β -p17opt#2-RL ($83 \pm 2\%$) as it was in clone β -p17opt#1-RL. These data would suggest that although the putative translation enhancer element RBS1 may function to enhance downstream translation in the context of the S1 mRNA, it is unable to do so in a heterologous mRNA. RBS1 is therefore necessary, but not sufficient, for optimal expression of a downstream ORF suggesting that other features of the S1 mRNA work in conjunction with RBS1 to promote ribosome access to downstream start sites.

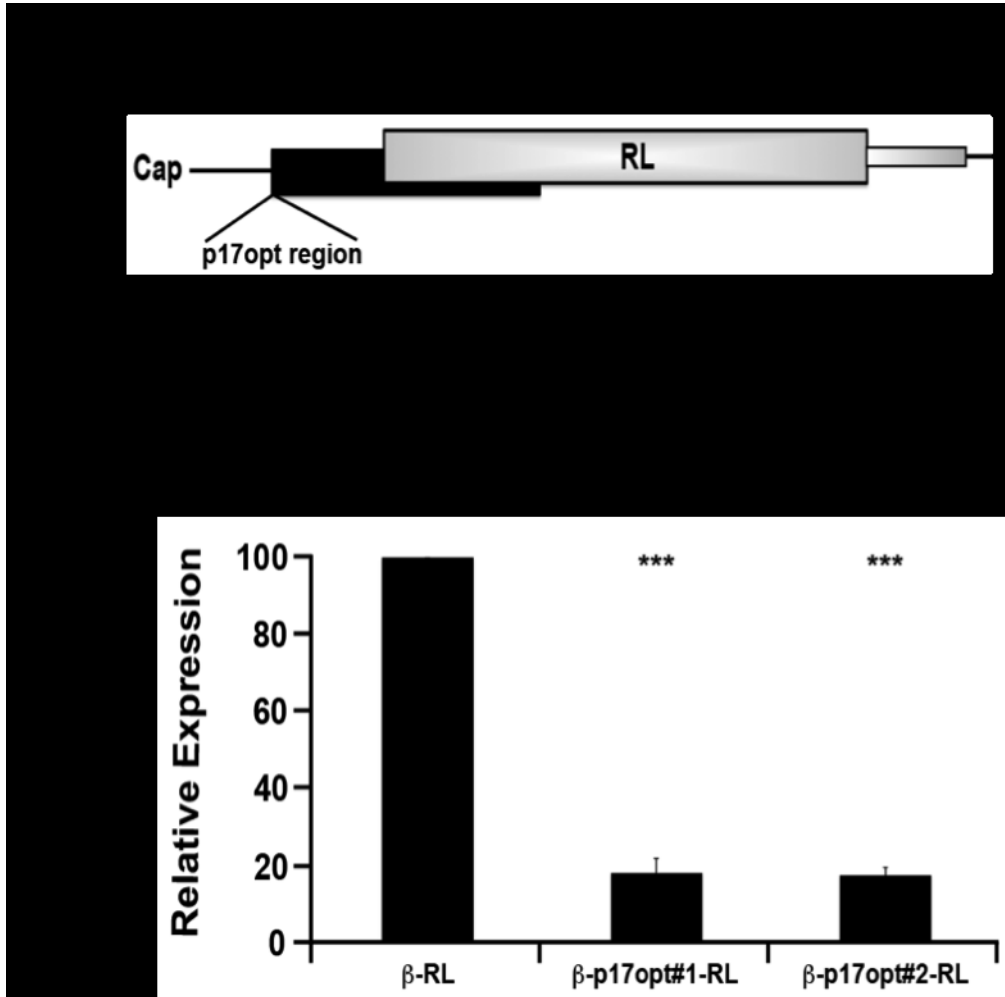


Figure 39. The optimized p17 start site functions according to the leaky scanning model when present within a heterologous mRNA. A. Diagram depicting the insertion of S1 nucleotides 267-320 or 260-393, both with an optimized p17 AUG codon into the UTR of β -RL, creating a bicistronic mRNA (β -p17opt#1RL and β -p17opt#2RL, respectively). **B.** The mono- and bi-cistronic constructs were *in vitro* transcribed and transfected into QM5 cells. Cell lysates were harvested and subjected to luciferase assay. Results are reported as the mean \pm S.E. (n=3) of the relative level of RL translation, normalized to the parental β -RL construct. Expression levels significantly different from the parental construct ($p < 0.001$) are indicated (***).

CHAPTER 4: Discussion

4.1 Overview

The S1 genome segment of the ARV is functionally tricistronic, encoding three independent protein products from three sequential, partially overlapping ORFs (Shmulevitz et al., 2002). This unusual tricistronic arrangement of ORFs must influence the mechanism(s) of translation control on the mRNA since the dogma of translation initiation, the cap-dependent scanning model, suggests that ribosomes would normally only efficiently translate the 5'-proximal ORF. The tricistronic nature of the S1 mRNA indicates that translation initiation complexes must bypass two uORFs and four methionine codons in order to reach the 3'-proximal σ C start site, which lies 630 nucleotides downstream from the 5'-cap. To add to the complexity of the S1 mRNA, ribosomes translating the mRNA generate a nonstructural, membrane-bound p10 FAST protein, a nonstructural nucleocytoplasmic shuttling protein, p17, and σ C, an essential structural protein involved in virus-cell attachment. Four alternate mechanisms of translation initiation may be responsible for initiation on the S1 mRNA; an IRES element, ribosomal reinitiation, ribosome shunting, and leaky scanning. Based on the suboptimal context of the p10 start site, it seems plausible that leaky scanning may be at least partially involved in downstream initiation. Previous studies (Shmulevitz and Duncan, 2000; Shmulevitz et al., 2002), and results presented herein, indicate that translation of the p10 and p17 ORFs are in fact coordinated via leaky scanning. The mechanism of translation initiation at the σ C AUG codon, the main subject of this research project, appears to occur by two independent mechanisms, context-independent leaky scanning and scanning-independent ribosome handoff from the 5'-cap.

4.2 Translation Of The σ C ORF Occurs Efficiently From The Full-Length mRNA

Although many plant and animal viruses appear to produce polycistronic mRNAs in which only the 5'-proximal AUG is translated, they in fact frequently harbour cryptic promoters and/or splice sites that position the "silent" 3'-cistron in the 5'-proximal position (Kozak, 2002). Northern blot analysis revealed a single S1-specific transcript in cells transfected with plasmid pARV-S1 (Figure 8A), indicating that translation of the σ C ORF occurs from the full-length, tricistronic S1 mRNA and not from alternate splicing to

generate a truncated mRNA that places the σ C AUG codon in the 5'-proximal position. This conclusion is further supported by RNA transfection studies using a non-functional cap analogue or a hairpin inserted in the 5'-UTR, both of which dramatically reduced or eliminated σ C expression (Figure 21). This would not be the case if RNA degradation generated a truncated, monocistronic mRNA for σ C expression. Expression of the σ C ORF therefore derives from a full-length S1 mRNA.

The scanning model of translation initiation predicts that the presence of uAUGs should impede translation of a downstream start codon since 40S subunits scan the mRNA until the first AUG codon in a favourable context is encountered (Kozak, 1989c). The efficiency with which ribosomes access the σ C AUG triplet was therefore examined by deleting the four AUG codons that are situated upstream of the σ C start site by site-directed mutagenesis, thus creating a monocistronic S1 mRNA (pARV-S1mono) where the σ C start site occurs in the 5'-proximal position. Quantitative Western blot analysis of lysates from cells transfected with pARV-S1mono revealed a 2.3-fold increase in σ C expression compared to σ C translation from the polycistronic mRNA (Figure 8B), although variability in the quantitative Western blots made this increase statistically insignificant. This result was confirmed via RNA transfection of a σ C-RL reporter mRNA that was also subjected to nucleotide point substitution to delete the four uAUGs (Figure 30; Mono). Analysis of luciferase activity from the reporter constructs revealed a significant 2.6-fold increase in translation initiation from the monocistronic mRNA compared to the parental σ C-RL construct. These results suggest that the uAUGs do exert an inhibitory effect on downstream translation initiation, although the extent of inhibition was relatively modest. By comparison, removal of the uORFs present within the yeast *GCN4*, mouse ATF4 and human GADD34 mRNAs, results in an approximate 30-500-fold increase in expression of the main ORF (Harding et al., 2000; Lee, Cevallos, and Jan, 2009; Mueller and Hinnebusch, 1986). Together, the above results indicate that σ C translation initiation occurs from the full-length S1 mRNA in a manner that is almost as efficient as linear scanning of a monocistronic version of the same mRNA, since translation of the downstream ORF appears to be relatively unaffected by the presence of uAUGs.

4.3 Quantitative Analysis Of Western Blots, Luciferase Assays And Real-Time PCR

The Western blots presented are representative of all blots analyzed for that particular set of constructs, and analysis of the blots was performed quantitatively (Figure 9). It should be noted that to accurately analyze the fold-change in protein band intensity, various factors had to be taken into consideration. For example, serial dilutions of lysates obtained from cells transfected with the parental and altered mRNA had to be loaded onto the same gel to obtain the linear range of exposure. The membrane also had to be probed for an internal control, such as actin, at the same time as the protein(s) of interest. Surprisingly, two-fold dilutions did not result in a linear range of exposure for the S1 encoded proteins, indicating that they fell outside of the linear range much more quickly than anticipated. For this reason, lysates were loaded in 1 μ g decreasing amounts. Also, a minimum of three independent experiments had to be analyzed in order to have confidence in the percent/fold change in expression reported. Knowing that such extensive measures must be undertaken to accurately interpret Western blot results, examination of the literature should be performed more critically. For example, translation of the human papillomavirus type 18 E1 protein was suggested to occur via ribosome shunting, regardless of the presence of the E7 ORF upstream (Remm, Remm, and Ustav, 1999). The Western blots presented in this report however, were not performed quantitatively (i.e. no serial dilution of lysates or loading control). A number of the blots are also under or over loaded, thus making interpretation of the results that much more difficult.

As with analysis of the Western blots, correct interpretation of the luciferase assays could only occur with examination of multiple independent experiments (Figure 25). I discovered that although the capping efficiency between *in vitro* transcription kits was approximately the same, slight variations might have occurred and with the variations in capping efficiency would come differences in protein expression. Also, due to unavoidable differences in seeding densities between experiments, luciferase activity obtained from each altered mRNA could only be compared to its respective parental construct *in vitro* transcribed from the same transcription kit and transfected on the same day. Again, examination of the literature revealed that not all experiments were conducted in such a quantitative manner and thus, the interpretation of these results

should be re-examined. For example, luciferase expression was used to analyze the effect the 3'-UTR of Bunyamwera orthobunyavirus S-segment has on translation efficiency (Blakqori, van Knippenberg, and Elliott, 2009). In this study, the authors describe the use of *in vitro* transcription kits in the production of luciferase reporter mRNAs, which were subsequently transfected into cells. Unfortunately, they do not indicate whether each experiment used a different batch of *in vitro* transcribed mRNA or whether the same mRNA was used each time. Also, a couple of their figures represent less than three experiments. The need to conduct quantitative experiments, as described for Western blot and luciferase assay analyses, is especially important when the change in expression level is minor (< 3-fold).

Similar cautions apply to qRT-PCR approaches to quantify transcripts. Normal qRT-PCR is performed in a quantitative manner, however, RNA transfection of *in vitro* transcribed mRNA adds another level of difficulty to the system. Due to the large amount of RNA added to the QM5 cells, a substantial quantity of the RNA remained on the surface of the cells at the time of harvesting. The presence of even minor amounts of residual RNA on the outside of cells interferes with accurate quantitation of the intracellular concentration of RNA. For this reason cells were treated with RNase A prior to RNA extraction to degrade any remaining extracellular RNA (Figure 23). I have yet to encounter any literature that takes this factor into consideration.

4.4 Expression Of The σ C ORF Is Not Mediated By Previously Described Alternate Translation Initiation Mechanisms

4.4.1 IRES-Independent

The cap-dependent scanning model of translation initiation cannot explain σ C ORF expression from the full-length S1 mRNA, and so the alternate models of translation initiation were examined. A common mechanism by which ribosomes bypass uAUGs and initiate internally, particularly on viral mRNAs, is through the use of an IRES element (Fitzgerald and Semler, 2009; Hellen and Sarnow, 2001). The highly structured IRES elements are normally found within the 5'-UTR of the mRNA and direct internal initiation in a cap-independent manner. Since the ARV S1 mRNA possesses a 5'-cap (Furuichi et al., 1975; Furuichi, Muthukrishnan, and Shatkin, 1975) and the 5'-leader is only 24 nucleotides long, it seems unlikely that the ARV S1 mRNA contains a previously

described IRES element. Analysis of the bicistronic construct in which the S1 mRNA was inserted downstream of the EGFP-encoding ORF provides additional evidence by failing to produce any trace of the σ C protein, even upon extended exposure of the fluorogram (Figure 13). Furthermore, co-transfection of QM5 cells with pARV-S1 and pPV2A, a plasmid expressing the poliovirus 2A protease, actually inhibited σ C translation (Figure 14B), contrary to the result expected if an IRES element were responsible for σ C initiation. The virally encoded 2A protease enhances IRES activity by cleaving eIF4G at its N-terminus, ultimately separating the regions that bind eIF3 and eIF4E, thus preventing cap-dependent 40S recruitment to the mRNA (Etchison et al., 1982; Krausslich et al., 1987). Excluding Hepatitis A virus, none of the other viral IRES elements require an intact eIF4G for proper functioning (Jackson, 2005), suggesting that the S1 mRNA is devoid of an IRES element. This hypothesis was confirmed by direct analysis of the importance of the 5'-cap on σ C translation through analysis of *in vitro* transcribed S1 mRNA with and without a functional cap structure and with a stable hairpin structure present at the 5'-terminus (Figure 21). The importance of the 5'-cap and an intact eIF4G protein for σ C translation indicates that internal initiation on the S1 mRNA occurs in a cap-dependent, IRES-independent manner.

4.4.2 Reinitiation-Independent

A translation termination-reinitiation mechanism was suggested to be responsible for translation initiation at the σ C ORF (Kozak, 2002). This mechanism suggests that the p10 ORF plays a dual role, to encode the p10 polypeptide and to escort ribosomes past the strong p17 start codon. This reinitiation theory is strengthened by the absence of extraneous AUG triplets in the 308 nucleotides that separates the p10 termination codon and the σ C start codon, and by the length of the intergenic region (~300 nucleotides), which would allow re-scanning ribosomes enough time to reacquire the eIF2-GTP-Met-tRNA_i ternary complex necessary to initiate translation at the σ C ORF. Cellular mRNAs, such as those encoding the glycine tRNA synthetase and the transcription factors C/EBP α and C/EBP β , utilize the presence of an uORF to shuttle ribosomes past a preferred start site (Calkhoven, Muller, and Leutz, 2000; Mudge et al., 1998). However, three lines of evidence show that σ C expression is not the result of reinitiation upon translation

termination of the p10 ORF. First, optimization of the p10 start site, which increases p10 translation ~6-fold, did not result in a concurrent increase in σ C synthesis (Figure 11) as would be expected due to the increased number of ribosomes potentially able to undergo reinitiation. Second, the presence of premature stop codons within the p10 reading frame (Figure 16) that should cause re-scanning ribosomes to encounter the p17 start codon did not diminish σ C translation. The strong context of the p17 AUG start codon, with the preferred A residue in the -3 position (Kozak, 1981; Kozak, 1984a), would be expected to at least partially inhibit scanning 40S subunits from reaching the σ C start site. Figures 29 and 30 demonstrate that the p17 start site is sufficient to block most scanning ribosomes. The inability of the p17 start site to impede scanning ribosomes when stop codons were inserted in the p10 ORF demonstrates that translation initiation at the σ C start codon does not proceed via a reinitiation mechanism. This is particularly true for the p10stp84 construct, which contains a 209 nucleotide intergenic region and when translated, produces a 20 amino acid peptide, since both of these factors satisfy the requirements for maximal reinitiation (Kozak, 2001a). Third, RNA transfection of constructs containing a p10 start site deletion, either by truncation of the 5'-end of the S1 mRNA (Figure 29) or nucleotide substitution (AUG to AUC; Figure 30), had no negative effect on translation initiation at the σ C start codon. If translation of the p10 ORF was required to escort ribosomes past the p17 start site, elimination of the p10 ORF should have resulted in a decrease in initiation at the σ C AUG codon. Cumulatively, these results provide strong evidence in support of a reinitiation-independent mechanism for σ C translation.

4.4.3 Ribosome Shunting

The best-studied examples of ribosomal shunting comes from the examination of translation initiation events on the 35S pgRNA of CaMV (Futterer et al., 1990; Futterer, Kiss-Laszlo, and Hohn, 1993; Park et al., 2001; Pooggin, Hohn, and Futterer, 2000), and the pgRNA of RTBV (Futterer et al., 1996; Pooggin et al., 2006), two plant pararetroviruses. In both examples, the 40S ribosomal subunit binds the 5'-cap and scans the mRNA until the first uORF is encountered. Translation, termination and release of the peptide encoded by uORFA must occur for shunting to proceed. The base of a strong stem-loop structure, which contains many uAUGs and can be divided into stem sections

1-3, is positioned six nucleotides downstream of the uORFA termination codon (Hemmings-Mieszczak, Steger, and Hohn, 1997; Pooggin, Hohn, and Futterer, 1998). Upon uORFA translation termination, the released 40S subunit still retaining initiation factors necessary for scanning and reinitiation but potentially not for unwinding secondary structure, shunts over an ~480 nucleotide structured region to reach the shunt landing site where the 40S subunit is able to scan the mRNA and reinitiate at the AUG codon of the first large viral ORF. The 19S RNA of CaMV acts as a monocistronic mRNA for the production of a transactivator/viroplasm (TAV) protein (Driesen et al., 1993) that transactivates the expression of several uORFs on the CaMV 35S RNA by enabling ribosome reinitiation (Futterer and Hohn, 1991; Park et al., 2001). In contrast, ribosome shunting on the RTBV does not require a TAV-like protein and translation initiation of ORFII and ORFIII occurs by leaky scanning (Futterer et al., 1997). Similar sORF-stem-mediated shunting mechanisms have recently been discovered in a mammalian retrovirus (Schepetilnikov et al., 2009) and on a cellular mRNA (Sherrill and Lloyd, 2008). Examination of the arrangement of ORFs on the ARV S1 mRNA indicates that a sORF-stem-mediated ribosome shunt mechanism, as just described, is not responsible for translation initiation at the σ C AUG codon. The ARV S1 mRNA does not encode a sORF, and if a stem-loop structure were present within the mRNA, it would have to be present within the coding region of the p10 and/or p17 ORFs.

Variation of the sORF-stem-mediated shunt mechanism has been described for adenovirus late mRNAs (Xi, Cuesta, and Schneider, 2004; Yueh and Schneider, 2000), Sendai virus Y mRNA (de Breyne et al., 2003), human papillomavirus E1 mRNA (Remm, Remm, and Ustav, 1999), and duck hepatitis B virus (Cao et al., 2009; Sen, Cao, and Tavis, 2004). Like the shunt mechanism described above, shunting on these viral mRNAs also occurs in a cap-dependent manner and requires limited scanning of the mRNA 5'-terminus by the 40S subunit before it is translocated to an internal position on the mRNA. Unlike the CaMV and RTBV shunt mechanisms, however, translation of a sORF does not appear to be required on these viral mRNAs. As with the shunt mechanism operating on CaMV, a virally encoded protein, L4-100K, enhances shunting on the adenovirus late mRNAs by selectively binding eIF4G and the viral tripartite leader sequence in a phosphotyrosine-dependent manner (Xi, Cuesta, and Schneider, 2004; Xi,

Cuesta, and Schneider, 2005). The only viral proteins that could participate in σ C translation initiation are those also translated from the S1 mRNA, p10 and p17, because no other viral proteins are present within the transfected cells. The ARV p10 protein is a plasma membrane-bound protein that induces cell-to-cell fusion (Shmulevitz and Duncan, 2000) and thus not a likely candidate for participation in the initiation reaction. The polypeptide encoded by the p17 ORF may function to reduce cell proliferation by activating p53 (Liu et al., 2005), therefore, it too is unlikely to be involved in translation initiation. Continued expression of the σ C ORF from the full-length monocistronic mRNA (Figure 8 and Figure 30), and from an mRNA that produces a truncated version of the p17 polypeptide (Figure 33) confirms that translation initiation at the internal σ C AUG codon does not require additional viral factors.

A common theme with all the shunting mechanisms presented is the requirement for limited scanning of the mRNA by the 40S subunit. Recruitment of the 40S subunit and its associated canonical initiation factors to the S1 mRNA in a cap-dependent manner (Figure 21) position the subunit such that it occupies the first 30-40 nucleotides of the mRNA (Kozak, 1977; Kozak and Shatkin, 1977). The bound subunit would therefore occlude the entire S1 5'-UTR and the first 5-10 nucleotides of the p10 ORF. Since optimization of the p10 ORF did not eliminate σ C expression (Figure 11 and Figure 22), shunting of the pre-initiation complex past the p10 and p17 start sites would require little, if any, scanning of the S1 mRNA. Truncation of the 5'-end of the S1 mRNA confirmed that in an RNA based transfection system, the 5'-proximal 147 nucleotides do not possess a *cis* element necessary for shunting ribosomes past the strong p17 start codon (Figure 29). This result is in contrast with a similar 5'-truncation experiment performed using a DNA plasmid expression system (Figure 15), where removal of the 5'-proximal 79 and 147 nucleotides eliminated both p10 and σ C expression. The DNA transfection result can be interpreted in one of two ways; first, deletion of both in-frame p10 AUG codons and subsequent inhibition in σ C expression is consistent with a role for the p10 ORF in escorting ribosomes past the strong p17 start site in a reinitiation-dependent fashion. Since reinitiation has already been ruled out as the mechanism responsible for initiation at the σ C start codon, the second possibility must be examined. The DNA plasmid 5'-truncation data is also consistent with the hypothesis that the truncations removed a *cis*

element necessary for shunting ribosomes past the p17 AUG codon. The reason for this apparent discrepancy between the DNA plasmid and RNA transfection based analysis systems is unknown, however, it has been reported that different transcription methods (i.e. transcription in the nucleus versus *in vitro* transcription) can result in different messenger ribonucleoprotein complexes and differential folding, ultimately producing contradictory results (Kataoka et al., 2000; Koh and Mauro, 2009). Nuclear transcription of the 5'-truncated constructs would result in spliced transcripts carrying vector-derived sequence at both the 5'- and 3'-termini, in the presence of a poly(A) tail and in the presence of cellular proteins added to the mRNA during splicing and nuclear export (Erkman and Kutay, 2004; Rodriguez, Dargemont, and Stutz, 2004). The *in vitro* transcribed RNA would possess none of these extraneous factors and would therefore be more likely to adopt a folding pattern similar to that conferred by the virally transcribed mRNA. For these reasons, the result obtained from the RNA transfected 5'-truncation constructs that suggested that no *cis* element necessary for ribosome shunting resides within the 5'-proximal 147 nucleotides is considered representative of the actual mechanism of translation initiation on the viral S1 mRNA. Taken together, the above results indicate that the S1 mRNA does not possess a *cis* element within the 5'-proximal 147 nucleotides necessary for translation initiation at the σ C start site, and internal initiation occurs independent of additional viral proteins and a sORF-stem-mediated ribosome shunting mechanism.

4.4.4 Leaky Scanning

The most common alternative mechanism of translation initiation, context-dependent leaky scanning, is a modification of the scanning model whereby ribosomes leak past the 5'-proximal AUG codon when they reside in a suboptimal context (Kozak, 2002). In mammals, the sequence ccA/GccAUGG is optimal for AUG triplet recognition, with an adenine in the -3 position (relative to the A of the AUG codon) being the most important and conserved nucleotide (Kozak, 1981; Kozak, 1984a; Kozak, 1987a). This optimal context normally results in almost complete inhibition of translation of a downstream ORF (for example, Chappell et al., 2006). In a now classical set of experiments, Kozak demonstrated that insertion of an AUG codon, with a A in the -3

position but differing in every other position of the consensus sequence, upstream of the preproinsulin gene was able to inhibit downstream expression by ~80%. Reiteration of the preproinsulin initiator codon in its natural context, with an A in the -3 position and a G in the +4 position, upstream of the preproinsulin gene completely abolished preproinsulin production (Kozak, 1984b). Also, insertion of the strong initiation signal (ccAacAUGG) upstream of the VP3 ORF of Simian virus 40 19S late mRNA inhibited VP3 expression up to 20-fold (Sedman and Mertz, 1988). I demonstrated a similar level of inhibition upon creation of an optimized start codon (ccAccAUGG) in the 5'-UTR of the β -RL mRNA construct, which decreased translation of the downstream ORF by ~95% (Figure 24). Many articles propose a leaky scanning model on their respective mRNAs, but close examination of the data would suggest something other than context-dependent leaky scanning was occurring (Castano, Ruiz, and Hernandez, 2009; Frederiks et al., 2009). The 1.6 kb subgenomic RNA of Pelargonium line pattern virus lacks a 5'-cap and 3' poly(A) tail but is functionally tricistronic encoding three distinct proteins, p7, p9.7 and p37. The 370 nucleotide region upstream of the p37 ORF contains a single AUG codon, in a poor context, which opens the p7 ORF. Point substitution of the p9.7 GUG codon to AUG increased p9.7 expression by ~4-fold, while residual p37 synthesis ranged from ~30-80%. Insertion of two additional AUG codons in a good context in the p9.7 AUG background, thus making the p37 start site the fifth AUG present on the mRNA, further reduced p37 expression to a residual ~20% (Castano, Ruiz, and Hernandez, 2009). Although the authors suggest a context-dependent leaky scanning mechanism for translation of all three ORFs, the 4-fold increase in p9.7 expression in the presence of an AUG start site and the lack of a concurrent decrease in p37 synthesis, along with the residual ~20% p37 expression in the presence of four uAUGs, would suggest that a proportion of 40S subunits initiating translation at the p37 ORF may do so via an alternate mechanism.

The ARV p10 start site lies in a suboptimal context, suggesting that leaky scanning may play a role in downstream initiation. Transfection of a DNA plasmid carrying an optimized p10 AUG codon decreased p17 production by ~8-fold (Figure 10) and it increased p10 expression ~6-fold (Figure 11), indicating that p10 and p17 expression is coordinated by leaky scanning. Although the early literature on leaky

scanning proposes a complete inhibition of downstream expression in the presence of an optimized uAUG (Kozak, 1984b; Kozak, 1986b), more recent, quantitative work demonstrates that the inhibition is not always complete (Castano, Ruiz, and Hernandez, 2009; Wang and Rothnagel, 2004). Flow cytometric analysis of an EGFP reporter present in transiently transfected mammalian cells revealed the production of biologically significant protein levels from an mRNA containing multiple uAUGs (Wang and Rothnagel, 2004). The presence of one uAUG in an optimal context reduced downstream expression by 70-90%, while the presence of two uAUGs, one in good context, the other optimal, did not inhibit expression any further. These results are in contrast to the radiolabeled immunoprecipitation results presented earlier that indicated that a single uAUG in an optimal context can completely (100%) inhibit downstream expression (Kozak, 1984b).

If the results presented by Wang and Rothnagel (2004) more accurately represent the ability of the 40S subunit to bypass an uAUG, the residual p17 expression was not unexpected. The approximate 2-fold decrease in σ C production observed upon p10 optimization is not proportional to the increase in p10 expression, suggesting that context-dependent leaky scanning past the p10 start site may play only a minor role in initiation of the 3'-proximal ORF. Not surprisingly, optimization of the p17 start site, which naturally possesses a strong context with an A in the -3 position, had no significant effect on translation initiation at the σ C AUG in the context of plasmid DNA transfections (Figure 11). These results were confirmed by RNA transfection of a reporter construct carrying either an optimized p10 or p17 start site (Figure 22). Once again, optimization of the p10 AUG codon had a more pronounced effect on internal initiation than did p17 optimization. Even though uAUG optimization did significantly affect σ C expression, there was a substantial level of translation retention, much more than anticipated according to the literature (Cao and Geballe, 1995; Futterer et al., 1997; Herzog, Guilley, and Fritsch, 1995; Kozak, 2002).

Remarkably, the inability of an optimized start site to eliminate downstream expression may be a particular feature of the S1 mRNA (Figure 24). One possible explanation for the residual luciferase activity due to internal initiation in the presence of an optimized p10 start codon is the proximity of the p10 AUG to the 5'-cap (Kozak,

1988; Kozak, 1991a; Sedman, Gelembiuk, and Mertz, 1990). Extension of the S1 5'-UTR with 77-nucleotides of heterologous sequence derived from the rabbit β -globin 5'-UTR actually increased, rather than decreased, the ability of the ribosome to initiate at the internal reporter ORF (Figure 26) indicating that the proximity of the p10 start site to the cap structure does not allow an elevated level of leak-through. Wang and Rothnagel (2004) suspected a similar cause for the significant level of residual downstream expression on their EGFP reporter mRNA that contained a 20-nucleotide 5'-UTR and an optimal uAUG. Extension of the EGFP reporter 5'-UTR to 94 nucleotides did not, however, affect translation initiation of the internal AUG codon (Wang and Rothnagel, 2004). Another interesting observation made from examining the effect of lengthening the S1 5'-UTR on internal initiation (Figure 26) was that in the framework of this mRNA, optimization of either the p10 or p17 start sites decreased translation of the reporter ORF to a similar extent (~30%). This suggests that whatever mechanism(s) ribosomes use to bypass the uORFs to reach the internal σ C start codon, it is specific for the S1 mRNA and functions with equal efficiency at the p10 and p17 AUGs.

As discussed in the section on reinitiation, the strong p17 start site naturally acts as a significant barrier to scanning ribosomes (Figure 29 and Figure 30). The single nucleotide point substitution (AUG to AUC) results presented in Figure 30 also demonstrate that the three methionine codons that reside within the p10 reading frame do not adversely affect translation initiation at the σ C AUG, even though Met4 (M4) is in a good context with a G in the -3 and +4 positions. The ability of an optimized p17 start site to decrease downstream initiation by no more than ~30% is somewhat surprising and suggests that some form of context-independent leaky scanning may be occurring on the S1 mRNA. Context-independent leaky scanning would require the 40S subunit to bypass an AUG codon despite the fact that it resides in an optimal context and for the subunit to continue scanning the mRNA until a more suitable start site is encountered. As demonstrated in other viral systems (Castano, Ruiz, and Hernandez, 2009; Futterer et al., 1997; Herzog, Guilley, and Fritsch, 1995), the lack of potential translation start codons between the p17 AUG triplet and the σ C initiation site, in any reading frame, indicates that AUG codons are under strong negative selection in this region, supporting the notion that ribosomes may scan this region of the S1 mRNA to reach the downstream start site.

The negative selection proposal is supported by the fact that 19 AUG codons are present in the 1011 nucleotides downstream of the σ C start site, which is in sharp contrast to the four methionines present in the 629 nucleotides upstream of σ C. Addition of AUGs in a strong context downstream of the p17 AUG codon confirmed that ribosomes undergo context-independent leaky scanning on the S1 mRNA (Figure 31) since the presence of eight uAUGs, six of which are in either a good or strong context, decreased but never fully eliminated downstream translation. In context-dependent leaky scanning, the insertion of fewer additional AUGs decreased internal initiation more dramatically (Futterer et al., 1997; Herzog, Guilley, and Fritsch, 1995). Interestingly, creation of two uAUGs in-frame with the p17 ORF reduced downstream translation initiation to a level (~70%) comparable to the creation of three in-frame uAUGs (Figure 32). This result would suggest that all ribosomes scanning this region have been effectively inhibited and that the residual translation occurring at the 3'-proximal ORF is occurring by another mechanism.

To evaluate the ability of ribosomes to traverse a different obstacle, a stable hairpin structure ($\Delta G = -60$ kcal/mol) known to inhibit scanning ribosomes on the 5' side of the hairpin (Kozak, 1986a; Kozak, 1989a; Pelletier and Sonenberg, 1985), was introduced into the S1 mRNA (Figure 27). Although insertion of the stable hairpin structure significantly inhibited translation of the σ C-RL reporter ORF regardless of its position within the S1 mRNA, it had a more pronounced effect when present within the p17 region (between S1 nucleotides 579 and 580) than it did when present within the p10 region (between S1 nucleotides 222 and 223). Also, the presence of two significant barriers to scanning ribosomes, the hairpin and an optimized AUG codon, still did not completely eliminate internal translation initiation and the extent to which these barriers functioned also differed. The more pronounced inhibitory effect on downstream initiation observed from construct p10opt hp 223, compared to σ C-RL hp 223, clearly demonstrates that 80S ribosomes translating the optimized p10 ORF are not disrupting the hairpin structure, as might have been expected (Kozak, 1989a). Such disruption would have allowed scanning 40S subunits to migrate through the unwound region and initiate internal translation at a higher frequency, which was not the case. The residual σ C translation in the presence of the hairpin structure is therefore unlikely to be due to such

an artifact. There is the possibility, however, that such a phenomenon is occurring upon p17 optimization (p17opt hp 579 vs σ C-RL hp 579). Ribosomes translating the optimized p10 ORF would be unable to unwind the hairpin located between S1 nucleotides 579 and 580 because the p10 ORF terminates well upstream of this position. The increase in reporter expression seen from p17opt hp 579 compared to σ C-RL hp 579 may be due to an increase in the number of ribosomes translating the p17 ORF, and thus enabling a more consistent flow of scanning 40S subunits through the hairpin. Ribosomes translating the p17 ORF would encounter a termination codon, however, approximately one-third of the way through the hairpin sequence. This would prevent further unwinding, although the extent of unwinding may have sufficiently affected the stability of the hairpin to enable a scanning subunit to migrate through the rest of the secondary structure. Why translating ribosomes might be able to unwind the hairpin when located within the p17 region and not when present within the p10 region is unknown. The influence translating ribosomes have on hairpin unwinding could be tested by point substitution of the either the p10 or p17 start sites. Removal of the initiation codon would prevent ribosome formation and thus should theoretically prevent hairpin unwinding.

Taken together, the results indicate a position-dependent effect of hairpin insertion, a finding similar to that demonstrated with a reporter mRNA (Babendure et al., 2006). Babendure and colleagues used a two-colour fluorescence assay for translation efficiency in living cells to demonstrate that shifting the hairpin by as little as nine nucleotides from the 5' cap modulated translation by 50-fold. A caveat must be made in regards to this comparison however. The hairpin location that resulted in a 50-fold increase in translation efficiency was ten nucleotides from the 5'-cap and the hairpin used had a thermal stability of $\Delta G = -25$ kcal/mol, while the hairpin used in the experiments was a minimum of 223 nucleotides from the 5'-cap and had a thermal stability of $\Delta G = -60$ kcal/mol. Also, when more thermodynamically stable hairpins were used, $> \Delta G = -40$ kcal/mol, the distance from the 5'-cap did not impact on translation efficiency (Babendure et al., 2006). Although the reason behind the potential position effect is unknown, it may be the result of either differences induced in mRNA secondary structure, or the hairpin located between S1 nucleotides 579 and 580 is able to inhibit not only context-independent leaky scanning ribosomes, but also ribosomes positioned within

this region of the mRNA via an as yet unidentified alternate mechanism (discussed below). Also, since hairpin insertion had a more pronounced effect on downstream inhibition than uAUG optimization, some ribosomes would appear to use a context-independent leaky scanning mechanism that does not allow them to circumvent a physical barrier like a hairpin structure. The level of downstream translation initiation in the presence of the hairpin may, therefore, reflect some form of scanning-independent ribosome migration.

The exact mechanism by which ribosomes are able to leak past uAUGs in an optimal context on the S1 mRNA is still unknown. However, I hypothesize that the S1 mRNA facilitates context-independent leaky scanning by directly or indirectly interacting with eIF1 and/or eIF1A bound to the 40S subunit. The initiation factors eIF1 and eIF1A play important roles in start codon recognition (Mitchell and Lorsch, 2008) with eIF1 being responsible for preventing premature engagement with a putative start codon by precluding the release of inorganic phosphate from eIF2 until an AUG codon is encountered (Algire, Maag, and Lorsch, 2005; Pestova and Kolupaeva, 2002). The initiation factor eIF1A facilitates pausing at the correct start codon long enough for initiation to proceed (Pestova and Kolupaeva, 2002). Studies have indicated that the N- and C-terminal tails of eIF1A are unstructured and play opposing roles in start codon recognition (Fekete et al., 2007; Pestova and Kolupaeva, 2002). The C-terminal tail naturally supports an open conformation on the 40S subunit, which promotes leaky scanning. The recruitment of a cellular factor or direct interaction with the 40S subunit by the S1 mRNA may prevent the proper functioning of either eIF1 or eIF1A, thus enabling context-independent leaky scanning.

Several approaches could be used to explore S1 RNA interactions with cellular initiation factors. A radiolabeled RNA probe containing the S1 mRNA region of interest could be used in electrophoretic mobility shift and nitrocellulose filter binding assays to test whether that particular region of the S1 mRNA was capable of interacting directly with cellular factors (Chappell, Edelman, and Mauro, 2004), followed by mass spectroscopy to identify the bound factors. The position of specific regions of the S1 mRNA on the 40S subunit in the initiation factor complex could be determined using UV cross-linking of the mRNA containing uniquely positioned 4-thiouridines (4-thioU;

Pisarev et al., 2008). The mRNA would be *in vitro* transcribed using 4-thiouridine instead of uridine, in the presence of ^{32}P . The ^{32}P -labelled 4-thioU mRNA would then be incubated with purified 48S complexes and irradiated at 360nm. The regions of the 40S subunit that cross-link to the S1 mRNA would be identified by electrophoresis. This cross-linking method is easiest to interpret with a minimal number of thiouridines present within the mRNA, therefore the S1 mRNA region selected for examination would have to be relatively small, which unfortunately, may not accurately represent the actual interactions within the full-length S1 mRNA due to differential folding of the mRNA. A similar approach using 6-thioguanosine has demonstrated that this purine in the -3 and +4 positions of a reporter mRNA interacts with eIF2 α and AA₁₈₁₈₋₁₈₁₉ in helix44 of 18S rRNA, respectively. This led the authors to hypothesize that these interactions help stabilize the changes that occur within the 48S initiation complex upon codon-anticodon base-pairing, which subsequently allows initiation to occur (Pisarev et al., 2006). Also, directed hydroxyl radical probing could be used to determine whether the locations/interactions of eIF1 and eIF1A on the 40S subunit are altered when bound to S1 mRNA compared to a control mRNA (Lomakin et al., 2003; Yu et al., 2009). In directed hydroxyl radical probing, specific cysteines on the surface of a protein (i.e. eIF1 or eIF1A) are tethered to Fe(II) by a linker. In the presence of H₂O₂ and ascorbic acid, hydroxyl radicals are generated near the Fe(II) site that are able to cleave the backbone of nearby RNA. The initiation factors eIF1 and eIF1A produce a predictable pattern of 18S rRNA cleavage in the presence of a reporter mRNA (Lomakin et al., 2003; Yu et al., 2009) and may thus produce an altered pattern of 18S rRNA cleavage when interacting with S1 mRNA.

The hairpin insertion data (Figure 27) also supports the idea that the purpose of the context-independent leaky scanning mechanism is to prevent initiation at uAUGs regardless of their context, since this mechanism does not seem to function (as efficiently) in the presence of a physical barrier like the hairpin structure. The inability of the context-independent scanning mechanism to propel ribosomes past physical barriers could be examined further by insertion of a G-quadruplex-forming sequence into the S1 mRNA (Halder, Wieland, and Hartig, 2009; Kumari, Bugaut, and Balasubramanian, 2008). RNA sequences with a minimum four interspersed “GGG” repeats can potentially

fold back to form stable G-quadruplex motifs, a four-stranded conformation composed of stacked guanine tetrads. The formation of such a structure has recently been shown to effectively inhibit scanning ribosomes from initiating downstream translation (Halder, Wieland, and Hartig, 2009; Kumari, Bugaut, and Balasubramanian, 2008). If the S1 mRNA does in fact utilize a context-independent leaky scanning mechanism of translation initiation, the presence of G-quadruplex physical barrier should prevent translation of the 3'-proximal ORF. Continued examination of the mechanism that controls context-independent leaky scanning on the ARV S1 mRNA and potentially on other polycistronic viral mRNAs (Castano, Ruiz, and Hernandez, 2009) may therefore aid in our understanding of translation on these mRNAs, and of the diversity and complexity of mechanisms that control eukaryotic translation initiation.

4.5 Ribosome Handoff

The inability of any of the known alternate translation initiation mechanisms to fully explain how ribosomes access the internal σ C AUG codon suggests that some novel form of translation initiation must also be occurring on the ARV S1 mRNA. The inability of either an optimized p10 or p17 start site, nor the presence of a multitude of additional AUGs in a strong context, to fully eliminate translation initiation from the 3'-proximal ORF suggests that some ribosomes access this region in a scanning-independent manner. As mentioned above, the well studied scanning-independent mechanism for internal translation initiation, the IRES element (Fitzgerald and Semler, 2009), is not responsible for downstream initiation on the S1 mRNA since translation initiation of the 3'-proximal ORF is cap-dependent (Figure 21) and independent of the 5'-proximal 147 S1 nucleotides (Figure 29).

Support for a 5' scanning-independent mechanism of translation initiation at the σ C start site comes from the inability to completely eliminate downstream initiation despite the presence of excessive numbers of upstream inhibitory elements (Figure 31 and Figure 32). Inhibition of downstream translation initiation plateaued at ~70%, suggesting that the context of the AUG triplets alone does not dictate ribosome recognition (Frederiks et al., 2009; Sen, Cao, and Tavis, 2004; Wang and Rothnagel, 2004), and that the 5' scanning-independent mechanism is likely responsible for at least

30% of the translation initiation events occurring at the σ C start site. This 5'-scanning independent model of translation initiation on the S1 mRNA was further supported by the inability of a stable hairpin structure to completely inhibit σ C-RL expression, regardless of its location within the mRNA (Figure 27). The residual luciferase activity upon hairpin insertion indicates that although up to two-thirds of ribosomes appear to scan the S1 mRNA to reach the σ C AUG codon, the other one-third of ribosomes that bind the 5'-cap are escorted past the hairpin and are thus competent to initiate translation at an internal start site.

Further support for the 5' scanning-independent nature of downstream initiation on the ARV S1 mRNA was provided by the addition of the 77-nucleotide rabbit β -globin 5'-UTR upstream of the full-length σ C-RL mRNA (β - σ CRL; Figure 26). In contrast to the literature (Kozak, 1991a; Slusher et al., 1991), extension of the relatively short S1 5'-UTR in the presence of an optimized p10 start site, slightly increased, rather than decreased, translation of the reporter ORF, suggesting that optimization of the p10 AUG codon also inhibits scanning-independent initiation. With only 24 nucleotides between the cap and the optimized p10 start site, ribosomes bound to the cap are more likely to recognize the p10 AUG codon and initiate translation than be able to undergo an alternate mechanism of initiation. By lengthening the 5' leader, ribosomes bound to the cap are no longer "forced" to initiate at the optimized p10 start site but are now free to translocate internally and initiate translation. The relief of σ C translation inhibition observed upon optimization of the p10 start codon in Figure 26 compared to Figure 22 suggests that ribosomes bound to the cap are translocated to an internal position along the mRNA without the need for scanning. The level of translation inhibition imposed by p17 start site optimization did not vary between experiments (Figure 22 and Figure 26) because the proportion of 40S subunits that are directed internally do not scan the mRNA upstream of the p17 start site and thus are not affected by the context of the p17 AUG codon. I believe that this is the first report of 5'-UTR extension relieving inhibition due to uORF optimization.

The 5' scanning-independent mechanism of translation initiation on the S1 mRNA, which I call ribosome handoff, requires the presence of a translation enhancer element located within S1 nucleotides 366-392. Progressively larger internal deletions of the S1

mRNA (Figure 34) revealed a 27-nucleotide region adjacent to the p17 start codon that promotes maximum ribosome access to a downstream ORF on the S1 mRNA. By removing a strong barrier to scanning ribosomes (i.e. the p17 start site), ribosomes should be free to reach the internal AUG codon independent of the translation enhancer element, if the element is only required to promote leaky scanning. This was not the case; the levels of luciferase activity obtained from constructs $\Delta 366-751RL$ and $\Delta 366-751RLM3$ were essentially the same (Figure 35), indicating that the 27-nucleotide element is not necessary for facilitating context-independent leaky scanning past the strong p17 start site. The translation enhancer element also functions in a length-independent manner (Figure 36), suggesting that this particular region of the S1 mRNA may be directly participating in ribosome recruitment.

Recent studies demonstrate that a nine-nucleotide sequence present in the 5' leader of the mRNA encoding the homeodomain protein Gtx is capable of acting as a ribosome recruitment site by base-pairing with 18S rRNA, and thus affecting the rate of translation (Chappell et al., 2006; Chappell, Edelman, and Mauro, 2000; Chappell, Edelman, and Mauro, 2004). According to photochemical cross-linking studies, the nine-nucleotide segment base-pairs to 18S rRNA (Hu et al., 1999), and was initially considered an IRES module because when present in multiple copies within the intergenic region of a bicistronic construct, it increased expression of the second cistron by 570-fold (Chappell, Edelman, and Mauro, 2000). Subsequent biochemical and functional analyses determined that the length of the complementary match directly correlated with the ability of the sequence to bind ribosomes and that a seven-nucleotide sequence maximally enhanced expression of a monocistronic reporter ~eight-fold (Chappell, Edelman, and Mauro, 2004). The intermolecular interaction between the nine-nucleotide element and 18S rRNA enables ribosomes to bypass uAUGs and stable hairpin structures, leading the authors to suggest that the Gtx element participates in ribosomal shunting (Chappell et al., 2006). Also, the shunting mechanism required for adenovirus late mRNA translation appears to require an intermolecular interaction between the viral tripartite leader and the 3' hairpin of 18S rRNA (Yueh and Schneider, 2000). Although there is no direct evidence to suggest that complementarity between the adenovirus tripartite leader and the 3' hairpin of 18S rRNA actually promotes rRNA-

mRNA interaction, deletion of the complementary elements suppressed shunting-mediated translation to almost background levels. This led the authors to hypothesize that such an interaction may be part of the shunting mechanism.

With the above studies in mind, closer examination of the 27-nucleotide enhancer element revealed the presence of two six-nucleotide sequences, designated RBS1 and RBS2, respectively, which are complementary to 18S rRNA (Figure 37). RBS1 is complementary to *Gallus gallus* 18S rRNA nucleotides 1549-1544, while RBS2 is complementary to nucleotides 101-96. On the basis of putative base-pairing between either of the RBSs and 18S rRNA, two different sets of point substitutions in RBS1 were made and shown to have a negative effect on the translation efficiency conferred by this region (Figure 37). Substitutions made within RBS2 had no effect on downstream translation. RBS1, but not RBS2 is also highly conserved in the S1 mRNAs of all avian reoviruses isolated from chickens and ducks (Figure 38). Moreover, fluorescent *in situ* hybridization using oligonucleotide probes complementary to the 18S rRNA of *Saccharomyces cerevisiae* identified the region complementary to RBS1, but not RBS2, as highly accessible (Behrens et al., 2003). The region of the 18S rRNA that is complementary to RCR1 corresponds to a loop between helices 46 and 47 (helices 41 and 42 in human 18S rRNA). Although preliminary, this data suggests a putative role for RBS1-18S rRNA base-pairing in the efficiency of internal initiation on the S1 mRNA and that this region (S1 nucleotides 370-375) participates in the ribosome handoff mechanism. To determine whether ribosome handoff is directly mediated by complementarity between RBS1 and 18S rRNA, experiments using altered S1 mRNA and yeast 18S rRNA could be conducted (Chappell et al., 2006). Experiments would be performed in a yeast strain lacking all chromosomal copies of the 35S rDNA but that episomally maintained a plasmid carrying either wild-type or altered 35S rRNA. The altered 35S rRNA would contain point substitutions within the 18S rRNA region complementary to RBS1. Luciferase activity would then be monitored from cells expressing the reporter S1 mRNA. Theoretically, the yeast strain carrying the 35S rRNA with alterations in RBS1 complementarity should result in decreased reporter activity. Point substitution of RBS1 to restore complementarity with the altered 35S rRNA should restore reporter activity and directly confirm that base-pairing between 18S rRNA and

RBS1 is required for maximal translation initiation at the 3'-proximal ORF on the S1 mRNA. Also, an intermolecular interaction between RBS1 and 18S rRNA could be observed through experiments using 2'-O-methyl-modified RNA oligonucleotides designed to block mRNA-rRNA base pairing by targeting either 18S rRNA nucleotides 1549-1544 or the RBS1 element in the σ C-RL reporter mRNA. This approach was used to show that the nine-nucleotide sequence found within the 5' leader of the Gtx homeodomain mRNA does directly interact with 18S rRNA (Panopoulos and Mauro, 2008). In these experiments, translation of mRNAs containing the Gtx 5' leader was decreased by >50% when oligonucleotides targeting either the mRNA or rRNA was used. Specificity was demonstrated by showing that translation of recombinant mRNAs was unaffected by control oligonucleotides.

Identification of the putative ribosome-binding site at S1 nucleotides 370-375 necessitated a second look at the results obtained from the AUG insertion experiments (Figure 32). The variability in effect on reporter expression from insertion of a single uAUG (M5-M7; ~40-60% reduction) may be due to the location of each insertion. The 5'-proximal insertion (M5) occurred upstream of RBS1, at S1 nucleotides 362-364, and was least inhibitory because the fraction of ribosomes interacting with RBS1 via the ribosome handoff mechanism would not be inhibited by M5. Insertion of M6 and M7 occurred downstream of RBS1, at S1 nucleotides 419-421 and 527-529, respectively. Ribosomes translocated internally by the handoff mechanism may scan the mRNA post-handoff and would thus encounter M6 or M7 and be inhibited from further scanning. They would not however, be completely inhibited due to the ability of the S1 mRNA to induce context-independent leaky scanning. The ~30% residual luciferase expression observed in the presence of all three AUG insertions (M5-7) would suggest that the S1 mRNA possesses a second element downstream of nucleotide 529 that also participates in ribosome handoff.

The location of RBS1 downstream of the p17 start codon, within the AUG-deficient region of the S1 mRNA, positions it in an ideal location for attracting 40S subunits. Theoretically, mRNA secondary structure could position 40S subunits bound to the 5'-cap in a position to simultaneously interact with RBS1, thus allowing the subunit to be handed off to an internal position where it is then capable of scanning the mRNA

until it encounters an AUG codon. A second look at the hairpin insertion data, however, does not completely agree with this theory. Insertion of the stable hairpin structure between S1 nucleotides 579 and 580 places it far enough downstream of RBS1 that 40S subunits handed off to RBS1 from the 5'-cap that resume scanning the S1 mRNA should be completely blocked, which they were not (Figure 27). The reason for this discrepancy is unknown, although a few possibilities might be considered. First, the residual luciferase activity observed from construct σ C-RL hp 579 could be due to 80S ribosomes translating the p17 ORF unwinding the hairpin and allowing trailing 40S subunits, present within this region of the S1 mRNA either by context-independent leaky scanning or ribosome handoff, to reach the internal start site via continuous scanning. The hairpin sequence used in the experiments described herein was the same as that originally used to demonstrate that a hairpin could inhibit 100% of scanning 40S subunits *in vitro*, as indicated by the lack of protein production and by the presence of only 40S subunits on the mRNA according to a polysome profile (Kozak, 1989a). That study also showed however, that an AUG codon in optimal context positioned upstream of the hairpin could direct a minor amount of protein synthesis, indicating that a minimal number of 80S elongating ribosomes can penetrate the hairpin. Thus, it is possible that the residual luciferase activity obtained from constructs σ C-RL hp 579 and p17opt hp 579 is due to unwinding of the hairpin. However, as mentioned previously, if hairpin unwinding were occurring, why was there no increase in reporter activity from construct p10opt hp 223? As mentioned in the previous section on leaky scanning, removal of the p10 or p17 start site should determine whether ribosome unwinding is responsible for the residual internal initiation. Second, although undetected in the series of experiments reported here, there may be an additional binding site downstream of the hairpin that enables an even more internal positioning of the 40S subunit. This second option would evoke a mechanism of translation initiation on the S1 mRNA that is a hybrid of the ribosome tethering and clustering hypotheses proposed by Mauro and colleagues (Chappell, Edelman, and Mauro, 2006). Tethering is a mechanism in which the ribosomal subunit reaches the initiation site by direct binding of the initiator Met-tRNA with the AUG codon, while bound to a fixed point on the mRNA, the 5'-cap for example. The clustering mechanism is a dynamic process that does not require fixed attachment, but does involve the

reversible binding of the ribosomal subunit to, and detachment from, various points on the mRNA (Figure 40). The data presented herein would suggest that 40S subunits bind and are tethered to the 5'-cap, at which point they interact not with the AUG codon, but with various points on the S1 mRNA due to a mRNA-18S rRNA intermolecular interaction. Perhaps a fraction of the ribosomal subunits bound to the S1 mRNA 5'-cap that undergo the hybrid mechanism (ribosome handoff), interact with RBS1, thus bypassing the intervening sequence and continue on to the downstream initiation site, while the other fraction of subunits reversibly interact with RBS1 and an as yet unidentified second binding site located downstream of S1 nucleotide 580. This could explain why RBS1 did not efficiently promote bypass of the strong p17 start codon when present in the β -globin-RL construct (Figure 39). According to the clustering hypothesis, this second binding site may reside downstream of the translation initiation site (Chappell, Edelman, and Mauro, 2006), an idea examined with the internal deletion experiments (Figure 34). The smallest internal deletion, encompassing the σ C AUG codon and the 3'-proximal 122 nucleotides (Δ 628-751RL), enabled efficient translation initiation of an internal reporter ORF, which suggests that if a second binding site exists, it would have to reside even further downstream than nucleotide 751. This is an unlikely situation, however, since the clustering model also proposes that translation decreases progressively at AUG codons located at increasing distances upstream or downstream from the ribosome recruitment element (Chappell, Edelman, and Mauro, 2006). Regardless of the exact mechanism of ribosome handoff, it does appear that ribosomal subunits may scan at least part of the 308 nucleotides between the p10 termination codon and the σ C AUG triplet, thus making the negative selection of AUG codons in this region advantageous not only for context-independent leaky scanning, but also for the ribosome handoff mechanism.

Although the role of the 3'-end of a mRNA in ribosome tethering or clustering has yet to be examined or discussed directly, the models were devised upon examination of polyadenylated mRNAs (Chappell, Edelman, and Mauro, 2006), and so it seems appropriate that mRNA circularization would also be a factor in the tethering and clustering models. Even though the virally transcribed S1 mRNA is non-polyadenylated,

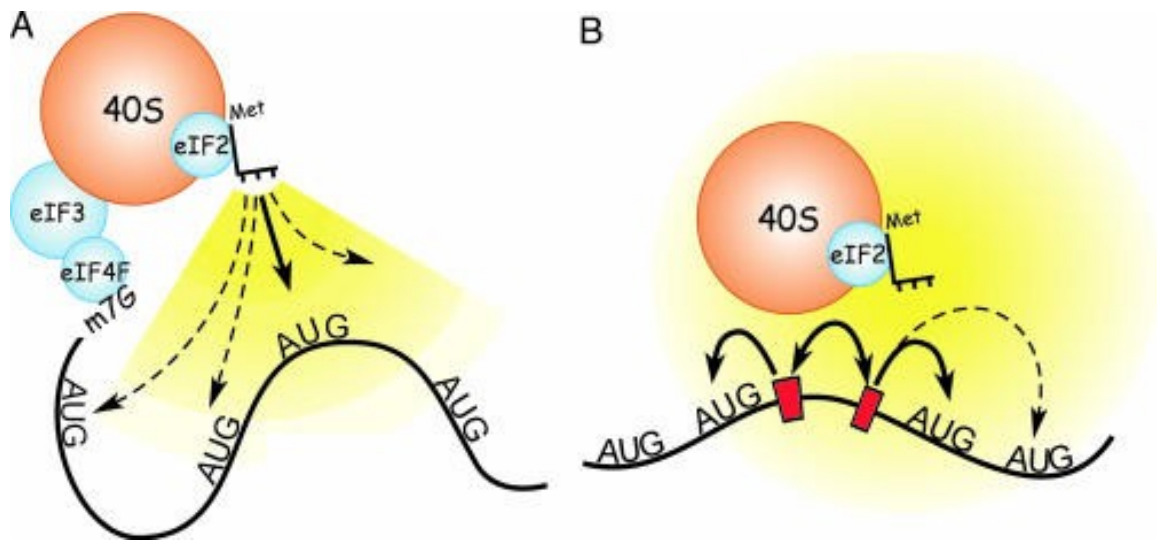


Figure 40. Schematic representations of the ribosomal tethering and clustering mechanisms of translation initiation. **A.** Representation of the hypothesized ribosomal tethering at the cap structure. The 40S ribosomal subunit can be tethered to the mRNA, for example to the 5' end of the mRNA at the cap structure (m7G). Here tethering occurs between the 40S subunit and the cap structure via the eIF4F complex of initiation factors and initiation factor eIF3. In both A and B, the range and probability of interaction between the 40S subunit and the various AUG codons is indicated schematically by the shaded yellow regions; brighter yellow indicates a higher probability of binding to an AUG codon in the vicinity (bold arrow). Pale yellow and dashed arrows indicate lower probabilities of binding to an AUG codon. **B.** Schematic model of translation initiation by means of dynamic ribosomal clustering. Clustering of the translation machinery (indicated by the double-headed arrow) involves binding to and detaching from sites in the mRNA (indicated by red bars), increasing the probability of binding to an AUG codon in the vicinity. Adapted from Chappell, Edelman and Mauro (2006) *PNAS* 103(48):18077-18082.

it may still play a role in mRNA circularization and translation initiation, as is the case for other, non-polyadenylated viral mRNAs (Guo, Allen, and Miller, 2001; Piron et al., 1998; Polacek, Friebe, and Harris, 2009; Wang, Browning, and Miller, 1997). Translation enhancement of the Dengue virus mRNA is postulated to involve PABP interaction with the A-rich sequence that flanks a secondary structure shaped like a dumbbell in an eIF4G-dependent manner (Polacek, Friebe, and Harris, 2009). Additionally, the uncapped, non-polyadenylated mRNA of BYDV possesses an extensive 3'-UTR that contains a translation enhancer element that is capable of binding eIF4G with high affinity (Treder et al., 2008) and is capable of interacting with a stem-loop structure found within the 5'-UTR (Rakotondrafara et al., 2006).

The role of the S1 3'-terminus in internal initiation was examined using 3'-truncations. Interestingly, truncation of the 3'-terminal nucleotides did exert a negative effect on σ C-RL reporter expression, although the level of inhibition was never greater than $35 \pm 5\%$ ($\Delta 50$; Figure 28), and the inhibition exerted by the smaller truncations was relieved by removal of the 3'-terminal 800 nucleotides. These results suggest that the 3'-end does exert some effect on translation, although it is still unclear whether this is a σ C-specific or global mRNA effect because the level of p10 and p17 expression upon 3'-truncation was not examined. The relief in translation inhibition observed upon truncation of the 3'-terminal 800 nucleotides suggests that this region may be involved in folding of the mRNA. Improper folding may occlude either the RBS1 or the σ C AUG codon itself, thus inhibiting translation. The extent of S1 mRNA circularization could be examined using atomic force microscopy (AFM; Wells et al., 1998). Well et al., (1998) demonstrated the reconstitution of an eIF4E/eIF4G/Pab1p complex with recombinant proteins, and showed by AFM microscopy that the complex can circularize capped, polyadenylated RNA. The ability of the parental or altered S1 mRNA to undergo circularization either alone, or in complex with one or more initiation factors could be examined by AFM. The requirement of the 3'-terminus in translation initiation adds to the importance of this region since it is well known that the conserved 3'-pentanucleotide 5'-UCAUC-3' found on the plus strands of all genome segments of all orthoreoviruses is necessary for genome packaging and virus replication (Duncan, 1999; McCrae, 1981; Roner and Roehr, 2006).

The ability of IRES elements to function within heterologous mRNAs is a defining characteristic of these extensive secondary structures (Jang et al., 1988; Pelletier and Sonenberg, 1988; Wilson et al., 2000b). The nine-nucleotide element found within the 5'-UTR of the homeodomain Gtx mRNA can be considered an IRES-module (Chappell, Edelman, and Mauro, 2000), but due to its size, it cannot form an IRES-like structure. The Gtx element does, however, function to increase internal initiation when present within a reporter mRNA (Chappell et al., 2006; Chappell, Edelman, and Mauro, 2000; Chappell, Edelman, and Mauro, 2004). I determined whether the p17opt region could autonomously direct context-independent leaky scanning and/or ribosome handoff by inserting either 54 or 134 S1 nucleotides surrounding an optimized p17 start site in front of the RL coding sequence within the β -RL construct, generating β -p17opt#1-RL and β -p17opt#2-RL, respectively. As demonstrated in Figure 39, both clones were unable to rescue downstream initiation even though clone β -p17opt#2-RL contains the putative RBS1 element. This demonstrates once again that outside of the full-length S1 mRNA, an uAUG codon with an optimized context is capable of severely inhibiting downstream initiation. The data also suggests that global mRNA folding may play a role in the proper functioning of the alternate translation initiation mechanisms, and that the S1 mRNA, potentially due to its folding, may recruit cellular *trans*-acting factors necessary for internal translation initiation. An alternative explanation for the lack of internal initiation from construct β -p17opt#2-RL is that this mRNA lacks an important second element. This second element may reside downstream of the σ C start site, as indicated by internal deletion data, and thus may not directly recruit the 40S subunit, but may be necessary for stabilizing the RBS1-18S rRNA interaction.

Despite these results, the occurrence of context-independent leaky scanning and/or ribosome handoff may not be limited to the ARV S1 mRNA, as various other viral and cellular mRNAs appear to utilize similar mechanisms (Anderson et al., 2007; Qiu, Cheng, and Pintel, 2007; Rogers, Edelman, and Mauro, 2004). The abundant R2 mRNA of Aleutian mink disease parvovirus is functionally tricistronic encoding the nonstructural protein NS2 and the two capsid proteins VP1 and VP2. Expression of the capsid proteins requires the presence of a *cis*-element within the NS2 gene that is location dependent, but VP1/VP2 expression is unaffected by the improvement or ablation of the NS2 AUG

codon (Qiu, Cheng, and Pintel, 2007). Although VP1/VP2 production does not require translation of the NS2 ORF *per se*, it does appear to require ribosome transit through the NS2 region since introduction of a stable hairpin structure into various regions of the NS2 gene severely inhibited translation of VP1/VP2. These results would suggest that perhaps ribosomes are able to leak past the NS2 start site, even when present in an optimal context, and continue scanning the mRNA until they reach the capsid AUG codons. The *cis*-acting element within the NS2 region may be required for inducing context-independent leaky scanning either by interacting with the ribosome or one of its initiation factors.

A key issue that must still be resolved regarding the context-independent leaky scanning and ribosome handoff mechanisms is the location of ribosomal subunits on the S1 mRNA. The location of 48S initiation complexes and 80S ribosomes on the S1 mRNA could be detected using an updated version of the toeprint experiment (Shirokikh et al., 2010). The advanced toeprinting approach uses DNA primers directed to different locations along the S1 mRNA and labeled with different fluorescent groups. The cDNA fragments produced from primer elongation are separated by capillary electrophoresis and the relative amounts of each fragment can be quantitatively determined. The advantages to this procedure include the ability to examine multiple locations along the mRNA concurrently and to precisely determine the type of ribosome-mRNA complex encountered by the elongating primer (e.g. 48S initiation complex or 80S terminating ribosome). Unfortunately, the results of these experiments will most likely be complicated by the number of potential ribosome-mRNA interaction sites, a problem already encountered with MRV S1 toeprinting (Doohan and Samuel, 1992).

Another issue yet to be tested directly or discussed is the ability of a single S1 mRNA species capable of expressing an integral membrane protein (p10) and two soluble proteins (p17 and σ C). Northern blot analysis revealed that S1 is in fact tricistronic and that σ C expression is not due to a monocistronic version of the S1 mRNA. This issue may be resolved by the ribosome filter hypothesis. The ribosome filter hypothesis posits that ribosomes are regulatory elements that affect the translation of mRNAs by binding differentially to them (Mauro and Edelman, 2002). According to the hypothesis, the ability of a particular ribosome to bind an mRNA, and thus its ability to efficiently

translate the mRNA, depends on the ribosomal protein and rRNA composition of that particular ribosome. The cell type, stage of cell differentiation, and subcellular location of the ribosome are all factors that influence ribosome heterogeneity (Mauro and Edelman, 2007; Rodriguez-Mateos et al., 2009; Tseng et al., 2008). I would expand the filter hypothesis by suggesting that not only does the type of ribosome bound to the mRNA affect translation efficiency, but the type of ribosome may also affect the translation initiation mechanism used by the ribosome to reach the start site. For example, one particular sub-set of 40S subunits when bound to the S1 5'-cap might be able to undergo context-independent leaky scanning, while a second sub-set of subunits are capable of initiating translation via ribosome handoff. What causes one particular set of ribosomes to bind the 5'-cap over another is still unknown. Examining ribosomes from different sources can test the notion that ribosome heterogeneity may be responsible for selection of the initiation mechanism. This test would be best performed *in vitro* where the contents of the reaction can easily be manipulated. Depending on the composition of the ribosome and the S1 mRNA examined, the level of σC expression may vary. Evidence in support of my expanded filter hypothesis comes from the examination of the use of the HCV IRES element in mammalian versus yeast cells. In mammalian cells the interaction between the IRES element and the 40S subunit is mediated between specific IRES-ribosomal protein contacts, which promotes formation of a stable binary complex that correctly positions the initiation codon in the ribosomal P-site (Pestova et al., 1998). The inability of the HCV IRES to function in *S. cerevisiae* has been attributed to differences in 40S ribosomal protein composition between the two cell types (Otto et al., 2002). Thus, the use of a specific mechanism for translation initiation is dictated by the arrangement of ribosome components.

4.6 The mechanism(s)

I propose a dual mechanism of translation initiation at the σC start site, context-independent leaky scanning and a 5' scanning-independent ribosome handoff mechanism from the 5'-cap (Figure 41), both of which are required for maximal protein production. Approximately two-thirds of the subunits undergo leaky scanning to express the p10 and p17 ORFs, while undefined features of the tricistronic S1 mRNA promote context-

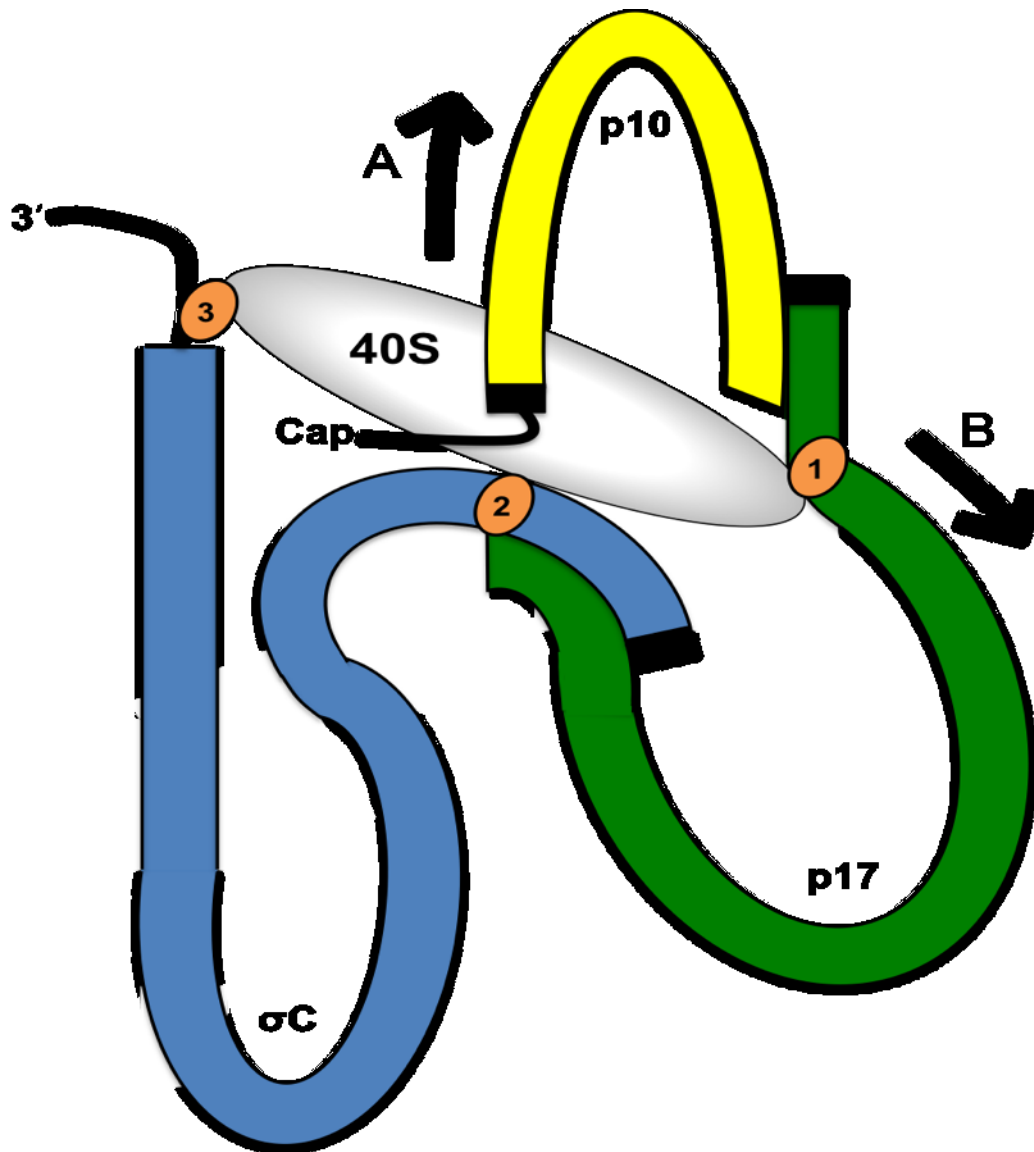


Figure 41. Model of translation initiation on the tricistronic S1 mRNA. Model illustrating the two ways in which the 40S ribosomal subunit can reach and initiate translation of the σ C ORF; **A.** context-independent leaky scanning **B.** ribosome handoff. **A.** The 40S subunit (large grey oval) binds to 5'-cap and can leaky scan to translate the S1 mRNA (AUG codons represented by black rectangles). **B.** Multiple interactions between the 40S subunit and the S1 mRNA, mediated by elements in the RNA (yellow ovals numbered 1-3), influence ribosome handoff downstream of the p17 start site. Subunits then scan part of the p17 ORF to access the σ C start site. Element 1: RBS1 is required to promote ribosome bypass of uAUGs. Element 2: a hypothetical second interaction site (there could be more) downstream of the σ C AUG codon that might stabilize 40S interactions with the S1 mRNA to promote handoff. Element 3: Element within the 3'-UTR that promotes pathway A and/or B translation of the S1 mRNA.

independent leaky scanning past the strong p17 start codon or other introduced barriers to scanning subunits. In ribosome handoff, approximately one-third of the 40S subunits that bind the 5'-cap do not scan the S1 mRNA, but are directly handed off downstream of the p17 start site. The putative RBS1-18S rRNA intermolecular interaction may be necessary for ribosome handoff, but as demonstrated by the insertion of an optimized p17 region into the β -RL construct (Figure 39), it alone is not sufficient for internal expression. As the model depicted in Figure 41 suggests, ribosome handoff is a complex process that may require the involvement of an additional element downstream of S1 nucleotide 751, as determined by the internal deletion constructs (Figure 34). The exact role this second element may play in the handoff mechanism is unknown, but most likely involves RBS1-18S rRNA stabilization rather than direct recruitment of the 40S subunit since translation efficiency diminishes with increasing distance between the subunit recruitment site and the initiation codon (Chappell, Edelman, and Mauro, 2006).

The reason for the evolution of this dual mechanism of translation initiation on the ARV S1 mRNA is unknown, however, several hypotheses are discussed below. The ARV S1 mRNA is unique in that it encodes three functionally different proteins; the integral membrane p10 FAST protein (Shmulevitz and Duncan, 2000), and the soluble proteins p17 (Costas et al., 2005; Liu et al., 2005) and σ C (Martinez-Costas et al., 1997; Shih et al., 2004). In the absence of transcription control to regulate expression of these three genes, this tricistronic mRNA uses translation control to regulate production of all three viral proteins. The minimal amount of p10 expressed, due to the weak start site, ensures that virus replication is complete before extensive syncytium formation occurs. The weak p10 start site also ensures that sufficient p17 is expressed via leaky scanning from the strong p17 start site. Although σ C is an essential structural protein, only 36 copies are required per virus particle (Benavente and Martinez-Costas, 2007; Martinez-Costas et al., 1997), indicating that the mechanism(s) that regulate its translation can be relatively less efficient.

Expression of multiple proteins from a single mRNA may serve to regulate the production of proteins required only in minimal amounts, but this strategy may also be a way of expanding the coding capacity of a limited-sized genome. The ARV S1 genome segment maximizes its coding capacity by truncating the σ C ORF by one-third compared

to its MRV counterpart, $\sigma 1$, to accommodate the p10 ORF. Truncation of σC eliminated its ability to cause hemagglutination and altered its recognition by cell surface receptors enabling ARV to bind and infect both mammalian and avian cells, while MRV cannot infect chicken embryo fibroblast cells (Benavente and Martinez-Costas, 2007). It is also interesting to note that the orthoreovirus FAST proteins initiate translation of their respective ORFs at AUG codons in a weak context (Duncan et al., 2004; Shmulevitz et al., 2002), and are encoded by the S1 genome segment, except for the baboon reovirus p15 protein (Dawe et al., 2005), suggesting that like ARV p10 and σC , the other FAST proteins are required only in limited concentrations and the genome segment within which they reside could tolerate modification. I believe that both mechanisms of translation initiation, neither of which is overly efficient, may be necessary to ensure that sufficient and appropriate quantities of all S1-encoded proteins are produced during virus infection.

4.7 Conclusions and perspectives

Translation initiation on eukaryotic mRNA is a complex process that requires a multitude of factors and can be accomplished in a variety of ways. This report adds to the possible mechanisms by which ribosomes can access internal initiation sites and commence translation. The ability of ribosomes to undergo context-independent leaky scanning suggests that the presence of a potential downstream ORF should not be discounted just because an uORF resides in an optimal context. Start codon context is clearly not the only factor regulating the ability of the ribosome to recognize a potential initiation site. The discovery of the ribosome handoff mechanism also expands the repertoire of the ribosome for internal initiation mechanisms. This hybrid mechanism uses features found within the other alternate mechanisms, like cap-dependency and direct interaction between the mRNA and the 40S ribosomal subunit, to facilitate internal initiation without the need for sacrificing coding capacity. The ARV apparently requires the production of all three S1-encoded proteins, and as such, imposed a selection for a means to express all three proteins in the appropriate quantities. The use of these two distinct mechanisms must satisfy this requirement.

Despite the discovery that mechanisms like context-independent leaky scanning

and ribosome handoff are being used on viral mRNAs, it is unlikely that many cellular mRNAs would be regulated in this way since almost half of all human mRNAs are monocistronic (Davuluri et al., 2000; Suzuki et al., 2000). It is not entirely improbable however, since the cellular machinery is clearly capable of using these novel translation initiation mechanisms. Although it was initially believed that less than 10% of vertebrate mRNAs contained uAUGs/uORFs (Kozak, 1987a), it is now believed that ~40% of human mRNAs contain complex 5'-leader sequences with uAUGs/uORFs, thus renewing interest in the role these features play in post-transcriptional gene regulation. Examining S1 mRNA mechanisms could therefore have much broader implications. One must also be reminded that other alternate mechanisms, like IRES elements and ribosome shunting, were first discovered by studying viral translation and are now known to operate on cellular mRNAs. The ability of cellular ribosomes to utilize such diverse means of initiating translation raises the possibility that initiation at internal AUGs may be far more common than currently appreciated.

The work reported herein expands not only our knowledge of the mechanism(s) of translation initiation on the tricistronic S1 mRNA of ARV, but on the capabilities of cellular 40S subunits. At one time 40S ribosomal subunits were thought to be limited to cap-dependent linear scanning along an mRNA, a constraint that is clearly not adhered to. Aside from the discovery of two novel forms of translation initiation, the most remarkable, and possibly important, discovery described in this report is the realization that ribosomal subunits themselves are versatile complexes that should be regarded as translation regulatory factors that can be manipulated to fit the needs of a particular mRNA or cellular state (Mauro and Edelman, 2002; Mauro and Edelman, 2007). Numerous diseases have been attributed to both specific and global disruptions in translation (Mauro and Edelman, 2007, and references therein). It is therefore conceivable that disruption of the ribosome filter may be partially responsible for these pathologies and that a better understanding of the filter will lead to therapeutic applications.

APPENDIX A: Letters Of Copyright Permission

Letter of Permission for Figure 1

ELSEVIER LICENSE TERMS AND CONDITIONS

Apr 15, 2010

This is a License Agreement between Trina Racine ("You") and Elsevier ("Elsevier") provided by Copyright Clearance Center ("CCC"). The license consists of your order details, the terms and conditions provided by Elsevier, and the payment terms and conditions.

All payments must be made in full to CCC. For payment instructions, please see information listed at the bottom of this form.

Supplier	Elsevier Limited The Boulevard,Langford Lane Kidlington,Oxford,OX5 1GB,UK
Registered Company Number	1982084
Customer name	Trina Racine
Customer address	5850 College St. Halifax, NS B3H 1X5
License Number	2410361368524
License date	Apr 15, 2010
Licensed content publisher	Elsevier
Licensed content publication	Current Opinion in Cell Biology
Licensed content title	Recent mechanistic insights into eukaryotic ribosomes
Licensed content author	Marina V Rodnina, Wolfgang

	Wintermeyer
Licensed content date	June 2009
Volume number	21
Issue number	3
Pages	9
Type of Use	Thesis / Dissertation
Portion	Figures/tables/illustrations
Number of Figures/tables/illustrations	1
Format	Print
You are an author of the Elsevier article	No
Are you translating?	No
Order Reference Number	
Expected publication date	May 2010
Elsevier VAT number	GB 494 6272 12
Permissions price	0.00 USD
Value added tax 0.0%	0.00 USD
Total	0.00 USD
Terms and Conditions	

INTRODUCTION

1. The publisher for this copyrighted material is Elsevier. By clicking "accept" in connection with completing this licensing transaction, you agree that the following terms and conditions apply to this transaction (along with the Billing and Payment terms and

conditions established by Copyright Clearance Center, Inc. ("CCC"), at the time that you opened your Rightslink account and that are available at any time at <http://myaccount.copyright.com>).

GENERAL TERMS

2. Elsevier hereby grants you permission to reproduce the aforementioned material subject to the terms and conditions indicated.

3. Acknowledgement: If any part of the material to be used (for example, figures) has appeared in our publication with credit or acknowledgement to another source, permission must also be sought from that source. If such permission is not obtained then that material may not be included in your publication/copies. Suitable acknowledgement to the source must be made, either as a footnote or in a reference list at the end of your publication, as follows:

“Reprinted from Publication title, Vol /edition number, Author(s), Title of article / title of chapter, Pages No., Copyright (Year), with permission from Elsevier [OR APPLICABLE SOCIETY COPYRIGHT OWNER].” Also Lancet special credit - “Reprinted from The Lancet, Vol. number, Author(s), Title of article, Pages No., Copyright (Year), with permission from Elsevier.”

4. Reproduction of this material is confined to the purpose and/or media for which permission is hereby given.

5. Altering/Modifying Material: Not Permitted. However figures and illustrations may be altered/adapted minimally to serve your work. Any other abbreviations, additions, deletions and/or any other alterations shall be made only with prior written authorization of Elsevier Ltd. (Please contact Elsevier at permissions@elsevier.com)

6. If the permission fee for the requested use of our material is waived in this instance, please be advised that your future requests for Elsevier materials may attract a fee.

7. Reservation of Rights: Publisher reserves all rights not specifically granted in the combination of (i) the license details provided by you and accepted in the course of this licensing transaction, (ii) these terms and conditions and (iii) CCC's Billing and Payment terms and conditions.

8. License Contingent Upon Payment: While you may exercise the rights licensed immediately upon issuance of the license at the end of the licensing process for the transaction, provided that you have disclosed complete and accurate details of your proposed use, no license is finally effective unless and until full payment is received from you (either by publisher or by CCC) as provided in CCC's Billing and Payment terms and conditions. If full payment is not received on a timely basis, then any license preliminarily granted shall be deemed automatically revoked and shall be void as if

never granted. Further, in the event that you breach any of these terms and conditions or any of CCC's Billing and Payment terms and conditions, the license is automatically revoked and shall be void as if never granted. Use of materials as described in a revoked license, as well as any use of the materials beyond the scope of an unrevoked license, may constitute copyright infringement and publisher reserves the right to take any and all action to protect its copyright in the materials.

9. Warranties: Publisher makes no representations or warranties with respect to the licensed material.

10. Indemnity: You hereby indemnify and agree to hold harmless publisher and CCC, and their respective officers, directors, employees and agents, from and against any and all claims arising out of your use of the licensed material other than as specifically authorized pursuant to this license.

11. No Transfer of License: This license is personal to you and may not be sublicensed, assigned, or transferred by you to any other person without publisher's written permission.

12. No Amendment Except in Writing: This license may not be amended except in a writing signed by both parties (or, in the case of publisher, by CCC on publisher's behalf).

13. Objection to Contrary Terms: Publisher hereby objects to any terms contained in any purchase order, acknowledgment, check endorsement or other writing prepared by you, which terms are inconsistent with these terms and conditions or CCC's Billing and Payment terms and conditions. These terms and conditions, together with CCC's Billing and Payment terms and conditions (which are incorporated herein), comprise the entire agreement between you and publisher (and CCC) concerning this licensing transaction. In the event of any conflict between your obligations established by these terms and conditions and those established by CCC's Billing and Payment terms and conditions, these terms and conditions shall control.

14. Revocation: Elsevier or Copyright Clearance Center may deny the permissions described in this License at their sole discretion, for any reason or no reason, with a full refund payable to you. Notice of such denial will be made using the contact information provided by you. Failure to receive such notice will not alter or invalidate the denial. In no event will Elsevier or Copyright Clearance Center be responsible or liable for any costs, expenses or damage incurred by you as a result of a denial of your permission request, other than a refund of the amount(s) paid by you to Elsevier and/or Copyright Clearance Center for denied permissions.

LIMITED LICENSE

The following terms and conditions apply only to specific license types:

15. **Translation:** This permission is granted for non-exclusive world **English** rights only unless your license was granted for translation rights. If you licensed translation rights you may only translate this content into the languages you requested. A professional translator must perform all translations and reproduce the content word for word preserving the integrity of the article. If this license is to re-use 1 or 2 figures then permission is granted for non-exclusive world rights in all languages.

16. **Website:** The following terms and conditions apply to electronic reserve and author websites: **Electronic reserve:** If licensed material is to be posted to website, the web site is to be password-protected and made available only to bona fide students registered on a relevant course if: This license was made in connection with a course, This permission is granted for 1 year only. You may obtain a license for future website posting, All content posted to the web site must maintain the copyright information line on the bottom of each image, A hyper-text must be included to the Homepage of the journal from which you are licensing at <http://www.sciencedirect.com/science/journal/xxxxx> or the Elsevier homepage for books at <http://www.elsevier.com> , and Central Storage: This license does not include permission for a scanned version of the material to be stored in a central repository such as that provided by Heron/XanEdu.

17. **Author website** for journals with the following additional clauses:

All content posted to the web site must maintain the copyright information line on the bottom of each image, and the permission granted is limited to the personal version of your paper. You are not allowed to download and post the published electronic version of your article (whether PDF or HTML, proof or final version), nor may you scan the printed edition to create an electronic version, A hyper-text must be included to the Homepage of the journal from which you are licensing at <http://www.sciencedirect.com/science/journal/xxxxx> , As part of our normal production process, you will receive an e-mail notice when your article appears on Elsevier's online service ScienceDirect (www.sciencedirect.com). That e-mail will include the article's Digital Object Identifier (DOI). This number provides the electronic link to the published article and should be included in the posting of your personal version. We ask that you wait until you receive this e-mail and have the DOI to do any posting. Central Storage: This license does not include permission for a scanned version of the material to be stored in a central repository such as that provided by Heron/XanEdu.

18. **Author website** for books with the following additional clauses: Authors are permitted to place a brief summary of their work online only. A hyper-text must be included to the Elsevier homepage at <http://www.elsevier.com>

All content posted to the web site must maintain the copyright information line on the bottom of each image You are not allowed to download and post the published electronic version of your chapter, nor may you scan the printed edition to create an

electronic version. Central Storage: This license does not include permission for a scanned version of the material to be stored in a central repository such as that provided by Heron/XanEdu.

19. **Website** (regular and for author): A hyper-text must be included to the Homepage of the journal from which you are licensing at <http://www.sciencedirect.com/science/journal/xxxxx>. or for books to the Elsevier homepage at <http://www.elsevier.com>

20. **Thesis/Dissertation**: If your license is for use in a thesis/dissertation your thesis may be submitted to your institution in either print or electronic form. Should your thesis be published commercially, please reapply for permission. These requirements include permission for the Library and Archives of Canada to supply single copies, on demand, of the complete thesis and include permission for UMI to supply single copies, on demand, of the complete thesis. Should your thesis be published commercially, please reapply for permission.

21. **Other Conditions**: None

Letter of Permission for Figure 2

ELSEVIER LICENSE TERMS AND CONDITIONS

Jun 11, 2010

This is a License Agreement between Trina Racine ("You") and Elsevier ("Elsevier") provided by Copyright Clearance Center ("CCC"). The license consists of your order details, the terms and conditions provided by Elsevier, and the payment terms and conditions.

All payments must be made in full to CCC. For payment instructions, please see information listed at the bottom of this form.

Supplier	Elsevier Limited The Boulevard,Langford Lane Kidlington,Oxford, OX5 1GB,UK
Registered Company Number	1982084
Customer name	Trina Racine
Customer address	5850 College St. Halifax, NS B3H 1X5
License Number	2445931195426
License date	Jun 11, 2010
Licensed content publisher	Elsevier
Licensed content publication	Cell
Licensed content title	Fidelity at the Molecular Level: Lessons from Protein Synthesis
Licensed content author	Hani S. Zaher, Rachel

	Green
Licensed content date	20 February 2009
Volume number	136
Issue number	4
Pages	17
Type of Use	Thesis / Dissertation
Portion	Figures/tables/illustrations
Number of Figures/tables/illustrations	1
Format	Both print and electronic
You are an author of the Elsevier article	No
Are you translating?	No
Order Reference Number	
Expected publication date	Jun 2010
Elsevier VAT number	GB 494 6272 12
Permissions price	0.00 USD
Value added tax 0.0%	0.00 USD
Total	0.00 USD
Terms and Conditions	

INTRODUCTION

1. The publisher for this copyrighted material is Elsevier. By clicking "accept" in connection with completing this licensing transaction, you agree that the following terms and conditions apply to this transaction (along with the Billing and Payment terms and conditions established by Copyright Clearance Center, Inc. ("CCC"), at the time that you opened your Rightslink account and that are available at any time at

<http://myaccount.copyright.com>).

GENERAL TERMS

2. Elsevier hereby grants you permission to reproduce the aforementioned material subject to the terms and conditions indicated.

3. Acknowledgement: If any part of the material to be used (for example, figures) has appeared in our publication with credit or acknowledgement to another source, permission must also be sought from that source. If such permission is not obtained then that material may not be included in your publication/copies. Suitable acknowledgement to the source must be made, either as a footnote or in a reference list at the end of your publication, as follows:

“Reprinted from Publication title, Vol /edition number, Author(s), Title of article / title of chapter, Pages No., Copyright (Year), with permission from Elsevier [OR APPLICABLE SOCIETY COPYRIGHT OWNER].” Also Lancet special credit - “Reprinted from The Lancet, Vol. number, Author(s), Title of article, Pages No., Copyright (Year), with permission from Elsevier.”

4. Reproduction of this material is confined to the purpose and/or media for which permission is hereby given.

5. Altering/Modifying Material: Not Permitted. However figures and illustrations may be altered/adapted minimally to serve your work. Any other abbreviations, additions, deletions and/or any other alterations shall be made only with prior written authorization of Elsevier Ltd. (Please contact Elsevier at permissions@elsevier.com)

6. If the permission fee for the requested use of our material is waived in this instance, please be advised that your future requests for Elsevier materials may attract a fee.

7. Reservation of Rights: Publisher reserves all rights not specifically granted in the combination of (i) the license details provided by you and accepted in the course of this licensing transaction, (ii) these terms and conditions and (iii) CCC's Billing and Payment terms and conditions.

8. License Contingent Upon Payment: While you may exercise the rights licensed immediately upon issuance of the license at the end of the licensing process for the transaction, provided that you have disclosed complete and accurate details of your proposed use, no license is finally effective unless and until full payment is received from you (either by publisher or by CCC) as provided in CCC's Billing and Payment terms and conditions. If full payment is not received on a timely basis, then any license preliminarily granted shall be deemed automatically revoked and shall be void as if never granted. Further, in the event that you breach any of these terms and conditions or any of CCC's Billing and Payment terms and conditions, the license is automatically

revoked and shall be void as if never granted. Use of materials as described in a revoked license, as well as any use of the materials beyond the scope of an unrevoked license, may constitute copyright infringement and publisher reserves the right to take any and all action to protect its copyright in the materials.

9. **Warranties:** Publisher makes no representations or warranties with respect to the licensed material.

10. **Indemnity:** You hereby indemnify and agree to hold harmless publisher and CCC, and their respective officers, directors, employees and agents, from and against any and all claims arising out of your use of the licensed material other than as specifically authorized pursuant to this license.

11. **No Transfer of License:** This license is personal to you and may not be sublicensed, assigned, or transferred by you to any other person without publisher's written permission.

12. **No Amendment Except in Writing:** This license may not be amended except in a writing signed by both parties (or, in the case of publisher, by CCC on publisher's behalf).

13. **Objection to Contrary Terms:** Publisher hereby objects to any terms contained in any purchase order, acknowledgment, check endorsement or other writing prepared by you, which terms are inconsistent with these terms and conditions or CCC's Billing and Payment terms and conditions. These terms and conditions, together with CCC's Billing and Payment terms and conditions (which are incorporated herein), comprise the entire agreement between you and publisher (and CCC) concerning this licensing transaction. In the event of any conflict between your obligations established by these terms and conditions and those established by CCC's Billing and Payment terms and conditions, these terms and conditions shall control.

14. **Revocation:** Elsevier or Copyright Clearance Center may deny the permissions described in this License at their sole discretion, for any reason or no reason, with a full refund payable to you. Notice of such denial will be made using the contact information provided by you. Failure to receive such notice will not alter or invalidate the denial. In no event will Elsevier or Copyright Clearance Center be responsible or liable for any costs, expenses or damage incurred by you as a result of a denial of your permission request, other than a refund of the amount(s) paid by you to Elsevier and/or Copyright Clearance Center for denied permissions.

LIMITED LICENSE

The following terms and conditions apply only to specific license types:

15. **Translation:** This permission is granted for non-exclusive world **English** rights only

unless your license was granted for translation rights. If you licensed translation rights you may only translate this content into the languages you requested. A professional translator must perform all translations and reproduce the content word for word preserving the integrity of the article. If this license is to re-use 1 or 2 figures then permission is granted for non-exclusive world rights in all languages.

16. **Website:** The following terms and conditions apply to electronic reserve and author websites: **Electronic reserve:** If licensed material is to be posted to website, the web site is to be password-protected and made available only to bona fide students registered on a relevant course if: This license was made in connection with a course, This permission is granted for 1 year only. You may obtain a license for future website posting, All content posted to the web site must maintain the copyright information line on the bottom of each image, A hyper-text must be included to the Homepage of the journal from which you are licensing at <http://www.sciencedirect.com/science/journal/xxxxx> or the Elsevier homepage for books at <http://www.elsevier.com>, and Central Storage: This license does not include permission for a scanned version of the material to be stored in a central repository such as that provided by Heron/XanEdu.

17. **Author website** for journals with the following additional clauses:

All content posted to the web site must maintain the copyright information line on the bottom of each image, and the permission granted is limited to the personal version of your paper. You are not allowed to download and post the published electronic version of your article (whether PDF or HTML, proof or final version), nor may you scan the printed edition to create an electronic version, A hyper-text must be included to the Homepage of the journal from which you are licensing at <http://www.sciencedirect.com/science/journal/xxxxx>, As part of our normal production process, you will receive an e-mail notice when your article appears on Elsevier's online service ScienceDirect (www.sciencedirect.com). That e-mail will include the article's Digital Object Identifier (DOI). This number provides the electronic link to the published article and should be included in the posting of your personal version. We ask that you wait until you receive this e-mail and have the DOI to do any posting. Central Storage: This license does not include permission for a scanned version of the material to be stored in a central repository such as that provided by Heron/XanEdu.

18. **Author website** for books with the following additional clauses: Authors are permitted to place a brief summary of their work online only. A hyper-text must be included to the Elsevier homepage at <http://www.elsevier.com>

All content posted to the web site must maintain the copyright information line on the bottom of each image You are not allowed to download and post the published electronic version of your chapter, nor may you scan the printed edition to create an electronic version. Central Storage: This license does not include permission for a scanned version of the material to be stored in a central repository such as that provided

by Heron/XanEdu.

19. **Website** (regular and for author): A hyper-text must be included to the Homepage of the journal from which you are licensing at <http://www.sciencedirect.com/science/journal/xxxxx>. or for books to the Elsevier homepage at <http://www.elsevier.com>

20. **Thesis/Dissertation**: If your license is for use in a thesis/dissertation your thesis may be submitted to your institution in either print or electronic form. Should your thesis be published commercially, please reapply for permission. These requirements include permission for the Library and Archives of Canada to supply single copies, on demand, of the complete thesis and include permission for UMI to supply single copies, on demand, of the complete thesis. Should your thesis be published commercially, please reapply for permission.

21. **Other Conditions**: None

Letter of Permission for Figure 4

Removed for privacy issues.

Letter of Permission for Figure 5

ELSEVIER LICENSE TERMS AND CONDITIONS

Apr 15, 2010

This is a License Agreement between Trina Racine ("You") and Elsevier ("Elsevier") provided by Copyright Clearance Center ("CCC"). The license consists of your order details, the terms and conditions provided by Elsevier, and the payment terms and conditions.

All payments must be made in full to CCC. For payment instructions, please see information listed at the bottom of this form.

Supplier	Elsevier Limited The Boulevard,Langford Lane Kidlington,Oxford, OX5 1GB,UK
Registered Company Number	1982084
Customer name	Trina Racine
Customer address	5850 College St. Halifax, NS B3H 1X5
License Number	2410370889565
License date	Apr 15, 2010
Licensed content publisher	Elsevier
Licensed content publication	Virology
Licensed content title	Structure of avian orthoreovirus virion by electron cryomicroscopy and image reconstruction
Licensed content author	Xing Zhang, Jinghua Tang, Stephen B. Walker, David O'Hara, Max L. Nibert, Roy Duncan, Timothy S.

	Baker
Licensed content date	5 December 2005
Volume number	343
Issue number	1
Pages	11
Type of Use	Thesis / Dissertation
Portion	Figures/tables/illustrations
Number of Figures/tables/illustrations	1
Format	Print
You are an author of the Elsevier article	No
Are you translating?	No
Order Reference Number	
Expected publication date	May 2010
Elsevier VAT number	GB 494 6272 12
Permissions price	0.00 USD
Value added tax 0.0%	0.00 USD
Total	0.00 USD
Terms and Conditions	

INTRODUCTION

1. The publisher for this copyrighted material is Elsevier. By clicking "accept" in connection with completing this licensing transaction, you agree that the following terms

and conditions apply to this transaction (along with the Billing and Payment terms and conditions established by Copyright Clearance Center, Inc. ("CCC"), at the time that you opened your Rightslink account and that are available at any time at <http://myaccount.copyright.com>).

GENERAL TERMS

2. Elsevier hereby grants you permission to reproduce the aforementioned material subject to the terms and conditions indicated.

3. Acknowledgement: If any part of the material to be used (for example, figures) has appeared in our publication with credit or acknowledgement to another source, permission must also be sought from that source. If such permission is not obtained then that material may not be included in your publication/copies. Suitable acknowledgement to the source must be made, either as a footnote or in a reference list at the end of your publication, as follows:

“Reprinted from Publication title, Vol /edition number, Author(s), Title of article / title of chapter, Pages No., Copyright (Year), with permission from Elsevier [OR APPLICABLE SOCIETY COPYRIGHT OWNER].” Also Lancet special credit - “Reprinted from The Lancet, Vol. number, Author(s), Title of article, Pages No., Copyright (Year), with permission from Elsevier.”

4. Reproduction of this material is confined to the purpose and/or media for which permission is hereby given.

5. Altering/Modifying Material: Not Permitted. However figures and illustrations may be altered/adapted minimally to serve your work. Any other abbreviations, additions, deletions and/or any other alterations shall be made only with prior written authorization of Elsevier Ltd. (Please contact Elsevier at permissions@elsevier.com)

6. If the permission fee for the requested use of our material is waived in this instance, please be advised that your future requests for Elsevier materials may attract a fee.

7. Reservation of Rights: Publisher reserves all rights not specifically granted in the combination of (i) the license details provided by you and accepted in the course of this licensing transaction, (ii) these terms and conditions and (iii) CCC's Billing and Payment terms and conditions.

8. License Contingent Upon Payment: While you may exercise the rights licensed immediately upon issuance of the license at the end of the licensing process for the transaction, provided that you have disclosed complete and accurate details of your proposed use, no license is finally effective unless and until full payment is received from you (either by publisher or by CCC) as provided in CCC's Billing and Payment terms and conditions. If full payment is not received on a timely basis, then any license

preliminarily granted shall be deemed automatically revoked and shall be void as if never granted. Further, in the event that you breach any of these terms and conditions or any of CCC's Billing and Payment terms and conditions, the license is automatically revoked and shall be void as if never granted. Use of materials as described in a revoked license, as well as any use of the materials beyond the scope of an unrevoked license, may constitute copyright infringement and publisher reserves the right to take any and all action to protect its copyright in the materials.

9. Warranties: Publisher makes no representations or warranties with respect to the licensed material.

10. Indemnity: You hereby indemnify and agree to hold harmless publisher and CCC, and their respective officers, directors, employees and agents, from and against any and all claims arising out of your use of the licensed material other than as specifically authorized pursuant to this license.

11. No Transfer of License: This license is personal to you and may not be sublicensed, assigned, or transferred by you to any other person without publisher's written permission.

12. No Amendment Except in Writing: This license may not be amended except in a writing signed by both parties (or, in the case of publisher, by CCC on publisher's behalf).

13. Objection to Contrary Terms: Publisher hereby objects to any terms contained in any purchase order, acknowledgment, check endorsement or other writing prepared by you, which terms are inconsistent with these terms and conditions or CCC's Billing and Payment terms and conditions. These terms and conditions, together with CCC's Billing and Payment terms and conditions (which are incorporated herein), comprise the entire agreement between you and publisher (and CCC) concerning this licensing transaction. In the event of any conflict between your obligations established by these terms and conditions and those established by CCC's Billing and Payment terms and conditions, these terms and conditions shall control.

14. Revocation: Elsevier or Copyright Clearance Center may deny the permissions described in this License at their sole discretion, for any reason or no reason, with a full refund payable to you. Notice of such denial will be made using the contact information provided by you. Failure to receive such notice will not alter or invalidate the denial. In no event will Elsevier or Copyright Clearance Center be responsible or liable for any costs, expenses or damage incurred by you as a result of a denial of your permission request, other than a refund of the amount(s) paid by you to Elsevier and/or Copyright Clearance Center for denied permissions.

LIMITED LICENSE

The following terms and conditions apply only to specific license types:

15. **Translation:** This permission is granted for non-exclusive world **English** rights only unless your license was granted for translation rights. If you licensed translation rights you may only translate this content into the languages you requested. A professional translator must perform all translations and reproduce the content word for word preserving the integrity of the article. If this license is to re-use 1 or 2 figures then permission is granted for non-exclusive world rights in all languages.

16. **Website:** The following terms and conditions apply to electronic reserve and author websites: **Electronic reserve:** If licensed material is to be posted to website, the web site is to be password-protected and made available only to bona fide students registered on a relevant course if: This license was made in connection with a course, This permission is granted for 1 year only. You may obtain a license for future website posting, All content posted to the web site must maintain the copyright information line on the bottom of each image, A hyper-text must be included to the Homepage of the journal from which you are licensing at <http://www.sciencedirect.com/science/journal/xxxxx> or the Elsevier homepage for books at <http://www.elsevier.com> , and Central Storage: This license does not include permission for a scanned version of the material to be stored in a central repository such as that provided by Heron/XanEdu.

17. **Author website** for journals with the following additional clauses:

All content posted to the web site must maintain the copyright information line on the bottom of each image, and the permission granted is limited to the personal version of your paper. You are not allowed to download and post the published electronic version of your article (whether PDF or HTML, proof or final version), nor may you scan the printed edition to create an electronic version, A hyper-text must be included to the Homepage of the journal from which you are licensing at <http://www.sciencedirect.com/science/journal/xxxxx> , As part of our normal production process, you will receive an e-mail notice when your article appears on Elsevier's online service ScienceDirect (www.sciencedirect.com). That e-mail will include the article's Digital Object Identifier (DOI). This number provides the electronic link to the published article and should be included in the posting of your personal version. We ask that you wait until you receive this e-mail and have the DOI to do any posting. Central Storage: This license does not include permission for a scanned version of the material to be stored in a central repository such as that provided by Heron/XanEdu.

18. **Author website** for books with the following additional clauses: Authors are permitted to place a brief summary of their work online only. A hyper-text must be included to the Elsevier homepage at <http://www.elsevier.com>

All content posted to the web site must maintain the copyright information line on the bottom of each image You are not allowed to download and post the published electronic version of your chapter, nor may you scan the printed edition to create an

electronic version. Central Storage: This license does not include permission for a scanned version of the material to be stored in a central repository such as that provided by Heron/XanEdu.

19. **Website** (regular and for author): A hyper-text must be included to the Homepage of the journal from which you are licensing at <http://www.sciencedirect.com/science/journal/xxxxx>. or for books to the Elsevier homepage at <http://www.elsevier.com>

20. **Thesis/Dissertation**: If your license is for use in a thesis/dissertation your thesis may be submitted to your institution in either print or electronic form. Should your thesis be published commercially, please reapply for permission. These requirements include permission for the Library and Archives of Canada to supply single copies, on demand, of the complete thesis and include permission for UMI to supply single copies, on demand, of the complete thesis. Should your thesis be published commercially, please reapply for permission.

21. **Other Conditions**: None

APPENDIX B: Plasmid list

Clone Name	Vector Backbone	Mutation	5' End Restriction Site	3' End Restriction Site
pARV-S1	pcDNA3	wt	HindIII	NotI
pS1-Mono	pcDNA3	Met 1-4 AUG to AUC	HindIII	NotI
p10opt	pcDNA3	cCAcCatgG	HindIII	NotI
p17opt	pcDNA3	CcacCatgG	HindIII	NotI
pS1-Apaadd 299	pcDNA3	Apa added to nt 299- 304	HindIII	NotI
p10opt-Apaadd 299	pcDNA3	Apa added to nt 299- 304	HindIII	NotI
p17opt-Apaadd 299	pcDNA3	Apa added to nt 299- 304	HindIII	NotI
pS1-FLAGp17	pcDNA3	FLAG insert using Apa	HindIII	NotI
p10optFLAGp17	pcDNA3	FLAG insert using Apa	HindIII	NotI
p17optFLAGp17	pcDNA3	FLAG insert using Apa	HindIII	NotI
pARV-Δ19	pcDNA3	truncation of 5' 19 nt	HindIII	NotI
pARV-Δ27	pcDNA3	truncation of 5' 27 nt	HindIII	NotI
pARV-Δ79	pcDNA3	truncation of 5' 79 nt	HindIII	NotI
pARV-Δ147	pcDNA3	truncation of 5' 147 nt	HindIII	NotI
pARV-Δ303	pcDNA3	truncation of 5' 303 nt	HindIII	NotI
p10stp84	pcDNA3	T to A pt mut	HindIII	NotI
p10stp243	pcDNA3	C to T and T to A pt mut	HindIII	NotI
pEGFP-N1		wt	AgeI	BsrGI
pEGFP-S1	pEGFP-N1	S1 inserted using NotI	AgeI	NotI
pS1-IRES-GFP	pEGFP-N1	Hind-S1-KpnI- IRES-AgeI	HindIII	BsrGI
pPV2A	pcDNA3	poliovirus 2A insert	HindIII	EcoRI
pσC-RL	pcDNA3	RL AUG to AGG	HindIII	NotI
p10opt	pcDNA3	cCAcCatgG	HindIII	NotI
p17opt	pcDNA3	CcacCatgG	HindIII	NotI
phpσC-RL	pcDNA3	hp insert b/w nt 1 & 2	HindIII	NotI

pσCRL-hp223	pcDNA3	NheI-hp-NheI b/w nt 222 & 223	HindIII	NotI
p10opt-hp223	pcDNA3	NheI-hp-NheI b/w nt 222 & 223	HindIII	NotI
pσCRL-hp579	pcDNA3	NheI-hp-NheI b/w nt 579 & 580	HindIII	NotI
p10opt-hp579	pcDNA3	NheI-hp-NheI b/w nt 579 & 580	HindIII	NotI
p17opt-hp579	pcDNA3	NheI-hp-NheI b/w nt 579 & 580	HindIII	NotI
p-RL	pcDNA3	RL wt with 3' 898 nt S1	BamHI	XbaI
pβ-RL	pcDNA3	β-globin 5'-UTR insert	HindIII	XbaI
pβ-ORF-RL	pcDNA3	nt 54 T to A pt mut	HindIII	XbaI
p17opt#1-RL	pcDNA3	S1 nt 267-320 with p17opt int	HindIII	XbaI
p17opt#2-RL	pcDNA3	S1 nt 260-393 with p17opt int	HindIII	XbaI
pβ-σCRL	pcDNA3	β-globin 5'-UTR insert	HindIII	NotI
pβ-p10opt	pcDNA3	β-globin 5'-UTR insert	HindIII	NotI
pβ-p17opt	pcDNA3	β-globin 5'-UTR insert	HindIII	NotI
pσCRL-M1	pcDNA3	Met 1 AUG to AUC pt mut	HindIII	NotI
pσCRL-M2	pcDNA3	Met 2 AUG to AUC pt mut	HindIII	NotI
pσCRL-M3	pcDNA3	Met 3 AUG to AUC pt mut	HindIII	NotI
pσCRL-M4	pcDNA3	Met 4 AUG to AUC pt mut	HindIII	NotI
pσCRL-M1+M2	pcDNA3	AUG to AUC	HindIII	NotI
pσCRL-M1+M3	pcDNA3	AUG to AUC	HindIII	NotI
pσCRL-M1+M4	pcDNA3	AUG to AUC	HindIII	NotI
pσCRL- M1+M2+M3	pcDNA3	AUG to AUC	HindIII	NotI
pσCRL-Mono	pcDNA3	All 4 AUGs to AUC	HindIII	NotI
pσCRL- MiniORF1	pcDNA3	insert 24 nt with two AUGs	HindIII	NotI
pσCRL-24nt int	pcDNA3	two AUGs pt mut to AUC	HindIII	NotI
pσCRL- MiniORF2	pcDNA3	insert 78 nt with four AUGs	HindIII	NotI
pσCRL-M5	pcDNA3	gcAaaAtGg (cap = pt mut)	HindIII	NotI
pσCRL-M6	pcDNA3	ttaacatGg (cap = pt)	HindIII	NotI

pσCRL-M7	pcDNA3	caacaAtgG (cap = pt mut)	HindIII	NotI
pS1-RL	pcDNA3	AUG to AUC b/w nt 632 to 732 T to G pt mut nt 520	HindIII	NotI
pσCRL-stp517	pcDNA3	T to G pt mut nt 520	HindIII	NotI
p10opt-stp517	pcDNA3	T to G pt mut nt 520	HindIII	NotI
p17opt-stp517	pcDNA3	T to G pt mut nt 520	HindIII	NotI
pΔ628-751RL	pcDNA3	nt 1-627 int upstream p-RL	HindIII	XbaI
pΔ593-751RL	pcDNA3	nt 1-592 int upstream p-RL	HindIII	XbaI
pΔ483-751RL	pcDNA3	nt 1-482 int upstream p-RL	HindIII	XbaI
pΔ423-751RL	pcDNA3	nt 1-422 int upstream p-RL	HindIII	XbaI
pΔ393-751RL	pcDNA3	nt 1-392 int upstream p-RL	HindIII	XbaI
pΔ366-751RL	pcDNA3	nt 1-365 int upstream p-RL	HindIII	XbaI
pΔ312-751RL	pcDNA3	nt 1-311 int upstream p-RL	HindIII	XbaI
pS1RL-M3	pcDNA3	Met 3 AUG to AUC	HindIII	NotI
pΔ366-751RL-M3	pcDNA3	Met 3 AUG to AUC	HindIII	XbaI
pΔ366-751intRL	pcDNA3	int 114 nt b/w nt 365 & A of RL	HindIII	XbaI
pΔ366-751RL-RCR1.1	pcDNA3	TTcatT (cap = pt mut)	HindIII	XbaI
pΔ366-751RL-RCR1.2	pcDNA3	ccTTcT (cap = pt mut)	HindIII	XbaI
pΔ423-751RL-RCR1.1	pcDNA3	TTcatT (cap = pt mut)	HindIII	XbaI
pΔ423-751RL-RCR2	pcDNA3	atTTcT (cap = pt mut)	HindIII	XbaI

APPENDIX C: Primer list

Primer Name	Sequence (5'to3')
Opt	
Hind ARV p10opt Fwd #2	ACTACTAAGCTTgcttttcaatcccttggtccaccatggtgcgatgcctccc gttcgtgtaacggtg
ARV p17 opt rnd 1 Fwd	gtagcggtgagttctggtaagcacCatgGaatggctccgccatacgacgtttg
ARV p17 opt rnd 1 Rev	CAAACGTCGTATGGCGGAGCCATTCCATGGTGCTTACCAGAACT CAACGCTAC
ARV p17opt rnd 2 Fwd	gctggtagcgttgagttctggtaaCcaccatggaatggctccgccatacg
ARV p17opt rnd 2 Rev	CGTATGGCGGAGCCATTCCATGGTGGTTACCAGAACTCAACGC TACCAGC

IRES

S1 Hind III Fwd #2	ACTACTAAGCTTGCTTTTTTCAATCCC
S1 Kpn I Rev #3	ACTACTGGTACCGATGAATAACCAATCC
SIG Kpn to Apa Fwd	gattggttattcatcGGgcCctttgtacgcctg
SIG Kpn to Apa Rev	caggcgtacaaaGGgcCCgatgaataaccaatc

Met AUG to AUC


p10 G27C QikChg Fwd	cccttgctcgtgatCctgcgatgcctccc
p10 G27C QikChg Rev	gggaggcatacgcagGatcgcgaacaaggg
p10 G36C QikChg Fwd	gtcgtatgctcgtatCctcccggttcgtg
p10 G36C QikChg Rev	cacgaaccgggaggGatacgcagcatcgac
p17 G295C QikChg Fwd	gttctgtaagcacaatCcaatggctccgccatac
p17 G295C QikChg Rev	gtatggcggagccattgGattgtgcttaccagaac
p10 G300C QikChg Fwd	gtaagcacaatgcaatCgctccgccatacgac
p10 G300C QikChg Rev	gtcgtatggcggagcGattgcattgtgcttac
p10G36Cp17 QikChg Fwd	gtcgtatCctgcgatCctcccggttcgtg
p10G36Cp17 QikChg Rev	cacgaaccgggaggGatacgcagGatcgcag
p10G300Cp17 QikChg Fwd	gtaagcacaatCcaatCgctccgccatacgac

p10G300Cp17 gtcgtatggcggagcGattgGattgtgcttac
 QikChg Rev
 Met 1 + 2 pt mut Fwd gttcgtcgatCctgcgtatCctccccggttcgtgtaacg
 Met 1 + 2 pt mut Rev cgttacacgaaccgggaggGatacgcagGatcgcagAAC

p10 stop insert

p10 stop insert nt 87 ggtaacgttcattgAcaggcagctcaaaac
 Fwd
 p10 stop insert nt 87 gttttgagctgcctgTcaatgaacgttacc
 Rev
 p10 stop int nt 244+246 gtcaaggcggacgctgcaTgAagtgtcttccatcg
 Fwd
 p10 stop inst nt cgatggaagacactTcAtgcagcgtccgccttgac
 244+246 Rev

3' truncations

ARV del 25nt 3' Rev  #2
 ARV del 50nt 3' Rev tacgcacggtcaaggaacgaatgttcgc
 ARV del 300nt 3' Rev cgtgagatttcccgtggacgacatcatataatcagtgc
 ARV del 500nt 3' Rev CGC CGT CAG CGA CAC TAA GCG GAG

Hairpins

S1 5' Nhe add step #1 gGGAGACCCAAGCTTgctAGttcaatcccttgttcgctcg
 Fwd
 S1 5' Nhe add step #1 cgacgaacaagggattgaaCTagcAAGCTTGGGTCTCCc
 Rev
 S1 5' Nhe add step #2 gGGAGACCCAAGCTTgctAGCtcaatcccttgttcgctcg
 Fwd
 S1 5' Nhe add step #2 cgacgaacaagggattgaGCTagcAAGCTTGGGTCTCCc
 Rev
 ARV Nhe add nt 223 ctatactgttgaaggctaGCgtcaaggcggacgctgcacg
 Fwd
 ARV Nhe add nt 223 cgtgcagcgtccgccttgacGctagccttacaacagtatag
 Rev
 ARV Nhe add 579 gcttactattctccccacagctaGcgttccattgctcatccgatcgg
 Fwd
 ARV Nhe add 579 CCGATCGGATGCAGGCAATGGAACGCTAGCGTGTGGGGAGAAT
 Rev AGTAGAGC
 Nhe hp Fwd ACTACTgctAGCattctgtctgttttgggggattgcaag
 Nhe hp Rev ACTACTgctagcTTA TAA AAG CAG TGG CTG CGG C
 T7 ARV 5' hp Fwd TAATACGACTCACTATAGGGAGAgctAGCattctgtctgttttggggg

Rnd Primers

ARV Hind III Fwd #3 ACTACTaagcttgcttttcaatcccttggtcg
Not I ARV S1 end ACTACTGCGGCCGCgatgaataaccaatcc
Rev
S1 end Rev #2 GAT GAA TAA CCA ATC CCA GTA CGG CGC C
RL end Rev TTATTGTTTCATTTTTGAGAACTCGC
Xba RL Fwd #2 ACTACTtctagaAgGgACTTCGAAAGTTTATGATCCAGAA
CAAAG
Xba RL Rev #2 ACTACTTCTAGAAATTATTGTTTCATTTTTGAGAACTCGC
TCAAC

qRT-PCR

RealTime Actin Fwd #1 ccagccatctttcttggtgta
RealTime Actin Rev #1 atgccagggtacattgtggt
RealTime ARV S1 Fwd #1 tgctataactggggctgacc
RealTime ARV S1 Rev #1 cacgtggaccctacaagtt
qRT-PCR RL Fwd ATCGGACCCAGGATTCTTTT
qRT-PCR RL Rev ACTCGCTCAACGAACGATTT

S1-RL

ARV Met 5 pt mut #2 Fwd cttgtcttatagttcattgggatCgcggtctcaatccatcgcagcg
ARV Met 5 pt mut #2 Rev cgctgcgatggattgagaccgcGatcccaatgaactataagacaag
ARV Met 6 pt mut Fwd gacttcgaacgtgactataagtcacGcgatttgacgccgatctatgaacg
ARV Met 6 pt mut Rev cgttcatagatcggcgcaaatcgcGatgacttatagtcacgttcgaagtc
ARV Met 6+7 pt mut Fwd gtcatcgcgatttgacgccgatctatCaacggctgaccaatctagaagcg
ARV Met 6+7 pt mut Rev cgcttctagattggcagccggtGatagatcggcgcaaatcgcgatgac
Xba RL ATG Fwd ACTACTtctagaATGACTTCGAAAGTTTATGATCCAG
ARV p17 stp 517 Fwd gcggtgattcggcgttcgctctctaGtcaacattgtcaagttttgtgagtacg
ARV p17 stp 517 Rev CGTACTCACAAATACTTGACAATGTTGACTAGAGAGCGAACCGGCGAAT
CAGCCGC

Internal Deletions

ARV Bam add nt 633 Fwd cttgtcttatagttcattgggatCCcggtctcaatccatcgcagcg

ARV Bam add nt 633 Rev cgctgcgatggattgagaccgGGatccaatgaactataagacaag

ARV Bam add nt 592 Rev ACTACTggatccAGG CAA TGG AAC GAT AGC GTG TGG GGA GAA T

Bam ARV nt 483 Fwd ACTACTggatccgggtccacgtgcggctgattc

Bam ARV nt 483 Rev ACTACTggatccTACAAGGTTGAGATAACAGAGTAGGCA ATTTGGAATAGAGAGGATGAG

ARV Bam nt 422 Rev ACTACTggatccCAATGTTAAAATACTGTGATGGGTCAGCCCCA GTTATAGC

ARV Bam nt 392 Rev ACTACTggatccCAGTTATAGCAGTAAATGATGGGATAG CAAGTTCGCGAAGTG

ARV Bam add nt 371 Fwd gctatcacttcgcgaacttgGGatcccatcttactgctataac

ARV Bam add nt 371 Rev gttatagcagtaaataatgatgggatCCcaagttcgcgaagtgatagc

A371RL add G rest site Fwd cgctatcacttcgcgaacttgGGATCCgGAATGACTTCGAAAGTTT AcGATCCAG

A371RL add G rest site Rev CTGGATCGTAAACTTTCGAAGTCATTCCGGATCCCAAGTTCGCG AAGTGATAGCG

A488RL add G rest site Fwd gcctactctgttatctcaaccttgaGGATCCgGAATGACTTCGAAAGTT TAcGATCCAGAACAAAGG

A488RL add G rest site Rev CCT TTG TTC TGG ATC GTA AAC TTT CGA AGT CAT TCC GGA TCC TAC AAG GTT GAG ATA ACA GAG TAG GC

Bam HI nt 389 Rev ACTACTggatccttatagcagtaaataatgatgggatagc

ARV Bam add nt 311 Rev ACTACTGGATCCTAT GGC GGA GCC ATT GCA TTG TGC

5' truncations

ARV del19ntT7LongFwd TAATACGACTCACTATAGGGAGAcgtcgatgctgcgtatgcc

ARV del27ntT7LongFwd TAATACGACTCACTATAGGGAGActgcgtatgcctcccggttc

ARV del79ntT7Long Fwd TAATACGACTCACTATAGGGAGAttcattgtcaggcagctcaaaac ac

ARVdel147ntT7Long Fwd TAATACGACTCACTATAGGGAGAtggccttatctagcggcgg

ARV del302ntT7LongFwd TAATACGACTCACTATAGGGAGAtccgccatacagcgtttgaagtg

T7

T7 B- GlobinUTRRLFwd TAATACGACTCACTATAGGGAGAGAATACAAAGCTTGCTTGT TCTTTTTGCAGAAGCTCAGAATAAACGCTCAACTTTGGCAGgc tagcATGACTTCGAAAGTTTATGATCCAGAACAAAG

T7B-GloUTRop RLFwd TAATACGACTCACTATAGGGAGAGAATACAAAGCTTGCTTGT
TCTTTTTGCAGAAGCTCAGAATAAACGCTCAACTaTGGCAGgc
tagcATGACTTCGAAAGTTTATGATCCAGAACAAAG

T7 S1 Long Fwd TAATACGACTCACTATAGGGAGAGCTTTTTCAATCCC
TTGTTCG

p17 FLAG

Apa FLAG Fwd ACTACTGGGCCCggtggcggagactacaaagaccatg
Apa FLAG Rev ACTACTGGGCCCAAG CTT GTC ATC GTC ATC CTT
GTA ATC
ARVwtApaaddnt302 Fwd gttctgtaagcacaATGcaaGggcCccgccatacgacgtttgaagtgaac
ARVwtApaaddnt302R ev GTTGCACTTCAAACGTCGTATGGCGGGGCCCTTGCATTGTGCTT
ACCAGAAC
ARVp17optApaaddnt 302 Fwd gttctgtaaCcacatggaaGggcCccgccatacgacgtttgaagtgaac
ARV p17opt Apa add nt 302 Rev GTTGCACTTCAAACGTCGTATGGCGGGGCCCTTCCATGGTGGT
TACCAGAAC
Xba del MCS Apa Fwd GCGGCCGCTCGAGCATGCATCTiGAGaGCCCTATTCT
ATAGTGTC
Xba del MCS Apa Rev GAC ACT ATA GAA TAG GGC TCT CAA GAT GCA TGC TCG
AGC GGC CGC

B-globin

B-Globin UTR RL Fwd #1 ACTACTAAGCTTGCTCCACCTTGGCAGGAATACAAAggctagcA
TGtCTTCGAAAGTTTATGATCCAGAACAAAG
B-Globin UTR RL Fwd #2 ACTACTAAGCTTGCTTTTGACACAACGTGTGTTTACTTGCAAT
CCCCAAAACAGACAGCTCCACCTTGGCAGGAATAC
B-Globin UTR opt pt mut RL Fwd cCCAAAACAGACAGCTCCACCATGGCAGGAATACAAAggctagc
B-Globin UTR opt pt mut RL Rev GCT AGC CTT TGT ATT CCT GCC ATG GTG GAG CTG TCT
GTT TTG GG
B-globin UTR ARV rnd 1 Fwd ACTACTggatccAGCTTCACAACAATCACCAACAGGATCCGAgct
tttcaatcccttggtc
B-glo opt ARV add "G" UTR Fwd **CAGACAGCTCCACCATGGgCAGGAATACAAAggatcc**
B-glo opt ARV add "G" UTR Rev GGA TCC TTT GTA TTC CTG CCC ATG GTG GAG CTG TCT G
B-glo p17opt add G Fwd gaatggctccgccatacgacgtttgGggatccGAATGACTTCGAAAGTTT
Ac
B-glo p17opt add G Rev GTAAACTTTTCGAAGTCATTCCGGATCCCCAAACGTCGTATGGCGG
AGCCATTC

Bam p17opt region Fwd ACTACTggatccggtagcgttgagttctggaaccacc
 Bam p17opt region Rev ACTACTggatccCAA ACG TCG TAT GGC GGA GCC ATT C
 ARV Bam nt 260 Fwd ACTACTggatccgtagcgttgagttctggaaccacc
 ARV Bam nt 393 Rev ACTACTggatccCCAGTTATAGCAGTAAATGATGGGATA GCAAGTTTCG

Met add p17 ORF

p17ORF Met add #1 Fwd cgattaatttctgtccgctatcacttcgcAaaAtGgctatcccatcattactgctat aactggggc
 p17ORF Met add #1 Rev GCCCCAGTTATAGCAGTAAATGATGGGATAGCCATTTTGCGAAG TGATAGCGGACAGAAATTAATCG
 p17ORF Met add #2 Fwd gggctgacctcacagtttaacatGgagctccacacactcatcctctc
 p17ORF Met add #2 Rev GAGAGGATGAGTGTGTGGGAGCTCCATGTTAAATACTGTGAT GGGTCAGCCC
 p17ORF Met add #3 Fwd ctgattcgccggttcgctctctattcaacaAtgGcaagtattgtgagtacgattgtgc tc
 p17ORF Met add #3 Rev GAGCACAATCGTACTCACAATACTTGCCATTGTTGAATAGAGA GCGAACC GGCGAATCAG

Δ366-751intRL

Bam GFP int Fwd ACTACTggatccCCACCTACGGCAAGCTGACCCTGAAGT TCATCTG
 Bam GFP int Rev #2 ACTACTggatccCGGGGTAGCGGCTGAAGCACTGCAC
 A371GFPintRL add 'cg' Fwd CGTGCAGTGCTCAGCCGCTACcgggatccGAATGACTTCGAAAG
 A371GFPintRL add 'cg' Rev CTTTCGAAGTCATTCCGGATCCCGGTAGCGGCTGAGCACTGCA CG

RBS1 & RBS2

ARV nt 370/1 pt mut Fwd #2 gtccgctatcacttcggaacttgctatTTcatTatttactgctataactgggatcc
 ARV nt 370/1 pt mut Rev #2 GGATCCCAGTTATAGCAGTAAATAATGAAATAGCAAGTTCGCGA AGTGATAGCGGAC
 ARV nt 372/3 pt mut Fwd ccgctatcacttcggaacttgctatccTTtcatttactgctataactggggctg
 ARV nt 372/3 pt mut Rev CAGCCCCAGTTATAGCAGTAAATGAAAGGATAGCAAGTTCGCG AAGTGATAGCGG
 ARV nt 388/9 pt mut Fwd cttgctatCccatcatttactgctatTTctggggctgacctcacagtttaac

ARV nt 388/9 pt mut GTTAAAATACTGTGATGGGTCAGCCCCAGAAATAGCAGTAAATG
Rev ATGGGATAGCAAG

Mini ORF1 & 2

Apa 1X FLAG Fwd ACTACTGggcCcgattacaaggAcGacgAcGacaagcgccatacgacgttt
gaagtg
Apa 1X FLAG ATG ACTACTGggcCcgattacaaggATGacgATGacaagcgccatacgacgttt
Fwd gaagtg
ARV WT Apa p17 ACTACTGggcCcTTGCATTGTGCTTACCAGAACTCAACG
Rev CTACC
ARV Apa p17opt Rev ACTACTGggcCcTTCCATGGTGGTTACCAGAACTCAAC
GCTAC

References

- Abastado, J. P., Miller, P. F., Jackson, B. M., and Hinnebusch, A. G. (1991). Suppression of ribosomal reinitiation at upstream open reading frames in amino acid-starved cells forms the basis for GCN4 translational control. *Mol Cell Biol* **11**(1), 486-96.
- Alam, J., and Cook, J. L. (1990). Reporter genes: application to the study of mammalian gene transcription. *Anal Biochem* **188**(2), 245-54.
- Algire, M. A., Maag, D., and Lorsch, J. R. (2005). Pi release from eIF2, not GTP hydrolysis, is the step controlled by start-site selection during eukaryotic translation initiation. *Mol Cell* **20**(2), 251-62.
- Ali, I. K., McKendrick, L., Morley, S. J., and Jackson, R. J. (2001). Activity of the hepatitis A virus IRES requires association between the cap-binding translation initiation factor (eIF4E) and eIF4G. *J Virol* **75**(17), 7854-63.
- Ambros, V. (1989). A hierarchy of regulatory genes controls a larva-to-adult developmental switch in *C. elegans*. *Cell* **57**(1), 49-57.
- Anderson, J. L., Johnson, A. T., Howard, J. L., and Purcell, D. F. (2007). Both linear and discontinuous ribosome scanning are used for translation initiation from bicistronic human immunodeficiency virus type 1 env mRNAs. *J Virol* **81**(9), 4664-76.
- Antin, P. B., and Ordahl, C. P. (1991). Isolation and characterization of an avian myogenic cell line. *Dev Biol* **143**(1), 111-21.
- Arias, C., Walsh, D., Harbell, J., Wilson, A. C., and Mohr, I. (2009). Activation of host translational control pathways by a viral developmental switch. *PLoS Pathog* **5**(3), e1000334.
- Attoui, H., Jaafar, F. M., Belhouchet, M., de Micco, P., de Lamballerie, X., and Brussaard, C. P. (2006). *Micromonas pusilla* reovirus: a new member of the family Reoviridae assigned to a novel proposed genus (Mimoreovirus). *J Gen Virol* **87**(Pt 5), 1375-83.
- Babendure, J. R., Babendure, J. L., Ding, J. H., and Tsien, R. Y. (2006). Control of mammalian translation by mRNA structure near caps. *RNA* **12**(5), 851-61.
- Barco, A., Feduchi, E., and Carrasco, L. (2000). A stable HeLa cell line that inducibly expresses poliovirus 2A(pro): effects on cellular and viral gene expression. *J Virol* **74**(5), 2383-92.

- Behrens, S., Ruhland, C., Inacio, J., Huber, H., Fonseca, A., Spencer-Martins, I., Fuchs, B. M., and Amann, R. (2003). In situ accessibility of small-subunit rRNA of members of the domains Bacteria, Archaea, and Eucarya to Cy3-labeled oligonucleotide probes. *Appl Environ Microbiol* **69**(3), 1748-58.
- Belsham, G. J. (2009). Divergent picornavirus IRES elements. *Virus Res* **139**(2), 183-92.
- Benavente, J., and Martinez-Costas, J. (2007). Avian reovirus: structure and biology. *Virus Res* **123**(2), 105-19.
- Bergenheim, N. C., Venta, P. J., Hopkins, P. J., Kim, H. J., and Tashian, R. E. (1992). Mutation creates an open reading frame within the 5' untranslated region of macaque erythrocyte carbonic anhydrase (CA) I mRNA that suppresses CA I expression and supports the scanning model for translation. *Proc Natl Acad Sci U S A* **89**(18), 8798-802.
- Berthelot, K., Muldoon, M., Rajkowitsch, L., Hughes, J., and McCarthy, J. E. (2004). Dynamics and processivity of 40S ribosome scanning on mRNA in yeast. *Mol Microbiol* **51**(4), 987-1001.
- Blakqori, G., van Knippenberg, I., and Elliott, R. M. (2009). Bunyamwera orthobunyavirus S-segment untranslated regions mediate poly(A) tail-independent translation. *J Virol* **83**(8), 3637-46.
- Bohnsack, M. T., Czaplinski, K., and Gorlich, D. (2004). Exportin 5 is a RanGTP-dependent dsRNA-binding protein that mediates nuclear export of pre-miRNAs. *RNA* **10**(2), 185-91.
- Bonneville, J. M., Sanfacon, H., Futterer, J., and Hohn, T. (1989). Posttranscriptional trans-activation in cauliflower mosaic virus. *Cell* **59**(6), 1135-43.
- Borman, A. M., and Kean, K. M. (1997). Intact eukaryotic initiation factor 4G is required for hepatitis A virus internal initiation of translation. *Virology* **237**(1), 129-36.
- Borman, A. M., Michel, Y. M., and Kean, K. M. (2000). Biochemical characterisation of cap-poly(A) synergy in rabbit reticulocyte lysates: the eIF4G-PABP interaction increases the functional affinity of eIF4E for the capped mRNA 5'-end. *Nucleic Acids Res* **28**(21), 4068-75.
- Brown, C. W., Stephenson, K. B., Hanson, S., Kucharczyk, M., Duncan, R., Bell, J. C., and Lichty, B. D. (2009). The p14 FAST protein of reptilian reovirus increases vesicular stomatitis virus neuropathogenesis. *J Virol* **83**(2), 552-61.

- Byrd, M. P., Zamora, M., and Lloyd, R. E. (2005). Translation of eukaryotic translation initiation factor 4GI (eIF4GI) proceeds from multiple mRNAs containing a novel cap-dependent internal ribosome entry site (IRES) that is active during poliovirus infection. *J Biol Chem* **280**(19), 18610-22.
- Cai, X., Hagedorn, C. H., and Cullen, B. R. (2004). Human microRNAs are processed from capped, polyadenylated transcripts that can also function as mRNAs. *RNA* **10**(12), 1957-66.
- Calkhoven, C. F., Muller, C., and Leutz, A. (2000). Translational control of C/EBPalpha and C/EBPbeta isoform expression. *Genes Dev* **14**(15), 1920-32.
- Cao, F., Scougall, C. A., Jilbert, A. R., and Tavis, J. E. (2009). Pre-P is a secreted glycoprotein encoded as an N-terminal extension of the duck hepatitis B virus polymerase gene. *J Virol* **83**(3), 1368-78.
- Cao, J., and Geballe, A. P. (1995). Translational inhibition by a human cytomegalovirus upstream open reading frame despite inefficient utilization of its AUG codon. *J Virol* **69**(2), 1030-6.
- Castano, A., Ruiz, L., and Hernandez, C. (2009). Insights into the translational regulation of biologically active open reading frames of Pelargonium line pattern virus. *Virology* **386**(2), 417-26.
- Chappell, S. A., Dresios, J., Edelman, G. M., and Mauro, V. P. (2006). Ribosomal shunting mediated by a translational enhancer element that base pairs to 18S rRNA. *Proc Natl Acad Sci U S A* **103**(25), 9488-93.
- Chappell, S. A., Edelman, G. M., and Mauro, V. P. (2000). A 9-nt segment of a cellular mRNA can function as an internal ribosome entry site (IRES) and when present in linked multiple copies greatly enhances IRES activity. *Proc Natl Acad Sci U S A* **97**(4), 1536-41.
- Chappell, S. A., Edelman, G. M., and Mauro, V. P. (2004). Biochemical and functional analysis of a 9-nt RNA sequence that affects translation efficiency in eukaryotic cells. *Proc Natl Acad Sci U S A* **101**(26), 9590-4.
- Chappell, S. A., Edelman, G. M., and Mauro, V. P. (2006). Ribosomal tethering and clustering as mechanisms for translation initiation. *Proc Natl Acad Sci U S A* **103**(48), 18077-82.
- Chen, D., and Patton, J. T. (1998). Rotavirus RNA replication requires a single-stranded 3' end for efficient minus-strand synthesis. *J Virol* **72**(9), 7387-96.
- Cigan, A. M., Feng, L., and Donahue, T. F. (1988). tRNAⁱ(met) functions in directing the scanning ribosome to the start site of translation. *Science* **242**(4875), 93-7.

- Costas, C., Martinez-Costas, J., Bodelon, G., and Benavente, J. (2005). The second open reading frame of the avian reovirus S1 gene encodes a transcription-dependent and CRM1-independent nucleocytoplasmic shuttling protein. *J Virol* **79**(4), 2141-50.
- Cuesta, R., Xi, Q., and Schneider, R. J. (2000). Adenovirus-specific translation by displacement of kinase Mnk1 from cap-initiation complex eIF4F. *EMBO J* **19**(13), 3465-74.
- Curran, J., and Kolakofsky, D. (1988). Scanning independent ribosomal initiation of the Sendai virus X protein. *EMBO J* **7**(9), 2869-74.
- Curran, J., and Kolakofsky, D. (1989). Scanning independent ribosomal initiation of the Sendai virus Y proteins in vitro and in vivo. *EMBO J* **8**(2), 521-6.
- Das, S., Ghosh, R., and Maitra, U. (2001). Eukaryotic translation initiation factor 5 functions as a GTPase-activating protein. *J Biol Chem* **276**(9), 6720-6.
- Das, S., and Maitra, U. (2001). Functional significance and mechanism of eIF5-promoted GTP hydrolysis in eukaryotic translation initiation. *Prog Nucleic Acid Res Mol Biol* **70**, 207-31.
- Davies, M. V., Pelletier, J., Meerovitch, K., Sonenberg, N., and Kaufman, R. J. (1991). The effect of poliovirus proteinase 2Apro expression on cellular metabolism. Inhibition of DNA replication, RNA polymerase II transcription, and translation. *J Biol Chem* **266**(22), 14714-20.
- Davuluri, R. V., Suzuki, Y., Sugano, S., and Zhang, M. Q. (2000). CART classification of human 5' UTR sequences. *Genome Res* **10**(11), 1807-16.
- Dawe, S., Corcoran, J. A., Clancy, E. K., Salsman, J., and Duncan, R. (2005). Unusual topological arrangement of structural motifs in the baboon reovirus fusion-associated small transmembrane protein. *J Virol* **79**(10), 6216-26.
- Dawe, S., and Duncan, R. (2002). The S4 genome segment of baboon reovirus is bicistronic and encodes a novel fusion-associated small transmembrane protein. *J Virol* **76**(5), 2131-40.
- de Breyne, S., Monney, R. S., and Curran, J. (2004). Proteolytic processing and translation initiation: two independent mechanisms for the expression of the Sendai virus Y proteins. *J Biol Chem* **279**(16), 16571-80.
- de Breyne, S., Simonet, V., Pelet, T., and Curran, J. (2003). Identification of a cis-acting element required for shunt-mediated translational initiation of the Sendai virus Y proteins. *Nucleic Acids Res* **31**(2), 608-18.

- de Breyne, S., Stalder, R., and Curran, J. (2005). Intracellular processing of the Sendai virus C' protein leads to the generation of a Y protein module: structure-functional implications. *FEBS Lett* **579**(25), 5685-90.
- de Breyne, S., Yu, Y., Unbehaun, A., Pestova, T. V., and Hellen, C. U. (2009). Direct functional interaction of initiation factor eIF4G with type 1 internal ribosomal entry sites. *Proc Natl Acad Sci U S A* **106**(23), 9197-202.
- Dever, T. E., Feng, L., Wek, R. C., Cigan, A. M., Donahue, T. F., and Hinnebusch, A. G. (1992). Phosphorylation of initiation factor 2 alpha by protein kinase GCN2 mediates gene-specific translational control of GCN4 in yeast. *Cell* **68**(3), 585-96.
- Dominguez, D. I., Ryabova, L. A., Pooggin, M. M., Schmidt-Puchta, W., Futterer, J., and Hohn, T. (1998). Ribosome shunting in cauliflower mosaic virus. Identification of an essential and sufficient structural element. *J Biol Chem* **273**(6), 3669-78.
- Donze, O., Jagus, R., Koromilas, A. E., Hershey, J. W., and Sonenberg, N. (1995). Abrogation of translation initiation factor eIF-2 phosphorylation causes malignant transformation of NIH 3T3 cells. *EMBO J* **14**(15), 3828-34.
- Doohan, J. P., and Samuel, C. E. (1992). Biosynthesis of reovirus-specified polypeptides: ribosome pausing during the translation of reovirus S1 mRNA. *Virology* **186**(2), 409-25.
- Dorner, A. J., Semler, B. L., Jackson, R. J., Hanecak, R., Duprey, E., and Wimmer, E. (1984). In vitro translation of poliovirus RNA: utilization of internal initiation sites in reticulocyte lysate. *J Virol* **50**(2), 507-14.
- Driesen, M., Benito-Moreno, R. M., Hohn, T., and Futterer, J. (1993). Transcription from the CaMV 19 S promoter and autocatalysis of translation from CaMV RNA. *Virology* **195**(1), 203-10.
- Duncan, R. (1996). The low pH-dependent entry of avian reovirus is accompanied by two specific cleavages of the major outer capsid protein mu 2C. *Virology* **219**(1), 179-89.
- Duncan, R. (1999). Extensive sequence divergence and phylogenetic relationships between the fusogenic and nonfusogenic orthoreoviruses: a species proposal. *Virology* **260**(2), 316-28.
- Duncan, R., Chen, Z., Walsh, S., and Wu, S. (1996). Avian reovirus-induced syncytium formation is independent of infectious progeny virus production and enhances the rate, but is not essential, for virus-induced cytopathology and virus egress. *Virology* **224**(2), 453-64.

- Duncan, R., Corcoran, J., Shou, J., and Stoltz, D. (2004). Reptilian reovirus: a new fusogenic orthoreovirus species. *Virology* **319**(1), 131-40.
- Duncan, R., Etchison, D., and Hershey, J. W. (1983). Protein synthesis eukaryotic initiation factors 4A and 4B are not altered by poliovirus infection of HeLa cells. *J Biol Chem* **258**(11), 7236-9.
- Duncan, R., Milburn, S. C., and Hershey, J. W. (1987). Regulated phosphorylation and low abundance of HeLa cell initiation factor eIF-4F suggest a role in translational control. Heat shock effects on eIF-4F. *J Biol Chem* **262**(1), 380-8.
- Duncan, R., Murphy, F. A., and Mirkovic, R. R. (1995). Characterization of a novel syncytium-inducing baboon reovirus. *Virology* **212**(2), 752-6.
- Duncan, R., and Sullivan, K. (1998). Characterization of two avian reoviruses that exhibit strain-specific quantitative differences in their syncytium-inducing and pathogenic capabilities. *Virology* **250**(2), 263-72.
- Elroy-Stein, O., and Merrick, W. C., Eds. (2007). Translation initiation via cellular internal ribosome entry sites. *Translational Control in Biology and Medicine*. Edited by M. B. Mathews, N. Sonenberg, and J. Hershey. New York: Cold Spring Harbor Laboratory Press.
- Erkmann, J. A., and Kutay, U. (2004). Nuclear export of mRNA: from the site of transcription to the cytoplasm. *Exp Cell Res* **296**(1), 12-20.
- Etchison, D., Hansen, J., Ehrenfeld, E., Edery, I., Sonenberg, N., Milburn, S., and Hershey, J. W. (1984). Demonstration in vitro that eucaryotic initiation factor 3 is active but that a cap-binding protein complex is inactive in poliovirus-infected HeLa cells. *J Virol* **51**(3), 832-7.
- Etchison, D., Milburn, S. C., Edery, I., Sonenberg, N., and Hershey, J. W. (1982). Inhibition of HeLa cell protein synthesis following poliovirus infection correlates with the proteolysis of a 220,000-dalton polypeptide associated with eucaryotic initiation factor 3 and a cap binding protein complex. *J Biol Chem* **257**(24), 14806-10.
- Fekete, C. A., Mitchell, S. F., Cherkasova, V. A., Applefield, D., Algire, M. A., Maag, D., Saini, A. K., Lorsch, J. R., and Hinnebusch, A. G. (2007). N- and C-terminal residues of eIF1A have opposing effects on the fidelity of start codon selection. *EMBO J* **26**(6), 1602-14.
- Fitzgerald, K. D., and Semler, B. L. (2009). Bridging IRES elements in mRNAs to the eukaryotic translation apparatus. *Biochim Biophys Acta* **1789**(9-10), 518-28.

- Fraser, C. S., Berry, K. E., Hershey, J. W., and Doudna, J. A. (2007). eIF3j is located in the decoding center of the human 40S ribosomal subunit. *Mol Cell* **26**(6), 811-9.
- Frederiks, F., Heynen, G. J., van Deventer, S. J., Janssen, H., and van Leeuwen, F. (2009). Two Dot1 isoforms in *Saccharomyces cerevisiae* as a result of leaky scanning by the ribosome. *Nucleic Acids Res* **37**(21), 7047-58.
- Furuichi, Y., Morgan, M., Muthukrishnan, S., and Shatkin, A. J. (1975). Reovirus messenger RNA contains a methylated, blocked 5'-terminal structure: m-7G(5')ppp(5')G-MpCp. *Proc Natl Acad Sci U S A* **72**(1), 362-6.
- Furuichi, Y., Muthukrishnan, S., and Shatkin, A. J. (1975). 5'-Terminal m-7G(5')ppp(5')G-m-p in vivo: identification in reovirus genome RNA. *Proc Natl Acad Sci U S A* **72**(2), 742-5.
- Futterer, J., Gordon, K., Sanfacon, H., Bonneville, J. M., and Hohn, T. (1990). Positive and negative control of translation by the leader sequence of cauliflower mosaic virus pregenomic 35S RNA. *EMBO J* **9**(6), 1697-707.
- Futterer, J., and Hohn, T. (1991). Translation of a polycistronic mRNA in the presence of the cauliflower mosaic virus transactivator protein. *EMBO J* **10**(12), 3887-96.
- Futterer, J., and Hohn, T. (1992). Role of an upstream open reading frame in the translation of polycistronic mRNAs in plant cells. *Nucleic Acids Res* **20**(15), 3851-7.
- Futterer, J., Kiss-Laszlo, Z., and Hohn, T. (1993). Nonlinear ribosome migration on cauliflower mosaic virus 35S RNA. *Cell* **73**(4), 789-802.
- Futterer, J., Potrykus, I., Bao, Y., Li, L., Burns, T. M., Hull, R., and Hohn, T. (1996). Position-dependent ATT initiation during plant pararetrovirus rice tungro bacilliform virus translation. *J Virol* **70**(5), 2999-3010.
- Futterer, J., Rothnie, H. M., Hohn, T., and Potrykus, I. (1997). Rice tungro bacilliform virus open reading frames II and III are translated from polycistronic pregenomic RNA by leaky scanning. *J Virol* **71**(10), 7984-9.
- Gallie, D. R. (1991). The cap and poly(A) tail function synergistically to regulate mRNA translational efficiency. *Genes Dev* **5**(11), 2108-16.
- Gard, G., and Compans, R. W. (1970). Structure and cytopathic effects of Nelson Bay virus. *J Virol* **6**(1), 100-6.

- Gebauer, F., and Hentze, M. W. (2004). Molecular mechanisms of translational control. *Nat Rev Mol Cell Biol* **5**(10), 827-35.
- Gingras, A. C., Kennedy, S. G., O'Leary, M. A., Sonenberg, N., and Hay, N. (1998). 4E-BP1, a repressor of mRNA translation, is phosphorylated and inactivated by the Akt(PKB) signaling pathway. *Genes Dev* **12**(4), 502-13.
- Grande, A., Rodriguez, E., Costas, C., Everitt, E., and Benavente, J. (2000). Oligomerization and cell-binding properties of the avian reovirus cell-attachment protein sigmaC. *Virology* **274**(2), 367-77.
- Grant, C. M., and Hinnebusch, A. G. (1994). Effect of sequence context at stop codons on efficiency of reinitiation in GCN4 translational control. *Mol Cell Biol* **14**(1), 606-18.
- Grant, C. M., Miller, P. F., and Hinnebusch, A. G. (1995). Sequences 5' of the first upstream open reading frame in GCN4 mRNA are required for efficient translational reinitiation. *Nucleic Acids Res* **23**(19), 3980-8.
- Gu, S., Jin, L., Zhang, F., Sarnow, P., and Kay, M. A. (2009). Biological basis for restriction of microRNA targets to the 3' untranslated region in mammalian mRNAs. *Nat Struct Mol Biol* **16**(2), 144-50.
- Guardado Calvo, P., Fox, G. C., Hermo Parrado, X. L., Llamas-Saiz, A. L., Costas, C., Martinez-Costas, J., Benavente, J., and van Raaij, M. J. (2005). Structure of the carboxy-terminal receptor-binding domain of avian reovirus fibre sigmaC. *J Mol Biol* **354**(1), 137-49.
- Guerra-Peraza, O., de Tapia, M., Hohn, T., and Hemmings-Mieszczak, M. (2000). Interaction of the cauliflower mosaic virus coat protein with the pregenomic RNA leader. *J Virol* **74**(5), 2067-72.
- Guo, L., Allen, E. M., and Miller, W. A. (2001). Base-pairing between untranslated regions facilitates translation of uncapped, nonpolyadenylated viral RNA. *Mol Cell* **7**(5), 1103-9.
- Haghighat, A., Mader, S., Pause, A., and Sonenberg, N. (1995). Repression of cap-dependent translation by 4E-binding protein 1: competition with p220 for binding to eukaryotic initiation factor-4E. *EMBO J* **14**(22), 5701-9.
- Halder, K., Wieland, M., and Hartig, J. S. (2009). Predictable suppression of gene expression by 5'-UTR-based RNA quadruplexes. *Nucleic Acids Res* **37**(20), 6811-7.

- Hambidge, S. J., and Sarnow, P. (1992). Translational enhancement of the poliovirus 5' noncoding region mediated by virus-encoded polypeptide 2A. *Proc Natl Acad Sci U S A* **89**(21), 10272-6.
- Harding, H. P., Novoa, I., Zhang, Y., Zeng, H., Wek, R., Schapira, M., and Ron, D. (2000). Regulated translation initiation controls stress-induced gene expression in mammalian cells. *Mol Cell* **6**(5), 1099-108.
- Hellen, C. U., and Sarnow, P. (2001). Internal ribosome entry sites in eukaryotic mRNA molecules. *Genes Dev* **15**(13), 1593-612.
- Hemmings-Mieszczak, M., Hohn, T., and Preiss, T. (2000). Termination and peptide release at the upstream open reading frame are required for downstream translation on synthetic shunt-competent mRNA leaders. *Mol Cell Biol* **20**(17), 6212-23.
- Hemmings-Mieszczak, M., Steger, G., and Hohn, T. (1997). Alternative structures of the cauliflower mosaic virus 35 S RNA leader: implications for viral expression and replication. *J Mol Biol* **267**(5), 1075-88.
- Henke, J. I., Goergen, D., Zheng, J., Song, Y., Schuttler, C. G., Fehr, C., Junemann, C., and Niepmann, M. (2008). microRNA-122 stimulates translation of hepatitis C virus RNA. *EMBO J* **27**(24), 3300-10.
- Herbreteau, C. H., Weill, L., Decimo, D., Prevot, D., Darlix, J. L., Sargueil, B., and Ohlmann, T. (2005). HIV-2 genomic RNA contains a novel type of IRES located downstream of its initiation codon. *Nat Struct Mol Biol* **12**(11), 1001-7.
- Herzog, E., Guilley, H., and Fritsch, C. (1995). Translation of the second gene of peanut clump virus RNA 2 occurs by leaky scanning in vitro. *Virology* **208**(1), 215-25.
- Hill, J. R., and Morris, D. R. (1993). Cell-specific translational regulation of S-adenosylmethionine decarboxylase mRNA. Dependence on translation and coding capacity of the cis-acting upstream open reading frame. *J Biol Chem* **268**(1), 726-31.
- Hinnebusch, A. G. (1997). Translational regulation of yeast GCN4. A window on factors that control initiator-trna binding to the ribosome. *J Biol Chem* **272**(35), 21661-4.
- Hinnebusch, A. G. (2005). Translational regulation of GCN4 and the general amino acid control of yeast. *Annu Rev Microbiol* **59**, 407-50.

- Hu, M. C., Tranque, P., Edelman, G. M., and Mauro, V. P. (1999). rRNA-complementarity in the 5' untranslated region of mRNA specifying the Gtx homeodomain protein: evidence that base-pairing to 18S rRNA affects translational efficiency. *Proc Natl Acad Sci U S A* **96**(4), 1339-44.
- Huang, H. K., Yoon, H., Hannig, E. M., and Donahue, T. F. (1997). GTP hydrolysis controls stringent selection of the AUG start codon during translation initiation in *Saccharomyces cerevisiae*. *Genes Dev* **11**(18), 2396-413.
- Humphreys, D. T., Westman, B. J., Martin, D. I., and Preiss, T. (2005). MicroRNAs control translation initiation by inhibiting eukaryotic initiation factor 4E/cap and poly(A) tail function. *Proc Natl Acad Sci U S A* **102**(47), 16961-6.
- Hunt, S. L., Hsuan, J. J., Totty, N., and Jackson, R. J. (1999). unr, a cellular cytoplasmic RNA-binding protein with five cold-shock domains, is required for internal initiation of translation of human rhinovirus RNA. *Genes Dev* **13**(4), 437-48.
- Hunt, S. L., and Jackson, R. J. (1999). Polypyrimidine-tract binding protein (PTB) is necessary, but not sufficient, for efficient internal initiation of translation of human rhinovirus-2 RNA. *RNA* **5**(3), 344-59.
- Hwang, W. L., and Su, T. S. (1998). Translational regulation of hepatitis B virus polymerase gene by termination-reinitiation of an upstream minicistron in a length-dependent manner. *J Gen Virol* **79** (Pt 9), 2181-9.
- Imataka, H., Gradi, A., and Sonenberg, N. (1998). A newly identified N-terminal amino acid sequence of human eIF4G binds poly(A)-binding protein and functions in poly(A)-dependent translation. *EMBO J* **17**(24), 7480-9.
- Jackson, R. J. (2005). Alternative mechanisms of initiating translation of mammalian mRNAs. *Biochem Soc Trans* **33**(Pt 6), 1231-41.
- Jackson, R. J., Kaminski, A., and Poyry, T. A., Eds. (2007). Coupled termination-reinitiation events in mRNA translation. *Translational Control in Biology and Medicine*. Edited by M. B. Mathews, N. Sonenberg, and J. Hershey. New York: Cold Spring Harbor Laboratory Press.
- Jackson, R. J., and Standart, N. (1990). Do the poly(A) tail and 3' untranslated region control mRNA translation? *Cell* **62**(1), 15-24.
- Jang, S. K., Krausslich, H. G., Nicklin, M. J., Duke, G. M., Palmenberg, A. C., and Wimmer, E. (1988). A segment of the 5' nontranslated region of encephalomyocarditis virus RNA directs internal entry of ribosomes during in vitro translation. *J Virol* **62**(8), 2636-43.

- Joachims, M., Van Breugel, P. C., and Lloyd, R. E. (1999). Cleavage of poly(A)-binding protein by enterovirus proteases concurrent with inhibition of translation in vitro. *J Virol* **73**(1), 718-27.
- Joklik, W. K. (1985). Recent progress in reovirus research. *Annu Rev Genet* **19**, 537-75.
- Jopling, C. L., Yi, M., Lancaster, A. M., Lemon, S. M., and Sarnow, P. (2005). Modulation of hepatitis C virus RNA abundance by a liver-specific MicroRNA. *Science* **309**(5740), 1577-81.
- Kahvejian, A., Svitkin, Y. V., Sukarieh, R., M'Boutchou, M. N., and Sonenberg, N. (2005). Mammalian poly(A)-binding protein is a eukaryotic translation initiation factor, which acts via multiple mechanisms. *Genes Dev* **19**(1), 104-13.
- Karlen, Y., McNair, A., Perseguers, S., Mazza, C., and Mermod, N. (2007). Statistical significance of quantitative PCR. *BMC Bioinformatics* **8**, 131.
- Kataoka, N., Yong, J., Kim, V. N., Velazquez, F., Perkinson, R. A., Wang, F., and Dreyfuss, G. (2000). Pre-mRNA splicing imprints mRNA in the nucleus with a novel RNA-binding protein that persists in the cytoplasm. *Mol Cell* **6**(3), 673-82.
- Kaufman, R. J., Murtha, P., and Davies, M. V. (1987). Translational efficiency of polycistronic mRNAs and their utilization to express heterologous genes in mammalian cells. *EMBO J* **6**(1), 187-93.
- Kerekatte, V., Keiper, B. D., Badorff, C., Cai, A., Knowlton, K. U., and Rhoads, R. E. (1999). Cleavage of Poly(A)-binding protein by coxsackievirus 2A protease in vitro and in vivo: another mechanism for host protein synthesis shutoff? *J Virol* **73**(1), 709-17.
- Koh, D. C., and Mauro, V. P. (2009). Reconciling contradictory reports regarding translation of BACE1 mRNA: initiation mechanism is altered by different expression systems. *RNA Biol* **6**(1), 54-8.
- Koromilas, A. E., Lazaris-Karatzas, A., and Sonenberg, N. (1992). mRNAs containing extensive secondary structure in their 5' non-coding region translate efficiently in cells overexpressing initiation factor eIF-4E. *EMBO J* **11**(11), 4153-8.
- Kozak, M. (1977). Nucleotide sequences of 5'-terminal ribosome-protected initiation regions from two reovirus messages. *Nature* **269**(5627), 391-4.

- Kozak, M. (1981). Possible role of flanking nucleotides in recognition of the AUG initiator codon by eukaryotic ribosomes. *Nucleic Acids Res* **9**(20), 5233-52.
- Kozak, M. (1984a). Point mutations close to the AUG initiator codon affect the efficiency of translation of rat preproinsulin in vivo. *Nature* **308**(5956), 241-6.
- Kozak, M. (1984b). Selection of initiation sites by eucaryotic ribosomes: effect of inserting AUG triplets upstream from the coding sequence for preproinsulin. *Nucleic Acids Res* **12**(9), 3873-93.
- Kozak, M. (1986a). Influences of mRNA secondary structure on initiation by eukaryotic ribosomes. *Proc Natl Acad Sci U S A* **83**(9), 2850-4.
- Kozak, M. (1986b). Point mutations define a sequence flanking the AUG initiator codon that modulates translation by eukaryotic ribosomes. *Cell* **44**(2), 283-92.
- Kozak, M. (1987a). An analysis of 5'-noncoding sequences from 699 vertebrate messenger RNAs. *Nucleic Acids Res* **15**(20), 8125-48.
- Kozak, M. (1987b). At least six nucleotides preceding the AUG initiator codon enhance translation in mammalian cells. *J Mol Biol* **196**(4), 947-50.
- Kozak, M. (1987c). Effects of intercistronic length on the efficiency of reinitiation by eucaryotic ribosomes. *Mol Cell Biol* **7**(10), 3438-45.
- Kozak, M. (1988). Leader length and secondary structure modulate mRNA function under conditions of stress. *Mol Cell Biol* **8**(7), 2737-44.
- Kozak, M. (1989a). Circumstances and mechanisms of inhibition of translation by secondary structure in eucaryotic mRNAs. *Mol Cell Biol* **9**(11), 5134-42.
- Kozak, M. (1989b). Context effects and inefficient initiation at non-AUG codons in eucaryotic cell-free translation systems. *Mol Cell Biol* **9**(11), 5073-80.
- Kozak, M. (1989c). The scanning model for translation: an update. *J Cell Biol* **108**(2), 229-41.
- Kozak, M. (1990). Downstream secondary structure facilitates recognition of initiator codons by eukaryotic ribosomes. *Proc Natl Acad Sci U S A* **87**(21), 8301-5.
- Kozak, M. (1991a). A short leader sequence impairs the fidelity of initiation by eukaryotic ribosomes. *Gene Expr* **1**(2), 111-5.

- Kozak, M. (1991b). Structural features in eukaryotic mRNAs that modulate the initiation of translation. *J Biol Chem* **266**(30), 19867-70.
- Kozak, M. (1992). Regulation of translation in eukaryotic systems. *Annu Rev Cell Biol* **8**, 197-225.
- Kozak, M. (1994). Features in the 5' non-coding sequences of rabbit alpha and beta-globin mRNAs that affect translational efficiency. *J Mol Biol* **235**(1), 95-110.
- Kozak, M. (1999). Initiation of translation in prokaryotes and eukaryotes. *Gene* **234**(2), 187-208.
- Kozak, M. (2001a). Constraints on reinitiation of translation in mammals. *Nucleic Acids Res* **29**(24), 5226-32.
- Kozak, M. (2001b). New ways of initiating translation in eukaryotes? *Mol Cell Biol* **21**(6), 1899-907.
- Kozak, M. (2002). Pushing the limits of the scanning mechanism for initiation of translation. *Gene* **299**(1-2), 1-34.
- Kozak, M. (2007). Lessons (not) learned from mistakes about translation. *Gene* **403**(1-2), 194-203.
- Kozak, M., and Shatkin, A. J. (1977). Sequences and properties of two ribosome binding sites from the small size class of reovirus messenger RNA. *J Biol Chem* **252**(19), 6895-908.
- Krausslich, H. G., Nicklin, M. J., Toyoda, H., Etchison, D., and Wimmer, E. (1987). Poliovirus proteinase 2A induces cleavage of eucaryotic initiation factor 4F polypeptide p220. *J Virol* **61**(9), 2711-8.
- Krowczynska, A., and Brawerman, G. (1986). Structural features of the 5' noncoding region of the rabbit globin messenger RNAs engaged in translation. *Proc Natl Acad Sci U S A* **83**(4), 902-6.
- Kumari, S., Bugaut, A., and Balasubramanian, S. (2008). Position and stability are determining factors for translation repression by an RNA G-quadruplex-forming sequence within the 5' UTR of the NRAS proto-oncogene. *Biochemistry* **47**(48), 12664-9.
- Kumimoto, H., Yamane, Y., and Ishizaki, K. (2005). Two haplotypes of 5' untranslated region in L-myc gene with different internal ribosome entry site activity. *Int J Oncol* **26**(1), 287-93.

- Latorre, P., Kolakofsky, D., and Curran, J. (1998). Sendai virus Y proteins are initiated by a ribosomal shunt. *Mol Cell Biol* **18**(9), 5021-31.
- Lazaris-Karatzas, A., Montine, K. S., and Sonenberg, N. (1990). Malignant transformation by a eukaryotic initiation factor subunit that binds to mRNA 5' cap. *Nature* **345**(6275), 544-7.
- Lazaris-Karatzas, A., Smith, M. R., Frederickson, R. M., Jaramillo, M. L., Liu, Y. L., Kung, H. F., and Sonenberg, N. (1992). Ras mediates translation initiation factor 4E-induced malignant transformation. *Genes Dev* **6**(9), 1631-42.
- Lazaris-Karatzas, A., and Sonenberg, N. (1992). The mRNA 5' cap-binding protein, eIF-4E, cooperates with v-myc or E1A in the transformation of primary rodent fibroblasts. *Mol Cell Biol* **12**(3), 1234-8.
- Lazarowitz, S. G., and Robertson, H. D. (1977). Initiator regions from the small size class of reovirus messenger RNA protected by rabbit reticulocyte ribosomes. *J Biol Chem* **252**(21), 7842-9.
- Lee, K. A., Edery, I., and Sonenberg, N. (1985). Isolation and structural characterization of cap-binding proteins from poliovirus-infected HeLa cells. *J Virol* **54**(2), 515-24.
- Lee, Y. Y., Cevallos, R. C., and Jan, E. (2009). An upstream open reading frame regulates translation of GADD34 during cellular stresses that induce eIF2alpha phosphorylation. *J Biol Chem* **284**(11), 6661-73.
- Lewis, S. M., and Holcik, M. (2008). For IRES trans-acting factors, it is all about location. *Oncogene* **27**(8), 1033-5.
- Lin, T. A., Kong, X., Haystead, T. A., Pause, A., Belsham, G., Sonenberg, N., and Lawrence, J. C., Jr. (1994). PHAS-I as a link between mitogen-activated protein kinase and translation initiation. *Science* **266**(5185), 653-6.
- Liu, H. J., Lin, P. Y., Lee, J. W., Hsu, H. Y., and Shih, W. L. (2005). Retardation of cell growth by avian reovirus p17 through the activation of p53 pathway. *Biochem Biophys Res Commun* **336**(2), 709-15.
- Livak, K. J., and Schmittgen, T. D. (2001). Analysis of relative gene expression data using real-time quantitative PCR and the 2^{(-Delta Delta C(T))} Method. *Methods* **25**(4), 402-8.
- Lloyd, R. E. (2006). Translational control by viral proteinases. *Virus Res* **119**(1), 76-88.

- Lomakin, I. B., Kolupaeva, V. G., Marintchev, A., Wagner, G., and Pestova, T. V. (2003). Position of eukaryotic initiation factor eIF1 on the 40S ribosomal subunit determined by directed hydroxyl radical probing. *Genes Dev* **17**(22), 2786-97.
- Lovett, P. S., and Rogers, E. J. (1996). Ribosome regulation by the nascent peptide. *Microbiol Rev* **60**(2), 366-85.
- Lowry, O. H., Rosebrough, N. J., Farr, A. L., and Randall, R. J. (1951). Protein measurement with the Folin phenol reagent. *J Biol Chem* **193**(1), 265-75.
- Lund, E., Guttinger, S., Calado, A., Dahlberg, J. E., and Kutay, U. (2004). Nuclear export of microRNA precursors. *Science* **303**(5654), 95-8.
- Luttermann, C., and Meyers, G. (2009). The importance of inter- and intramolecular base pairing for translation reinitiation on a eukaryotic bicistronic mRNA. *Genes Dev* **23**(3), 331-44.
- Luukkonen, B. G., Tan, W., and Schwartz, S. (1995). Efficiency of reinitiation of translation on human immunodeficiency virus type 1 mRNAs is determined by the length of the upstream open reading frame and by intercistronic distance. *J Virol* **69**(7), 4086-94.
- Macejak, D. G., and Sarnow, P. (1991). Internal initiation of translation mediated by the 5' leader of a cellular mRNA. *Nature* **353**(6339), 90-4.
- Martinez-Costas, J., Grande, A., Varela, R., Garcia-Martinez, C., and Benavente, J. (1997). Protein architecture of avian reovirus S1133 and identification of the cell attachment protein. *J Virol* **71**(1), 59-64.
- Martinez-Costas, J., Varela, R., and Benavente, J. (1995). Endogenous enzymatic activities of the avian reovirus S1133: identification of the viral capping enzyme. *Virology* **206**(2), 1017-26.
- Mason, P. W., Bezborodova, S. V., and Henry, T. M. (2002). Identification and characterization of a cis-acting replication element (cre) adjacent to the internal ribosome entry site of foot-and-mouth disease virus. *J Virol* **76**(19), 9686-94.
- Matsuda, D., and Dreher, T. W. (2006). Close spacing of AUG initiation codons confers dicistronic character on a eukaryotic mRNA. *RNA* **12**(7), 1338-49.
- Mauro, V. P., and Edelman, G. M. (2002). The ribosome filter hypothesis. *Proc Natl Acad Sci U S A* **99**(19), 12031-6.

- Mauro, V. P., and Edelman, G. M. (2007). The ribosome filter redux. *Cell Cycle* **6**(18), 2246-51.
- McCrae, M. A. (1981). Terminal structure of reovirus RNAs. *J Gen Virol* **55**(Pt 2), 393-403.
- Meijer, H. A., and Thomas, A. A. (2002). Control of eukaryotic protein synthesis by upstream open reading frames in the 5'-untranslated region of an mRNA. *Biochem J* **367**(Pt 1), 1-11.
- Mendez, R., Myers, M. G., Jr., White, M. F., and Rhoads, R. E. (1996). Stimulation of protein synthesis, eukaryotic translation initiation factor 4E phosphorylation, and PHAS-I phosphorylation by insulin requires insulin receptor substrate 1 and phosphatidylinositol 3-kinase. *Mol Cell Biol* **16**(6), 2857-64.
- Merrill, M. K., Dobrikova, E. Y., and Gromeier, M. (2006). Cell-type-specific repression of internal ribosome entry site activity by double-stranded RNA-binding protein 76. *J Virol* **80**(7), 3147-56.
- Meyers, G. (2003). Translation of the minor capsid protein of a calicivirus is initiated by a novel termination-dependent reinitiation mechanism. *J Biol Chem* **278**(36), 34051-60.
- Miller, P. F., and Hinnebusch, A. G. (1989). Sequences that surround the stop codons of upstream open reading frames in GCN4 mRNA determine their distinct functions in translational control. *Genes Dev* **3**(8), 1217-25.
- Miller, W. A., Waterhouse, P. M., and Gerlach, W. L. (1988). Sequence and organization of barley yellow dwarf virus genomic RNA. *Nucleic Acids Res* **16**(13), 6097-111.
- Mitchell, S. F., and Lorsch, J. R. (2008). Should I stay or should I go? Eukaryotic translation initiation factors 1 and 1A control start codon recognition. *J Biol Chem* **283**(41), 27345-9.
- Miyagi, Y., Sugiyama, A., Asai, A., Okazaki, T., Kuchino, Y., and Kerr, S. J. (1995). Elevated levels of eukaryotic translation initiation factor eIF-4E, mRNA in a broad spectrum of transformed cell lines. *Cancer Lett* **91**(2), 247-52.
- Montero, H., Arias, C. F., and Lopez, S. (2006). Rotavirus Nonstructural Protein NSP3 is not required for viral protein synthesis. *J Virol* **80**(18), 9031-8.
- Morris, D. R., and Geballe, A. P. (2000). Upstream open reading frames as regulators of mRNA translation. *Mol Cell Biol* **20**(23), 8635-42.

- Mudge, S. J., Williams, J. H., Eyre, H. J., Sutherland, G. R., Cowan, P. J., and Power, D. A. (1998). Complex organisation of the 5'-end of the human glycine tRNA synthetase gene. *Gene* **209**(1-2), 45-50.
- Mueller, P. P., and Hinnebusch, A. G. (1986). Multiple upstream AUG codons mediate translational control of GCN4. *Cell* **45**(2), 201-7.
- Muthukrishnan, S., Both, G. W., Furuichi, Y., and Shatkin, A. J. (1975). 5'-Terminal 7-methylguanosine in eukaryotic mRNA is required for translation. *Nature* **255**(5503), 33-7.
- Napthine, S., Lever, R. A., Powell, M. L., Jackson, R. J., Brown, T. D., and Brierley, I. (2009). Expression of the VP2 protein of murine norovirus by a translation termination-reinitiation strategy. *PLoS One* **4**(12), e8390.
- Nibert, M. L., and Schiff, L., Eds. (2001). Reoviridae. Vol. 2. Fields Virology. Edited by D. M. Knipe, and P. M. Howley. New York: Lippincott Williams & Wilkins.
- Olsen, P. H., and Ambros, V. (1999). The lin-4 regulatory RNA controls developmental timing in *Caenorhabditis elegans* by blocking LIN-14 protein synthesis after the initiation of translation. *Dev Biol* **216**(2), 671-80.
- Otero, L. J., Ashe, M. P., and Sachs, A. B. (1999). The yeast poly(A)-binding protein Pab1p stimulates in vitro poly(A)-dependent and cap-dependent translation by distinct mechanisms. *EMBO J* **18**(11), 3153-63.
- Otto, G. A., Lukavsky, P. J., Lancaster, A. M., Sarnow, P., and Puglisi, J. D. (2002). Ribosomal proteins mediate the hepatitis C virus IRES-HeLa 40S interaction. *RNA* **8**(7), 913-23.
- Panopoulos, P., and Mauro, V. P. (2008). Antisense masking reveals contributions of mRNA-rRNA base pairing to translation of Gtx and FGF2 mRNAs. *J Biol Chem* **283**(48), 33087-93.
- Paraskeva, E., Gray, N. K., Schlager, B., Wehr, K., and Hentze, M. W. (1999). Ribosomal pausing and scanning arrest as mechanisms of translational regulation from cap-distal iron-responsive elements. *Mol Cell Biol* **19**(1), 807-16.
- Park, H. S., Himmelbach, A., Browning, K. S., Hohn, T., and Ryabova, L. A. (2001). A plant viral "reinitiation" factor interacts with the host translational machinery. *Cell* **106**(6), 723-33.
- Passmore, L. A., Schmeing, T. M., Maag, D., Applefield, D. J., Acker, M. G., Algire, M. A., Lorsch, J. R., and Ramakrishnan, V. (2007). The eukaryotic translation initiation factors eIF1 and eIF1A induce an open conformation of the 40S ribosome. *Mol Cell* **26**(1), 41-50.

- Patton, J. T., and Gallegos, C. O. (1988). Structure and protein composition of the rotavirus replicase particle. *Virology* **166**(2), 358-65.
- Patton, J. T., and Gallegos, C. O. (1990). Rotavirus RNA replication: single-stranded RNA extends from the replicase particle. *J Gen Virol* **71 (Pt 5)**, 1087-94.
- Patton, J. T., and Spencer, E. (2000). Genome replication and packaging of segmented double-stranded RNA viruses. *Virology* **277**(2), 217-25.
- Pause, A., Belsham, G. J., Gingras, A. C., Donze, O., Lin, T. A., Lawrence, J. C., Jr., and Sonenberg, N. (1994). Insulin-dependent stimulation of protein synthesis by phosphorylation of a regulator of 5'-cap function. *Nature* **371**(6500), 762-7.
- Peabody, D. S. (1989). Translation initiation at non-AUG triplets in mammalian cells. *J Biol Chem* **264**(9), 5031-5.
- Pelletier, J., and Sonenberg, N. (1985). Insertion mutagenesis to increase secondary structure within the 5' noncoding region of a eukaryotic mRNA reduces translational efficiency. *Cell* **40**(3), 515-26.
- Pelletier, J., and Sonenberg, N. (1988). Internal initiation of translation of eukaryotic mRNA directed by a sequence derived from poliovirus RNA. *Nature* **334**(6180), 320-5.
- Perry, R. P., and Kelley, D. E. (1976). Kinetics of formation of 5' terminal caps in mRNA. *Cell* **8**(3), 433-42.
- Pestova, T. V., Hellen, C. U., and Shatsky, I. N. (1996). Canonical eukaryotic initiation factors determine initiation of translation by internal ribosomal entry. *Mol Cell Biol* **16**(12), 6859-69.
- Pestova, T. V., and Kolupaeva, V. G. (2002). The roles of individual eukaryotic translation initiation factors in ribosomal scanning and initiation codon selection. *Genes Dev* **16**(22), 2906-22.
- Pestova, T. V., Lomakin, I. B., Lee, J. H., Choi, S. K., Dever, T. E., and Hellen, C. U. (2000). The joining of ribosomal subunits in eukaryotes requires eIF5B. *Nature* **403**(6767), 332-5.
- Pestova, T. V., Shatsky, I. N., Fletcher, S. P., Jackson, R. J., and Hellen, C. U. (1998). A prokaryotic-like mode of cytoplasmic eukaryotic ribosome binding to the initiation codon during internal translation initiation of hepatitis C and classical swine fever virus RNAs. *Genes Dev* **12**(1), 67-83.

- Pillai, R. S., Bhattacharyya, S. N., Artus, C. G., Zoller, T., Cougot, N., Basyuk, E., Bertrand, E., and Filipowicz, W. (2005). Inhibition of translational initiation by Let-7 MicroRNA in human cells. *Science* **309**(5740), 1573-6.
- Piron, M., Vende, P., Cohen, J., and Poncet, D. (1998). Rotavirus RNA-binding protein NSP3 interacts with eIF4GI and evicts the poly(A) binding protein from eIF4F. *EMBO J* **17**(19), 5811-21.
- Pisarev, A. V., Chard, L. S., Kaku, Y., Johns, H. L., Shatsky, I. N., and Belsham, G. J. (2004). Functional and structural similarities between the internal ribosome entry sites of hepatitis C virus and porcine teschovirus, a picornavirus. *J Virol* **78**(9), 4487-97.
- Pisarev, A. V., Hellen, C. U., and Pestova, T. V. (2007). Recycling of eukaryotic posttermination ribosomal complexes. *Cell* **131**(2), 286-99.
- Pisarev, A. V., Kolupaeva, V. G., Pisareva, V. P., Merrick, W. C., Hellen, C. U., and Pestova, T. V. (2006). Specific functional interactions of nucleotides at key -3 and +4 positions flanking the initiation codon with components of the mammalian 48S translation initiation complex. *Genes Dev* **20**(5), 624-36.
- Pisarev, A. V., Kolupaeva, V. G., Yusupov, M. M., Hellen, C. U., and Pestova, T. V. (2008). Ribosomal position and contacts of mRNA in eukaryotic translation initiation complexes. *EMBO J* **27**(11), 1609-21.
- Pisarev, A. V., Shirokikh, N. E., and Hellen, C. U. (2005). Translation initiation by factor-independent binding of eukaryotic ribosomes to internal ribosomal entry sites. *C R Biol* **328**(7), 589-605.
- Polacek, C., Friebe, P., and Harris, E. (2009). Poly(A)-binding protein binds to the non-polyadenylated 3' untranslated region of dengue virus and modulates translation efficiency. *J Gen Virol* **90**(Pt 3), 687-92.
- Poncet, D., Aponte, C., and Cohen, J. (1993). Rotavirus protein NSP3 (NS34) is bound to the 3' end consensus sequence of viral mRNAs in infected cells. *J Virol* **67**(6), 3159-65.
- Pooggin, M. M., Hohn, T., and Fütterer, J. (1998). Forced evolution reveals the importance of short open reading frame A and secondary structure in the cauliflower mosaic virus 35S RNA leader. *J Virol* **72**(5), 4157-69.
- Pooggin, M. M., Hohn, T., and Fütterer, J. (2000). Role of a short open reading frame in ribosome shunt on the cauliflower mosaic virus RNA leader. *J Biol Chem* **275**(23), 17288-96.

- Pooggin, M. M., Ryabova, L. A., He, X., Futterer, J., and Hohn, T. (2006). Mechanism of ribosome shunting in Rice tungro bacilliform pararetrovirus. *RNA* **12**(5), 841-50.
- Powell, M. L., Napthine, S., Jackson, R. J., Brierley, I., and Brown, T. D. (2008). Characterization of the termination-reinitiation strategy employed in the expression of influenza B virus BM2 protein. *RNA* **14**(11), 2394-406.
- Poyry, T. A., Kaminski, A., Connell, E. J., Fraser, C. S., and Jackson, R. J. (2007). The mechanism of an exceptional case of reinitiation after translation of a long ORF reveals why such events do not generally occur in mammalian mRNA translation. *Genes Dev* **21**(23), 3149-62.
- Poyry, T. A., Kaminski, A., and Jackson, R. J. (2004). What determines whether mammalian ribosomes resume scanning after translation of a short upstream open reading frame? *Genes Dev* **18**(1), 62-75.
- Qiu, J., Cheng, F., and Pintel, D. (2007). The abundant R2 mRNA generated by aleutian mink disease parvovirus is tricistronic, encoding NS2, VP1, and VP2. *J Virol* **81**(13), 6993-7000.
- Racine, T., Barry, C., Roy, K., Dawe, S. J., Shmulevitz, M., and Duncan, R. (2007). Leaky scanning and scanning-independent ribosome migration on the tricistronic S1 mRNA of avian reovirus. *J Biol Chem* **282**(35), 25613-22.
- Racine, T., Hurst, T., Barry, C., Shou, J., Kibenge, F., and Duncan, R. (2009). Aquareovirus effects syncytiogenesis by using a novel member of the FAST protein family translated from a noncanonical translation start site. *J Virol* **83**(11), 5951-5.
- Rakotondrafara, A. M., Polacek, C., Harris, E., and Miller, W. A. (2006). Oscillating kissing stem-loop interactions mediate 5' scanning-dependent translation by a viral 3'-cap-independent translation element. *RNA* **12**(10), 1893-906.
- Rasmussen, E. B., and Lis, J. T. (1993). In vivo transcriptional pausing and cap formation on three Drosophila heat shock genes. *Proc Natl Acad Sci U S A* **90**(17), 7923-7.
- Remm, M., Remm, A., and Ustav, M. (1999). Human papillomavirus type 18 E1 protein is translated from polycistronic mRNA by a discontinuous scanning mechanism. *J Virol* **73**(4), 3062-70.
- Reynolds, J. E., Kaminski, A., Kettinen, H. J., Grace, K., Clarke, B. E., Carroll, A. R., Rowlands, D. J., and Jackson, R. J. (1995). Unique features of internal initiation of hepatitis C virus RNA translation. *EMBO J* **14**(23), 6010-20.

- Roberts, L. O., Seamons, R. A., and Belsham, G. J. (1998). Recognition of picornavirus internal ribosome entry sites within cells; influence of cellular and viral proteins. *RNA* **4**(5), 520-9.
- Rodnina, M. V., and Wintermeyer, W. (2009). Recent mechanistic insights into eukaryotic ribosomes. *Curr Opin Cell Biol* **21**(3), 435-43.
- Rodriguez, M. S., Dargemont, C., and Stutz, F. (2004). Nuclear export of RNA. *Biol Cell* **96**(8), 639-55.
- Rodriguez-Mateos, M., Garcia-Gomez, J. J., Francisco-Velilla, R., Remacha, M., de la Cruz, J., and Ballesta, J. P. (2009). Role and dynamics of the ribosomal protein P0 and its related trans-acting factor Mrt4 during ribosome assembly in *Saccharomyces cerevisiae*. *Nucleic Acids Res* **37**(22), 7519-32.
- Rogers, G. W., Jr., Edelman, G. M., and Mauro, V. P. (2004). Differential utilization of upstream AUGs in the beta-secretase mRNA suggests that a shunting mechanism regulates translation. *Proc Natl Acad Sci U S A* **101**(9), 2794-9.
- Ron, D., and Harding, H. P., Eds. (2007). eIF2alpha phosphorylation in cellular stress responses and disease. *Translational Control in Biology and Medicine*. Edited by M. B. Mathews, N. Sonenberg, and J. Hershey. New York: Cold Spring Harbor Laboratory Press.
- Roner, M. R., and Roehr, J. (2006). The 3' sequences required for incorporation of an engineered ssRNA into the Reovirus genome. *Virol J* **3**, 1.
- Rosenwald, I. B., Hutzler, M. J., Wang, S., Savas, L., and Fraire, A. E. (2001). Expression of eukaryotic translation initiation factors 4E and 2alpha is increased frequently in bronchioloalveolar but not in squamous cell carcinomas of the lung. *Cancer* **92**(8), 2164-71.
- Roy, B., Vaughn, J. N., Kim, B. H., Zhou, F., Gilchrist, M. A., and Von Arnim, A. G. The h subunit of eIF3 promotes reinitiation competence during translation of mRNAs harboring upstream open reading frames. *RNA* **16**(4), 748-61.
- Ryabova, L. A., Pooggin, M. M., and Hohn, T. (2002). Viral strategies of translation initiation: ribosomal shunt and reinitiation. *Prog Nucleic Acid Res Mol Biol* **72**, 1-39.
- Ryabova, L. A., Pooggin, M. M., and Hohn, T. (2006). Translation reinitiation and leaky scanning in plant viruses. *Virus Res* **119**(1), 52-62.

- Sachs, M. S., Wang, Z., Gaba, A., Fang, P., Belk, J., Ganesan, R., Amrani, N., and Jacobson, A. (2002). Toeprint analysis of the positioning of translation apparatus components at initiation and termination codons of fungal mRNAs. *Methods* **26**(2), 105-14.
- Salsman, J., Top, D., Boutilier, J., and Duncan, R. (2005). Extensive syncytium formation mediated by the reovirus FAST proteins triggers apoptosis-induced membrane instability. *J Virol* **79**(13), 8090-100.
- Samols, M. A., Skalsky, R. L., Maldonado, A. M., Riva, A., Lopez, M. C., Baker, H. V., and Renne, R. (2007). Identification of cellular genes targeted by KSHV-encoded microRNAs. *PLoS Pathog* **3**(5), e65.
- Schepetilnikov, M., Schott, G., Katsarou, K., Thiebauld, O., Keller, M., and Ryabova, L. A. (2009). Molecular dissection of the prototype foamy virus (PFV) RNA 5'-UTR identifies essential elements of a ribosomal shunt. *Nucleic Acids Res* **37**(17), 5838-47.
- Schneider, R., and Sonenberg, N., Eds. (2007). Translation Control in Cancer Development and Progression. Translation Control in Biology and Medicine. Edited by M. B. Mathews, N. Sonenberg, and J. Hershey. New York: Cold Spring Harbor Laboratory Press.
- Schuler, M., Connell, S. R., Lescoute, A., Giesebrecht, J., Dabrowski, M., Schroeer, B., Mielke, T., Penczek, P. A., Westhof, E., and Spahn, C. M. (2006). Structure of the ribosome-bound cricket paralysis virus IRES RNA. *Nat Struct Mol Biol* **13**(12), 1092-6.
- Searfoss, A., Dever, T. E., and Wickner, R. (2001). Linking the 3' poly(A) tail to the subunit joining step of translation initiation: relations of Pab1p, eukaryotic translation initiation factor 5b (Fun12p), and Ski2p-Slh1p. *Mol Cell Biol* **21**(15), 4900-8.
- Sedman, S. A., Gelembiuk, G. W., and Mertz, J. E. (1990). Translation initiation at a downstream AUG occurs with increased efficiency when the upstream AUG is located very close to the 5' cap. *J Virol* **64**(1), 453-7.
- Sedman, S. A., and Mertz, J. E. (1988). Mechanisms of synthesis of virion proteins from the functionally bigenic late mRNAs of simian virus 40. *J Virol* **62**(3), 954-61.
- Sen, N., Cao, F., and Tavis, J. E. (2004). Translation of duck hepatitis B virus reverse transcriptase by ribosomal shunting. *J Virol* **78**(21), 11751-7.

- Shabalina, S. A., Ogurtsov, A. Y., Rogozin, I. B., Koonin, E. V., and Lipman, D. J. (2004). Comparative analysis of orthologous eukaryotic mRNAs: potential hidden functional signals. *Nucleic Acids Res* **32**(5), 1774-82.
- Sherrill, K. W., and Lloyd, R. E. (2008). Translation of ciAP2 mRNA is mediated exclusively by a stress-modulated ribosome shunt. *Mol Cell Biol* **28**(6), 2011-22.
- Shih, W. L., Hsu, H. W., Liao, M. H., Lee, L. H., and Liu, H. J. (2004). Avian reovirus sigmaC protein induces apoptosis in cultured cells. *Virology* **321**(1), 65-74.
- Shirokikh, N. E., Alkalaeva, E. Z., Vassilenko, K. S., Afonina, Z. A., Alekhina, O. M., Kisselev, L. L., and Spirin, A. S. Quantitative analysis of ribosome-mRNA complexes at different translation stages. *Nucleic Acids Res* **38**(3), e15.
- Shirokikh, N. E., and Spirin, A. S. (2008). Poly(A) leader of eukaryotic mRNA bypasses the dependence of translation on initiation factors. *Proc Natl Acad Sci U S A* **105**(31), 10738-43.
- Shmulevitz, M., and Duncan, R. (2000). A new class of fusion-associated small transmembrane (FAST) proteins encoded by the non-enveloped fusogenic reoviruses. *EMBO J* **19**(5), 902-12.
- Shmulevitz, M., Yameen, Z., Dawe, S., Shou, J., O'Hara, D., Holmes, I., and Duncan, R. (2002). Sequential partially overlapping gene arrangement in the tricistronic S1 genome segments of avian reovirus and Nelson Bay reovirus: implications for translation initiation. *J Virol* **76**(2), 609-18.
- Siridechadilok, B., Fraser, C. S., Hall, R. J., Doudna, J. A., and Nogales, E. (2005). Structural roles for human translation factor eIF3 in initiation of protein synthesis. *Science* **310**(5753), 1513-5.
- Slusher, L. B., Gillman, E. C., Martin, N. C., and Hopper, A. K. (1991). mRNA leader length and initiation codon context determine alternative AUG selection for the yeast gene MOD5. *Proc Natl Acad Sci U S A* **88**(21), 9789-93.
- Spahn, C. M., Jan, E., Mulder, A., Grassucci, R. A., Sarnow, P., and Frank, J. (2004). Cryo-EM visualization of a viral internal ribosome entry site bound to human ribosomes: the IRES functions as an RNA-based translation factor. *Cell* **118**(4), 465-75.
- Spandidos, D. A., and Graham, A. F. (1976). Physical and chemical characterization of an avian reovirus. *J Virol* **19**(3), 968-76.

- Stripecke, R., Oliveira, C. C., McCarthy, J. E., and Hentze, M. W. (1994). Proteins binding to 5' untranslated region sites: a general mechanism for translational regulation of mRNAs in human and yeast cells. *Mol Cell Biol* **14**(9), 5898-909.
- Sullivan, C. S., and Ganem, D. (2005). MicroRNAs and viral infection. *Mol Cell* **20**(1), 3-7.
- Suzuki, Y., Ishihara, D., Sasaki, M., Nakagawa, H., Hata, H., Tsunoda, T., Watanabe, M., Komatsu, T., Ota, T., Isogai, T., Suyama, A., and Sugano, S. (2000). Statistical analysis of the 5' untranslated region of human mRNA using "Oligo-Capped" cDNA libraries. *Genomics* **64**(3), 286-97.
- Swaminathan, S. (2008). Noncoding RNAs produced by oncogenic human herpesviruses. *J Cell Physiol* **216**(2), 321-6.
- Szamecz, B., Rutkai, E., Cuchalova, L., Munzarova, V., Herrmannova, A., Nielsen, K. H., Burela, L., Hinnebusch, A. G., and Valasek, L. (2008). eIF3a cooperates with sequences 5' of uORF1 to promote resumption of scanning by post-termination ribosomes for reinitiation on GCN4 mRNA. *Genes Dev* **22**(17), 2414-25.
- Tarun, S. Z., Jr., and Sachs, A. B. (1996). Association of the yeast poly(A) tail binding protein with translation initiation factor eIF-4G. *EMBO J* **15**(24), 7168-77.
- Tejada, S., Lobo, M. V., Garcia-Villanueva, M., Sacristan, S., Perez-Morgado, M. I., Salinas, M., and Martin, M. E. (2009). Eukaryotic initiation factors (eIF) 2alpha and 4E expression, localization, and phosphorylation in brain tumors. *J Histochem Cytochem* **57**(5), 503-12.
- Thiebauld, O., Schepetilnikov, M., Park, H. S., Geldreich, A., Kobayashi, K., Keller, M., Hohn, T., and Ryabova, L. A. (2009). A new plant protein interacts with eIF3 and 60S to enhance virus-activated translation re-initiation. *EMBO J* **28**(20), 3171-84.
- Treder, K., Kneller, E. L., Allen, E. M., Wang, Z., Browning, K. S., and Miller, W. A. (2008). The 3' cap-independent translation element of Barley yellow dwarf virus binds eIF4F via the eIF4G subunit to initiate translation. *RNA* **14**(1), 134-47.
- Tseng, H., Chou, W., Wang, J., Zhang, X., Zhang, S., and Schultz, R. M. (2008). Mouse ribosomal RNA genes contain multiple differentially regulated variants. *PLoS One* **3**(3), e1843.
- Van Eden, M. E., Byrd, M. P., Sherrill, K. W., and Lloyd, R. E. (2004). Translation of cellular inhibitor of apoptosis protein 1 (c-IAP1) mRNA is IRES mediated and regulated during cell stress. *RNA* **10**(3), 469-81.

- Vattem, K. M., and Wek, R. C. (2004). Reinitiation involving upstream ORFs regulates ATF4 mRNA translation in mammalian cells. *Proc Natl Acad Sci U S A* **101**(31), 11269-74.
- Ventoso, I., MacMillan, S. E., Hershey, J. W., and Carrasco, L. (1998). Poliovirus 2A proteinase cleaves directly the eIF-4G subunit of eIF-4F complex. *FEBS Lett* **435**(1), 79-83.
- von Der Haar, T., Ball, P. D., and McCarthy, J. E. (2000). Stabilization of eukaryotic initiation factor 4E binding to the mRNA 5'-Cap by domains of eIF4G. *J Biol Chem* **275**(39), 30551-5.
- Walsh, D., and Mohr, I. (2004). Phosphorylation of eIF4E by Mnk-1 enhances HSV-1 translation and replication in quiescent cells. *Genes Dev* **18**(6), 660-72.
- Walsh, D., and Mohr, I. (2006). Assembly of an active translation initiation factor complex by a viral protein. *Genes Dev* **20**(4), 461-72.
- Walsh, D., Perez, C., Notary, J., and Mohr, I. (2005). Regulation of the translation initiation factor eIF4F by multiple mechanisms in human cytomegalovirus-infected cells. *J Virol* **79**(13), 8057-64.
- Wang, S., Browning, K. S., and Miller, W. A. (1997). A viral sequence in the 3'-untranslated region mimics a 5' cap in facilitating translation of uncapped mRNA. *EMBO J* **16**(13), 4107-16.
- Wang, X. Q., and Rothnagel, J. A. (2004). 5'-untranslated regions with multiple upstream AUG codons can support low-level translation via leaky scanning and reinitiation. *Nucleic Acids Res* **32**(4), 1382-91.
- Wehner, K. A., and Sarnow, P., Eds. (2007). Regulation of mRNA molecules by microRNAs. *Translational Control in Biology and Medicine*. Edited by M. B. Mathews, N. Sonenberg, and J. Hershey. New York: Cold Spring Harbor Laboratory Press.
- Wells, S. E., Hillner, P. E., Vale, R. D., and Sachs, A. B. (1998). Circularization of mRNA by eukaryotic translation initiation factors. *Mol Cell* **2**(1), 135-40.
- Wightman, B., Burglin, T. R., Gatto, J., Arasu, P., and Ruvkun, G. (1991). Negative regulatory sequences in the lin-14 3'-untranslated region are necessary to generate a temporal switch during *Caenorhabditis elegans* development. *Genes Dev* **5**(10), 1813-24.
- Wightman, B., Ha, I., and Ruvkun, G. (1993). Posttranscriptional regulation of the heterochronic gene lin-14 by lin-4 mediates temporal pattern formation in *C. elegans*. *Cell* **75**(5), 855-62.

- Williams, M. A., and Lamb, R. A. (1989). Effect of mutations and deletions in a bicistronic mRNA on the synthesis of influenza B virus NB and NA glycoproteins. *J Virol* **63**(1), 28-35.
- Wilson, J. E., Pestova, T. V., Hellen, C. U., and Sarnow, P. (2000a). Initiation of protein synthesis from the A site of the ribosome. *Cell* **102**(4), 511-20.
- Wilson, J. E., Powell, M. J., Hoover, S. E., and Sarnow, P. (2000b). Naturally occurring dicistronic cricket paralysis virus RNA is regulated by two internal ribosome entry sites. *Mol Cell Biol* **20**(14), 4990-9.
- Wu, L., Fan, J., and Belasco, J. G. (2006). MicroRNAs direct rapid deadenylation of mRNA. *Proc Natl Acad Sci U S A* **103**(11), 4034-9.
- Xi, Q., Cuesta, R., and Schneider, R. J. (2004). Tethering of eIF4G to adenoviral mRNAs by viral 100k protein drives ribosome shunting. *Genes Dev* **18**(16), 1997-2009.
- Xi, Q., Cuesta, R., and Schneider, R. J. (2005). Regulation of translation by ribosome shunting through phosphotyrosine-dependent coupling of adenovirus protein 100k to viral mRNAs. *J Virol* **79**(9), 5676-83.
- Yu, Y., Marintchev, A., Kolupaeva, V. G., Unbehaun, A., Veryasova, T., Lai, S. C., Hong, P., Wagner, G., Hellen, C. U., and Pestova, T. V. (2009). Position of eukaryotic translation initiation factor eIF1A on the 40S ribosomal subunit mapped by directed hydroxyl radical probing. *Nucleic Acids Res* **37**(15), 5167-82.
- Yueh, A., and Schneider, R. J. (1996). Selective translation initiation by ribosome jumping in adenovirus-infected and heat-shocked cells. *Genes Dev* **10**(12), 1557-67.
- Yueh, A., and Schneider, R. J. (2000). Translation by ribosome shunting on adenovirus and hsp70 mRNAs facilitated by complementarity to 18S rRNA. *Genes Dev* **14**(4), 414-21.
- Zaher, H. S., and Green, R. (2009). Fidelity at the molecular level: lessons from protein synthesis. *Cell* **136**(4), 746-62.
- Zhang, X., Tang, J., Walker, S. B., O'Hara, D., Nibert, M. L., Duncan, R., and Baker, T. S. (2005). Structure of avian orthoreovirus virion by electron cryomicroscopy and image reconstruction. *Virology* **343**(1), 25-35.
- Zhang, Y., Dolph, P. J., and Schneider, R. J. (1989). Secondary structure analysis of adenovirus tripartite leader. *J Biol Chem* **264**(18), 10679-84.

(2001). New synthetic Renilla gene and assay system increase expression, reliability, and sensitivity. . Zhuang, Y., Butler, B., Hawkins, E., Paguio, A., Orr, L., Wood, M., and Wood, K. V.